2022, 23, 2
العلوم الأساسية والتطبيقية
Basic and Applied Sciences
ISSN: 1658-0311 Online ISSN: 1658-8371

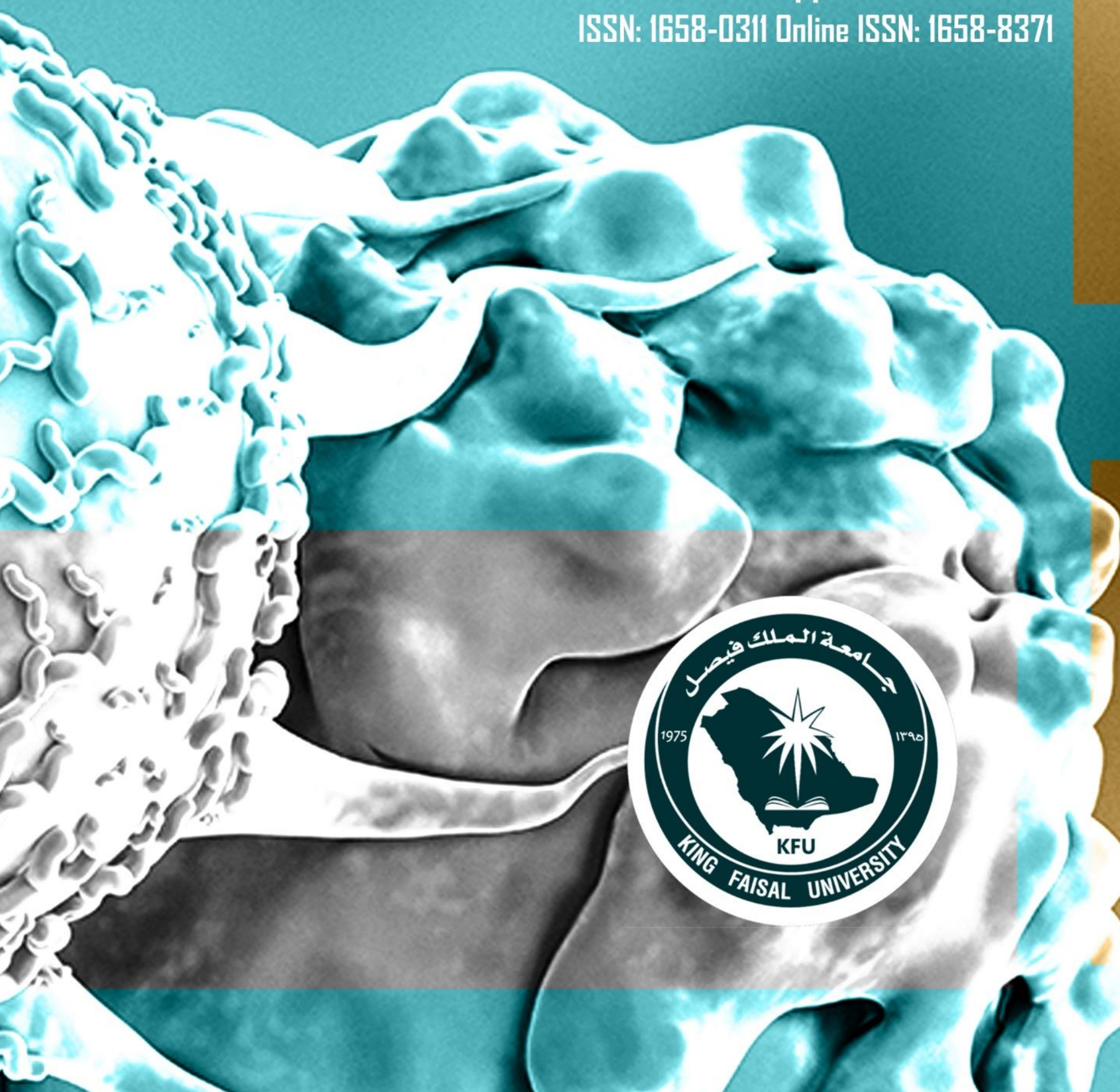

SJKFU

المجلة العلمية لجامعة الملك فيصل

The Scientific Journal of King Faisal University

In this Issue: Identifying Novel Targetable Chromosomal Alterations in Ovarian Cancer

Description

King Faisal University has two open-access refereed journals published bi-annually. The first is 'The Scientific Journal of King Faisal University: Humanities and Management Sciences' (ISSN: 1319-6944, E-ISSN: 1658-838x), issued in March and September and named in the Arab Impact Factor. The second is 'The Scientific Journal of King Faisal University: Basic and Applied Sciences' (ISSN: 1658-0311, E-ISSN: 1658-8371), which is published in June and December and indexed in Scopus. The two journals were founded in 2000 under the guidance of the Scientific Council of the University. Editors-in-chief are as follows: Prof. Khalid S. Al Abdulsalam (2000-2), Prof. Adel I. Al Afaleq (2002-14), Dr Muhammed S. Al Wasli (2014-15), Prof. Ghazi F. Basiouni (2015-2020) and Prof. Abdulrahman E. Al Lily (2020-present).

Correspondence

Editor-in-Chief, Scientific Journal of King Faisal University
P.O. Box 400 Al Ahsa, 31982, Saudi Arabia
00966135895238, 00966135895237
scijkfu@kfu.edu.sa

وصف المجلة

تصدر جامعة الملك فيصل مجلتين علميتين محكمتين نصف سنوية وذات "الوصول المفتوح". الأولى هي "المجلة العلمية لجامعة الملك فيصل: العلوم الإنسانية والإدارية" (ردمد مطبوع: 1319-6944، ردمد إلكتروني: ×838-1658)، والتي تصدر في مارس وسبتمبر وهي مسجلة في قاعدة بيانات معامل التصنيف العربي. الثانية هي "المجلة العلمية لجامعة الملك فيصل: العلوم الأساسية والتطبيقية" (ردمد مطبوع: 0311-1658، ردمد إلكتروني: 1658-8371)، والتي تصدر في يونيو وديسمبر وهي مفهرسة في سكوبس. بدأ إصدار المجلتين في عام 1420هـ (2000م)، تحت إشراف المجلس العلمي للجامعة. أول رئيس لهيئة التحرير أ.د. خالد سعد آل عبدالسلام (12/4/1419هـ)، تلاه أ.د. عادل إبراهيم العفالق (12/6/1421هـ)، عقبه د. محمد سعد الوصالي (17/7/1432هـ)، وجاء بعده أ.د. غازي فيصل بسيوني (11/1/1433هـ)، وحالياً أ.د. عبدالرحمن عيسى الليلي (5/5/1441هـ).

المراسلات العامة

رئيس هيئة التحرير، المجلة العلمية لجامعة الملك فيصل
ص. ب 400 الأحساء 31982، المملكة العربية السعودية
00966135895238، 00966135895237
scijkfu@kfu.edu.sa

Table of Contents

جدول المحتويات

The Scientific Journal of King Faisal University

Basic and Applied Sciences

Coral Mitigates High-energy Marine Floods: Numerical Analysis on Flow–Coral Interaction

N.A.K Nandasena [1] and Irshaad Chawdhary [2]

[1] Civil and Environmental Engineering Department, United Arab Emirates University, Al Ain, United Arab Emirates

[2] Auckland Council, Henderson, New Zealand

LINK	RECEIVED	ACCEPTED	PUBLISHED ONLINE	ASSIGNED TO AN ISSUE
https://doi.org/10.37575/b/sci/220007	27/02/2022	16/06/2022	16/06/2022	01/12/2022
NO. OF WORDS	**NO. OF PAGES**	**YEAR**	**VOLUME**	**ISSUE**
6099	6	2022	23	2

ABSTRACT

This paper investigates the effect of coral reef roughness on mitigating marine floods by using numerical analysis. The study includes two ocean bathymetries — idealised bathymetry with 1% gradient and real bathymetry — for Gold Coast, Australia. The results indicate that characteristics of the marine flood (wave height and period), coral roughness, and shape of the bathymetry are key to the mitigation of marine floods. Wave height reduction behind the reef and at the shore increases with the incident wave height of the marine flood. The maximum reduction behind the reef is around 60% for both bathymetries for the incident wave height of 4 m. When the incident wave period increases from 10 min to 20 min, the wave height reduction increases to 60% but increases from 20 min to 40 min, decreasing the reduction to as little as 3% behind the reef for the ideal bed condition. However, the marine floods caused by longer period waves can be slowed by higher coral roughness compared to the floods caused by relatively shorter period waves. The wave force reduction behind the reef increases with the incident wave height of the marine flood. The wave force reduction is greater than the wave height reduction behind the reef.

KEYWORDS

Marine flood; roughness; coral; numerical modelling; long-period waves

CITATION

Nandasena, N.A.K. and Chawdhary, I. (2022). Coral mitigates high-energy marine floods: Numerical analysis on flow—coral interaction. *The Scientific Journal of King Faisal University: Basic and Applied Sciences*, **23**(2), 1–6. DOI: 10.37575/b/sci/220007

1. Introduction

Coral reef ecosystems thrive in tropical waters of the Pacific, Indian and Caribbean oceans (Pandolfi *et al.*, 2003). Coral reefs are considered a natural barrier system against marine floods caused by high-energy wave events such as tsunamis and storms (Kunkel *et al.*, 2006; Beck *et al.*, 2018). Complex hydrodynamic processes including wave reflection, refraction and breaking occur near and over coral reefs. Reef structure morphology, flow depth over the reef, reef width and coral surface roughness are some of the important parameters that help to assess wave energy reduction (Brander, 2004). Other parameters, such as the location of the coral reef relative to wave source, coral health and coral continuum, also influence the performance of the coral reef in wave energy reduction (Cochard *et al.*, 2008). The effect of coral reefs on wave energy mitigation reduces where the reefs are located close to the shoreline or where the wave heights and wave lengths are considerably large (Kunkel *et al.*, 2006). Waves propagating over a coral reef surface undergo a complex transformation, mainly because of rapid change in water depth, irregularities of reef geometry, and variability in surface roughness conditions (Brander, 2004), which creates a complex hydrodynamic environment (Philpott, 2016). Due to changes in ocean bathymetry, waves shoal, reflect, refract and break while propagating over the reef structure (Hardy *et al.*, 1990). Reef flats have surface roughness due to the presence of coral growth and the continual sedimentation process by biological and wave depositional processes (Flood, 2011). The surface roughness of coral varies considerably with types of coral since coral formation and growth are influenced by biological and morphological processes (Gourlay, 1996). Corals branch out in the presence of sunlight (Chappell, 1980), and slow-growing globular coral structures are observed where the light availability is limited. Conversely, hydrodynamic stresses have adverse effects on the coral morphology (Chappell, 1980), especially on branching corals such as staghorn corals, which are dislodged and damaged due to wave forces (Harmelin-Vivien, 1994). However, the globular corals can withstand damaging wave forces without being severely affected (Chappell, 1980). These constant changes in coral structure influence the overall roughness. In their study, Madin and Connolly (2006) provided a general framework for understanding and predicting the effects of hydrodynamic disturbances on coral reef communities with the coefficient of drag. Undoubtedly, these findings provide an insight into reef hydrodynamics; however, there is still a lack of fundamental studies such as numerical analysis and controlled experimental investigations to demonstrate the mechanism of wave energy dissipation over coral reefs. Such studies could also provide a better understanding of the role of coral reefs in the mitigation of marine floods. This study aimed to elucidate the effect of the roughness of coral reefs on mitigating marine floods in numerical modelling. A one-dimensional depth-integrated numerical model was developed to simulate the long-period marine flood propagation under the effect of coral reef roughness. The numerical results were analysed to report the effect of coral reefs' roughness on the reduction of wave height and wave force behind the reef and at the shoreline against the incident wave characteristics, and the effect of bed slope.

2. Material and Methods

2.1. Governing Equations

A depth-integrated modelling approach was used to simulate marine flood propagation by long-period waves. The governing laws were the conservation of mass and momentum (Kowalik, 2012). The representative forms of those laws are given as:

Continuity equation

$$\frac{\partial \xi}{\partial t}+\frac{\partial Q}{\partial x}=0 \tag{1}$$

Corresponding Author: N.A.K Nandasena 00966525304576, n.nandasena@uaeu.ac.ae

Momentum equation

$$\frac{\partial Q}{\partial t}+\frac{\partial\left(\frac{Q^2}{h}\right)}{\partial x}+gh\frac{\partial \xi}{\partial x}+\frac{\tau}{\rho}=0 \tag{2}$$

where ξ is the sea surface elevation, t the time, x the longitudinal co-ordinate, Q the discharge along the x-direction per unit width, h the sea depth, g the gravitational acceleration, τ the bottom shear stress along the x-direction, and ρ the seawater density (Yasuda, 2019). The bottom shear stress can be modelled by Nandasena *et al.* (2008):

$$\tau=\frac{\rho g n^2}{h^{\frac{7}{3}}}Q^2 \tag{3}$$

where n is the bed resistance given in Manning's roughness coefficient.

For seabed roughness without coral, the value of Manning's roughness of 0.025 s/m$^{1/3}$ (Goto *et al.*, 1997) was considered in the model. The coefficient of friction (f) for the coral reef zone in the shallow sea (depth from 30 m to 60 m) ranging between 0.05 m/s and 0.40 m/s and thus the corresponding Manning's roughness (n) ranging between 0.1 s/m$^{1/3}$ and 0.25 s/m$^{1/3}$ (Cialone *et al.*, 2008) were considered in the model. The density of seawater was 1029 kg/m³ in the model (Nandasena *et al.*, 2008).

2.2. Coral Bed Profile

Two bed profiles were considered, namely an idealized profile with a constant bed slope and a profile for Gold Coast, Australia, based on the Great Barrier Reef depth and elevation model (GBRDM). Fig. 1a displays the idealized ocean bed profile, which consisted of a flat ocean floor at a depth of 4,000 m and extending from origin to a horizontal distance of 50 km. The horizontal profile was identified as a linear zone and was the origin of the wave generation (generation boundary). Beyond the linear zone, the bed had an increasing slope with a constant gradient of 1 in 100. Fig. 1b represents the actual bed profile for Gold Coast, Australia. The profile was drawn using the actual bathymetry elevation contours, made available by James Cook University and The Reef and Rainforest Centre Australia as part of their project 3D GBR (Great Barrier Reef): high-resolution depth model for the Great Barrier Reef and the Coral Sea. The bed consisted of a near-horizontal abyssal plain at 4,900 m depth for a distance of about 50 km, beyond which the bathymetry increased from deep ocean to about 200 m depth within a 100 km horizontal distance and at an average gradient of 1 in 20 (5%). Beyond 100 m depth, the bathymetry increased gently, with the slope between 50 m depth and the shoreline being less than 0.5%. The coral zone was defined between depths of 50 m and 25 m to have similar coral width, as in case of the Fig. 1a. A lagoon area, behind the reef, is depicted in Fig. 1b; however, due to the gentle slope of the Gold Coast profile, the extent of the lagoon water was almost three times wider than that in the idealized case (Fig. 1a).

2.3. Model Set-up

A finite difference scheme with a staggering space grid and leap-frog time method was used to solve the governing equations. The discretization sizes were Δx = 10 m and time step Δt = 0.04 s and allowed for non-dispersive wave propagation (Kowalik, 2012). The water depth at the wave generation boundary was at least 4000 m, depicting the marine flood origination in the deep sea. Flood waves were modelled by long-period waves with T_p = 10 min (relatively short), 20 min (moderate) and 40 min (relatively long). The wave height at the generation boundary was set to H_b = 0.5.

Figure 1: Bed profiles for simulation: (a) cross-section of the idealized bed at 1% gradient, (b) cross-section of Gold Coast from GBRDEM. Insets show the location of the coral reef in the bed. The wave generation boundary was at 0 m. 1.0 m, 2.0 m, and 4.0 m. For each bed profile and flood characteristics, three different cases were analysed.

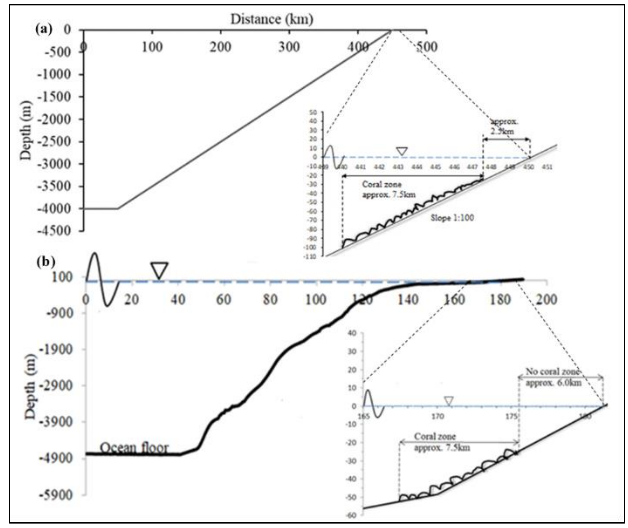

Case 1: seabed without corals – a constant bed roughness of Manning's (n) = 0.025 s/m$^{1/3}$ (Levin and Nosov, 2019).

Case 2: seabed with corals of low resistance – a bed roughness of Manning's (n) = 0.025 s/m$^{1/3}$ for the seabed, and corals with Manning's roughness (n) of 0.1 s/m$^{1/3}$ (Cialone *et al.*, 2008).

Case 3: seabed with corals of high resistance – a bed roughness of Manning's (n) = 0.025 s/m$^{1/3}$ for the seabed, and corals with Manning's roughness (n) of 0.25 s/m$^{1/3}$ (Cialone *et al.*, 2008).

The model predicted the temporal and spatial variation in sea surface elevation (i.e. wave height) and water particle velocity (flow velocity) in the computational domain (Fig. 1). The percentage reduction of wave height and wave force (hydrodynamic force) behind the coral reef and at the shoreline was estimated relative to the no coral case. The following key assumptions were made for the model. The waves were purely sinusoidal and long-period at the wave generation boundary. The flow above the corals and the flow through the corals were not considered separately (i.e. the two-layer flow was not considered). The energy dissipation of waves was only caused by the roughness of the corals and seabed. The length of the coral reef was infinitely long parallel to the shoreline. The coral reef was considered parallel to the shoreline and perpendicular to wave propagation. Corals were of uniform roughness, and this was modelled by Manning's roughness coefficient.

3. Results

The effect of coral roughness on mitigating marine floods was assessed by calculating the percentage reduction in wave height at the end of the coral zone (i.e. at 25 m sea depth behind the reef) and at the shoreline compared with the no coral condition. Wave energy is proportional to the square of the wave height (Sorensen, 2006); therefore, the assessment of the wave height at the end of the coral zone determines the effect of coral roughness on flood energy reduction. Fig. 2 displays the temporal variation in the sea surface behind the reef for the wave characteristics and coral roughness on the idealized bed profile.

Figure 2: Temporal variation in sea surface elevation behind the reef on the idealized bed profile (Fig. 1a). (a) H_b = 0.5 m and T_p = 10 min, (b) H_b = 4 m and T_p = 10 min, and (c) H_b = 4 m and T_p = 40 min. The red line shows the case without coral, and the blue and black lines show the cases of Manning's roughness of 0.1 and 0.25, respectively.

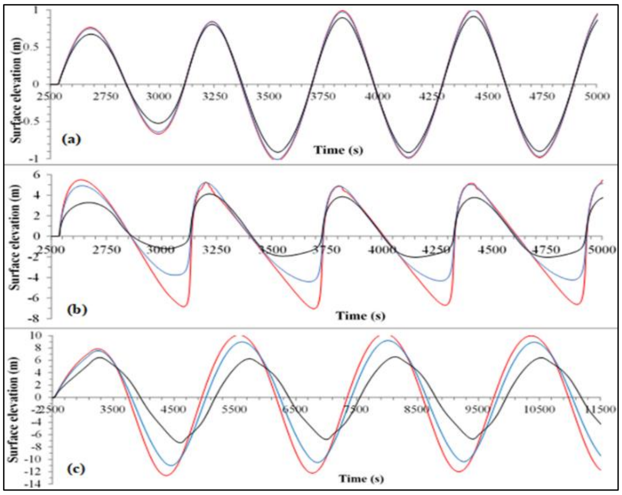

When the roughness of the reef increased, the fluctuation of the sea surface decreased. But it was not significant for marine floods with a small wave height and a relatively shorter wave period (Fig. 2a). The roughness effect of the sea bed and coral increased when the sea depth decreased (Eq. 3). Therefore, theoretically, the effect of coral roughness on wave trough is significant. In this study, this effect was evident for larger waves despite their wave period (Fig. 2b–c). For small waves, it was not significant, as the temporal change in the sea depth caused by the fluctuation of the sea surface was minimal (Fig. 2a). Wave deformation was increased when wave height increased. With the travel distance, the sinusoidal shape of the waves changed for the high waves with a relatively shorter wave period (Fig. 2b). When the high waves with a relatively longer wave period moved over the coral reef with higher roughness, they were subjected to phase lag (Fig. 2c). This indicated that marine floods with a longer period can be slowed by higher coral roughness. Fig. 3 shows the temporal variation in the sea surface behind the reef for the wave characteristics and coral roughness on the Gold Coast bed profile.

Figure 3: Temporal variation in sea surface elevation behind the reef on the Gold Coast bed profile (Fig. 1b). (a) H_b = 0.5 m and T_p = 10 min at the generation boundary, and (b) H_b = 4 m and T_p = 40 min. The red line shows the case without coral, and the blue and black lines show the cases of Manning's roughness of 0.1 and 0.25, respectively.

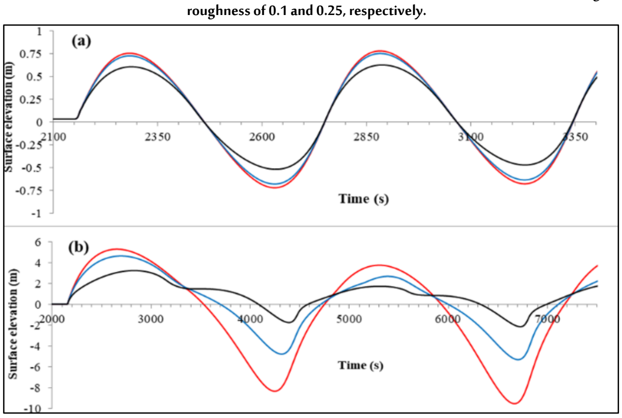

The bed profile has a convex shape compared to the idealized bed (Fig. 1a). The effect of the sea bed was significant; therefore, a flatter wave crest and steeper wave trough were observed for the high waves with a relatively longer wave period (Fig. 3b). The reef has a relatively shallow sea depth compared to that of the idealized bed (Fig. 1a); this resulted in a significant reduction in wave height behind the reef (Fig. 3). These observations confirmed that wave characteristics of the marine flood, coral roughness, and shape of the sea bed are key to controlling the mitigation of marine floods. The effect of coral roughness on mitigating the marine flood on the idealized bed is displayed in Fig. 4 and Fig. 5.

Figure 4: Marine flood mitigation potential of the coral reef on the idealized bed profile (Fig. 1a) with wave height. (a, b, and c) wave height reduction behind the reef and (d, e, and f) wave height reduction at the shoreline compared to the case without reef. The thick and dotted lines show the results for Manning's roughness of 0.25 and 0.1, respectively. H_b and T_p are the wave height and wave period at the generation boundary, respectively.

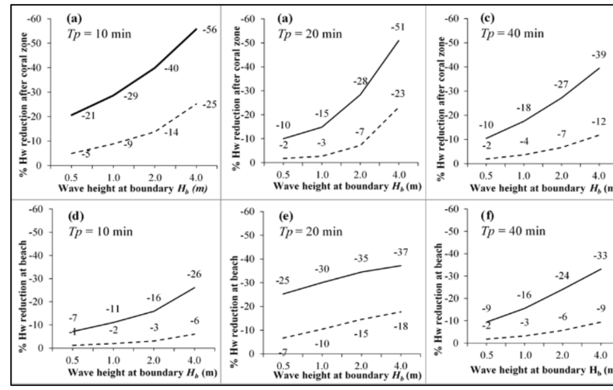

Figure 5: Marine flood mitigation potential of the coral reef on the idealized bed profile (Fig. 1a) with wave period. (a, b, and c) wave height reduction behind the reef and (d, e, and f) wave height reduction at the shore compared to the case without reef. Thick and dotted lines show the results for Manning's roughness of 0.25 and 0.1, respectively. H_b and T_p are the wave height and wave period at the generation boundary, respectively.

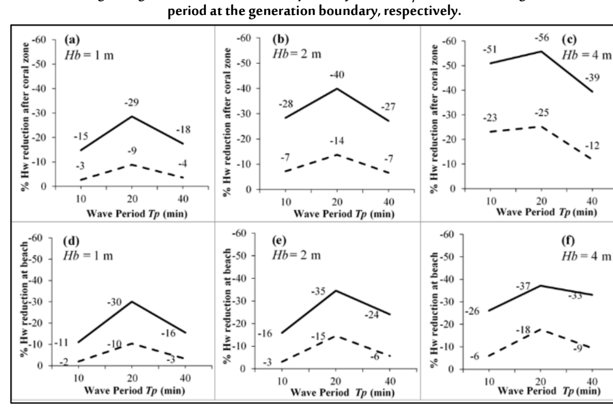

Regardless of the wave period, the coral reef reduced the wave height behind the reef and at the shoreline with the magnitude of the marine flood (Fig. 4). When the roughness was increased twofold, the reduction in wave height was increased from 2.2 times to as high as five times behind the reef for the cases studied. The reduction in the wave height at the shoreline was smaller compared to that behind the reef since the bed roughness from the reef end to the shoreline was not higher than that from the reef. The relationship between the wave period and the effect of coral roughness on mitigating the marine flood was complex (Fig. 5). When the wave period increased from 10 min to 20 min, the reduction in wave height increased, whereas during the wave period from 20 min to 40 min, the reduction in wave height decreased (Fig. 5). Despite the wave height, the marine flood with a wave period of 20 min was largely mitigated by the coral reef on the idealized bed (Fig. 1a). Table 1 shows the effect of coral roughness on mitigating the marine flood on the Gold Coast bed. The percentage reduction in wave height was similar to the case of the idealized bed (Fig. 4).

Table 1: Marine flood mitigation potential of the coral reef on the Gold Coast bed profile (Fig. 1b). Wave height reduction behind the reef and at the shoreline compared to the case without reef. H_b and T_p are the wave height and wave period at the generation boundary, respectively.

	Wave height reduction %					
	The roughness of corals (Manning's roughness coefficient = 0.1)					
H_b (m)	Behind the coral zone			At the shore		
	T_p = 10 min	T_p = 20 min	T_p = 40 min	T_p = 10 min	T_p = 20 min	T_p = 40 min
0.5	4	4	7	2	3	11
1.0	8	6	12	4	5	16
2.0	16	13	20	7	7	21
4.0	28	26	33	10	10	22
	The roughness of corals (Manning's roughness coefficient = 0.25)					
H_b (m)	Behind the coral zone			At the shore		
	T_p = 10 min	T_p = 20 min	T_p = 40 min	T_p = 10 min	T_p = 20 min	T_p = 40 min
0.5	16	18	26	4	11	32
1.0	33	26	36	20	16	36
2.0	51	37	49	28	24	40
4.0	65	57	64	36	35	43

When the wave height increased, the percentage reduction in wave height behind the reef and at the shoreline increased. The reduction in wave height was greater behind the reef than at the shoreline. When the wave period increased from 10 min to 20 min, the reduction in wave height decreased, whereas when the wave period increased from 20 to 40 min, the reduction in wave height increased. This is contrary to the case of the idealized bed. The maximum efficiency of corals on the idealized bed in mitigating the marine floods was with a wave period of 20 min (Fig. 5), but the efficiency was minimum for the same coral on the Gold Coast bed. This indicates that the relationship between the wave period and the bed slope is not simple like the wave height and bed slope when assessing the mitigation potential of coral reefs. Wave energy reduction is mainly determined by the effect of coral roughness and waves shoaling in this study. The roughness effect from corals is determined by water particle velocity (Eq. 3), which is a function of wave height and wave period. When the wave period increases, water particle velocity first increases and then decreases for the ideal bathymetry. However, this phenomenon is challenged by the shoaling effect of the Gold Coast bed due to its complexity. Therefore, we need experimental and field data to confirm the results. Table 2 shows the reduction in the force of the marine floods by the coral reef.

Table 2: Mitigation potential of the coral reef on the idealized and Gold Coast bed profiles (Fig. 1). H_b and T_p are the wave height and wave period at the generation boundary, respectively. Note that the force is calculated as the multiplication of the density of seawater, flow depth (= still sea depth + water surface elevation), and the square of water particle velocity (Nandasena *et al.*, 2008).

Force reduction behind the coral reef %						
	The roughness of corals (Manning's roughness coefficient $n = 0.1$)					
H_b (m)	Coral reef on the idealized bed			Coral reef on the Gold Coast bed		
	$T_p = 10$ min	$T_p = 20$ min	$T_p = 40$ min	$T_p = 10$ min	$T_p = 20$ min	$T_p = 40$ min
0.5	4	13	5	8	7	22
1.0	9	22	9	18	13	33
2.0	18	34	17	30	21	45
4.0	17	44	25	43	45	56
	The roughness of corals (Manning's roughness coefficient $n = 0.25$)					
H_b (m)	Coral reef on the idealized bed			Coral reef on the Gold Coast bed		
	$T_p = 10$ min	$T_p = 20$ min	$T_p = 40$ min	$T_p = 10$ min	$T_p = 20$ min	$T_p = 40$ min
0.5	22	51	25	38	35	63
1.0	39	66	40	61	51	75
2.0	59	78	56	76	66	83
4.0	77	85	69	91	82	88

The marine flood force is calculated as the multiplication of density of seawater, flow depth (= still sea depth + water surface elevation), and the square of water particle velocity (Nandasena *et al.*, 2008). When the wave height increased, the percentage reduction in the force increased. Regardless of the wave period, the percentage reduction in the force was greater than the reduction in wave height behind the reef. No significant difference in the reduction of the force was observed between the idealized and Gold Coast profiles. For the idealized bed, the maximum reduction of the force was achieved for the case with the waves of $H_b = 4$ m and $T_p = 20$ min, whereas for the Gold Coast bed, it was the case with waves of $H_b = 4$ m and $T_p = 10$ min.

4. Discussion

Coastal areas are subject to more frequent extreme flooding caused by tsunamis and big storms because of sea level rises due to global warming (Rovere *et al.*, 2017). Submarine barriers such as coral reefs can play a significant role to dissipate the flow of energy, thereby reducing potential damage to the coastline. The quantitative meta-analysis conducted by Ferrario *et al.* (2014) indicated that coral reefs in the Indian, Pacific and Atlantic Oceans dissipate 97% of the wave energy that would otherwise impact shorelines. Fernando *et al.* (2005) found a strong correlation between the water inundation and the extent of the coral and rock reef cover with a visible reduction in flow velocity when the tsunami approached the coral reef. Corals cause drastic wave attenuation (as much as 80%–95%) and act as submerged breakwaters (Lugo-Fernández *et al.*, 1994; Frihy *et al.*, 2004). This study also confirmed that the coral reef about 7.5 km long in the wave direction reduced the wave height to 65% and the wave force to 91% if the roughness of the reef was 0.25 s/m$^{1/3}$.

Inundation distance was largely determined by wave height and coastal topography; however, human modification of the reef did not contribute to the magnitude of damage on land (Baird *et al.*, 2005). In a numerical simulation, Kunkel *et al.* (2006) found that a sufficiently wide barrier reef within a metre or two of the surface reduces run-up on land by the order of 50%. They noted that the effectiveness depends on the amplitude and wavelength of the incident tsunami, as well as the geometry and health of the reef and the offshore distance of the reef. Both reflection and frictional dissipation are significant in reducing the energy transmitted over the reef. The broader and shallower the reef, the more protection it provides. This study shows that when the wave height increased, the percentage reduction in both wave height and wave force behind the reef increased. However, when the wave period increased, the reduction in wave height behind the reef first increased and then decreased for the reef on the idealized bed, and this was the opposite on the Gold Coast bed.

Many researchers have attempted to quantify the reef roughness by using numerical assessment and conducting field studies (Nunes and Pawlak, 2008). The rugosity index, the simple indicator for reef roughness, is calculated as $R_i = 1 - D_l/C_l$, where D_l is the direct tape length and C_l is the draped chain length over the reef (Fuad, 2010). A higher rugosity index represents greater coral roughness. Leon *et al.* (2015) explained the digital terrain model technique for surface roughness measurement, which involves using high spatial resolution photography of the reef surface, along with the Lidar and Global Positioning System data. A field study at John Brewer reef included measurement of reef-flat surface undulations and observation of non-linear oscillatory wave propagation over the reef flat. The study showed that the hydraulic reef roughness ranged between 0.04 m and 0.1 m. The flow resistance provided by the corals is due to their density and bonding with the platform (Massel, 2013). A study conducted by Lugo-Fernández *et al.* (1998) indicated that the wave attenuation characteristics for any reef depend on the reef morphology, such as reef geometry, coral alignments, and bottom friction. The reef morphology changes continually with extreme wave impacts, and therefore using a typical surface drag coefficient for all reefs would not be precise (Lugo-Fernández *et al.*, 1998). At scales of 1 m to 10 m, the most obvious physical feature of coral reefs is that they are remarkably rough, having bottom drag coefficients that are typically ten times larger (or more) than the typical value of 0.0025 found for muddy or sandy sea beds (Lugo-Fernández *et al.*, 1998). However, a numerical model study based on including the steady-state finite difference model indicated that the coefficient of friction (cf) for coral typically ranges between 0.05 m/sec and 0.4 m/sec, which correlates with Manning's roughness (n) of 0.1 s/m$^{1/3}$ and 0.25 s/m$^{1/3}$, respectively (Cialone *et al.*, 2008). In this study, we used the definition of Cialone *et al.* (2008). To the best of our knowledge, an accurate estimation of coral roughness in terms of flow–coral interaction (reef hydrodynamics) is not yet available. Therefore, large-scale experimental studies are needed to explore it.

Model simulation studies for the 2007 Solomon Islands earthquake showed that coral reef in the GBR region attenuated wave amplitude by at least 50% and delayed the tsunami arrival time at the shoreline by 15 min (Cummins, 2008). The roughness is important in determining the effect of the fringing reef on tsunami inundation, and based on sensitivity analysis, smooth reefs are more likely to increase the onshore velocity than rough reefs (Gelfenbaum *et al.*, 2011). The flow velocity impeded by the corals found its way to the land with greater intensity through low resistance paths created by anthropogenic coral removal, much the same way as water jetting through dead vegetation in wetlands (Granata *et al.*, 2001) and shore-normal gaps in coastal vegetation (Thuy *et al.*, 2009). Numerical simulation by Gelfenbaum *et al.* (2011) confirmed that healthy, rough coral reefs that are wide, high and without unnecessary channels offer the greatest protection from destructive tsunamis. In their experiment with a uniform array of rods, Fernando *et al.* (2008) simulated the gap effect in coral reefs. Coral reefs substantially decreased the flow velocity due to the increase in the bottom drag coefficient, which was a strong function of the coral porosity. Increased flow velocity through the gap was observed, which was a strong function of porosity, in addition to a suite of other parameters that accounts for waves, corals, water depth and gap size.

Gawehn *et al.* (2016) classified long-period waves into four different classes: resonant, standing, progressive-growing and progressive-dissipative waves. The results of their study indicated that wave resonance caused prolonged, large-amplitude water surface oscillations at the inner reef flat ranging in wave height from 0.14 m to 0.83 m. The waves had non-linear, bore-like wave shapes, which are likely to have a greater impact on the shoreline than regular, sinusoidal waveforms. We reported similar wave shapes at the reef (Fig. 3b); however, corals with high roughness of the Gold Coast bed profile can mitigate wave energy behind the reef by up to 88% with wave period. Reef shape to the characteristics of incident waves is an important factor controlling the hydrodynamic process over the reef platform surfaces (Mandlier and Kench, 2012). Elliptical and circular reefs could create distinctive wave convergence zones while linear platforms do not superimpose reef-flat waves. Our study also found that the mitigation potential of coral reefs is greatly controlled by the bed slope off the reef. Wave height reduction behind the reef was highest for the linear bed profile but lowest for the convex shape bed profile (Gold Coast profile) for the incident waves of 20 min.

The results of this numerical study confirmed that coral has an important role in marine flood reduction, and therefore protection of reef-building corals is important from an engineering perspective. Many researchers have realized the importance of corals and raised concerns regarding coral degeneration due to human developments and climate change. Government institutions and research centres are trying to control the adverse factors affecting coral degeneration and considering innovating and aspiring measures of forming artificial coral reefs by studying the behaviour of corals in a simulator environment. Further work is needed to address the issues of coral degeneration and the revival of reef morphology. Basic numerical and controlled experimental studies are pertinent for elucidating the rationales behind coral reef hydrodynamics that help to understand the mitigation potential of large coral reefs on a real scale.

5. Conclusions

The effect of roughness of coral reefs on mitigating marine floods caused by long-period waves was analysed using one-dimensional numerical simulations. The reduction in wave height and hydrodynamic force behind the coral reef were tested against the magnitude of marine floods subjected to the roughness of coral reefs. The reduction in wave height behind the reef and at the shoreline increases with the magnitude of the marine flood. The effect of wave period is not similar to the effect of wave height when assessing the mitigation potential of coral reefs on the sea bed. However, the marine floods caused by longer period waves can be slowed by higher coral roughness compared to the floods caused by shorter period waves. Despite the wave period, the reduction in wave force is greater than the reduction in wave height behind the reef. This study is limited in its scope and only provides long-wave behaviour over coral reefs for selective profiles and coral roughness in a one-dimensional numerical simulation. Further assessments are required to consider two-dimensional changes in bathymetry, wave breaking, and spatial change in coral roughness over the reef, non-uniformity of coral reef in sea depth, and wave hydrodynamics through the porous coral colonies.

Biographies

N.A.K. Nandasena

Civil and Environmental Engineering Department, United Arab Emirates University, Al Ain, United Arab Emirates, n.nandasena@uaeu.ac.ae, 00966525304576

Dr Nandasena, who is Sri Lankan, obtained a PhD in Civil and Environmental Engineering from Saitama University. He was a postdoctoral fellow of the Japan Society for the Promotion of Science. His research focus is high-energy coastal disasters, and he is known as a leading researcher in the field of boulder transport by tsunamis. He is a member of Inundation Signatures on Rocky Coastlines, National Science Foundation-funded Research Coordination Network, in the USA. He conducted field surveys in Japan after the 2011 Great East Japan tsunami.

Irshaad Chawdhary

Auckland Council, Henderson, New Zealand, irshaad.chawdhary@aucklandcouncil.govt.nz , 006493010101

Mr Chawdhary, who is Indian, is a Senior Development Engineer at Auckland Council based in Auckland, New Zealand. He obtained a master's degree in Civil and Environmental Engineering from the University of Auckland. He is interested in the concept of ecosystem-based disaster risk reduction and testing the capability of coral reefs to mitigate high-energy wave events. He is also involved in various domestic and international projects on parks, transportation, water services, and other typical city government services. He is a member of the New Zealand (NZ) Coastal Society and Engineers NZ.

Acknowledgements

This research was funded by the Start-up Grant Scheme – G00003262.

References

Baird, A.H., Campbell, S.J., Anggoro, A.W., Ardiwijaya, R.L., Fadli, N., Herdiana, Y., Kartawijaya, T., Mahyiddin, D., Mukminin, A., Pardede, S.T., Pratchett, M.S., Rudi, E. and Siregar, A.M. (2005). Acehnese reefs in the wake of the Asian tsunami. *Current Biology*, **15**(21), 1926–30.

Beck, M.W., Losada, I.J., Menéndez, P., Reguero, B.G., Díaz-Simal, P. and Fernández, F. (2018). The global flood protection savings provided by coral reefs. *Nature Communications*, **9**(1), 2186.

Brander, R.W. (2004). Spatial and temporal variations in wave characteristics across a reef platform, warraber Island, Torres Strait, Australia. *Marine Geology*, **207**(1), 169–84.

Chappell, J. (1980). Coral morphology diversity and reef growth. *Nature*, **286**(5770), 249–52.

Cialone, M.A., Brown, M.E., Smith, J.M. and Hathaway, K.K. (2008). *Southeast Oahu Coastal Hydrodynamic Modeling with ADCIRC and STWAVE*. Coastal and Hydraulics Laboratory, Vicksburg, MS: U.S. Army Corps of Engineer.

Cochard, R., Ranamukhaarachchi, S., Shivakoti, G.P., Shipin, O.V., Edwards, P.J. and Seeland, K.T. (2008). The 2004 tsunami in aceh and Southern Thailand: A review on coastal ecosystems, wave hazards and vulnerability. *Perspectives in Plant Ecology, Evolution and Systematics*, **10**(1), 3–40.

Cummins, P.R., Kong, L.S. and Satake, K. (2008). Introduction to "Tsunami science four years after the 2004 Indian Ocean tsunami, part i: modelling and hazard assessment". *Pure and Applied Geophysics*, **165**, (n/a), 1983–9.

Ferrario, F., Beck, M.W., Storlazzi, C.D., Micheli, F., Shepard, C.C. and Airoldi, L. (2014). The effectiveness of coral reefs for coastal hazard risk reduction and adaptation. *Nature Communications*, **5**(3794), 1–9.

Fernando, H.J.S., McCulley, J.L., Mendis, S.G., and Perera, K. (2005). Coral poaching worsens tsunami destruction in Sri Lanka. *Eos Trans. AGU*, **86**(33), 301–4.

Fernando, H.J.S., Samarawickrama, S.P., Balasubramanian, S., Hettiarachchi, S.S.L. and Voropayev, S. (2008). Effects of porous barriers such as coral reefs on coastal wave propagation. *Journal of Hydro-environment Research*, **1**(3-4), 187–94.

Flood, P. (2011). *Reefal Sediments*. Encyclopedia of Modern Coral Reefs – Structure, Form and Process. Netherlands: Springer.

Frihy, O.E., El Ganaini, M.A., El Sayed, W.R. and Iskander, M.M. (2004). The role of fringing coral reef in beach protection of Hurghada, Gulf of Suez, Red Sea of Egypt. *Ecological Engineering*, **22**(1), 17–25.

Fuad, M.A. (2010). *Coral reef Rugosity and Coral Biodiversity*. Master's Dissertation, International Institute for Geo-Information Science and Earth Observation, Enschede, Netherland.

Gelfenbaum, G., Apotsos, A., Stevens, A.W. and Jaffe, B. (2011). Effects of fringing reefs on tsunami inundation: American Samoa. *Earth Science Review*, **107**(1-2), 12–22.

Gourlay, M.R. (1996). Wave set-up on coral reefs. 2. Set-up on reefs with various profiles. *Coastal Engineering*, **28**(1-4), 17–55.

Goto, C., Ogawa, Y., Shuto, N. and Imamura, F. (1997). *Numerical Method of Tsunami Simulation with the Leap-Frog Scheme*. IUGG/IOC Time Project: Intergovernmental Oceanographic Commission of UNESCO. Paris: Manuals and Guides, 35.

Granata, T., Serra, T., Colomer, J., Casamitjana, X., Duarte, C. and Gacia, E. (2001). Flow and particle distribution in a nearshore seagrass meadow before and after a storm. *Marine Ecology-progress Series*, **218**, (n/a), 95–106.

Gawehn, M., van Dongeren, A., van Rooijen, A., Storlazzi, C.D., Cheriton, O.M. and Reniers, A. (2016). Identification and classification of very low frequency waves on a coral reef flat. *Journal of Geophysical Research: Oceans*, **121**(10), 7560–74.

Hardy, T.A., Young, I.R., Nelson, R.C. and Gourlay, M.R. (1990). Wave attenuation on an offshore coral reef. In: *Coastal Engineering Proceedings*, 1(22).

Harmelin-Vivien, M.L. (1994). The effects of storms and cyclones on coral reefs: A review. *Journal of Coastal Research*, **12**(n/a), 211–31.

Kowalik, Z. (2012). *Introduction to Numerical Modeling of Tsunami Waves. Institute of Marine Science*. Fairbanks: University of Alaska.

Kunkel, C.M., Hallberg, R.W. and Oppenheimer, M. (2006). Coral reefs reduce tsunami impact in model simulations. *Geophysical Research Letters*, **33**(L23612), 1– 4.

Levin, B.W. and Nosov, M. (2009). *Physics of Tsunamis*. Switzerland: Springer International Publishing.

Leon, J.X., Roelfsema, C.M., Saunders, M.I. and Phinn, S.R. (2015). Measuring coral reef terrain roughness using 'Structure-from-Motion' close-range photogrammetry. *Geomorphology*, **242**(n/a) 21–28.

Lugo-Fernández, A., Hernandez-Avila, M.L. and Roberts, H.H. (1994). Wave-energy distribution and hurricane effects on Margarita Reef, southwestern Puerto Rico. *Coral Reefs*, **13**(1), 21–32.

Lugo-Fernández, A., Roberts, H.H. and Wiseman, W.J. (1998). Water level and currents of tidal and infragravity periods at Tague Reef, St. Croix (USVI), *Coral Reefs*, **17**(4), 343–9.

Massel, S.R. (2013). *Ocean Surface Waves - Their Physics and Prediction*. Poland: World Scientific Publishing.

Madin, J., and Connolly, S. (2006). Ecological consequences of major hydrodynamic disturbances on coral reefs. *Nature*, **444**(n/a), 477–80.

Mandlier, P.G., and Kench, P.S. (2012). Analytical modelling of wave refraction and convergence on coral reef platforms: Implications for island formation and stability. *Geomorphology*, **150–160**(n/a), 84–92.

Nandasena, N.A.K., Tanaka, N., and Tanimoto, K. (2008). Tsunami current inundation of ground with coastal vegetation effects: an initial step towards a natural solution for tsunami amelioration. *Journal of Earthquake and Tsunami*, **2**(2), 157–171.

Nunes, V., and Pawlak, G. (2008). Observations of bed roughness of a coral reef. *Journal of Coastal Research*, **24**(sp2), 39–50.

Pandolfi, J.M., Bradbury, R.H., Sala, E., Hughes, T.P., Bjorndal, K.A., Cooke, R.C., McArdle, D., McClenachan, L., Newman, M.J.H., Paredes, G., Warner, R.R., and Jackson, J.B.C. (2003). Global trajectories of the long-term decline of coral reef ecosystems. *Science*, **301**(5635), 955–8.

Philpott, O. (2016). *The Effects of Reef Surface Roughness on Wave Process: Fatato, Funafuti, Atoll, Tuvalu*. Master's Dissertation, University of Auckland, Auckland, New Zealand.

Rovere, A., Casella, E., Harris, D.L., Lorscheid, T., Nandasena, N.A.K., Dyer, B., Sandstrom, M.R., Stocchi, P., D'Andrea, W.J., Raymo, M.E. (2017). Giant boulders and Last Interglacial storm intensity in the North Atlantic, *Proceedings of the National Academy of Sciences*, **114** (46), 12144–9.

Sorensen, R. M. (2006). *Basic Coastal Engineering*. New York, USA: Springer.

Thuy, N.B., Tanimoto, K., Tanaka, N., Harada, K., and Iimura, K. (2009). Effect of open gap in coastal forest on tsunami run-up––investigations by experiment and numerical simulation. *Ocean Engineering*, **36**(15–16), 1258–69.

Yasuda, H. (2009). One-Dimensional Study on Propagation of Tsunami Wave in River Channels. *Journal of Hydraulic Engineering*, **136**(2), 93–105.

The Scientific Journal of King Faisal University

Basic and Applied Sciences

Reactivity Indices for the Coronene Nanocrystals and Their Derivatives: Modeling Approach

Abdelkareem Almeshal

Department of Physics, College of Science and Arts in Al-Mithnab, Qassim University, Al-Mithna, Saudi Arabia

LINK	RECEIVED	ACCEPTED	PUBLISHED ONLINE	ASSIGNED TO AN ISSUE
https://doi.org/10.37575/b/sci/220011	08/03/2022	04/09/2022	04/09/2022	01/12/2022
NO. OF WORDS	**NO. OF PAGES**	**YEAR**	**VOLUME**	**ISSUE**
3690	5	2022	23	2

ABSTRACT

The modeling approach was applied for the study of the reactivity of pristine and the substitution and absorption of doped coronene nanocrystals with nitrogen and boron under different cases. The reactivity indices of doped coronene molecules were investigated by adopting the Density Function Theory (DFT) code under the SIESTA and Hückel method schemes, which were performed using WebMO. We calculated reactivity indices that were placed into an orbital molecular frame. The results showed that the replacement and absorption of the effects of the doped coronene molecule with nitrogen increased the reactivity of the coronene nanocrystals. The pure coronene molecule is the molecule that has the largest energy gap. The hardness value of doped coronene substituted with a nitrogen atom decreases. The magnitude of chemical potential and electrophilicity for doped coronene with a nitrogen molecule has higher values than all compound cases studied. Moreover, the reactivity indices for the para position are low, so the compound will be less stable and highly reactive compared to the other positions. Therefore, substitution and absorption of doped coronene nanocrystals with nitrogen, and also the para position for doping with nitrogen and boron cases, will be a candidate for studying reactivity in the future.

KEYWORDS

Chemical potential; coronene nanocrystals and their derivatives; electrophilic; energy gap; hardness; modeling approach

CITATION

Almeshal, A. (2022). Reactivity indices for the coronene nanocrystals and their derivatives: Modeling approach. *The Scientific Journal of King Faisal University: Basic and Applied Sciences*, **23**(2), 7–11. DOI: 10.37575/b/sci/220011

1. Introduction

In recent years, the attention given to organic crystals has increased due to their low heaviness and price tag, which can be shown by substituting transition raw material oxides within large amounts of available carbon-based crystals (Devi *et al.*, 2020; Lee *et al.*, 2018; Mauger *et al.,* 2019; Vadehra *et al.,* 2014; Zhu *et al.,* 2018). Graphene-based materials are at present widely valued for their possible uses as devices and adsorbents. The electronic properties and reactivity of graphene can be improved by doping with transition metals or heteroatoms. Coronene composites can be employed as small graphene quantum dots (Malček and Cordeiro, 2018). Coronene nanocrystals have been used in the creation of graphene (Kato *et al.,* 2021; Saha and Bhattacharyya, 2018). The properties of pure coronene and its boron nitride substitution were considered (Dosso *et al.,* 2020; Kurita, 2000; Vessally *et al.,* 2017). Lithium as a dopant has already been reported to reduce the stability of coronene more than three times (Forozmand and Biglari, 2021). The substitution and absorption of doped coronene nanocrystals with nitrogen are of interest in scientific circles concerning their use in the field of nanomaterial science, biosensors, environmental pollution remediation, drug delivery, and several other areas (Kato *et al.,* 2021).

Molecular modeling is the best-developed field to simulate any molecule or system to recognize and predict its behavior. It has further uses in engineering and material sciences, including nanoscience materials and electronics, which cover numerous areas of investigation dealing with things that are scaled in nanometers and that are expected to change the manufacturing sector in the coming decades (Müller and Gubbins, 1998; MacDonell and Schuurman, 2018; Cygan, 2001; Mekky, 2020). Computational software has proven to be an important exploratory tool, and our plan is to bring this technology to the classroom and apply it to examining the doping of nitrogen and boron into carbon compounds (Amin and Deraz 2000; Petrushenko, 2019; Zhu *et al.,* 2018).

The examination of the adsorption actions of the graphene, fullerene, carbon, and coronene ring complexes' theoretical composites can provide important data about their reactivity and electronic and structural tracts (Almuqrin *et al.,* 2021; Wiśniewski and Gauden, 2009).

The reactivity descriptors widely used by computational scientists contain the highest occupied molecular orbital (HOMO) energies, global hardness or chemical hardness, electrophilicity, and chemical potential, as shown by Koopmans' formulas (Bassi *et al.,* 2020). A thorough consideration of the stability of a doped system as visualized in the previous studies requires assessing the above descriptors for discovering potential synthetic uses in the future (Belghiti *et al.,* 2016; Bhawsar *et al.,* 2015; Jaufeerally *et al.,* 2013; Mujica-Martínez and Arce, 2010; Qiang *et al.,* 2016; Yadav *et al.,* 2016; Mekky, 2018).

In this paper, we propose that substitution and absorption of doped coronene nanocrystals with nitrogen, as well as the para position for doping with nitrogen and boron cases, will be a candidate for studying reactivity in the future.

2. Methods and Calculations

Calculations were carried out using the Density Function Theory (DFT) in the SIESTA code. It is used to obtain the relaxed geometry of the considered composites, the optimum structural geometry of the fragments shown in Figures 1, 2, and 3 come to be reached up to all forces in general on atoms are lesser than 0.05 V/Ang. Energy with a cutoff of 200 Ry is measured in the SIESTA calculations and to carry out the measurements to examine electronic properties.

Once the inter-atom forces were smaller than 40 me V/A, the systems were measured completely optimized. The last step was to compute the mean-field Hamiltonians of the full junctions after fixing the geometry of the junctions. SIESTA is a self-consistent density functional theory method that uses norm-conserving pseudo-potentials and a linear combination of atomic orbital basis (LCAOB) to execute effective calculations (Soler *et al.,* 2002; Sozykin, 2021).

Corresponding Author: Abdelkareem Almeshal 00966555141402, amshl@qu.edu.sa

WebMO is a web-based interface for computational physics and chemistry packages (Perri and Weber, 2014; Schmidt and Polik, 2021). It allows the user to set up, run, and visualize physical and chemical calculations from a web browser, smartphone, or tablet. It is used to model and study the reactivity parameters of coronene nanocomposites and their derivatives. Substitution and absorption of doped coronene nano molecules by nitrogen and boron (with ortho and meta and para) positions are displayed in Figures 1 and 2. All models involved in this study are presented in Figures 1 and 2.

Figure 1: Structure of (a) pure coronene, substitutional doped coronene with (b) nitrogen, and (c) boron molecules and absorbed (d) nitrogen, and (e) boron molecules inside coronene.

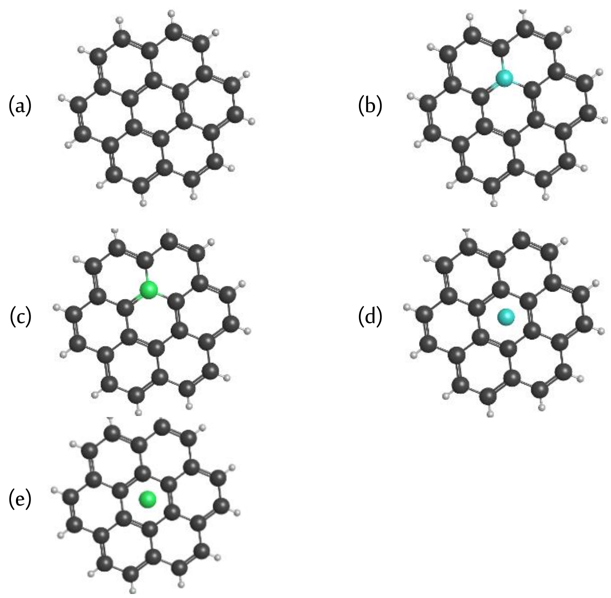

Figure 2: Structure of substitutional doped coronene with nitrogen (a, b, and c), and boron (d, e, and f) molecules at the (ortho & meta & para) positions.

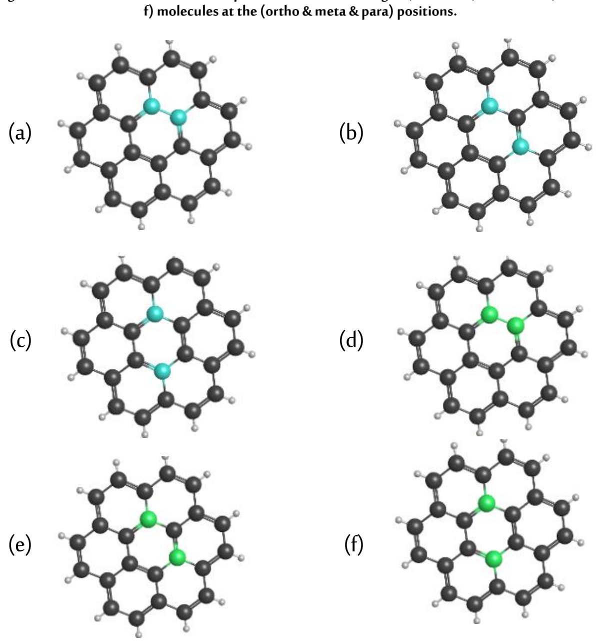

These have been examined by assuming the Hückel method. Merging mechanic cleanups through a Hückel orbital scheming is a rapid approach to optimizing geometry and assessing molecular orbitals devoid of exhausting a computational engine. To show molecular orbitals, WebMO uses the Extended Hückel Theory (EHT) Molecular Orbital method. The Hückel Molecular Orbital (HMO) concept is a very simple theorem for examining both sigma and pi-molecular orbitals of carbon systems.

EHT covers the important components of the molecular orbital principle at a minimum level. Typically, EHT with a very low computational request suggests a qualitatively valuable explanation of the electronic structure of molecules.

The objective of WebMO's EHT execution is computational efficiency.

3. Results and Discussion

Reactivity is the impetus by which material needs to undergo a chemical reaction with an overall flow of energy, either alone or with other substances. The reactivity index is the traditional theoretical quantity used to calculate the relative rate of identical reactions occurring at various positions in a compound or in different compounds.

For the calculations of inclusive identifiers of reactivity, the Lowest Unoccupied Molecular Orbital (LUMO) and HOMO energies are used. The reactivity indices are hardness, energy gap, electrophilicity, and chemical potential, symbolled as η, ΔE, ω, and μ, respectively (Mekky, 2014; Islam *et al.,* 2019) These are determined using the formulas below, based on E_{HOMO} and E_{LUMO}:

$$\Delta E = E_{gap} = (E_{LUMO} - E_{HOMO}) \quad (1)$$

where

$$\mu = (E_{LUMO} + E_{HOMO}) / 2, \quad (2)$$

$$\eta = (E_{LUMO} - E_{HOMO}) / 2, \text{ and} \quad (3)$$

$$\omega = \mu^2/2\,\eta. \quad (4)$$

The doping of nitrogen and boron atoms in coronene is performed to obtain the worked models. For the heterostructure, only in the central ring of coronene, we replace C atoms with B and N. It is worth noting that the purpose of this paper is to examine the replacement and absorption effects of the doped coronene molecule on coronene reactivity indices. The energy gap (E_{LUMO}-E_{HOMO}) is a significant stability index that maintenances telling the reactivity (stability) of the studied molecule. The reactivity is different from the kind with dopants. The substitution of doped coronene by a nitrogen atom has the lowest energy gap, as shown in Figure 3(a). It allows this lower gap to be the softest molecule and more reactive than all the cases studied. The pure coronene molecule is the molecule that has the largest energy gap.

Figure 3: (a) energy gaps, (b) hardness, (c) chemical potential, and (d) electrophilic of coronene and its substituted N and B derivatives.

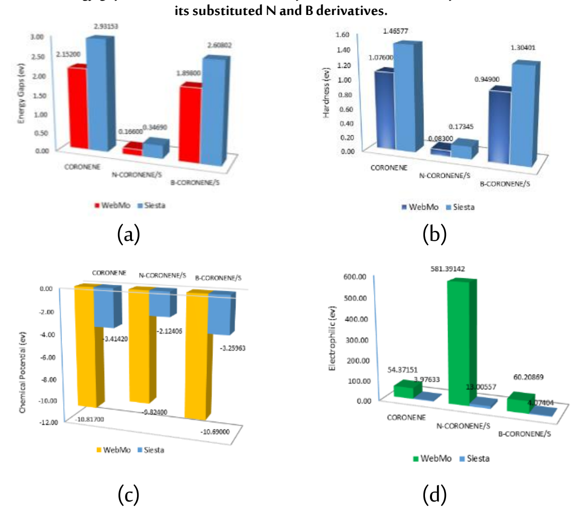

As shown in Figure 3(b), among all other molecules in the study case, the hardness value of doped coronene substitution with the nitrogen atom is lower. Thus, it is observed that coronene doped with nitrogen is more reactive than in other recent cases.

From SIESTA and WebMO simulations, the hardness of the pure coronene molecule is estimated to be 1.47 and 1.08 eV, respectively (Figure 3[b]), and the value decreases due to the replacement of carbon with nitrogen and boron atoms. In the case of nitrogen substitution, the lower value of chemical hardness means that the stability of the studied system decreases, and it will come to be more reactive.

Generally, the chemical potential is defined as the negative of electronegativity, and it describes the trend of gaining electrons in the direction of the molecule. Electrons in general flow from low to high electronegativity areas up to the electronegativity value of the constituent system neutralizes. The magnitude of chemical potential for doped coronene with nitrogen molecules has higher values than all compound cases studied (figure 3[c]) when determined using SIESTA and WebMO calculations.

The coronene compound doped with a nitrogen atom has nearly as high an electrophilicity value as all compound cases studied (Figure 3[d]). The results illustrate the compound that has the slightest energy gap. Therefore, it is polarizable and is associated with a greater chemical reactivity and smaller stability, and it is labeled as a soft molecule.

As shown in Figure 2, we found several possible formations for both the nitrogen and boron atoms occupying the central ring of the coronene model. The two substituent atoms are adjacent at the ortho substitution. If there is one C atom between the two atoms, then it is in the meta substitution, whereas para substitution inserts two C atoms between the two atoms.

The meta and para substitution slightly decreases the energy gaps of N and B of the doped coronene in comparison to the ortho position. Figures 4(a) and 5(a) summarize these effects. This illuminates the dependence of energy gaps on the sites N and B of the doped coronene molecules.

The LUMOs–HOMOs gap explains the reactivity and stability of the composites. At the para position, the energy gap is lower than in the two other positions; the compound at the para position is less stable and more reactive. Correspondingly, the energy gap at the ortho position is large, so the compound will be highly stable and less reactive compared to the other positions.

As shown in Figures 4(b) and 5(b), the nitrogen and boron substitutions lead to a decrease in meta and para position hardness compared with the ortho position hardness. On the other hand, the lowest single value for hardness is the para doped B and N system position. So, the coronene that dopes with nitrogen is the more reactive.

In Figures 4(c) and 5(c), the most chemical-potential molecule value is coronene doped with N and B at the ortho position, but the lowest chemical-potential molecule value in each is at the para position. The more reactive one is the compound structure at the para position.

Assuming SIESTA yields better results, the N and B substitution becomes equally good in terms of reactivity, which is described in Figures 4(a) and 5 (a) by similar ΔE values of 0.225 eV and 0.231 eV.

Figure 4: (a) energy gaps, (b) hardness,(c) chemical potential, and (d) electrophilic of coronene and its substituted N derivatives for (ortho & meta & para) positions.

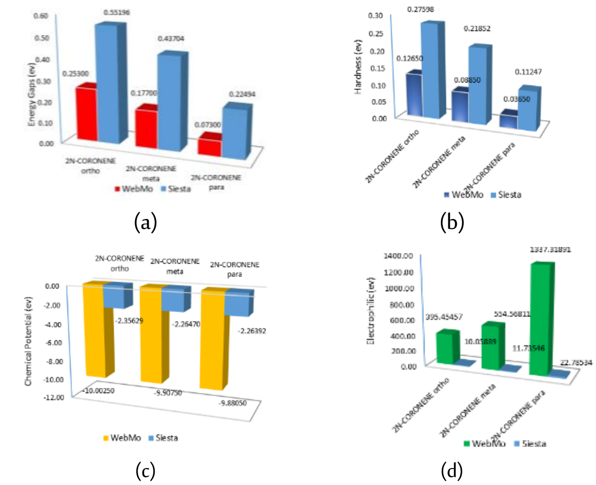

Figure 5: (a) energy gaps, (b) hardness,(c) chemical potential, and (d) electrophilic of coronene and its substituted B derivatives for (ortho & meta & para) positions.

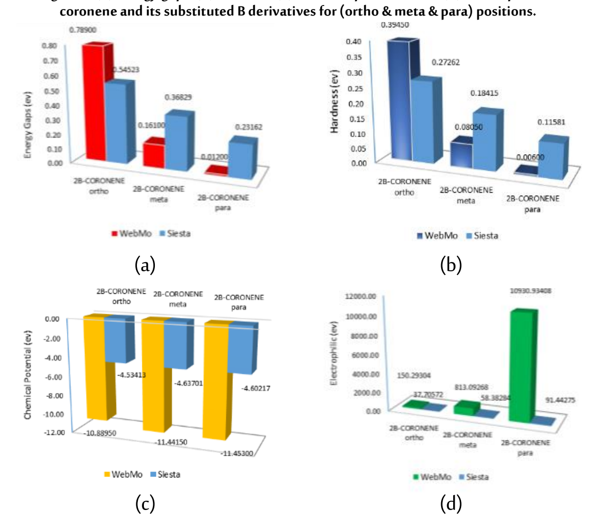

The electrophilicity of the modified coronene rises from ortho to para, which once again confirms the reduction in chemical stability, as shown in Figures 4(d) and 5(d), supporting the theory of optimal electrophilicity. Because the molecule of the para position system becomes less stable than that of the other position systems, this will demonstrate a higher propensity to accumulate extra electronic charges from the surroundings.

As shown earlier in Figures 1 (b) and (c), we identified the hollow absorption sites to demonstrate that the hollow positions are the most favorable for the absorption of nitrogen and boron atoms. Doping with the B atom does not increase the energy gap from Figure 6(a), whereas the addition of the N atom to the molecule's central ring results in a decrease, with the weakest energy gap being lower than pristine coronene, as seen in Figure 6(a). This narrower gap makes it more reactive than in other situations. The largest energy difference is present in the pure coronene compound.

Figure 6: (a) energy gaps, (b) hardness, (c) chemical potential, and (d) electrophilic of coronene and its absorbed N and B molecules inside coronene.

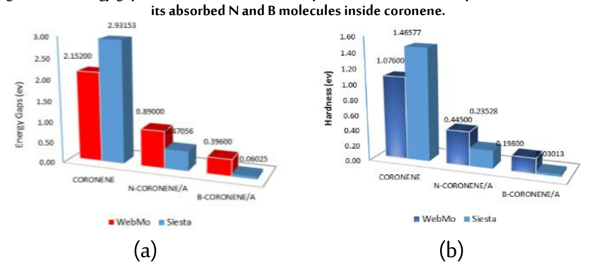

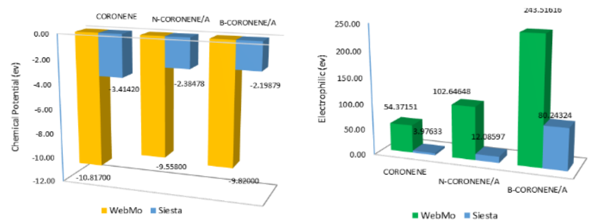

(c) (d)

The most reactive and unstable compound in this sequence, as shown in Figure 6(b), was absorbed by coronene B, and its reactivity was also accompanied by lower hardness values. The most stable compound was the pure coronene compound, which is also confirmed by its elevated hardness values.

The chemical potential of coronene and its absorbed N and B derivatives are shown in Figure 6(c). For pristine coronene, the highest value was observed, and for coronene absorbed B, the lowest value was measured.

It has been observed from Figure 6(d) that the highest electrophilicity index value of the coronene absorbed B molecule is obtained from the considered molecules.

4. Conclusions

A modeling approach is performed using the Density Function Theory (DFT) and the Extended Hückel Theory (EHT) methods to study the reactivity indices for pristine coronene and doped coronene with nitrogen and boron atoms and the position of doping in the molecule. The results obtained for the reactivity indices show that the most reactive study case is the most stable, depending on the values of the energy gap (E_{LUMO}-E_{HOMO}). Assuming SIESTA yields better results, the N and B substitutions become equally good in terms of reactivity. The studies show that doping decreases some of the above reactivity indices significantly while some increase occurs compared to pure coronene, suggesting that one can induce a significant change in doped coronene reactivity with nitrogen and the para position doping.

Biography

Abdelkareem Almeshal

Department of Physics, College of Science and Arts in Al-Mithnab, Qassim University, Al-Mithna, Saudi Arabia, ahm1971123@yahoo.com, amshl@qu.edu.sa, 00966555141402

Dr Almeshal, Saudi, holds a PhD in Solid State Physics (Nanotechnology) from Lancaster University, UK. He is a Saudi Assistant Professor and Dean of the Faculty of Science and Arts in Al-Mithnab. He has published five ISI/Scopus-indexed articles with global publishers (Elsevier, Springer). In addition, he has attended several conferences, including EPSRC Thermoelectric Network (UK); MOLESCO International Workshop on Molecular-Scale Electronics (UK); the International Conference on the Theory of Molecular-Scale Transport (UK); Molecular-Scale Thermoelectricity, Materials, Measurements, and Modelling (UK); the International Conference on Molecular-scale Charge and Thermal Transport (Switzerland); and Some Applications of Solid-State Physics (online–Egypt). Dr Almeshal's special research interests are charge transport, materials, the theory of molecular-scale transport, nanoelectronics, and thermoelectricity. ORCID: 0000-0001-6601-0816.

References

Almuqrin, A.H., Al-Otaibi, J.S., Mary, Y.S. and Mary, Y.S. (2021). DFT computational study towards investigating psychotropic drugs, promazine and trifluoperazine adsorption on graphene, fullerene and carbon cyclic ring nanoclusters. *Spectrochimica Acta - Part A: Molecular and Biomolecular Spectroscopy*, **246**(n/a), 119012. DOI: 10.1016/j.saa.2020.119012

Amin, N.H. and Deraz, N.M. (2000). Decomposition of H_2O_2 on pure and ZnO-treated Co_3O_4 / Al_2O_3 solids. *Technology*, **2**(n/a), 45–58.

Bassi, M.A., Lopez, M.A., Confalone, L., Gaudio, R.M., Lombardo, L. and Lauritano, D. (2020). Applied Koopman operator theory for power systems technology. *Nature*, **388**(n/a), 539–47.

Belghiti, M.E., Karzazi, Y., Dafali, A., Obot, I.B., Ebenso, E.E., Emran, K.M., Bahadur, I., Hammouti, B. and Bentiss, F. (2016). Anti-corrosive properties of 4-amino-3,5-bis(disubstituted)-1,2,4-triazole derivatives on mild steel corrosion in 2 M H_3PO_4 solution: experimental and theoretical studies. *Journal of Molecular Liquids*, **216**(n/a), 874–86. DOI: 10.1016/j.molliq.2015.12.093

Bhawsar, J., Jain, P.K. and Jain, P. (2015). Experimental and computational studies of nicotiana tabacum leaves extract as green corrosion inhibitor for mild steel in acidic medium. *Alexandria Engineering Journal*, **54**(3), 769–75. DOI: 10.1016/j.aej.2015.03.022

Cygan, R.T. (2001). Molecular modeling in mineralogy and geochemistry. *Reviews in Mineralogy and Geochemistry*, **42**(1), 1–35. DOI: 10.2138/rmg.2001.42.1

Devi, N., Ghosh, S.K., Perla, V.K. and Mallick, K. (2020). Organic-inorganic complexation chemistry-mediated synthesis of bismuth-manganese bimetallic oxide for energy storage application. *ACS Omega*, **5**(30), 18693–9. DOI: 10.1021/acsomega.0c01576

Dosso, J., Battisti, T., Ward, B.D., Demitri, N., Hughes, C.E., Williams, P.A., Harris, K.D.M. and Bonifazi, D. (2020). Boron–nitrogen-doped nanographenes: A synthetic tale from borazine precursors. *Chemistry - A European Journal*, **26**(29), 6608–21. DOI: 10.1002/chem.201905794

Forozmand, N. and Biglari, Z. (2021). Influence of lithiation on electro-optical properties of disk-like coronene molecule. *Physica E: Low-Dimensional Systems and Nanostructures*, **134**(n/a). DOI: 10.1016/j.physe.2021.114838

Islam, M.J., Zannat, A., Kumer, A., Sarker, N. and Paul, S. (2019). The prediction and theoretical study for chemical reactivity, thermophysical and biological activity of morpholinium nitrate and nitrite ionic liquid crystals: A DFT study. *Advanced Journal of Chemistry-Section A*, **2**(4), 316–26. DOI: 10.33945/sami/ajca.2019.4.5

Jaufeerally, N.B., Abdallah, H.H. and Ramasami, P. (2013). Novel silanetellones: Structures, ionization potentials, electron affinities, singlet-triplet gaps and Kohn-Sham HOMO-LUMO gaps of the X_2SiTe and XYSiTe (X, Y=H, F, Cl, Br, I and CN) molecules. *Computational and Theoretical Chemistry*, **1016**(n/a), 62–72. DOI: 10.1016/j.comptc.2013.04.010

Kato, M., Masese, T. and Yoshii, K. (2021). Coronene: A high-voltage anion de-insertion cathode for potassium-ion battery. *New Journal of Chemistry*, **45**(11), 4921–4.

Kurita, N. (2000). Molecular orbital calculations on lithium absorption in boron-or nitrogen-substituted disordered carbon. *Carbon*, **38**(1), 65–75. DOI: 10.1016/S0008-6223(99)00100-1

Lee, S., Kwon, G., Ku, K., Yoon, K., Jung, S.K., Lim, H.D. and Kang, K. (2018). Recent progress in organic electrodes for Li and Na rechargeable ratteries. *Advanced Materials*, **30**(42), e1704682. DOI: 10.1002/adma.201704682

MacDonell, R.J. and Schuurman, M.S. (2018). Substituent effects on the nonadiabatic dynamics of ethylene: π-donors and π-acceptors. *Chemical Physics*, **515**(n/a), 360–8. DOI: 10.1016/j.chemphys.2018.09.012

Malček, M. and Cordeiro, M.N.D.S. (2018). A DFT and QTAIM study of the adsorption of organic molecules over the copper-doped coronene and circumcoronene. *Physica E: Low-Dimensional Systems and Nanostructures*, **95**(n/a), 59–70. DOI: 10.1016/j.physe.2017.09.004

Mauger, A., Julien, C., Paolella, A., Armand, M. and Zaghib, K. (2019). Recent progress on organic electrodes materials for rechargeable batteries and supercapacitors. *Materials*, **12**(11), 1770. DOI: 10.3390/ma12111770

Mekky, A.H. (2014). Molecular properties of nanoscale fullerene based systems as a corrosion inhibitors. *Nano Science and Nano Technology*, **8**(12), 482–88.

Mekky, A.H. (2018). Investigation of the influence of Br- and As-doped silica single-wall nanotubes: Hartree–Fock method. *Bulletin of Materials Science*, **41**(6), 164. DOI: 10.1007/s12034-018-1668-1

Mekky, A.H. (2020). Electrical and Optical Simulation of Hybrid Perovskite-Based Solar Cell at Various Electron Transport Materials and Light Intensity. *Annales de Chimie: Science Des Materiaux*, **44** (3), 179–

84. DOI: 10.18280/acsm.440304.

Mujica-Martínez, C.A. and Arce, J.C. (2010). Mini-bandstructure tailoring in pi-conjugated periodic block copolymers using the envelope crystalline-orbital method. *International Journal of Quantum Chemistryonal Journal*, **110**(13), 2532–40. DOI: 10.1002/qua

Müller, E.A. and Gubbins, K.E. (1998). Molecular simulation study of hydrophilic and hydrophobic behavior of activated carbon surfaces. *Carbon*, **36**(10), 1433–8. DOI: 10.1016/S0008-6223(98)00135-3

Perri, M.J. and Weber, S.H. (2014). Web-based job submission interface for the GAMESS computational chemistry program. *Journal of Chemical Education*, **91**(12), 2206–8. DOI: 10.1021/ed5004228.

Petrushenko, I.K. (2019). A DFT study of hydrogen adsorption on h-BN: Boron doping effects. *Journal of Nano- and Electronic Physics*, **11**(2), 1–5. DOI: 10.21272/jnep.11(2).02024

Qiang, Y., Zhang, S., Xu, S. and Li, W. (2016). Experimental and theoretical studies on the corrosion inhibition of copper by two indazole derivatives in 3.0% NaCl solution. *Journal of Colloid and Interface Science*, **472**(n/a), 52–9. DOI: 10.1016/j.jcis.2016.03.023

Saha, B. and Bhattacharyya, P.K. (2018). Density functional study on the adsorption of 5-membered N-heterocycles on B/N/BN-doped graphene: Coronene as a model system. *ACS Omega*, **3**(12), 16753–68. DOI: 10.1021/acsomega.8b02340

Schmidt, J.R. and Polik, W.F. (2021). *WebMO Enterprise*, Version 20.0.012e; WebMO LLC: Holland, MI, USA, 2021. Holland, MI, USA: WebMO LLC. Available at: http://www.webmo.net (accessed on 1/12/2021).

Soler, J.M., Artacho, E., Gale, J.D., García, A., Junquera, J., Ordejón, P. and Sánchez-Portal, D. (2002). The SIESTA method for ab initio order-N materials simulation. *Journal of Physics Condensed Matter*, **14**(11), 2745–79. DOI: 10.1088/0953-8984/14/11/302

Sozykin, S.A. (2021). GUI4dft — A SIESTA oriented GUI. *Computer Physics Communications*, **262**(n/a), 107843. DOI: 10.1016/j.cpc.2021.107843

Vadehra, G.S., Maloney, R.P., Garcia-Garibay, M.A. and Dunn, B. (2014). Naphthalene diimide based materials with adjustable redox potentials: Evaluation for organic lithium-ion batteries. *Chemistry of Materials*, **26**(24), 7151–7. DOI: 10.1021/cm503800r

Vessally, E., Soleimani-Amiri, S., Hosseinian, A., Edjlali, L. and Bekhradnia, A. (2017). A comparative computational study on the BN ring doped nanographenes. *Applied Surface Science*, **396**(n/a), 740–5. DOI: 10.1016/j.apsusc.2016.11.019

Wiśniewski, M. and Gauden, P.A. (2009). The HSAB principle as a means to interpret the reactivity of carbon nanotubes. *Applied Surface Science*, **255**(9), 4782–6. DOI: 10.1016/j.apsusc.2008.11.090

Yadav, M., Gope, L., Kumari, N. and Yadav, P. (2016). Corrosion inhibition performance of pyranopyrazole derivatives for mild steel in HCl solution: Gravimetric, electrochemical and DFT studies. *Journal of Molecular Liquids*, **216**(n/a), 78–86. DOI: 10.1016/j.molliq.2015.12.106.

The Scientific Journal of King Faisal University

Basic and Applied Sciences

Identifying Novel Targetable Chromosomal Alterations in Ovarian Cancer: Using Germline Copy Number Variation Association Analysis

Hanan Mohamed Abd Elmoneim[1, 2], Rehab Kamal Mohammed [2], Reda Fikry Abd El-Meguid [2], Heba Mohammed Tawfik [2], Manal Ismail Abd Elghany [2], Halah Tariq Albar [3], Mohammed Abubakr Mohammed Basalamah [1] and Nisreen Dahi Mohamed Toni [2]

[1] Department of Pathology, Faculty of Medicine, Umm Al-Qura University, Makkah, Saudi Arabia
[2] Department of Pathology, Faculty of Medicine, Minia University, Minia, Egypt
[3] Department of Physiology, Faculty of Medicine, Umm Al-Qura University, Makkah, Saudi Arabia

LINK	RECEIVED	ACCEPTED	PUBLISHED ONLINE	ASSIGNED TO AN ISSUE
https://doi.org/10.37575/b/med/220015	04/04/2022	04/09/2022	04/09/2022	01/12/2022
NO. OF WORDS	**NO. OF PAGES**	**YEAR**	**VOLUME**	**ISSUE**
7729	8	2022	23	2

ABSTRACT

The heterogeneity of ovarian cancer (Ov Ca) is attributed to multiple genetic and epigenetic changes, rendering it difficult to detect the most relevant molecular alterations. Identifying copy number variations (CNVs) will be helpful in screening patients with a familial history and will ultimately facilitate early diagnosis. This work aims to determine germline CNVs that may be associated with risks for different subtypes of ovarian cancer. Using Affymetrix genome-wide human SNP 6.0 arrays, 138 germline DNA samples of non-familial ovarian cancer were analysed using Golden Helix (SVS7) software. CNVs overlapping the EYA2 (20q13.12) and WNK1 (12p13.33) genes are the top hits with a significant p-value (<0.05). Deletion is more frequent in normal and low-grade carcinomas. Commonly, ovarian cancer is copy neutral (CN2) or has copy number gains (CN3). Amplification at these locations is associated with high-grade cases, which have worse overall survival rates. A CN3 in the WNK1 gene is associated with a higher expression of mRNA. It could be concluded that ovarian cancer is associated with CN3s where the segments of DNA overlap WNK1 and EYA2. The oncogenic effect of WNK1 and EYA2 on ovaries may serve as prognostic markers for ovarian cancer.

KEYWORDS
Copy number variations; EYA2; ovarian cancer; WNK1

CITATION
Abd Elmoneim, H.M., Mohammed, R.K., Abd El-Meguid, R.F., Tawfik, H.M., Abd Elghany, M.I., Albar, H.T., Basalamah, M.A.M. and Toni, N.D.M. (2022). Identifying novel targetable chromosomal alterations in ovarian cancer: Using germline copy number variation association analysis. *The Scientific Journal of King Faisal University: Basic and Applied Sciences*, **23**(2), 12–9. DOI: 10.37575/b/med/220015

1. Introduction

Ovarian carcinoma (Ov Ca) is the seventh most common malignancy in women. It is a major public health problem, as there are more than 190,000 new cases of Ov Ca worldwide every year, with multiple etiologic hypotheses for ovarian carcinogenesis. There are neither applicable biomarkers to ascertain early disease nor consistent prognostic markers for predicting clinical response to treatment (Concolino *et al.*, 2018; Siegel *et al.*, 2019; Webb and Jordan, 2017). The heterogeneity of Ov Ca leads to a histopathologic subtype that carries distinct genetic events with complex genomic alterations. Hence, the importance of recognising disease diversity has clinical implications for the strategies of early detection, prevention and treatment (Alexandrova *et al.*, 2020; Kossai *et al.*, 2018).

Copy number variations (CNVs) are duplications or deletions of several kilo-base or more segments of nuclear DNA. CNVs are associated with the risk of developing common diseases, including cancers (Concolino *et al.*, 2018; C. Lee *et al.*, 2007). The recent application of genotyping platforms reliably detects copy number information that serves as another intense basis of genetic variability to outline complex molecular and biochemical interactions within the human genome (C. Lee *et al.*, 2007).

Eyes absent (*EYA*), homologous to the Drosophila eyes absent genes, form a family of genes first identified in Drosophila and other organisms (mice, humans, molluscs, nematodes). *EYA2*, mapped to chromosome 20q13 and *EYA* mutations, are associated with multi-organ birth defects in humans (Zhang *et al.*, 2005). *EYA*s are required for the development of multiple organs and have correspondingly been implicated in multiple disorders. Increasing evidence points to an oncogenic, pro-metastatic and angiogenic function for *EYA*. *EYA2* functions as a transcriptional coactivator to activate a variety of target genes involved in cell cycle progression and differentiation in several tissues (Tadjuidje and Hegde, 2013). Overexpression of *EYA*s occurs in tumorigenesis and metastasis processes by working on the tumour microenvironment to activate tumour cell growth. *EYA2* mRNA is highly expressed in most human cancers, such as ovarian, prostate, lung, breast and urinary tract, while its expression is low in colon cancer (Liu *et al.*, 2019; Tadjuidje and Hegde, 2013).

*WNK*s (with no lysine [K]) express four isoforms belonging to the serine/threonine kinases family of genes (Xu *et al.*, 2000). *WNK* family proteins play an integral role in cell proliferation, differentiation and carcinogenesis (Moniz and Jordan, 2010). *WNK1* is located in Chr12p13.33, and allelic losses in the Chr12p12.2-p13 region that harbours *WNK1* are in breast and ovarian cancers. *WNK1* point mutations are associated with breast, prostate, ovarian, colorectal, lung and thyroid cancers, which confirms its potential role in tumorigenesis and metastasis formation (Kori and Yalcin Arga, 2018; Rodan and Jenny, 2017).

CNVs could play a substantial role in conferring Ov Ca. This study aims to identify germline CNVs that may be associated with risks for different subtypes of Ov Ca. The use of a genome-wide copy number analysis-testing platform would enable the identification of novel and potentially targetable chromosomal alterations of therapeutic significance.

2. Materials and Methods

2.1. Cohort:

The samples consist of 138 germline DNA of non-familial ovarian cancer drawn from a CA-125 screened cohort of individuals with peripheral blood samples from 1996, which was a collaborative work between Harvard Medical School and the Chinese University of Hong Kong. The cohort is composed of ethnically homogeneous women

Corresponding Author: Hanan Mohamed Abd Elmoneim 00966594455902, hmnour@uqu.edu.sa

(Chinese descent) obtained from an ethnically homogeneous population to avoid detection of CNVs related to differences in ethnicity and not to an ovarian cancer genetic signature. The study population is aged 15–94 years (mean=49.8) and presents with different pathological subtypes of Ov Ca. The Ov Ca cases in this cohort are divided into three groups based on age: the smallest group involves cases younger than 21 years (1.5%), the second ranges between 21–45 years (22%) and the most common group consists of patients older than 45 (76.5%). Most of the cases are serous carcinoma subtypes (31.1%), followed by endometrioid carcinoma (20.5%), then clear cell carcinoma (12.9%), while other types represent 34.4%. Overall survival curves in this cohort show that the worst survival rate is the malignant mixed Mullerian tumour (MMMT), followed by adenocarcinomas and serous carcinomas, while maximum survival is detected in clear cell carcinoma and endometrioid carcinoma. Tumour grades are classified into a low grade (63%) and high grade (37%), and the cases comprise stage I (38.5%), stage II (15.4%), stage III (36.9%) and stage IV (9.2%). Normal controls (30 samples) are from an ethnically homogeneous population to avoid the detection of CNVs related to differences in ethnicity and not related to an ovarian cancer genetic signature.

All procedures implemented in this study have been approved by IRB and/or the national research ethics committee in agreement with the 1964 Helsinki Declaration and its later amendments.

2.2. Study Outline:

Affymetrix genome- wide human SNP 6.0 arrays

DNA from 138 Ov Ca cases belonging to different grades, stages and subtypes with Affymetrix genome-wide human SNP 6.0 arrays were analysed using Affymetrix Genotyping Console (GTC) software to generate copy number, loss of heterozygosity (LOH) and segmentation data from the raw intensity values (CEL files). All cases were processed according to the manufacturer's protocol (Affymetrix Santa Clara, CA, USA).

Affymetrix GTC generates copy number and segmentation data using the Birdseed v2 algorithm. Golden Helix software (SVS7) provides advantages in correcting the batch effect as well as detecting the t-wave effect to minimise noisiness and eliminate false-positive results. The software suite also has a module to carry out association analysis. Segmentation algorithms convert the log-ratio data to copy number segments to yield a list of inherited and de novo CNVs on a univariate and multivariate basis. CNVs that did not have a significant p-value for association analysis between cancer and normal groups were excluded. The results provide heat map pictures of multiple genetic loci of lesions associated with Ov Ca and provide avenues for further identification of oncogenes and tumour suppressor genes involved in Ov Ca.

2.3. Copy Number Validation:

TaqMan DNA copy number validation by qPCR

DNA from 138 ovarian cancer cell lines were used for TaqMan quantitative polymerase chain reaction (qPCR; Life Technologies, CA) validation in addition to human and HapMap samples. HapMap cell lines NA10851 and NA12878 (Coriell Institute) were used as references for qPCR validation. DNA was extracted from all cell lines using Puregene DNA Purification Kit (Gentra Systems). Copy Caller software was used to analyse the copy number experiments provided by Applied Biosystems.

The genomic coordinates of the top hits from the Golden Helix analysis were extracted from the association analysis table. The copy number states of the top CNVs were validated using qPCR. TaqMan qPCR was preferred because it has a more reliable primer design, which is more specific and sensitive. Each experiment was repeated three times, using three replicates of the same sample in each run to ensure consistency of results.

2.4. NanoString Validation:

NanoString nCounter analysis techniques (NanoString Technologies, WA) were performed to confirm the results detected by association analysis. NanoString technology was used to further confirm the copy number state of a specific DNA segment that was seen to be significantly associated with serous ovarian cancer.

For NanoString analysis, samples representing different copy number states of two specific CNV segments previously identified by Golden Helix analysis were used. DNA samples from four commercially available cell lines were also included for use in further functional follow-up studies to assess the copy number states in these cell lines. NanoString's workflow has three different primers built into the array to obtain triplicate results for further confirmation.

2.5. RNA qPCR for EYA2 and WNK1 Protein Expression:

We performed quantitative-RT-PCR (qRT-PCR) to test the gene expression among samples with different copy number states to find a relationship between the copy number state and the expression. Total RNA was first extracted from cell lines and reverse transcribed. The cDNA was then used for TaqMan qPCR analysis. Each experiment was repeated three times, using three replicates of the same sample in each run to ensure consistency of results.

SYBR® Green I (Life Technologies, CA) was used to perform real-time PCR with synthesised single-stranded cDNA from RNA extracted from Ov Ca cell lines (A2780, HOSE-636 and OV CAR3& CAOV3). RNA expression analysis was performed for the selected genes (*WNK1* and *EYA2*) to identify their expression amount and to link the expression to the copy number state of each sample. The coordinates of CNV segments that overlapped the genes of interest were detected by Golden Helix software analysis (*WNK1*: coordinates hg19, chr12:867,000-875,750; coordinates hg18, chr12:737,261-746,011 and *EYA2* coordinates hg19, chr20:45,778,000-5,788,000; coordinates hg18, chr20:45,211,407-45,221,407). According to these coordinates, primers were designed to detect the mRNA of the following:

*WNK1*_5' CAGTTGCGACACAACCCTCGGT

*WNK1*_3' TGGGAAGCCCTGGTACAGAACA

*EYA2*_5' AGACCTGGCTACAGCTCCGAGC

*EYA2*_3' ACATTGACACAGTTGGGCCGGGA

The output of the qPCR was analysed to detect the mRNA expression of every sample. The results were compared to the CNV state of the DNA of the same sample for the same segment previously tested by Golden Helix analysis and confirmed by TaqMan qPCR.

2.6. Data Analysis:

The data were analysed with Affymetrix GTC software to generate copy number, LOH and segmentation data from the raw intensity values (CEL files). Analysis was performed on the detected CNV regions using the following statistical tests for CNV association analysis: Correlation/Trend Test, Armitage Trend Test, Exact Form of Armitage Test, (Pearson) Chi-Squared Test, Fisher's Exact Test, Odds Ratio with Confidence Limits, Analysis of Deviance, F-Test, Logistic Regression and Linear Regression.

3. Results

On the one hand, for each histopathological type (irrespective of the stage), some CNVs were shared by all subtypes of Ov Ca. On the other hand, other CNVs specific to each subtype were not identified when the samples were compared to HapMap. In another trial to find CNVs among different groups according to the stage of cancer (among cases of stages I, II, III and IV), all shared some CNVs, but when comparing each stage separately to HapMap, unique CNVs (correlated with higher grade and stage) could be found among each stage, which may be of prognostic importance in Ov Ca. In this study, most cases were of the serous carcinoma subtype (31.1%), followed by endometrioid carcinoma (20.5%), clear cell carcinoma (12.9%) and other types (34.4%). Similarities in gene expression could be seen between the serous and endometrioid subtypes and between the clear cell and endometrioid subtypes.

Association analysis was performed on the detected CNV regions, dividing the cases into two groups (Ov Ca samples and normal control group) using the statistical tests mentioned in section 2.6. For association analysis, the –log10 p-value for all chromosomes was plotted for all cases using a Manhattan Plot of the corrected data. Association analysis detected six significant top hits that characterised cancer cases from the control ethnically homogeneous age-matched normal group (see Table 1). The most significant detected CNVs are at six locations: 20q13.12 overlapping the *EYA2* gene, 12p13.33 overlapping the *WNK1*, 12p11.22 overlapping the *KLHDC5*, 13q13.3 overlapping the *CSNK1A1L*, 18q22.1 overlapping the *CCDC102B* and 5q11.2 overlapping the *PLK2* (see Figures 1 and 2). *KLHDC5*, *CSNK1A1L* and *CCDC102B* are pseudogenes that do not have previous research on their biological roles. The most significant detected genes that have p-values <0.05 are *WNK1* and *EYA2*, which have previously been described as the carcinogenesis pathways of many cancers: CN_623069 overlapping the *EYA2* (20q13.12) gene at location chr12:867,000-875,750 and CN_874978 overlapping the *WNK1* (12p13.33) gene at location chr20:45,778,000-45,788,000.

For validation studies using cell lines, the work focused on *WNK1* and *EYA2* genes and carried out DNA copy number analysis in conjunction with RNA expression analysis. DNA copy number analysis used two methods, namely, TaqMan qPCR and NanoString assays. The Ov Ca cell lines included SKOV3, OVCAR5, 2008, CAOV3, A2780 and HOSE636. DNA was also extracted from HapMap cell lines NA12878 and NA10851, which were used as controls.

The first validation method, TaqMan qPCR, was performed to measure the copy number states of the DNA extracted from different Ov Ca samples and the HapMap cell lines that were previously analysed using Golden Helix. The second technique for validation was NanoString, and the results of the two validation steps were compared with each other and with the arrays detected in CN states.

The two assays for validation correctly recapitulated the results of the arrays in the Golden Helix analysis for HapMap cell lines. The CN states for ovarian cancer cell lines were also in agreement with the predominant CN state in ovarian cancer detected by Golden Helix arrays analysis. Therefore, the copy number states of the most significant CNVs associated with Ov Ca were confirmed and validated.

Table 1 shows the results of our extensive association analysis using Golden Helix software with the p-value for each association. The most significant hits that overlap genes are presented in descending order of p- values.

The output data of the association analysis, which nominated significant CNV regions, distinguish ovarian cancer from normal cases. These CNVs overlap known genes and pseudogenes listed in the associated gene column.

The first column in the table represents the chromosome, the second column is the cytoband location in the chromosome and the third column is the exact starting genomic coordinate of the CNV segment in the chromosome. The p-value is presented in the highlighted fifth column, and the last column lists the –log10 p-value.

Table 1: The output data of association analysis using Golden Helix software nominated significant CNV regions that distinguish ovarian cancer from normal cases

Chromosome	Cytoband	Position	Associated gene	T-test P	Regression-log10 P
20	q13.12	45780094	EYA2	0.002857	2.61044
12	p13.33	869251	WNK1	0.010271	2.052746
12	p11.22	28095546	KLHDC5	0.01287	1.963284
13	q13.3	38072024	CSNK1A1L	0.040633	1.43374
18	q22.1	66742743	CCDC102B	0.045041	1.385111
5	q11.2	57326015	PLK2	0.052274	1.312454

Figure 1: Heat map of the copy number gain overlapping the *EYA2* gene in cancer cases

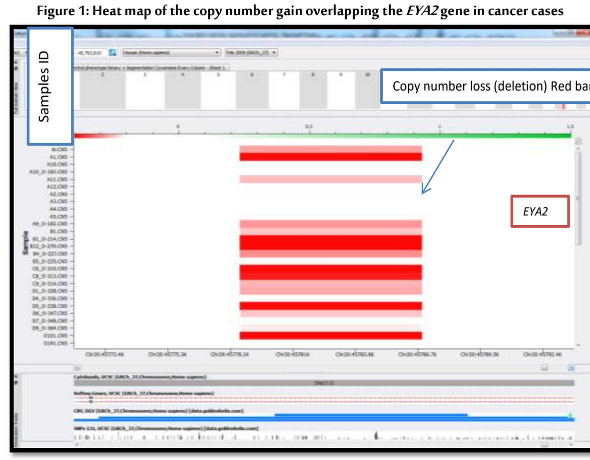

Figure 1 is a heat map of the copy number loss detected at the location of the *EYA2* gene (Chr20q13.12) in normal cases; however, ovarian cancer cases show a copy neutral (CN2) state in the same segment. This means that cancer cases have more copies in the Chr20q13.12 location than the normal control group. Red bars represent the areas of copy number loss, while the white bars represent CN2 cases. The X-axis represents the exact position of the copy number variation segment, and the Y-axis represents the ID of the studied ovarian cancer samples.

Figure 2: Heat map of the copy number gain overlapping the *WNK1* gene in cancer cases

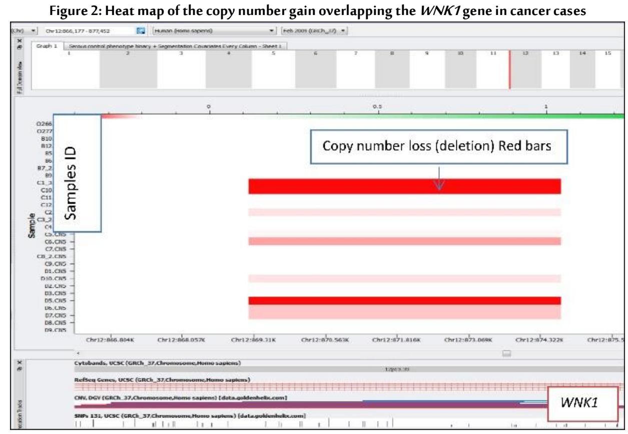

Figure 2 is a heat map of the copy number loss detected at the location of the *WNK1* gene (Chr12p13.33) in normal cases. The ovarian cancer cases show either a CN2 state or copy number gain (CN3) in the same segment. This means that cancer cases have more copies in the Chr12p13.33 location than the normal control group. The red bars represent the areas of copy number loss, while the white bars represent the CN2 regions. The X-axis represents the exact position of the copy number variation segment, and the Y-axis represents the ID of the studied ovarian cancer samples.

In the CNVs overlapping *EYA2* and *WNK1*, deletion is more frequent in normal and in some low-grade cancers, while Ov Ca is chiefly CN2 or has CN3, giving a clue to the possible oncogenic role of these two genes in Ov Ca.

Validation of the resulting top hits was performed using two different techniques: TaqMan qPCR and NanoString copy number analysis. The results of the two validation steps were compared to each other and the arrays detected in CN states. TaqMan qPCR was performed to measure the copy number states of the DNA extracted from different Ov Ca and the HapMap cell lines that were previously analysed using Golden Helix. The CNV segment that overlaps the *EYA2* gene (see Figure 3) shows that the copy number states used in NanoString (panel-A) are identical to the results obtained from Golden Helix analysis (panel-B). This means that the CNV segment overlapping the *EYA2* gene was successfully validated and its true CNV is related to Ov Ca. For the CNV segment that overlaps the *WNK1* gene (see Figure 4), the copy number states used in NanoString (panel-A) are identical to the results obtained from Golden Helix analysis (panel-B). The CNV segment overlapping the *WNK1* gene was successfully validated and its true CNV is related to the cancer cases.

Figure 3: Expected versus detected CNV (*EYA2*)

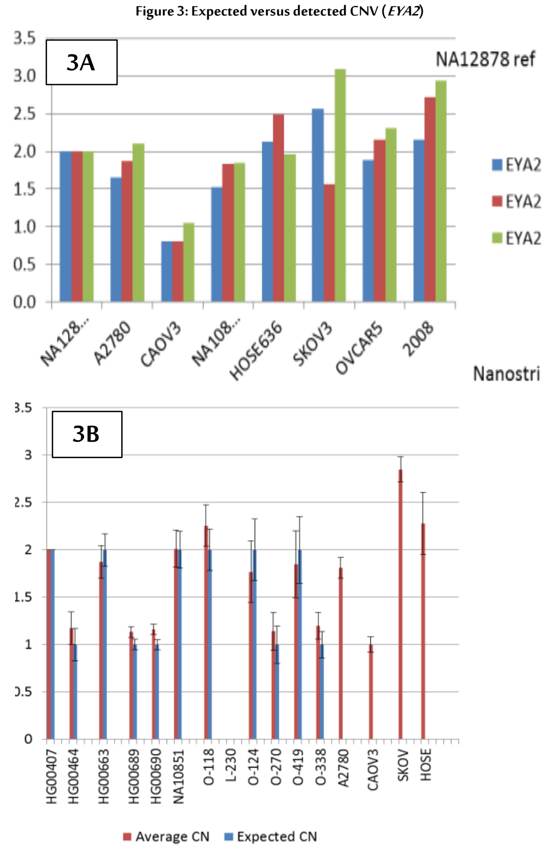

Figure 3 presents illustrations of copy number state validation using the NanoString technique. Picture (A) shows the copy number state of different samples using three different primers. Picture (B) compares the CN state of NanoString and the CN state of TaqMan qPCR with successful validation. The CNV segment that overlaps the *EYA2* gene is tested, and all samples of the NanoString copy number states (Figure 3A) are identical to the results obtained from the Golden Helix analysis in Figure 3B. This means that the CNV segment overlapping the *EYA2* gene is successfully validated and its true CNV is related to the carcinoma samples.

Figure 4. Expected versus detected CNV (*WNK1*)

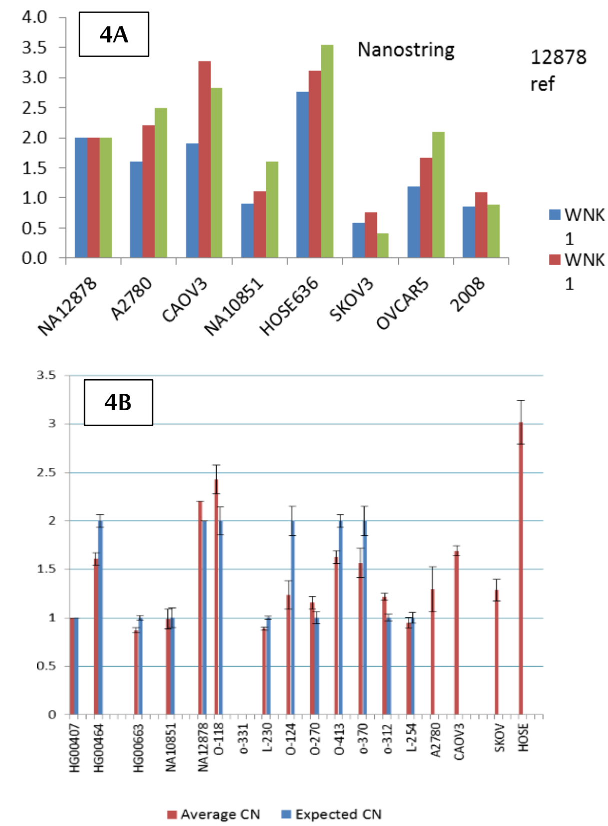

Figure 4 presents illustrations of copy number state validation using the NanoString technique. Figure 4A shows the copy number state of different samples using three different primers. Figure 4B compares the CN state of NanoString and the CN state of TaqMan qPCR with successful validation. The CNV segment that overlaps the *WNK1* gene is tested, and all samples used in the NanoString copy number states (Figure 4A) are identical to the results obtained from the Golden Helix analysis in Figure 4B. This means that the CNV segment overlapping the *WNK1* gene is successfully validated and its true CNV is related to the serous carcinoma samples.

The two assays for validation correctly recapitulated the results of the Golden Helix arrays analysis for the HapMap cell lines. The CN states for Ov Ca cell lines were also in agreement with the predominant CN state in ovarian cancer detected by Golden Helix arrays analysis. Therefore, the copy number states of the most significant CNVs associated with Ov Ca were confirmed and validated.

For *WNK1*, the RNA expression was seen to increase with a higher DNA copy number in the same segment (Figure 5). However, in the case of *EYA2*, no consistent correlation was detected between the DNA copy number state and the RNA expression level in the cell lines tested (Figure 6), which may be explained by the presence of many factors affecting the *EYA2* expression other than the copy number state. Our study confirmed frequent amplification at the segment overlapped by *WNK1* (Chr12p13.33), with concordant mRNA overexpression in many Ov Ca cell lines.

Figure 5. The DNA copy number state and mRNA expression of the *WNK1* gene

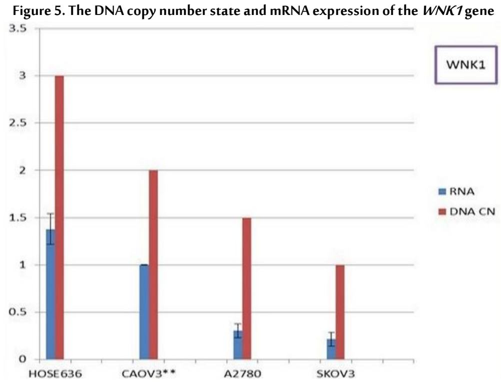

Figure 5 shows the validation of Ov Ca samples with different copy number states detected by Golden Helix analysis using TaqMan qPCR. The graph compares the DNA copy number state (red bars) and the RNA expression state of the same samples (blue bars).

Figure 6. The DNA copy number state and mRNA expression of the *EYA2* gene

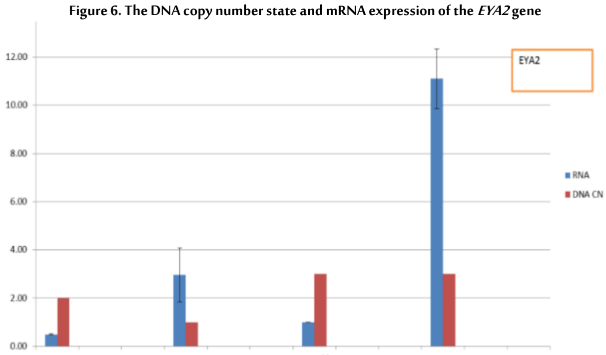

Figure 6 shows the validation of Ov Ca samples with different copy number states detected by Golden Helix analysis using TaqMan qPCR. The graph compares the DNA copy number state (red bars) and the RNA expression state of the same samples (blue bars).

4. Discussion

The high mortality rate of Ov Ca arises from a lack of diagnostic symptoms, the absence of effective biomarkers to identify early stages and missing reliable prognostic markers. The heterogeneous nature of Ov Ca histologic subtypes may affect treatment modalities and disease prognosis (Kobel *et al.*, 2008). Evaluating the molecular changes, copy, content and structure associated with epithelial Ov Ca arising in distinct genetic backgrounds offer approaches to therapeutic intervention (George *et al.*, 2013).

In this study, a germline association study using blood from patients with ovarian cancer was carried out using the genome-wide human SNP array 6.0, which contains 906,600 probes for SNPs and 946,000 probes for the detection of CNV loci. Affymetrix GTC was used to generate copy numbers, LOH and segmentation of the raw data (CEL files). The presence of CNVs specific to each histopathological subtype in this study indicates that each subtype of ovarian cancer has distinctive CNVs that may lead to better identification of the pathogenesis of Ov Ca to invent early screening tools. Therefore, future analysis integrating chromatin features into the CNV selection process could identify other CNVs missed in this analysis that are associated with cancer risk (Walker *et al.*, 2017). Ov Ca heterogeneity will also have affected the ability to identify risk loci, as common variant risk regions are different for different histopathological types of Ov Ca (Lawrenson *et al.*, 2019). In this study, a germline association study using blood from patients with ovarian carcinoma using the genome-wide human SNP array 6.0 can reveal novel genes worthy of follow-up for cancer susceptibility.

The most significant CNVs detected were 20q13.12 overlapping the *EYA2* gene and 12p13.33 overlapping the *WNK1* gene (p-values <0.05), which have previously been described as some of the carcinogenesis pathways of many cancers. The *EYA* family form a mutual transcription factor complex that supports the proliferation and survival of progenitor cells. The expression of *EYA* in adult tissue is associated with the origin and development of diverse tumour types. *EYA* proteins also contain protein tyrosine phosphatase activity, which plays a crucial role in breast cancer growth and metastasis as well as guiding cells to the repair pathway upon DNA damage (Blevins *et al.*, 2015). The epigenetic silencing of *EYA2* is a common incident in pancreatic cancers, and its constant expression limits the growth and metastases of adenocarcinoma (Vincent *et al.*, 2014). *EYA* proteins have multipurpose biochemical activities, which are associated with different cellular functions, and elevated *EYA* ranks of expression might enhance resistance to DNA-damaging therapeutic regimens frequently consumed in cancer therapy (Blevins *et al.*, 2015; Tadjuidje and Hegde, 2013). *EYA* proteins affect advanced cancer progression via their role as pro-proliferative and anti-apoptotic factors. A tough DNA damage response pathway comprises the regulation of H2AX phosphorylation via *EYA2* to facilitate proper cell cycle progression upon injury (Sousounis *et al.*, 2020). The most eminent cell cycle regulators, cyclin D1, p27 and *c-myc*, are target genes of the *EYA* transcriptional stimulators. CDK6 expression enhances the degradation of the *EYA2* protein (Kohrt *et al.*, 2014). Overexpression of micro RNAs-30a in lung adenocarcinoma cells can inhibit cell migration and invasion, which is partially attributed to the decrease in *EYA2* expression. These results may be used in the future as a new prospective target for the treatment of lung adenocarcinoma (Yuan *et al.*, 2016).

Using SNP arrays to detect CNVs has many benefits such as being cost-effective and requiring fewer samples per experiment compared to other techniques (Winchester *et al.*, 2009). For validation studies using cell lines focused on *WNK1* and *EYA2* genes, CN states for ovarian cancer cell lines are also in agreement with the predominant CN state in ovarian cancer detected by Golden Helix array analysis. If copy number-driven alteration in gene expression is a common attribute of the genomic panorama, it is likely that epigenetic modifications will further polish gene expression in favour of tumour growth (Bowtell, 2010).

Herein, the detected CNVs overlapping *EYA2* and *WNK1* give a clue to the possible oncogenic role of these two genes in Ov Ca. Amplification at these locations is associated with high-grade tumours, which have a worse overall survival rate. *WNK1* and *EYA2* amplifications are significantly associated with high-grade tumours, which indicates the possible oncogenic activity of both genes, and *WNK1* and *EYA2* may serve as prognostic markers for Ov Ca. These results are in agreement with other studies that suggest the oncogenic role of *WNK1* and *EYA2* in different cancer types (Costa *et al.*, 2015; Li *et al.*, 2018). A significant association is also found between higher expression and end-stage ovarian cancer along with poor prognosis (Xu *et al.*, 2019). *WNK1* plays an essential role in early embryonic angiogenesis regulation through oxidative stress response kinase. Emerging evidence suggests that ion homeostasis is important for cell migration in many cell types and Akt phosphorylation of *WNK1* may affect its targeting and interaction with downstream targets (Huang *et al.*, 2020). Generally, the functional diversity of *WNK1* offers positive feedback loops for the amplification of tumour growth. *WNK1* can promote tumorigenesis by stimulating tumour angiogenesis. Thus, a *WNK1* signalling cascade might be a multi-purpose focus for blended cancer therapy. The inhibition of *WNK1* may be a potent anti-cancer therapy (Sie *et al.*, 2020).

Targeting *EYA* may inhibit the growth and progression of multiple tumour types (Zhou *et al.*, 2018). *EYA2* has a higher expression and copy number in ovarian cancer than in normal human ovaries, which is consistent with similar observations in breast cancer that are in concordance with this work (Xu *et al.*, 2019). In the case of *EYA2*, no consistent correlation has been detected between DNA copy number state and RNA expression level in the cell lines tested. This may be attributed to any other biological factor that increases the *EYA2* expression that is not related to the increase in the copy number state. Further research is needed to detect the cause of the high expression of *EYA2*. A somatic study of ovarian cancers, especially epithelial, identified a high expression of *EYA2* mRNA in different types of malignant cells. A high copy number is directly associated with the mRNA expression level of *EYA2*. In Ov Ca cell lines, up-regulation of *EYA2* has also been shown to push the tumour growth of cells and is related to the genomic amplification of its locus in Ov Ca specimens. Up-regulation of *EYA2* has been associated with the activation of tumour growth and decreased overall survival, especially in epithelial Ov Ca (Zhang *et al.*, 2005), which aligns with these results. The 20q13.12 amplification was observed in multiple tumours, and it encodes 11 genes, one of which is *EYA2*. However, the current association contrasts with other findings that reported improved overall survival with chr20q13.12 amplification (Xie *et al.*, 2012). Early-stage Ov Ca is commonly asymptomatic, and nearly 75% of women have the progressive disease at diagnosis. Hence, Ov Ca is the leading cause of death among gynaecological cancers, as it represents 4% of all cancers in women. Overall survival is highly dependent on the stage of Ov Ca, and five-year survival is 80–90% in patients with early-stage compared with 25% for patients with advanced stage. Therefore, early screening for Ov Ca increases survival among patients (Alexandrova *et al.*, 2020).

Gene amplification and an increase in the DNA copy number of a chromosomal segment often lead to an increase in oncogene expression in many human cancers (Li *et al.*, 2017). There is frequent amplification at the segment overlapped by *WNK1* (Chr12p13.33) with concordant mRNA overexpression in many Ov Ca cell lines. Members of the *WNK* family have been shown to modulate MAPK signalling. *WNK1* activates the ERK5-MAP kinase (MAPK) cascade in addition to the regulatory role of the TGF-β-Smad signalling cascade (B. H. Lee *et al.*, 2007). Phosphatidylinositol 3-kinase PI3K-activating hormones phosphorylate *WNK1* by AKT1 and SGK1 (Cheng and Huang, 2011). Transient transfection studies of *WNK1* revealed that overexpression of *WNK1* leads to the activation of ERK5 (Wang and Tournier, 2006). Many studies emphasise that *WNK1* functions as a MAP4K in the MAPK pathways (Sun *et al.*, 2006). *EYA2* is a co-factor for the *SIX1* gene that induces TGF-β signalling to activate the epithelial-mesenchymal transition as well as stimulate metastasis (Blevins *et al.*, 2015). MAPK positively regulates *EYA*. EGFR/RAS/MAPK signalling phosphorylates *EYA* as a downstream, and the two MAPK phosphorylation sites detected in *EYA* positively standardise *EYA* activity in vivo (Tootle *et al.*, 2003). The activation of RAS/MAPK can potentiate *EYA*-mediated transactivation, whereby in the absence of RAS/MAPK signalling, it can trigger some transcription. However, when the signal occurs, this function is potentiated such that target genes may be activated to advanced levels. An alternative role for RAS/MAPK is to grant more activation potential to *EYA* to overwhelm the negative regulation of specific target genes (Silver *et al.*, 2003).

Our study may present comprehensive data assembled to our knowledge; however, there are potential limitations. The sample size is small, so it is necessary to apply the same study outline to a larger sample size to confirm our association analysis for ovarian cancer. Furthermore, although using peripheral blood samples and cell lines allows the analysis of the germline, tissue samples from the same patients could strengthen the results. The tissue samples in this study, however, had intrinsic noise, which led to unreliable results.

To summarise, preliminary evidence for CNVs in two potential oncogenes (*WNK1* and *EYA2*) using Affymetrix SNP 6.0 arrays was found and was associated significantly with high-grade Ov Ca cases. This may confer risk to Ov Ca that needs extended study on a bigger sample size to confirm the association analysis.

5. Conclusion

There is evidence of cross-talk between the *WNK1* and *EYA2* genes and the *MAPK* signalling pathways, which is a common ovarian carcinogenic pathway detected in many reports. The detected CNV genes might not be the aetiology, but they may overlap *WNK1* and *EYA2*, which share the same pathway. The potential diagnostic and therapeutic values of these genes may help in early diagnosis and proper management to minimise the high mortality rate of this disease. Ovarian carcinomas are associated with copy number gains at the segments of DNA overlapping *WNK1* and *EYA2*. This may support the hypothesis that both *WNK1* and *EYA2* have an oncogenic effect on ovaries. The copy number gain of the *WNK1* gene is associated with a higher expression of mRNA.

6. Recommendations

Applying the same study outline in a bigger sample size to confirm the association analysis of ovarian cancer is recommended. Performing functional analysis of *WNK1* and *EYA2* on ovarian cancer cell lines (overexpression and knocking down) will explore the effect of gene overexpression on cell proliferation or division and will knock down the same genes by comparing the effect on cells.

Biographies

Hanan Mohamed Abd Elmoneim

Department of Pathology, Faculty of Medicine, Umm Al-Qura University, Makkah, Kingdom of Saudi Arabia, Department of Pathology, Faculty of Medicine, Minia University, Minia, Egypt, 00966594455902, hmnour@uqu.edu.sa

Dr Abd Elmoneim is an Egyptian professor with a PhD in pathology from Glasgow University, Scotland, United Kingdom. In 2012, she became a professor of pathology and was elected head of the Department of Pathology, Faculty of Medicine, Minia University, Egypt. Currently, she is a professor of pathology in the Faculty of Medicine, Umm Al-Qura University, Makkah, Saudi Arabia and a pathology consultant at the Umm Al-Qura University Medical Centre. She has published 35 ISI/Scopus-indexed scientific papers with special research interests in breast, urogenital and molecular pathology. ORCID: 0000-0003-1715-5060.

Rehab Kamal Mohammed

Department of Pathology, Faculty of Medicine, Minia University, Minia, Egypt, 00201027267773, rehab_kemo@yahoo.com

Dr Kamal is an Egyptian associate professor of pathology, department of pathology, faculty of Medicine, Minia university, Minia, Egypt. She has MD in pathology at the Faculty of Medicine, Minia University, Minia, Egypt. She is a pathology consultant at the pathology department, Minia University Hospital, Faculty of Medicine, Minia, Egypt. She has published 8 ISI/Scopus-indexed scientific papers. Dr Kamal has a special research interests in the liver pathology, gastrointestinal pathology, pathology of soft tissue tumors, anatomical pathology and molecular pathology.

Reda Fikry Abd El-Meguid

Department of Pathology, Faculty of Medicine, Minia University, Minia, Egypt, 00201004964423, redhal3@hotmail.com

Dr Abd El-Meguid is an Egyptian professor of pathology. He is an MD in pathology at the Faculty of Medicine, Minia University, Minia, Egypt. He is a professor in the Department of Pathology at the College of Medicine, University of Minia, Egypt. He is also a pathology consultant at the Minia University Hospital, Faculty of Medicine, Minia. He has published 16 ISI/Scopus-indexed scientific papers with special research interests in breast, gastrointestinal and anatomical pathology.

Heba Mohammed Tawfik

Department of Pathology, Faculty of Medicine, Minia University, Minia, Egypt, 00201006767744, heba.kamel@mu.edu.eg

Dr Tawfik is an Egyptian professor with a PhD in pathology from Glasgow Caledonian University, Scotland, United Kingdom. She is the current head of the Department of Pathology, College of Medicine, Minia University, Egypt. She has been a member of the Higher Promotion Committee of Pathology in the Supreme Council of Universities in Egypt for two rounds. She has published 25 ISI/Scopus-indexed scientific papers with special research interests in breast, urogenital and anatomical pathology. She has participated in many conferences in Scotland, Turkey and Egypt.

Manal Ismail Abd Elghany

Department of Pathology, Faculty of Medicine, Minia University, Egypt, 00201005765568, manal.abdelghany@mu.edu.eg

Dr Abd-Elghany is an Egyptian associate professor. She was awarded her Ph.D from Liverpool University, United Kingdom. She is a pathology consultant at the Minia University Hospital, Faculty of Medicine. She is certified trainer in Research Ethics (Maryland, USA). She has published 18 ISI/Scopus-indexed scientific papers and has special research interests in prostate pathology, anatomical and molecular pathology. She is also interested in medical education and quality management. Currently she is excutive manager of Technology Innovation and Commercialization Office (TICO), and TISC moderator at Minia University.

Halah Tariq Albar

Department of Physiology, Faculty of Medicine, Umm Al-Qura University, Makkah, Saudi Arabia, 00966554413222, halbar@live.com

Dr Albar is a Saudi assistant professor. She received her PhD in Physiology in 2018 from the University of Manchester, United Kingdom. She was the vice head of the Physiology Department from 2019 until 2021. Currently, she is the academic lead of the MBBS program, Faculty of Medicine, Umm Al-Qura University, Makkah, Saudi Arabia. She is also a general practitioner at the Umm Al-Qura University Medical Centre. Her special research interests are women's health and kidney and endocrine disorders.

Mohammed Abubakr Mohammed Basalamah

Department of Pathology, Faculty of Medicine, Umm Al-Qura University, Makkah, Kingdom of Saudi Arabia, 00966503516809, mabasalamah@uqu.edu.sa

Dr Basalamah is a Saudi associate professor in pathology. He is currently the chairman of the Pathology Department, Faculty of Medicine, Umm Al-Qura University. He has a PhD in molecular and cellular pathology from the University of North Carolina. He has published 21 ISI/Scopus-indexed scientific papers with special research interests in pathological changes at the molecular and cellular levels. He has most recently studied vitamin D protective effects against toxicities and pulsed laser effects on different organs and tissues of animal models.

Nisreen Dahi Mohamed Toni

Department of Pathology, Faculty of Medicine, Minia University, Minia, Egypt, 00201005420266, nisreen.toni@mu.edu.eg

Dr Toni has been an Egyptian associate professor of pathology at pathology department, Faculty of Medicine, Minia University since 2019. She was a fellow of the Molecular Genetic Research Unit, Department of Pathology, Brigham and Women's Hospital, Harvard Medical School, USA, from 2009–2011. She received an MD in pathology from the Faculty of Medicine, Minia University. Minia. She has published 8 ISI/Scopus-indexed scientific papers with special research interests in pathology of the female genital system molecular pathology, immunohistochemistry, cytogenetics, tissue culture and anatomical pathology.

Acknowledgements

The authors acknowledge Dr Charles Lee and Dr Sunita R Setlur at the Brigham and Women's Hospital, Harvard Medical School, Boston MA, USA, for general supervision of the research group. They also gratefully acknowledge the Faculty of Medicine at Minia University for its financial support.

References

Alexandrova, E., Pecoraro, G., Sellitto, A., Melone, V., Ferravante, C., Rocco, T., Guacci, A., Giurato, G., Nassa, G., Rizzo, F., Weisz, A. and Tarallo, R. (2020). An overview of candidate therapeutic target genes in ovarian cancer. *Cancers (Basel),* **12**(6), 1470.

Blevins, M.A., Towers, C.G., Patrick, A.N., Zhao, R. and Ford, H.L. (2015). The SIX1-EYA transcriptional complex as a therapeutic target in cancer. *Expert Opin Ther Targets,* **19**(2), 213–25.

Bowtell, D.D. (2010). The genesis and evolution of high-grade serous ovarian cancer. *Nat Rev Cancer,* **10**(11), 803–8.

Cheng, C.J. and Huang, C.L. (2011). Activation of PI3-kinase stimulates endocytosis of ROMK via Akt1/SGK1-dependent phosphorylation of WNK1. *J Am Soc Nephrol,* **22**(3), 460–71.

Concolino, P., Rizza, R., Mignone, F., Costella, A., Guarino, D., Carboni, I., Capoluongo, E., Santonocito, C., Urbani, A. and Minucci, A. (2018). A comprehensive BRCA1/2 NGS pipeline for an immediate Copy Number Variation (CNV) detection in breast and ovarian cancer molecular diagnosis. *Clin Chim Acta,* **480**(n/a), 173–9.

Costa, A.M., Pinto, F., Martinho, O., Oliveira, M.J., Jordan, P. and Reis, R.M. (2015). Silencing of the tumor suppressor gene WNK2 is associated with upregulation of MMP2 and JNK in gliomas. *Oncotarget,* **6**(3), 1422–34.

George, J., Alsop, K., Etemadmoghadam, D., Hondow, H., Mikeska, T., Dobrovic, A., deFazio, A., Australian Ovarian Cancer Study, G., Smyth, G.K., Levine, D.A., Mitchell, G. and Bowtell, D.D. (2013). Nonequivalent gene expression and copy number alterations in high-grade serous ovarian cancers with BRCA1 and BRCA2 mutations. *Clin Cancer Res,* **19**(13), 3474–84.

Huang, C.-L., Jian, X. and Yuh, C.-H. (2020). WNK1-OSR1/SPAK Kinase cascade is important for angiogensis. *Transactions of the American Clinical and Climatological Association,* **131**(n/a), 140–6.

Kobel, M., Kalloger, S.E., Boyd, N., McKinney, S., Mehl, E., Palmer, C., Leung, S., Bowen, N.J., Ionescu, D.N., Rajput, A., Prentice, L.M., Miller, D., Santos, J., Swenerton, K., Gilks, C.B. and Huntsman, D. (2008). Ovarian carcinoma subtypes are different diseases: implications for biomarker studies. *PLoS Med,* **5**(12), e232.

Kohrt, D., Crary, J., Zimmer, M., Patrick, A.N., Ford, H.L., Hinds, P.W. and Grossel, M.J. (2014). CDK6 binds and promotes the degradation of the EYA2 protein. *Cell Cycle,* **13**(1), 62–71.

Kori, M. and Yalcin Arga, K. (2018). Potential biomarkers and therapeutic targets in cervical cancer: Insights from the meta-analysis of transcriptomics data within network biomedicine perspective. *PLoS One,* **13**(7), e0200717.

Kossai, M., Leary, A., Scoazec, J.Y. and Genestie, C. (2018). Ovarian Cancer: A Heterogeneous Disease. *Pathobiology,* **85**(1-2), 41–9.

Lawrenson, K., Song, F., Hazelett, D.J., Kar, S.P., Tyrer, J., Phelan, C.M., Corona, R.I., Rodriguez-Malave, N.I., Seo, J.H., Adler, E., Coetzee, S.G., Segato, F., Fonseca, M.A.S., Amos, C.I., Carney, M.E., Chenevix-Trench, G., Choi, J., Doherty, J.A., Jia, W., Jin, G.J., Kim, B.G., Le, N.D., Lee, J., Li, L., Lim, B.K., Adenan, N.A., Mizuno, M., Park, B., Pearce, C.L., Shan, K., Shi, Y., Shu, X.O., Sieh, W., Australian Ovarian Cancer Study, G., Thompson, P.J., Wilkens, L.R., Wei, Q., Woo, Y.L., Yan, L., Karlan, B.Y., Freedman, M.L., Noushmehr, H., Goode, E.L., Berchuck, A., Sellers, T.A., Teo, S.H., Zheng, W., Matsuo, K., Park, S., Chen, K., Pharoah, P.D.P., Gayther, S.A. and Goodman, M.T. (2019). Genome-wide association studies identify susceptibility loci for epithelial ovarian cancer in East Asian women. *Gynecol Oncol,* **153**(2), 343–55.

Lee, B.H., Chen, W., Stippec, S. and Cobb, M.H. (2007). Biological cross-talk between WNK1 and the transforming growth factor beta-Smad signaling pathway. *J Biol Chem,* **282**(25), 17985–96.

Lee, C., Iafrate, A.J. and Brothman, A.R. (2007). Copy number variations and clinical cytogenetic diagnosis of constitutional disorders. *Nat Genet,* **39**(7 Suppl), S48–54.

Li, C., Lin, C., Cong, X. and Jiang, Y. (2018). PDK1-WNK1 signaling is affected by HBx and involved in the viability and metastasis of hepatic cells. *Oncol Lett,* **15**(4), 5940–6.

Li, X., Liu, Y., Lu, J. and Zhao, M. (2017). Integrative analysis to identify oncogenic gene expression changes associated with copy number variations of enhancer in ovarian cancer. *Oncotarget,* **8**(53), 91558–67.

Liu, Z., Zhao, L. and Song, Y. (2019). Eya2 Is overexpressed in human prostate cancer and regulates docetaxel sensitivity and mitochondrial membrane potential through AKT/Bcl-2 signaling. *Biomed Res Int,* **2019**(n/a), 3808432.

Moniz, S. and Jordan, P. (2010). Emerging roles for WNK kinases in cancer. *Cell Mol Life Sci,* **67**(8), 1265–76.

Rodan, A.R. and Jenny, A. (2017). WNK Kinases in Development and Disease. *Curr Top Dev Biol,* **123**(n/a), 1–47.

Sie, Z.L., Li, R.Y., Sampurna, B.P., Hsu, P.J., Liu, S.C., Wang, H.D., Huang, C.L. and Yuh, C.H. (2020). WNK1 Kinase Stimulates Angiogenesis to Promote Tumor Growth and Metastasis. *Cancers (Basel),* **12**(3), 575.

Siegel, R.L., Miller, K.D. and Jemal, A. (2019). Cancer statistics, 2019. *CA Cancer J. Clin,* **69**(1), 7–34.

Silver, S.J., Davies, E.L., Doyon, L. and Rebay, I. (2003). Functional dissection of eyes absent reveals new modes of regulation within the retinal determination gene network. *Mol Cell Biol,* **23**(17), 5989–99.

Sousounis, K., Bryant, D.M., Martinez Fernandez, J., Eddy, S.S., Tsai, S.L., Gundberg, G.C., Han, J., Courtemanche, K., Levin, M. and Whited, J. L. (2020). Eya2 promotes cell cycle progression by regulating DNA damage response during vertebrate limb regeneration. *eLife,* **9**(n/a), e51217.

Sun, X., Gao, L., Yu, R.K. and Zeng, G. (2006). Down-regulation of WNK1 protein kinase in neural progenitor cells suppresses cell proliferation and migration. *J. Neurochem,* **99**(4), 1114–21.

Tadjuidje, E. and Hegde, R.S. (2013). The Eyes Absent proteins in development and disease. *Cell Mol Life Sci,* **70**(11), 1897–913.

Tootle, T.L., Silver, S.J., Davies, E.L., Newman, V., Latek, R.R., Mills, I.A., Selengut, J.D., Parlikar, B.E. and Rebay, I. (2003). The transcription factor Eyes absent is a protein tyrosine phosphatase. *Nature,* **426**(6964), 299–302.

Vincent, A., Hong, S.M., Hu, C., Omura, N., Young, A., Kim, H., Yu, J., Knight, S., Ayars, M., Griffith, M., Van Seuningen, I., Maitra, A. and Goggins, M. (2014). Epigenetic silencing of EYA2 in pancreatic adenocarcinomas promotes tumor growth. *Oncotarget* **5**(9), 2575–87.

Walker, L.C., Marquart, L., Pearson, J.F., Wiggins, G.A., O'Mara, T.A., Parsons, M.T., Bcfr, Barrowdale, D., McGuffog, L., Dennis, J., Benitez, J., Slavin, T.P., Radice, P., Frost, D., Embrace, Godwin, A.K., Meindl, A., Schmutzler, R.K., Collaborators, G.S., Isaacs, C., Peshkin, B.N., Caldes, T., Hogervorst, F.B., Hebon, Lazaro, C., Jakubowska, A., Montagna, M., Investigators, K. C., Chen, X., Offit, K., Hulick, P.J., Andrulis, I.L., Lindblom, A., Nussbaum, R.L., Nathanson, K.L., Chenevix-Trench, G., Antoniou, A.C., Couch, F.J. and Spurdle, A.B. (2017). Evaluation of copy-number variants as modifiers of breast and ovarian cancer risk for BRCA1 pathogenic variant carriers. *Eur J Hum Genet,* **25**(4), 432–8.

Wang, X. and Tournier, C. (2006). Regulation of cellular functions by the ERK5 signalling pathway. *Cell Signal,* **18**(6), 753–60.

Webb, P.M. and Jordan, S.J. (2017). Epidemiology of epithelial ovarian cancer. *Best Practice and Research, Clinical Obstetrics and Gynaecology,* **41**(n/a), 3–14.

Winchester, L., Yau, C., and Ragoussis, J. (2009). Comparing CNV detection methods for SNP arrays. *Brief Funct Genomic Proteomic,* **8**(5), 353–66.

Xie, T., G, D.A., Lamb, J.R., Martin, E., Wang, K., Tejpar, S., Delorenzi, M., Bosman, F.T., Roth, A.D., Yan, P., Bougel, S., Di Narzo, A.F., Popovici, V., Budinska, E., Mao, M., Weinrich, S.L., Rejto, P.A. and Hodgson, J.G. (2012). A comprehensive characterization of genome-wide copy number aberrations in colorectal cancer reveals novel oncogenes and patterns of alterations. *PLoS One,* **7**(7), e42001.

Xu, B., English, J.M., Wilsbacher, J.L., Stippec, S., Goldsmith, E.J. and Cobb, M.H. (2000). WNK1, a novel mammalian serine/threonine protein kinase lacking the catalytic lysine in subdomain II. *J Biol Chem,* **275**(22), 16795–801.

Xu, H., Jiao, Y., Yi, M., Zhao, W. and Wu, K. (2019). EYA2 correlates with clinico-pathological features of breast cancer, promotes tumor proliferation, and predicts poor survival. *Frontiers in Oncology,* **9**(n/a), 26.

Yuan, Y., Zheng, S., Li, Q., Xiang, X., Gao, T., Ran, P., Sun, L., Huang, Q., Xie, F., Du, J. and Xiao, C. (2016). Overexpression of miR-30a in lung adenocarcinoma A549 cell line inhibits migration and invasion via targeting EYA2. *Acta Biochim Biophys Sin (Shanghai),* **48**(3), 220–8.

Zhang, L., Yang, N., Huang, J., Buckanovich, R., Liang, S., Barchetti, A., Vezzani, C., O'Brien-Jenkins, A., Wang, J., Ward, M. and Courreges, M. (2005). Transcriptional coactivator *Drosophila* eyes absent homologue 2 is up-regulated in epithelial ovarian cancer and promotes tumor growth.*Cancer Research.,* **65**(n/a), 925–32.

Zhou, H., Zhang, L., Vartuli, R.L., Ford, H.L. and Zhao, R. (2018). The eya phosphatase: Its unique role in cancer. *Int J Biochem Cell Biol,* **96**(n/a), 165–70.

The Scientific Journal of King Faisal University

Basic and Applied Sciences

Egyptian Imports from Food Groups in Light of COVID-19: An Econometric Study

Mona Hosny Gad Ali [1] and Eman Fakhry Yousif Ahmed [2]

[1] Department of Agricultural Policy Research and Project Evaluation, Agricultural Economics Research Institute, Agriculture Research Centre, Cairo, Egypt

[2] Department of Agricultural Economics, Faculty of Agriculture, Ain Shams University, Cairo, Egypt

LINK	RECEIVED	ACCEPTED	PUBLISHED ONLINE	ASSIGNED TO AN ISSUE
https://doi.org/10.37575/b/agr/220017	04/04/2022	01/12/2022	01/12/2022	01/12/2022
NO. OF WORDS	**NO. OF PAGES**	**YEAR**	**VOLUME**	**ISSUE**
7284	8	2022	23	2

ABSTRACT

This study aims to identify the extent to which COVID-19 impacted Egyptian imports. It includes two main sections. The first section identifies the repercussions of COVID-19 on some global and local economic indicators – especially the recession that most of the world's economies are experiencing in light of the continuing COVID-19 outbreaks. The Egyptian economy achieved a general growth rate in 2020, at a time when the entire world was experiencing economic stagnation; this was due to the Egyptian government's set of measures and a lack of direction towards a complete closure. The second part examines demand determinants for Egyptian imports of meat, dairy, oils, cereals, sugar and wheat using ARDL models according to the bounds testing approach to cointegration. This was accomplished by studying the extent to which dependent variables have a long-term equilibrium relationship, as well as the value of imports with lag periods, gross domestic products, relative prices, effective real exchange rates, liberalisation policies, COVID-19 effects on imports and forecasting demand for Egyptian imports.

KEYWORDS

ARDL-UECM, economic growth, exchange rate, relative prices, SARIMA, trade policies

CITATION

Ali, M.H.G. and Ahmed, E.F.Y. (2022). Egyptian imports from food groups in light of COVID-19: An econometric study. *The Scientific Journal of King Faisal University: Basic and Applied Sciences*, **23**(2), 20–7. DOI: 10.37575/b/agr/220017

1. Introduction

The coronavirus 'COVID-19' outbreak occurred globally in several waves. Because most countries implemented ban, closure and social distancing policies to confront the virus's spread on a human level, the repercussions of that crisis included the financial, economic, social and human fields. Many economic sectors, such as tourism and aviation, were also negatively affected. Other sectors, such as the digital economy and the manufacture of medicines and masks, nonetheless, achieved many gains. In addition, the environment benefitted directly from the suspension of thousands of factories that used fossil fuels, resulting in a decline in carbon dioxide (CO_2) emissions. Although COVID-19 containment measures abruptly disrupted international merchandise trade and affected food trade (Vickers *et al.*, 2020), the Egyptian economy has proven resilient to the immense human and financial costs caused by the global COVID-19 pandemic. This is explained by the successful implementation of the economic reform programme since 2016, which has provided more fiscal space to withstand the adverse impact of the COVID-19 crisis. In addition, the Egyptian government's rapid response and proactive measures to limit the virus's impact, which have been implemented since March 2020, enabled the country to avoid a full lockdown (IFPRI, 2020).

Despite this containment, the weak global trade during COVID-19 is a major reason to reduce Egypt's exports. Furthermore, some countries have taken protectionist trade measures, while others have issued tenders for more purchases, and many major exporters have imposed various forms of trade restrictions to increase local food security. Therefore, this study intends to answer the following questions: (1) What impact has the COVID-19 pandemic had on Egypt's total imports, particularly meat, dairy, oils, grains and sugars, as well as wheat imports? (2) Does the policy of economic liberalisation have a positive or negative role in Egyptian foreign trade during the COVID-19 pandemic, especially in meat, dairy, oils, cereal and sugars, as well as wheat imports?

This research mainly aims to investigate the determinants of demand for Egyptian imports from certain food groups in light of COVID-19, through the following methods:

- Recognising the repercussions of COVID-19 on some global and local economic indicators.
- Reviewing the Egyptian economic policies used to face the repercussions of the spread of COVID-19.
- Studying the short-term impact of the value of imports of some studied food groups with a lag period, gross domestic product, relative prices, effective real exchange rates, liberalisation policy and COVID-19.
- Investigating the extent to which the studied variables in the total import demand model and the demand models for each of the groups – meat, dairy, oils, grains, wheat and sugar – have a stable long-term relationship.
- Forecasting demand for Egyptian imports from certain studied food groups.

2. Materials and Methods

2.1. Research Method:

The unit root test of the augmented Dickey–Fuller Test was conducted using the following equations:

- $\Delta Y_t = \gamma Y_{t-1} + \sum_{j=1}^{p}(\delta_j \Delta Y_{t-j}) + e_t \rightarrow \ H_0\,; \gamma = 0,\ H_0\,; \gamma < 0 \rightarrow$ *without* intercept(η_μ)
- $\Delta Y_t = \propto + \gamma Y_{t-1} + \sum_{j=1}^{p}(\delta_j \Delta Y_{t-j}) + e_t \ \rightarrow \ H_0\,; \gamma = 0,\ H_0\,; \gamma < 0 \rightarrow$ *with* intercept(η_μ)
- $\Delta Y_t = \propto + \beta t + \gamma Y_{t-1} + \sum_{j=1}^{p}(\delta_j \Delta Y_{t-j}) + e_t \ \rightarrow \ H_0\,; \gamma = 0,$ $H_0\,; \gamma < 0 \rightarrow$ *with* trend and intercept ($\eta_{\mu\tau}$)

It was found that some of the studied variables were stationary at level and others with first difference. Therefore, the autoregressive distributed lag [ARDL (p, q)] approach and the unrestricted equilibrium correction model (ARDL-UECM) were both used in order to show the equilibrium relationship of the determinants of demand for Egyptian imports. Particular attention was given to imports of certain food groups in the short and long term, and the elasticity of short and long term was estimated by using economic theory in terms of acceptance and interpretation of the results.

The determinants of import demand from some food groups were studied using the bound test from January 2010–April 2021

Corresponding Author: Eman Fakhry Yousif Ahmed 00201141722425, eman_youssif1@agr.asu.edu.eg

according to the World Trade Classification (CAPMAS Statistical and UN Comtrade databases).

The following are the estimated model variables (Rihan, 2021; AMIS, 2020; Vickers *et al.*, 2020; Aljebrin, 2012):

$$\mathrm{Y_t} \uparrow = \mathcal{F}\big(\mathrm{Y_{(t-P)}} \uparrow \mathrm{RGDP_{(t-q1)}} \uparrow \mathrm{Pall_{(t-q2)}} \uparrow \mathrm{REER_{(t-q3)}} \uparrow \mathrm{Dex_{(t-q4)}} \uparrow \mathrm{DC19_{(t-q5)}} \downarrow\big)$$

$$\mathrm{YM_t} \uparrow = \mathcal{F}\big(\mathrm{YM_{(t-P)}} \uparrow \mathrm{RGDP_{(t-q1)}} \uparrow \mathrm{Pmeat_{(t-q2)}} \uparrow \mathrm{REER_{(t-q3)}} \uparrow \mathrm{Dex_{(t-q4)}} \uparrow \mathrm{DC19_{(t-q5)}} \downarrow\big)$$

$$\mathrm{YD_t} \uparrow = \mathcal{F}\big(\mathrm{YD_{(t-P)}} \uparrow \mathrm{RGDP_{(t-q1)}} \uparrow \mathrm{Pdairy_{(t-q2)}} \uparrow \mathrm{REER_{(t-q3)}} \uparrow \mathrm{Dex_{(t-q4)}} \uparrow \mathrm{DC19_{(t-q5)}} \downarrow\big)$$

$$\mathrm{YO_t} \uparrow = \mathcal{F}\big(\mathrm{YO_{(t-P)}} \uparrow \mathrm{RGDP_{(t-q1)}} \uparrow \mathrm{Poils_{(t-q2)}} \uparrow \mathrm{REER_{(t-q3)}} \uparrow \mathrm{Dex_{(t-q4)}} \uparrow \mathrm{DC19_{(t-q5)}} \downarrow\big)$$

$$\mathrm{YC_t} \uparrow = \mathcal{F}\big(\mathrm{YC_{(t-P)}} \uparrow \mathrm{RGDP_{(t-q1)}} \uparrow \mathrm{Pcereals_{(t-q2)}} \uparrow \mathrm{REER_{(t-q3)}} \uparrow \mathrm{Dex_{(t-q4)}} \uparrow \mathrm{DC19_{(t-q5)}} \downarrow\big)$$

$$\mathrm{YWH_t} \uparrow = \mathcal{F}\big(\mathrm{YWH_{(t-P)}} \uparrow \mathrm{RGDP_{(t-q1)}} \uparrow \mathrm{Pcereals_{(t-q2)}} \uparrow \mathrm{REER_{(t-q3)}} \uparrow \mathrm{Dex_{(t-q4)}} \uparrow \mathrm{DC19_{(t-q5)}} \downarrow\big)$$

$$\mathrm{YS_t} \uparrow = \mathcal{F}\big(\mathrm{YS_{(t-P)}} \uparrow \mathrm{RGDP_{(t-q1)}} \uparrow \mathrm{Psugar_{(t-q2)}} \uparrow \mathrm{REER_{(t-q3)}} \uparrow \mathrm{Dex_{(t-q4)}} \uparrow \mathrm{DC19_{(t-q5)}} \downarrow\big)$$

Where:

Y_t	; The total value of Egyptian imports in million dollars.
YM_t	; The value of Egyptian imports of meat.
YD_t	; The value of Egyptian imports of dairy products.
YO_t	; The value of Egyptian imports of oils.
YC_t	; The value of Egyptian imports of cereals.
YWh_t	; The value of Egyptian imports of wheat and meslin.
YS_t	; The value of Egyptian imports of sugars.
$RGDP_t$	; GDP in millions of dollars at constant prices (2015 = 100).
$Pall_t$	; Relative prices (world price index/consumer price index in Egypt) (2015 = 100).
$Pmeat_t$	; The relative prices of meat.
$Pdairy_t$	; The relative prices of milk.
$Poils_t$	; The relative prices of oils.
$Pcereals_t$	; The relative prices of cereals.
$Psugar_t$	; The relative prices of sugars.
$REER38_t$	; Effective real exchange rate for trading partners.
Dex_t	; Dummy variable that expresses the liberalisation of the exchange rate for the local currency.
$Dc19_t$	; Dummy variable that expresses COVID-19.

Based on the results in Table 1, the ARDL (p, q) has been applied as proposed by Pesaran *et al.* (2001) by using the bounds testing approach to cointegration to estimate the long- and short-term elasticity; based on the study variables, the ARDL models (p, q1, q2, ..., qn) can be estimated using the following formulas:

$$\begin{aligned} ln\mathrm{Y_t} = {} & \beta_0 + \pi_1 \mathrm{lnY_{t-1}} + \pi_2 \mathrm{lnRGDP_{t-1}} + \pi_3 \mathrm{lnPall_{t-1}} + \pi_4 \mathrm{lnREER_{t-1}} \\ & + \pi_5 \mathrm{Dex_{t-1}} + \pi_6 \mathrm{DC19_{t-1}} + \sum_{i=1}^{p} \gamma_i \Delta \mathrm{lnY_{t-i}} \\ & + \sum_{i=1}^{q1} \delta_1 \Delta \mathrm{lnRGDP_{t-i}} + \sum_{i=1}^{q2} \delta_2 \Delta \mathrm{lnPall_{t-i}} \\ & + \sum_{i=1}^{q3} \delta_3 \Delta \mathrm{lnREER_{t-i}} + \sum_{i=1}^{q4} \delta_4 \Delta \mathrm{Dex_{t-i}} \\ & + \sum_{i=1}^{q5} \delta_5 \Delta \mathrm{DC19_{t-i}} + \varepsilon_t \rightarrow \text{Total Import Model} \end{aligned}$$

$$\begin{aligned} ln\mathrm{YM_t} = {} & \beta_0 + \pi_1 \mathrm{lnYM_{t-1}} + \pi_2 \mathrm{lnRGDP_{t-1}} + \pi_3 \mathrm{lnPmeat_{t-1}} + \pi_4 \mathrm{lnREER_{t-1}} \\ & + \pi_5 \mathrm{Dex_{t-1}} + \pi_6 \mathrm{DC19_{t-1}} + \sum_{i=1}^{p} \gamma_i \Delta \mathrm{lnYM_{t-i}} \\ & + \sum_{i=1}^{q1} \delta_1 \Delta \mathrm{lnRGDP_{t-i}} + \sum_{i=1}^{q2} \delta_2 \Delta \mathrm{lnPmeat_{t-i}} \\ & + \sum_{i=1}^{q3} \delta_3 \Delta \mathrm{lnREER_{t-i}} + \sum_{i=1}^{q4} \delta_4 \Delta \mathrm{Dex_{t-i}} \\ & + \sum_{i=1}^{q5} \delta_5 \Delta \mathrm{DC19_{t-i}} + \varepsilon_t \rightarrow \text{Meat Model} \end{aligned}$$

$$\begin{aligned} ln\mathrm{YD_t} = {} & \beta_0 + \pi_1 \mathrm{lnYD_{t-1}} + \pi_2 \mathrm{lnRGDP_{t-1}} + \pi_3 \mathrm{lnPdairy_{t-1}} + \pi_4 \mathrm{lnREER_{t-1}} \\ & + \pi_5 \mathrm{Dex_{t-1}} + \pi_6 \mathrm{DC19_{t-1}} + \sum_{i=1}^{p} \gamma_i \Delta \mathrm{lnYD_{t-i}} \\ & + \sum_{i=1}^{q1} \delta_1 \Delta \mathrm{lnRGDP_{t-i}} + \sum_{i=1}^{q2} \delta_2 \Delta \mathrm{lnPdairy_{t-i}} \\ & + \sum_{i=1}^{q3} \delta_3 \Delta \mathrm{lnREER_{t-i}} + \sum_{i=1}^{q4} \delta_4 \Delta \mathrm{Dex_{t-i}} \\ & + \sum_{i=1}^{q5} \delta_5 \Delta \mathrm{DC19_{t-i}} + \varepsilon_t \rightarrow \text{Dairy Model} \end{aligned}$$

$$\begin{aligned} ln\mathrm{YO_t} = {} & \beta_0 + \pi_1 \mathrm{lnYO_{t-1}} + \pi_2 \mathrm{lnRGDP_{t-1}} + \pi_3 \mathrm{lnPoils_{t-1}} + \pi_4 \mathrm{lnREER_{t-1}} \\ & + \pi_5 \mathrm{Dex_{t-1}} + \pi_6 \mathrm{DC19_{t-1}} + \sum_{i=1}^{p} \gamma_i \Delta \mathrm{lnYO_{t-i}} \\ & + \sum_{i=1}^{q1} \delta_1 \Delta \mathrm{lnRGDP_{t-i}} + \sum_{i=1}^{q2} \delta_2 \Delta \mathrm{lnPoils_{t-i}} \\ & + \sum_{i=1}^{q3} \delta_3 \Delta \mathrm{lnREER_{t-i}} + \sum_{i=1}^{q4} \delta_4 \Delta \mathrm{Dex_{t-i}} \\ & + \sum_{i=1}^{q5} \delta_5 \Delta \mathrm{DC19_{t-i}} + \varepsilon_t \rightarrow \text{Oils Model} \end{aligned}$$

$$\begin{aligned} ln\mathrm{YC_t} = {} & \beta_0 + \pi_1 \mathrm{lnYC_{t-1}} + \pi_2 \mathrm{lnRGDP_{t-1}} + \pi_3 \mathrm{lnPcereals_{t-1}} + \pi_4 \mathrm{lnREER_{t-1}} \\ & + \pi_5 \mathrm{Dex_{t-1}} + \pi_6 \mathrm{DC19_{t-1}} + \sum_{i=1}^{p} \gamma_i \Delta \mathrm{lnYC_{t-i}} \\ & + \sum_{i=1}^{q1} \delta_1 \Delta \mathrm{lnRGDP_{t-i}} + \sum_{i=1}^{q2} \delta_2 \Delta \mathrm{lnPcereals_{t-i}} \\ & + \sum_{i=1}^{q3} \delta_3 \Delta \mathrm{lnREER_{t-i}} + \sum_{i=1}^{q4} \delta_4 \Delta \mathrm{Dex_{t-i}} \\ & + \sum_{i=1}^{q5} \delta_5 \Delta \mathrm{DC19_{t-i}} + \varepsilon_t \rightarrow \text{Cereals Model} \end{aligned}$$

$$\begin{aligned} ln\mathrm{YWH_t} = {} & \beta_0 + \pi_1 \mathrm{lnYWH_{t-1}} + \pi_2 \mathrm{lnRGDP_{t-1}} + \pi_3 \mathrm{lnPcereals_{t-1}} \\ & + \pi_4 \mathrm{lnREER_{t-1}} + \pi_5 \mathrm{Dex_{t-1}} + \pi_6 \mathrm{DC19_{t-1}} \\ & + \sum_{i=1}^{p} \gamma_i \Delta \mathrm{lnYWH_{t-i}} + \sum_{i=1}^{q1} \delta_1 \Delta \mathrm{lnRGDP_{t-i}} \\ & + \sum_{i=1}^{q2} \delta_2 \Delta \mathrm{lnPcereals_{t-i}} + \sum_{i=1}^{q3} \delta_3 \Delta \mathrm{lnREER_{t-i}} \\ & + \sum_{i=1}^{q4} \delta_4 \Delta \mathrm{Dex_{t-i}} + \sum_{i=1}^{q5} \delta_5 \Delta \mathrm{DC19_{t-i}} + \varepsilon_t \\ & \rightarrow \text{Wheat Model} \end{aligned}$$

$$\begin{aligned} ln\mathrm{YS_t} = {} & \beta_0 + \pi_1 \mathrm{lnYS_{t-1}} + \pi_2 \mathrm{lnRGDP_{t-1}} + \pi_3 \mathrm{lnPsugar_{t-1}} + \pi_4 \mathrm{lnREER_{t-1}} \\ & + \pi_5 \mathrm{Dex_{t-1}} + \pi_6 \mathrm{DC19_{t-1}} + \sum_{i=1}^{p} \gamma_i \Delta \mathrm{lnYS_{t-i}} \\ & + \sum_{i=1}^{q1} \delta_1 \Delta \mathrm{lnRGDP_{t-i}} + \sum_{i=1}^{q2} \delta_2 \Delta \mathrm{lnPsugar_{t-i}} \\ & + \sum_{i=1}^{q3} \delta_3 \Delta \mathrm{lnREER_{t-i}} + \sum_{i=1}^{q4} \delta_4 \Delta \mathrm{Dex_{t-i}} \\ & + \sum_{i=1}^{q5} \delta_5 \Delta \mathrm{DC19_{t-i}} + \varepsilon_t \rightarrow \text{Sugar Model} \end{aligned}$$

Where β_0 expresses the intercept parameter; ε_t represents the random error term; π_i denotes the long-term coefficients; γ_i, δ_j stand for the short-term coefficients; and the long-term effect of the variable $\mathrm{lnRGDP_{t-1}}$, for example, is $[-\pi_2/\pi_1]$, as the short-term effect of the real GDP variable is the first difference coefficient δ_1. The ARDL-UECM models were estimated using the following formulas:

$$\begin{aligned} \Delta ln\mathrm{Y_t} = {} & \beta_0 + \delta_1 \Delta \mathrm{lnRGDP_t} + \delta_2 \Delta \mathrm{lnPall_t} + \delta_3 \Delta \mathrm{lnREER_t} + \delta_4 \Delta \mathrm{Dex_t} + \delta_5 \Delta \mathrm{DC19_t} \\ & + \psi \mathrm{ECT_{t-1}} \end{aligned}$$

$$\begin{aligned} \Delta ln\mathrm{YM_t} = {} & \beta_0 + \delta_1 \Delta \mathrm{lnRGDP_t} + \delta_2 \Delta \mathrm{lnPmeat_t} + \delta_3 \Delta \mathrm{lnREER_t} + \delta_4 \Delta \mathrm{Dex_t} \\ & + \delta_5 \Delta \mathrm{DC19_t} + \psi \mathrm{ECT_{t-1}} \end{aligned}$$

$$\begin{aligned} \Delta lnYD_\mathrm{t} = {} & \beta_0 + \delta_1 \Delta \mathrm{lnRGDP_t} + \delta_2 \Delta \mathrm{lnPdairy_t} + \delta_3 \Delta \mathrm{lnREER_t} + \delta_4 \Delta \mathrm{Dex_t} \\ & + \delta_5 \Delta \mathrm{DC19_t} + \psi \mathrm{ECT_{t-1}} \end{aligned}$$

$$\begin{aligned} \Delta lnYO_\mathrm{t} = {} & \beta_0 + \delta_1 \Delta \mathrm{lnRGDP_t} + \delta_2 \Delta \mathrm{lnPoils_t} + \delta_3 \Delta \mathrm{lnREER_t} + \delta_4 \Delta \mathrm{Dex_t} \\ & + \delta_5 \Delta \mathrm{DC19_t} + \psi \mathrm{ECT_{t-1}} \end{aligned}$$

$$\begin{aligned} \Delta lnYC_\mathrm{t} = {} & \beta_0 + \delta_1 \Delta \mathrm{lnRGDP_t} + \delta_2 \Delta \mathrm{lnPcereals_t} + \delta_3 \Delta \mathrm{lnREER_t} + \delta_4 \Delta \mathrm{Dex_t} \\ & + \delta_5 \Delta \mathrm{DC19_t} + \psi \mathrm{ECT_{t-1}} \end{aligned}$$

$$\begin{aligned} \Delta lnYWH_\mathrm{t} = {} & \beta_0 + \delta_1 \Delta \mathrm{lnRGDP_t} + \delta_2 \Delta \mathrm{lnPcereals_t} + \delta_3 \Delta \mathrm{lnREER_t} + \delta_4 \Delta \mathrm{Dex_t} \\ & + \delta_5 \Delta \mathrm{DC19_t} + \psi \mathrm{ECT_{t-1}} \end{aligned}$$

$$\begin{aligned} \Delta lnYS_\mathrm{t} = {} & \beta_0 + \delta_1 \Delta \mathrm{lnRGDP_t} + \delta_2 \Delta \mathrm{lnPsugar_t} + \delta_3 \Delta \mathrm{lnREER_t} + \delta_4 \Delta \mathrm{Dex_t} \\ & + \delta_5 \Delta \mathrm{DC19_t} + \psi \mathrm{ECT_{t-1}} \end{aligned}$$

Since $\mathrm{ECT_{t-1}}$ expresses the error-correction limit, ψ represents the speed of the correction, and the most significant statistical formula that is consistent with economic logic and with different lag periods has been reached, the model formula ARDL (p, q) is appropriate via the lowest value of information criteria, such as AIC, SC and HQ. According to the boundary test, the F-distribution is non-standard, where the two critical values are taken from the Pesaran table.

It had predicted according to the parameters estimated from the cointegration models, as well as the forecast based on the seasonality of demand using SARIMA, where the time series can be clarified

$\{Z_t | t = 1,2, \ldots, k\}$ with the $SARIMA(p,d,q)(P,D,Q)_S$ model and mean μ, as well as with the Box–Jenkins model (Abdel Rahman, 2002), as shown below:

$$\Phi(B^S)\varphi(B)(1-B)^d(1-B^s)^D(Y_t-\mu) = \Theta(B^S)\theta(B)\varepsilon_t \rightsquigarrow SARIMA(p,d,q)(P,D,Q)_S$$

AR	$\varphi(B) = 1 - \varphi_1 B - \varphi_2 B^2 - \cdots - \varphi_p B^p$	Polynomials of the order p
Seasonal AR	$\Phi(B^S) = 1 - \Phi_1 B^S - \Phi_2 B^{2S} - \cdots - \Phi_P B^{PS}$	Polynomials of the order P
MA	$\theta(B) = 1 - \theta_1 B - \theta_2 B^2 - \cdots - \theta_q B^q$	Polynomials of the order q
Seasonal MA	$\Theta(B^S) = 1 - \Theta_1 B^S - \Theta_2 B^{2S} - \cdots - \Theta_Q B^{QS}$	Polynomials of the order Q

p	: Non-seasonal AR model rank	P	: Seasonal AR Model Rank
d	: Non-seasonal integration (number of differences)	D	: Seasonal integration (number of seasonal differences)
q	: Non-seasonal MA model rank	Q	: Seasonal MA model rank
S	: Period of seasonal pattern recurrence equal to 12 for monthly data	Y_t	: actual time series data during period t
		B	: lag factor

ε_t : It is the white noise process under the hypothesis of $\varepsilon_t \sim \mathrm{WN}(0, \sigma^2)$, and the root of each $\varphi(Z) = 0, \theta(Z) = 0$ must lie outside the unit circle.

2.2. Data:

To solve the above problem, this study uses macroeconomic indicator data from the World Bank, the Organisation for Economic Cooperation and Development and the Arab Monetary Fund. The Egyptian economic policies implemented to confront the COVID-19 repercussions from 14 February 2020 to 20 December 2021 were obtained through the Ministry of Planning and Economic Development, IFPRI, Egypt and the World Trade Organization.

The data for the food groups studied from January 2010–April 2021 were related to joint integration models obtained from the Comtrade database, the Food and Agriculture Organization of the United Nations (FAO), the Central Agency for Public Mobilisation and Statistics, the Bruegel database, the UNCTAD and other relevant studies.

3. Literature Review

3.1. The Impact of COVID-19 on Some Global Macroeconomic Indicators:

The pandemic is causing massive economic disruptions at the international level through concurrent shocks, including decreased domestic and external demand, lower oil prices, disruptions in trade and global value chains and tightened financial conditions due to lower global demand. Commodity prices fell; the Egyptian economy stumbled as a result of the Egyptian government's rapid response and proactive measures to limit the virus's impact, which were implemented in March 2020 (IFPRI, 2022).

3.1.1. GDP Growth Responses at the Global Economy Level During the COVID-19 Pandemic

The global economy witnessed a recession during the emergence of COVID-19 – the 'deepest global recession' since World War II – with the contraction rate reaching about 3.5% in 2020. However, economists expect a strong recovery in economic growth. The World Bank anticipates that in 2021 the economy will expand by about 5.6% at the global level, and about 5.4% in advanced economies, while the International Monetary Fund (IMF, 2021), expects the global economy will grow by 5.9% and 4.9% in 2021 and 2022, respectively. In addition, the global recession's economic impact will largely occur in emerging markets and other developing countries that depend on global trade, tourism and remittances from abroad (World Bank, 2021; 2022; Figure 1).

Figure 1: The evolution of the recession state that most of the world's economies are experiencing in light of the continuing COVID-19 outbreak in comparison to the Egyptian economy from 2000–2023.

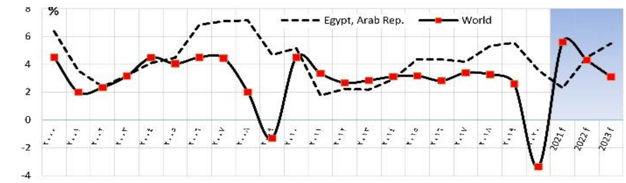

Source (data collected and calculated):
- www.worldbank.org
- World Bank (2021) Global Economic Prospects, Washington, DC, World Bank. https://doi.org/10.1596/978-1-4648-1665-9

In this context, World Bank experts (World Bank, 2021; 2022) believe that there are two scenarios for global economic growth beyond 2021. The first is a 'faltering recovery', in which the global economy slows in response to the possibility of another COVID-19 outbreak, leading to increasing inflationary pressures and a sharp tightening in global financial conditions over the next two years. The second scenario is 'sustainable expansion', which simulates COVID-19 containment due to a vaccine and reopening, implying that current signs of recovery may be fleeting and that policymakers must exploit one of the current opportunities to implement reforms that enhance economic growth.

The Fund also warns of the consequences of different paths of recovery among countries based on vaccine availability. A rapid return to normal economic activity is expected in advanced economies. The rise in inflationary pressures is one of the most serious challenges facing both advanced and developing economies (Arab Monetary Fund, 2021). According to the Organisation for Economic Cooperation and Development (OECD statistical databases), the global economy will grow by 2.56% in 2021 and 4.458% in 2022. These expectations are attributed to the global economy's strong recovery as a result of accommodative fiscal and monetary policies, as well as the steady increase in the number of vaccinators. However, this recovery is uneven, with several countries still facing various challenges that threaten the recovery's sustainability.

3.1.2. GDP Growth Responses at the Egyptian Economy Level During the COVID-19 Pandemic

The Egyptian economy is an exceptional case during the emergence of COVID-19. At a time when the rest of the world was experiencing economic stagnation, the Egyptian economy grew in 2020, as shown in Figure 1. However, Egypt's GDP growth rate in 2019 was about 5.6%, indicating that it still decreased by about 1.9% points in 2020 and 3.3% points in 2021, ending with 3.6% and 2.3%, respectively. This is due to a set of measures implemented by the Egyptian government to address the COVID-19 repercussions, which is a part of the economic reforms that succeeded in confronting the crisis. The stimulation of internal demand for goods and services, as well as the lack of a trend towards complete closure also aided the country's GDP during the pandemic (Arab Monetary Fund, 2021).

In 2022, the World Bank (2021) expects the growth rate to increase to about 4.5%, while the Arab Monetary Fund (2021) anticipates it to rise to about 5.4%. This indicates an increase in the overall growth rate, which could be due to a rise in the number of vaccine recipients in Egypt and the second phase of the structural economic reform programme. The Egyptian government programme aimed at making all commercial, agricultural, industrial and economic activities flexible, as well as the possibility of increasing the number of tourists, as shown in Figure 1.

3.1.3. World Trade Volume in Relation to Egyptian Trade

The global health crisis caused by the COVID-19 outbreak has had severe repercussions on the level of economic activity (International Monetary Fund, 2020), with general bans and widespread closures being implemented to slow the spread of the virus. Ninety-three countries applied temporary export measures, while 105 countries implemented temporary import measures to facilitate access to essential medical supplies or food (International Trade Centre, 2020).

Consequently, world exports and imports were affected by the COVID-19 outbreak and the closure of borders between some countries, including China, the European Union and the United States, as shown in Figure 2. In 2020, The World Trade Organization expected a 13% to 32% decline in commodities in global trade due to the pandemic. In 2021, international trade was expected to recover at rates ranging from 21% to 24%, and the state adopted appropriate policies to support it and controlled the rates of disease outbreaks by receiving vaccines (International Monetary Fund, 2020).

In 2022, a relative recovery of the international trade exchange was expected (Arab Monetary Fund, 2021; International Monetary Fund, 2021), including at the level of merchandise trade or some services trade activities, as a result of increased levels of flexibility in global supply chains, the benefits of digital transformation in trade exchange processes and the liberalisation of international trade flows. Countries with an increasing share of tourism and travel in GDP are expected to witness a significant decline, with travel restrictions and ongoing fears of contagion likely to affect tourism activity.

Figure 2: The global and Egyptian trade movement in light of the COVID-19 outbreak.

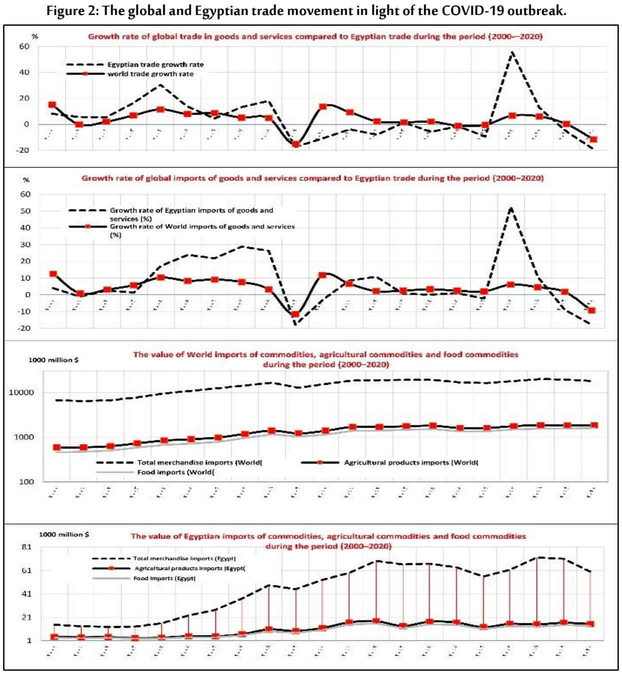

At the local level, the Information and Decision Support Centre (2021) indicated that Egypt's five largest trading partners account for 41% of Egyptian imports in 2020, with China in the lead with about 18%, followed by America, Germany, Italy and Turkey at 7%, 6%, 5% and 5%, respectively. However, the volume of Egypt's non-oil imports from China fell to \$11.6 billion in 2020, compared to \$12.4 billion in 2019. In terms of Egyptian exports, the United Arab Emirates (UAE), Saudi Arabia, Turkey, America and Italy accounted for 35% of them in 2020. Also, Egypt's non-oil exports to the UAE increased by about \$2.9 billion in 2020, compared to \$2.1 billion in 2019.

3.2. Egypt's COVID-19 Economic Policy Responses in Comparison:

Despite the Egyptian government's ban and social distancing measures, certain economic policies were needed to withstand the repercussions of the COVID-19 outbreak from 14 February 2020 to 20 December 2021 (IFPRI, 2022; Ministry of Planning and Economic Development, 2021; World Trade Organization, 2021):

3.2.1. Implemented Egyptian Trade Policies

The Egyptian government has banned the export of pulses twice, the first was on 28 March 2020, and the second was in October 2020, each of which lasted for three months. To achieve self-sufficiency in strategic food products, the import of white sugar was banned for three months to protect the local industry from fluctuations in international sugar prices.

The Egyptian government has changed the policies of import tenders for wheat, in which suppliers, starting on 3 April 2020, were required to replace any shipments affected by COVID-19 transport restrictions with wheat from another location and bear the cost. A shipment of wheat that had already been sold to an Egyptian buyer was suspended by Romania, due to its ban on grain exports to countries outside the European Union, including Egypt.

3.2.2. Some of the Implemented Egyptian Fiscal and Monetary Policies

The Central Bank of Egypt implemented two policies. The first focused on expanding investment opportunities to relieve expected pressures on the currency by issuing certificates of deposits at a new rate of 15% for one year. The second centred on the reduction in interest rates, which resulted in a 3% drop in borrowing rates to stimulate industries and increase demand.

In conjunction with the state's monetary policy, on 15 March 2020, the Central Bank and the Prime Ministry implemented a set of fiscal policies directed to private companies in the form of financial support, without specifying a time for these policies to end, as well as rural income assistance. They aided Egyptian farmers by extending the moratorium on agricultural land taxation for two years and deferring the payment of farmers' debts for six months. The wheat price was set at 700 pounds/ardab (1 ardab = 155 kg) to support farmers and increase wheat reserves, covering seven months.

4. Results and Discussion

4.1. Demand Determinants for Some Egyptian Food Imports in Light of COVID-19:

4.1.1. Unit Root Test Results (Augmented Dickey–Fuller Test)

The unit root was tested to determine the cointegration rank (Shrestha and Chowdhury, 2005) of the previously described models' studied variables and choose the analysis method. If all variables are stationary at level, the OLS–VAR method is used, but if all the variables are un-stationary at level, the VECM method or the causality test is used. Moreover, if some of the variables are stationary at level and the others with first difference, the ARDL models are used (Table 1).

Table 1: Unit root test of the determinants of Egyptian food import demand during the COVID-19 pandemic from January 2020 – April 2021 using the augmented Dickey–Fuller test. The results of first differences.

variable	Intercept(η_{μ})		Trend and intercept ($\eta_{\mu\tau}$)		Decision
	Test statistic	AIC	Test statistic	AIC	
Y_t	(-12.64)***	15.72	(-12.61)***	15.73	I(1)
YM_t	(-12.13)***	9.58	(-12.12)***	9.59	I(1)
YD_t	(-14.44)***	7.93	(-14.39)***	7.94	I(1)
YO_t	(-19.46)***	10.17	(-19.39)***	10.19	I(1)
YC_t	(-10.39)***	11.85	(-10.36)***	11.87	I(1)
YWh_t	(-11.49)***	12.68	(-11.53)***	12.69	I(1)
YS_t	(-17.05)***	9.73	(17.01)***	9.74	I(1)
$RGDP_t$	(-15.18)***	19.04	(-14.75)***	19.06	I(1)
$Pall_t$	(-7.66)***	-2.95	(-7.63)***	-2.93	I(1)
$Pfood_t$	(-7.46)***	-3.52	(-7.43)***	-3.51	I(1)
$Pmeat_t$	(-10.44)***	-4.15	(-10.52)***	-4.15	I(1)
$Pdairy_t$	(-8.99)***	-3.50	(-9.01)***	-3.49	I(1)
$Poils_t$	(-8.26)***	-2.66	(-6.82)***	-2.68	I(1)
$Pcereals_t$	(-9.77)***	-2.94	(-9.75)***	-2.92	I(1)
$Psugar_t$	(-7.81)***	-1.54	(-6.43)***	-1.96	I(1)
$REER38_t$	(-10.28)***	6.71	(-10.24)***	6.73	I(1)

Notes: ***, ** and * denote significance at 1%, 5% and 10% levels, respectively.
Critical values 10% 5% 1%
Withconst (n = 135): -2.578 -2.883 -3.479
Withconst & time (n = 135): -3.147 -3.444 -4.027

Source: Authors' results were obtained using the EViews9.5 econometrics package.

Table 1 shows the unit root test results (using the augmented Dickey–Fuller test), highlighting the stationarity of some study variables after obtaining the first differences. In the Egyptian Total Imports model, some independent variables (i.e. $RGDP_t$, $Pall_t$, $REER38_t$) were non-stationary at level but stationary in the first differential, integrated at order one [I (1)]. Moreover, in the meat group model, some independent variables (i.e. $RGDP_t$, $Pmeat_t$, $REER38_t$) were non-stationary at level but stationary in the first differential. In the dairy group model, some independent variables (i.e. $RGDP_t$, $Pdairy_t$, $REER38_t$) were also non-stationary at level but stationary in the first differential. Similarly, in the oil group model, several of the independent variables (i.e. $RGDP_t$, $Poils_t$, $REER38_t$) were non-stationary at level but stationary in the first differential.

With the cereal and wheat models, the independent variables $RGDP_t$, $Pcereals_t$ and $REER38_t$ were found to be non-stationary at level but stationary in the first differential. It was also found that in the sugar model, the independent variables $RGDP_t$, $Psugar_t$ and $REER38_t$ were non-stationary at level but were stationary in the first differential. Therefore, one of the solutions to the series' instability is to take the difference.

4.1.2. Discussing the Results of the Estimated Models

Table 2 shows that the explanatory variables studied (i.e. the value of imports with a lag period, GDP, relative prices, the effective real exchange rate, the liberation policy and COVID-19) explain about 46% of the changes in the total demand for Egyptian imports. This percentage improved at the level of the meat group and dairy models, while it decreased at the level of the cereals group. This required studying the demand for wheat alone, without the other cereals, resulting in a high interpretation rate of about 92%.

It was found that the error correction limit coefficient was negative and statistically significant for the studied models. This means that the determinants of demand for total Egyptian imports and the imports of the studied food groups cointegrate when the value of imports is a dependent variable; this effect is supported in short- and long-term dynamic models (Table 2).

Furthermore, the estimated intercept parameter of the two models of demand for meat and sugar imports was found to be positive, indicating that there is a part of the import at the level of those two groups that does not depend on the studied factors, particularly consumer response to import prices. This may be due to the seasonality of demand for meat during Eid al-Adha and for sugar during the holy month of Ramadan each year. In addition, the state's support for some imported food groups obscures the consumers' real demand for sugar in response to prices, especially wheat, which accounts for the largest share of the Egyptian food import basket (Table 2).

It was also revealed that the explanatory variables studied were integrated at a significant level of 1%. The F-statistic value was greater than the critical values for the corresponding upper bound at the 1% level of significance for each of the total imports of meat, dairy, oil, cereals and sugar, while there is a cointegration between the studied variable of wheat demand at a significant level of 5%. This means that there is a long-term equilibrium relationship between the variables studied in those models (Table 2).

4.2. Discussion of the Results in Relation to the Estimated Variables:

4.2.1. Real GDP

The real GDP variable had a positive and statistically significant impact on total Egyptian imports in both the short and long term. According to economic theory, an increase in real GDP always leads to an increase in import level, as the coefficient of elasticity was about 1.11 and 1.77 in the short and long term, respectively (Table 2).

For the studied food group, the impact of the real GDP variable on dairy, oils, cereals and wheat imports was positive. However, it was not significant at the level of the wheat model alone. A 1% increase in real GDP will result in an increase in dairy, oils, cereals and wheat imports by 3.58%, 10.04%, 1.63% and 0.26% in the short term, and about 7.31%, 7.73%, 2.33% and 2.4% in the long term, respectively. In contrast, a 1% increase in real GDP will lead to a decrease in meat and sugar imports by 2.76% and 6.2% in the short term, and about 7.57% and 10.6% in the long term, respectively (Tables 2, 3 and 4).

4.2.2. Relative Prices

To obtain suitable time series for relative prices, the same base year was used for the studied consumer price indices (2015 = 100), and the index numbers for food groups were taken from the FAO data. The relative prices (Monthly Bulletin of Statistics [MBS] Online) of the demand model for total Egyptian imports were estimated by dividing the world price index by the consumer price index in Egypt. Moreover, the relative prices of the demand model for meat imports were estimated by dividing the meat price index (taken from the FAO data) by the consumer price index for the food and drink section of Egypt (CAPMAS); a similar formula was employed for the rest of the relative prices of the food group models studied.

The effect of relative prices on total Egyptian imports was positive in the short and long term, with elasticity coefficients of 0.045 and 0.072, respectively, but it was statistically insignificant (Table 2).

At the food group level (Tables 2, 3 and 4), it was found that the relative prices of dairy, oils, cereals and wheat had a positive and statistically significant effect on their total imports in the long term, with elasticity coefficients of 0.82, 1.53, 0.48 and 0.844, respectively. Meanwhile, the relative prices of meat and sugar had a negative and statistically significant effect on their total imports in the long term, with elasticity coefficients of -2.74 and -1.33, respectively. This means that imports of milk, oils, cereals and wheat are less sensitive to price increases than imports of meat and sugar.

It was also discovered that the relative prices of meat, dairy, oils, wheat and sugar had a negative impact on their total imports in the short term, with elasticity coefficients of -0.35, -0.99, -0.63, -0.31 and -0.78, respectively. This means that imports of these food groups are more sensitive to price increases in the short term, but meat and oils were statistically insignificant (Tables 2, 3 and 4).

Table 2: Cointegration estimation using the bound test for total, meat and dairy imports from January 2020–April 2021.

Dependent Var	Total import, $Ln(Y_t)$		Meat import, $Ln(YM_t)$		Dairy import, $Ln(YD_t)$	
	Coef.	t	Coef.	t	Coef.	t
$\Delta Ln(RGDP_t)$	1.11	2.80***	-2.76	-2.2**	3.58	3.6***
$\Delta Ln(Pall_t)$	0.045	0.816				
$\Delta Ln(Pmeat_t)$			-0.35	-0.451		
$\Delta Ln(Pmeat_{t-1})$			1.72	2.19**		
$\Delta Ln(Pdairy_t)$					-0.99	-1.89*
$\Delta Ln(reer38_t)$			0.68	3.1***	-1.15	2.36**
ΔDex_t	-0.084	-1.77*			-0.54	-2.5**
$\Delta Dc19_t$	-0.152	-3.3***	-0.158	-1.82*	-0.04	-0.43
ETC_{t-1}	-0.626	-7.4***	-0.37	-5.5***	-0.49	-6.5***
$Ln(RGDP_t)$	1.77	3.05***	-7.57	-2.3**	7.31	3.9***
$Ln(Pall_t)$	0.072	0.820				
$Ln(Pmeat_t)$			-2.74	-3.0***		
$Ln(Pdairy_t)$					0.82	2.5**
$Ln(reer38_t)$			1.88	3.7***	-0.85	-1.23
Dex_t	-0.133	-1.83*			-1.10	-2.8***
$Dc19_t$	-0.24	-3.87***	-0.43	-1.92*	-0.08	-0.43
C	-13.75	-1.87*	91.34	2.2**	-84.1	-3.7***
R^2	0.46		0.696		0.49	
F-statistic	24.03***		44.45***		17.3***	

Notes: ***, ** and * denote significance at 1%, 5% and 10% levels, respectively.
F-bounds test = 10.46, 5.12, 6.88 for total, meat and dairy imports, respectively, Critical Value [I (1)] = 5.06 (1%), [I (0)] = 3.74 (1%)
Source: Authors' results were obtained using the EViews9.5 econometrics package and Gretl

4.2.3. Effective Real Exchange Rate

Effective real exchange rates for 38 of Egypt's trading partners were obtained from Bruegel databases during the study period; since it is a case of depreciation of the local currency, the economic theory refers to an increase in exports and a decrease in import volume. For this reason, an overvaluation of the local currency can artificially make imports less expensive when compared to locally exchangeable products, increasing imports.

At the level of the studied food group (Table 2), the effective real exchange rate had a positive and statistically significant effect on meat imports in both the short and long term. This implies a deterioration of the local currency value against a rise of the foreign currency value as a result of higher demand for meat imports and the consequent price increases. This is because the short- and long-term elasticity were at about 0.68 and 1.88, respectively.

It was also found that the effective real exchange rate had a negative impact on dairy, oils and wheat imports in the short and long term, with elasticity coefficients of -1.15, -3.92 and -0.39 in the short term and about -0.85, -0.49 and -0.65 in the long term, respectively. However, it was statistically insignificant in the long term (Tables 2, 3 and 4).

4.2.4. The Impact of the Economic Reform Policy

Egypt's great dependence on global markets for food imports led to high import costs; nonetheless, the macroeconomic situation has significantly improved as a result of the immediate responses implemented by the Egyptian government with the support of the International Monetary Fund since November 2016 (Ali and Attala, 2021; USDA, 2020). Accordingly, it was necessary to include a dummy variable in the studied models to express the economic reform policy as one during the period (November 2016–April 2021) and zero otherwise.

In the short term, the economic reform policy had a negative and significant impact on total, dairy, oils and wheat imports. Their elasticity coefficients were -0.084, -0.54, -2.07 and -0.20, respectively. Moreover, the policy had a positive yet insignificant effect on sugar imports, with an elasticity coefficient of 0.49 (Tables 2, 3 and 4).

In the long term, it was found that the economic reform policy had a negative and significant impact on total and dairy imports, with elasticity coefficients of -0.133 and -1.10, respectively. In addition, the policy had a positive yet insignificant impact on imports of oils, cereals, wheat and sugar, with elasticity coefficients of 0.219, 0.10, 0.24 and 0.84, respectively (Tables 2, 3 and 4).

4.2.5. Impact of COVID-19

COVID-19-induced shocks (AMIS, 2020; USDA, 2020; Mohamed, 2015) began to affect food markets in April 2020. This led to a decline in oil prices and a slowdown in feed demand. Also, despite sufficient global supplies, many major exporters imposed various forms of trade restrictions to increase domestic food security. Accordingly, a dummy variable was introduced in the studied models to express the impact of COVID-19 on Egyptian imports, especially food groups, with a value of one during the period (March 2020–April 2021) and zero otherwise.

According to the estimates (Tables 2, 3 and 4), COVID-19 had a negative impact on total Egyptian imports and all the studied imported food groups. The elasticity coefficients for total, meat, dairy, oil, cereal, wheat and sugar imports were -0.152, -0.158, -0.04, -0.33, 0.088, -0.01 and 0.71, respectively, in the short term. In the long term, these were about -0.24, -0.43, -0.08, -0.62, -0.125, 0.08, and -1.2, respectively. This shows the significance of total Egyptian, meat, oil and sugar imports.

Table 3: Cointegration estimation for oil and sugar imports using the bound test during the period (January 2020–April 2021).

Dependent Var	Oils import, $Ln(YO_t)$		Sugar import, $Ln(YS_t)$	
	Coef.	t	Coef.	t
$\Delta Ln(RGDP_t)$	10.41	2.7***	-6.2	-2.6**
$\Delta Ln(Poils_t)$	-0.63	-0.83		
$\Delta Ln(Psugar_t)$			-0.78	-2.1**
$\Delta Ln(reer38_t)$	-3.92	-2.1**		
ΔDex_t	-2.07	-1.97*	0.49	1.59
$\Delta Dc19_t$	-0.33	-1.7*	-0.71	-2.4**
ETC_{t-1}	-0.54	-6.8***	-0.59	-7.4***
$Ln(RGDP_t)$	7.73	2.3**	-10.6	-2.6**
$Ln(Poils_t)$	1.53	3.5***		
$Ln(Psugar_t)$			-1.33	-2.1**
$Ln(reer38_t)$	-0.49	-0.37		
Dex_t	0.219	0.286	0.84	1.63
$Dc19_t$	-0.62	-1.7*	-1.2	-2.6**
C	-91.1	-2.4**	138	2.7***
$\bar{R}^2$	0.45		0.42	
F-statistic	7.94***		18.5***	
F-Bounds Test Critical Value	8.02*** [I(1)] = 4.68 (1%), [I (0)] = 3.41 (1%)		11.12*** [I(1)] = 5.06 (1%), [I (0)] = 3.74 (1%)	

Notes: ***, ** and * denote significance at 1%, 5% and 10% level, respectively.
Source: Authors' results were obtained using the EViews9.5 econometrics package and Gretl.

Table 4: Cointegration estimation for cereal and wheat imports using the bound test during the period (January 2020–April 2021).

Dependent Var	Cereal import, $Ln(YC_t)$		Wheat import, $Ln(YWh_t)$	
	Coef.	t	Coef.	t
$\Delta Ln(Pcereals_t)$	0.337	2.03**	-0.31	-3.1***
$\Delta Ln(reer38_t)$			-0.39	-2.1**
ΔDex_t	0.07	0.786	-0.20	-1.9*
ΔDex_{t-1}			-0.09	-1.9*
$\Delta Dc19_t$	-0.088	-0.95	-0.01	-0.47
ETC_{t-1}	-0.70	-8.3***	-0.11	-3.9***
$Ln(RGDP_t)$	2.33	2.06**	2.4	1.29
$Ln(Pcereals_t)$	0.48	2.1**	0.844	2.7***
$Ln(reer38_t)$			-0.65	-0.97
Dex_t	0.10	0.786	0.24	0.603
$Dc19_t$	-0.125	-0.97	-0.08	-0.47
C	-23.7	-1.66	-19.4	-0.90
$\bar{R}^2$	0.19		0.922	
F-statistic	6.12***		145.4***	
F-Bounds Test Critical Value	13.93*** [I(1)] = 5.06 (1%), [I (0)] = 3.74 (1%)		4.31** [I(1)] = 3.79 (5%), [I (0)] = 2.62 (5%)	

Notes: ***, ** and * denote significance at 1%, 5% and 10% levels, respectively.
Source: Authors' results were obtained using the EViews9.5 econometrics package and Gretl.

4.3. Expected Demand for Egyptian Imports from Specific Food Groups:

Forecasting the value of Egyptian imports from some of the studied food groups during the period (January 2022–December 2023) can be studied using parameters estimated from ARDL models, as well as forecasting based on demand seasonality using SARIMA models. The following are the prediction results (Tables 5 and 6):

- Total Egyptian imports are expected to reach their lowest level during April 2022 (about $5,643 million, compared to about $5,624 million in April 2023). The maximum is expected in December 2022 with about $6,608 million, compared to about $6,928 million in December 2023 ($ARIMA(1.1.1)X(2.0.2)_{12}$). The average is about $6,253 million per month in 2022, and about $6,429 million per month in 2023 (ARDL model).
- According to the seasonality forecast, total Egyptian imports from the meat group would reach a low in February 2022 at about $135.2 million, and a high of about $266.8 million in July 2022. The average is about $77 million per month in 2022 and about $97.15 million per month in 2023.
- According to the seasonal forecast, total Egyptian imports of the dairy group would reach a low in October 2022 at about $26.7 million, and a high of about $73.4 million in April 2022. The average is about $119.3 million per month in 2022 and about $175 million per month in 2023.
- At the level of the total Egyptian imports of oils, the values estimated from the ARDL model increased when compared to the prediction via the $ARIMA(2.0.0)X(2.1.2)_{12}$ model. According to the seasonal forecast, it would reach a low of about $30.7 million in December 2022, and a high of about $157 million in May 2022.
- On the level of total Egyptian wheat imports, it has been found that the best model that can be relied upon in future prediction is Brown's linear exp.; thus, the total value of Egyptian imports is expected to reach a minimum of $169.7 million in July 2022 and a maximum of about $255.9 million in January 2023.
- It was found that the total Egyptian imports of sugar would reach a low of about $6.78 million in March 2023, and a high of about $38.9 million in September 2022. The expected average is about $41.4 million per month in 2022 and about $58.7 million per month in 2023.

Table 5: Forecasting the value of Egyptian meat, dairy and total imports in million dollars during the period (January 2022–December 2023).

Appreciation method	Total Imports		Meat Imports		Dairy Imports	
	ARDL,F	SARIMA	ARDL,F	SARIMA	ARDL,F	SARIMA
2022M01	6002	5852	88.1	151.8	86.1	49.6
2022M03	6268	6377	72.4	137.1	105.9	67.1

2022M05	6303	5987	73.0	166.3	118.9	72.5
2022M07	6298	6253	74.4	266.8	125.8	50.4
2022M09	6280	6051	75.5	228.8	128.8	38.8
2022M11	6271	6052	81.3	197.7	139.4	39.4
2023M01	6420	5849	83.0	165.7	157.0	53.6
2023M03	6459	6632	83.8	171.8	167.5	67.6
2023M05	6442	6027	90.8	164.9	173.8	66.6
2023M07	6439	6310	99.7	183.1	176.4	49.1
2023M09	6420	6175	103.9	197.3	177.9	37.2
2023M10	6411	6411	109.5	175.6	173.4	31.2
2023M11	6398	6230	114.3	184.4	191.5	41.5
2023M12	6384	6928	123.4	145.4	195.1	50.1
ThaiL coef.	0.06	-	0.19	-	0.33	-

Notice: -ARDL, F denote prediction using the ARDL Model according to the results in Table 2.
- SARIMA denotes prediction using seasonal ARIMA (SARIMA) models.
Source: Authors' results were obtained using the EViews9.5 econometrics package and STATGRAPHICS.

Table 6: Estimated value of Egyptian imports of oil, sugar, cereal and wheat in million dollars during the period (January 2022–December 2023).

Appreciation method	Oil Imports		Sugars Imports		Wheat Imports	
	ARDL,F	SARIMA	ARDL,F	SARIMA	ARDL,F	SARIMA
2022M01	419.4	96.5	11.56	17.82	256.8	221.6
2022M03	371.0	121.4	6.92	9.53	236.2	235.4
2022M05	376.5	157.0	32.11	15.95	237.7	236.9
2022M07	370.4	77.3	47.14	19.53	172.6	169.7
2022M09	352.2	80.0	77.19	38.88	226.4	225.7
2022M11	391.5	91.1	90.74	33.95	231.9	231.2
2023M01	536.9	101.6	46.68	15.35	256.6	255.9
2023M03	521.2	122.2	29.05	6.78	236.0	235.4
2023M05	542.1	137.8	54.94	13.06	237.5	236.9
2023M07	539.5	90.7	50.64	16.56	172.4	169.7
2023M09	528.4	78.2	94.89	35.87	226.3	225.7
2023M10	488.0	101.0	89.43	32.23	234.0	233.5
2023M11	618.5	96.8	87.67	30.93	231.7	231.2
2023M12	658.2	49.8	60.17	21.57	209.7	209.2
ThaiL coef.	0.50	-	0.38	-	0.08	-

Notice: -ARDL, F denotes prediction using the ARDL Model according to the results in Tables 3 and 4.
- SARIMA denotes prediction using seasonal ARIMA (SARIMA) models.
Source: Authors' results were obtained using the EViews9.5 econometrics package and STATGRAPHICS.

5. Conclusion

The results are as follows:

- When the demand for food commodities, especially wheat and meslin, is studied separately from the demand for the rest of the cereal group, the estimated results improve significantly.
- In addition to the state's support for some imported food groups, the demand for the meat and sugar groups is due to the seasonality of demand, making the consumer's real demand for them in response to prices unclear, especially wheat and meslin, which accounts for the largest share of the Egyptian food import basket.
- An increase in real GDP always leads to a boost in import level.
- Importing meat, dairy, oils, wheat and sugar is more sensitive to price increases in the short term.
- In the long term, importing milk, oils, cereal and wheat is less sensitive to price increases than importing meat and sugar.
- COVID-19 had a negative impact on total Egyptian imports and all imported food groups studied.

Biographies

Mona Hosny Gad Ali

Department of Agricultural Policy Research and Project Evaluation, Agricultural Economics Research Institute, Agriculture Research Centre, Cairo, Egypt, 00201010698859, jasmen_m201050@yahoo.com

Dr Ali, PhD (Ain Shams University), is an Egyptian Assistant Professor of Agricultural Economics and a member of the Centre for Contract Agriculture research team. Preparation and analysis of reports on the current situation and outlook for several commodities, as well as food security reports. Experience with statistical analysis approaches such as the Simultaneous Equation Model (2SLS, 3SLS, SUR, GLS), Data Envelopment Analysis (DEA), VAR Model, ARDL Model, AIDS Model and Linear Expenditure System using Excel, SPSS, EViews, DEA P., ITSM, STATGRAPHICS, Gretl, and others.

Eman Fakhry Yousif Ahmed

Department of Agricultural Economics, Faculty of Agriculture, Ain Shams University, Cairo, Egypt, 00201141722425, eman_youssif1@agr.asu.edu.eg

Dr Ahmed, PhD (Ain Shams University), is an Egyptian who has spent the last 21 years working in the Department of Agricultural Economics, Faculty of Agriculture, Ain Shams University. She is fluent in Arabic and English. She has 6 e-books in various fields from the Faculty of Agriculture, Ain Shams University: four in Arabic (agricultural economic resources, agricultural price analysis, project feasibility study and international agricultural trade) and two in English (economics of Egyptian agriculture and business administration).

References

Abdel Rahman, A.M. (2002). *Turuq Altanabuw Alahisayiy, Aljuz' Alawl* 'Statistical Prediction Methods, Part 1'. Available at: http://www.abarry.ws/StatisticalForecast.pdf (accessed on 6/03/2022) [In Arabic]

Agricultural Market Information System. (2020). *AMIS Market Monitor*. Available at: https://reliefweb.int/sites/reliefweb.int/files/resources/AMIS_Market_Monitor_current.pdf (accessed on 06/03/2021)

Aljebrin, M.A. and Ibrahim, M.A. (2012). *The determinants of the demand for imports in GCC countries*. International Journal of Economics and Finance, **4**(3), 126–38.

Ali, M.H.G. and Attala, M.A. (2021). Dirasat 'iiqtisadiat qiasiat li'athar muhadadat altadakhum aleam wa'asear alghidha' ealaa alaistiqrar alaiqtisadaa faa misr 'An econometric study of the impact of headline and food price inflation determinants on economic stability in Egypt'. *JAESS*, **12**(7), 573–85, DOI: 10.21608/JAESS.2021.81903.1012. [In Arabic]

Arab Monetary Fund. (2021). *Arab Economic Outlook Report*. Available at: https://www.amf.org.ae/en/arab-economic-outlook/fifteenth-edition-arab-economic-outlook-report-october (accessed on 21/12/2021)

Box, E.P., Jenkins, G.M., Reinsel, G.C. and Ljung, G.M. (2016). *Time Series Analysis: Forecasting and Control*. 5th edition. New Jersey: John Wiley and Sons Inc. Available at: https://eg1lib.org/book/2613644/2c4d65 (accessed on 06/03/2022)

Bruegel. (2021). *Real Effective Exchange Rates for 178 Countries: A New Database, Bruegel*. Available at: https://www.bruegel.org/ (accessed on 26/01/2022)

Egypt's Central Agency for Public Mobilization and Statistics (CAPMAS). (2010 -2021). *Annual Consumer Price Index Urban: According to the Food, Beverage and Tobacco Section*. Available at: https://www.capmas.gov.eg/ (accessed on 06/10/2021)

IFPRI, Egypt. (2022). *COVID-19 Food Policy Response Monitor for Egypt*. Available at: https://egyptssp.ifpri.info/2022/03/06/COVID-19-food-policy-response-monitor-for-egypt-2/(accessed on 06/03/2022)

IFPRI 'International Food Policy Research Institute'. (2020). *COVID-19 and the Egyptian Economy, from Reopening to Recovery: Alternative Pathways and Impacts on Sectors, Jobs, and Households*. Available at: https://doi.org/10.2499/p15738coll2.134162 (accessed on 27/01/2022)

Information and Decision Support Center (IDSC). (2021). *Egypt: IDSC*. Available at: https://www.idsc.gov.eg/InfoMedia/List/1 (accessed on 21/01/2022)

International Monetary Fund (IMF). (2020). *World economic outlook: the great lockdown*. Washington, DC. Available at: https://www.imf.org/en/Publications/WEO/Issues/2020/04/14/weo-april-2020 (accessed on 27/01/2022)

International Monetary Fund (IMF). (2021). *World economic outlook: Recovery during pandemic—health concerns, supply disruptions, and price pressures*. Washington, DC. Available at: https://www.imf.org/en/Publications/WEO/Issues/2021/10/12/world-economic-outlook-october-2021 (accessed on 06/03/2022)

International Trade Center (ITC). (2020). *SME Competitiveness Outlook: Executive summary—COVID-19: The great lockdown and its impact on small business*. Available at: https://www.intracen.org/uploadedFiles/intracenorg/Content/Publications/ITC_SMECO-2020ExSummary_EN_web.pdf(accessed on 06/03/2022)

MBS 'Monthly Bulletin of Statistics Online'. (2010-2021). *Price indices: Consumer Price Indices*. UNdata, a World of Information. Available at: https://unstats.un.org/unsd/mbs/app/DataSearchTable.aspx (accessed on 06/10/2021)

Ministry of Planning and Economic Development. (2021). *Egypt's COVID-19 Policy Tracker*. Available at: http://policytracker.mped.gov.eg/(accessed on 20/12/2021)

Mohamad, N.M.A. (2015). Egypt's trade during COVID-19 crisis: An assessment of responses, and implications. *International Trade* *and Cooperation, Egypt*, PART 1. 7(n/a), 107–120. Available at: https://www.kiep.go.kr/galleryExtraDownload.es?bid=0026&list_no=9311&seq=7 (accessed on 14/12/2021)

OECD Statistics 'Organization for Economic Co-operation and Development'. (2010 -2021). *GDP in Millions of Dollars at Constant Prices*. Available at: https://stats.oecd.org/index.aspx?DataSetCode=EO (accessed on 06/10/2021)

Pesaran, M.H., Shin, Y. and Smith, R.J. (2001). Bounds testing approaches to the analysis of level relationships. *Journal of Applied Econometrics*, **16**(3), 289–326.

Rihan, M.K. (2021). *Muhadarat Fi Alaiqtisad Alqiasii* 'Lectures in econometrics'. Cairo, Egypt: Ain Shams University Library. [In Arabic]

Safoulanitou, L.N. and Ndinga, M.A. (2010). An empirical analysis of the determinants of food imports in Congo. *African Economic Research Consortium: Research Department, Working Papers*, **195**(n/a), 9–25. Available at: https://aercafrica.org/wp-content/uploads/2018/07/RP195.pdf (accessed on 16/12/2021)

Shrestha, M.B. and Chowdhury, K. (2005). ARDL modelling approach to testing the financial liberalization hypothesis. *Department of Economics, University of Wollongong, WP* **05-15**(n/a), 1–30. Available at: https://ro.uow.edu.au/commwkpapers/121(accessed on 06/03/2022)

UN Comtrade 'International Trade Statistics Database'. (2010 -2021). *The value of Egyptian imports from some food groups in million dollar*s. Available at: https://comtrade.un.org/db/mr/rfcommoditieslist.aspx(accessed on 06/10/2021)

USDA 'Foreign Agricultural Service'. (2020). *Grain: World Markets and Trade, Global Market Analysis*. Available at: https://downloads.usda.library.cornell.edu/usda-esmis/files/zs25x844t/q811m414s/ff365r040/grain.pdf (accessed on 30/06/2021)

USDA 'Foreign Agricultural Service'. (2020). *Egypt Retail Foods*. Report number: EG2020-0032. Available at: https://www.fas.usda.gov/data/egypt-retail-foods-4 (accessed on 30/06/2021)

Vickers, B., Ali, S., Zhuawu, C., Zimmermann, A., Attaallah, H. and Dervisholli, E. (2020). Impacts of the COVID-19 Pandemic on Food Trade in the Commonwealth. Commonwealth Secretariat and FAO: London International Trade Working Paper 2020/15. ISSN: 2413 –3175.

World Bank. (2021). *Global Economic Prospects*. Washington, DC. DOI: 10.1596/978-1-4648-1665-9. Available at: https://elibrary.worldbank.org/doi/abs/10.1596/978-1-4648-1665-9 (accessed on 26/12/2021)

World Bank. (2022). *Global Economic Prospects*. Available at: https://elibrary.worldbank.org/doi/abs/10.1596/978-1-4648-1758-8 (accessed on 06/03/2022)

World Bank. (2000 - 2020). *Imports of Goods and Services (Annual % Growth*). Available at: https://data.worldbank.org/ (accessed on 03/03/2022)

World Trade Organization 'WTO'. (2021).COVID-19: *Agricultural Measures*. Available at: https://www.wto.org/english/tratop_e/covid19_e/ag_trade_measures_e.htm (accessed on 06/12/2021)

WTO 'Stats'. (2000 -2020). *Growth Rate of Trade of Goods and Services*. Available at: https://stats.wto.org/(accessed on 03/03/2022)

The Scientific Journal of King Faisal University

Basic and Applied Sciences

Ultra-Short Pulses Generation of Free Electron Laser

Thair Abdulkareem Khalil Al-Aish[1] and Hanady Amjed Kamil[2]

[1] Department of Physics, College of Education for Pure Sciences Ibn Al-Haitham, University of Baghdad, Baghdad, Iraq
[2] Directorate of Education of First Karkh, Ministry of Education, Baghdad, Iraq

LINK	RECEIVED	ACCEPTED	PUBLISHED ONLINE	ASSIGNED TO AN ISSUE
https://doi.org/10.37575/b/sci/220045	06/10/2022	01/12/2022	01/12/2022	01/12/2022
NO. OF WORDS	**NO. OF PAGES**	**YEAR**	**VOLUME**	**ISSUE**
3643	5	2022	23	2

ABSTRACT

The major problem facing the development of civil and military laser applications lies in the attempts to obtain short pulses close to the length of the bond that connects the atoms of certain materials. In this paper, an executable program has been constructed to simulate and analyze the generation of ultra-short free electron laser pulses; it contains several parameters directing the creation of short pulses within a time duration of femtoseconds (fs). On analyzing the simulation results, it can be concluded that it is possible to generate ultra-short pulses with a duration of about 7.4 – 87.4 fs with the storage ring free-electron laser Fabry–Perot resonator with noticeably short wavelengths (11.4–190.2) for the output laser beam.

KEYWORDS

Homogenous broadening; SR-FEL; undulator; energy spread gain; Q- switching

CITATION

Al-Aish, T.A.K. and Kamil, H.A. (2022). Ultra-short pulses generation of free electron laser. *The Scientific Journal of King Faisal University: Basic and Applied Sciences*, **23**(2), 28–32. DOI: 10.37575/b/sci/220045

1. Introduction

The number of laser applications is constantly increasing in the civil and military fields due to the generation of very short-wavelength laser beams. The fields in which these are used include nonlinear optics, the spectroscopy of materials, medical treatment, the destruction of military targets, plasma remote sensing, high-speed photography, space, and astronomy (Haarlammert and Zacharias, 2009; Kamil and Al-Aish, 2022; Al-Aish and Jawad, 2017; Benson *et al*., 2011; Varro, 2012).

Conventional laser oscillators have been used to create these ultra-short pulses primarily using the mode-locked oscillation technique. The pulse generated by this technique has a duration roughly the inverse of the gain width. One of the first successful attempts to generate ultrashort pulses was in 1986, using Ti:Sapphire as a preferred gain medium with good beam quality and high output power (Moulton, 1986).

However, due to the short bandwidth of the pulses, this technique has fallen short of producing a series of short pulses in less than a picosecond. Nonetheless, the gain spectrum width of a free electron laser (FEL) is essentially very wide in contrast to that of most conventional lasers, thus enabling a FEL to create ultra-short pulses. The storage ring free-electron laser (SR-FEL) is a self-mode locked optical system and represents a technique to produce a shorter-wavelength beam laser (Varro, 2012; Hannon, 2008; Mahmood and Al-Aish, 2020; Al-Aish, 2017; Kamil *et al*., 2019).

In this paper, the undulator parameters have been altered to produce short pulses at a femtosecond time duration with the Fabry–Perot resonator. In contrast, the optical pulses of an SR-FEL are several picoseconds, full width at half maximum.

2. The Technique and Implementation of the Work

The ability of energy spread sources to prompt additional gain broadening, homogeneously and non-homogeneously, should be considered when designing a Fabry–Perot resonator for the FEL gain medium. This will simultaneously lead to an increase in longitudinal modes, besides those already present within the gain profile in the ultra-short wavelength region, mainly owing to long cavity length. These broadening effects significantly influence the small signal gain and saturation intensity. The homogenous broadening $\left(\frac{\Delta\omega}{\omega}\right)_{hom}$ (as a gain spectrum) is related to L_u (the length of the undulator) and N_u (the number of electron wavelengths), which can be written as

$$\left(\frac{\Delta\omega}{\omega}\right)_{hom} = \frac{1}{2}\, N_u \tag{1}$$

where ω is the angular frequency.

The number N_u is given by the equation below (Al-Aish and Kamil, 2022; Parvin *et al*., 1997; Mehravaran and Dorranian, 2010; Kawamura *et al*., 1987):

$$N_u = \frac{L_u}{\lambda_u} \tag{2}$$

where L_u is the length of the undulator and λ_u is the wavelength of an electron.

The nonhomogeneous broadening is due to energy spread $\in_s$ of the electron beam and emittance $\in_i$ $(i = x + y)$ as follows (Parvin *et al*., 2012):

$$\in_s = 4\,\sigma\, N_u \tag{3}$$

where σ is the natural root-mean-square energy spread with values ranging from 0.001-0.0001.

Fine alteration of pulse duration can be conducted by adjusting the energy emittance $\in_i$ of the storage ring, such that equal to zero is in correspondence with fs duration and $\in_s$ equal to one is attributed to the picosecond pulse length.

The emittance of the $\in_i$ electron beam is one of the critical factors concerning the storage ring for FEL operations. At relatively small values of energy spread, the total broadening $\left(\frac{\Delta\omega}{\omega}\right)_{total}$ in an FEL for both homogenous and nonhomogeneous effects can be written as (Parvin *et al*., 2012; Dattoli *et al*., 1993).

$$\left(\frac{\Delta\omega}{\omega}\right)_{total} = \left(\frac{\Delta\omega}{\omega}\right)_{hom} \sqrt{1 + \in_i^2 + \in_s^2} \tag{4}$$

The gain broadening corresponds to a greater number of longitudinal modes, leading to shorter pulses and a significant reduction in the output intensity. Absorption losses in SR-FEL are the main reason

Corresponding Author: Thair Abdulkareem Khalil Al-Aish 009647801693969, thair.ak.i@ihcoedu.uobaghdad.edu.iq

behind power growth and gain reduction. A small signal gain and corresponding losses of the resonator are the basis of the FEL system.

The primary purpose of technology is to create a laser beam that has high power with exceedingly small $\in_s$, broadening, and $\in_i$. The generation of pulses of femtosecond duration, where one or sometimes several pulses are circulating in the laser resonator, is mainly achieved through the mode-locking technique. For passive Q switching (self-Q switching), the losses are automatically modulated with a saturable absorber. Modulation is responsible for the loss in the resonator, which arises from the radiative damping of electron energy in the undulator (Penzkofer, 1988).

The round-trip time τ_r of the resonator is equal to the inverse value of the free spectral range (FSR) of the resonator (see Figure 1), which is given by the equation (Parvin *et al.*, 2012; Dattoli *et al.*, 1993; Penzkofer, 1988; Davis, 1996).

$$\tau_r = \frac{1}{FSR} = \frac{2L}{c} \tag{5}$$

where L is the length of the Fabry–Perot resonator and c is the velocity of light.

The number of the n_{mode} is given by

$$n_{mode} = \Delta v_{gain}\, \tau_r \tag{6}$$

where Δv_{gain} is the gain bandwidth. The duration of the mode-locked pulses τ can be written in the following equation:

$$\tau = \frac{\tau_r}{n_{mode}} = \frac{1}{\Delta v_{gain}} \tag{7}$$

Figure 1: The round-trip time duration of the mode-locked pulses.

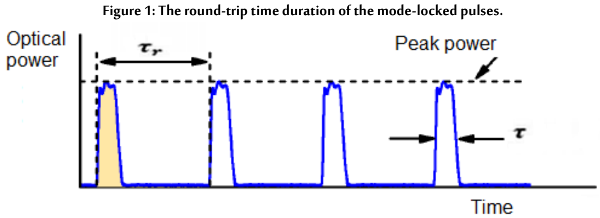

The homogenous broadening $\left(\frac{\Delta\omega}{\omega}\right)_{hom}$, depends on the number of undulator periods N_u in the half-maximum full width, and can be written in the following equation:

$$\Delta\omega_{hom} = \frac{2\pi c}{\lambda\, N_u} \tag{8}$$

where λ is the wavelength of the output laser.

$$\lambda = \frac{\lambda_u}{2\gamma^2}\left(1 + \frac{k^2}{2}\right) \tag{9}$$

$$\gamma = \frac{E_e}{m_e c^2} \tag{10}$$

$$k = \frac{e\, \beta\, \lambda_u}{2\pi\, m_e c} \tag{11}$$

where γ is the relativistic Lorentz factor, E_e the electron beam energy, m_e the electron mass, β the magnetic field, and k the undulator parameter (Dhedan *et al.*, 2022; Ali *et al.*, b2022; Al-Aish *et al.*, 2019).

The FEL comprises four main parts (electron gun, linear accelerator, undulator, and Fabry–Perot resonator), as shown in Figure 2.

Figure 2: The four main parts of the FEL.

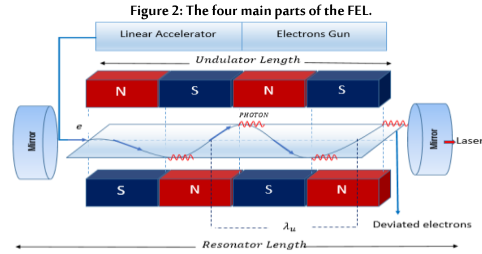

The reflection of the output mirror R is given below (Davis, 1996):

$$R = 1 - A - T \tag{12}$$

where A is the absorption loss and T the transmittance of the output mirror. It can be calculated by (Parvin *et al.*, 2012):

$$T = \frac{AR[g_0 L + \ln R]}{1 - R} \tag{13}$$

where g_0 is the small signal gain per unit length, written by the equation emittance ($\in_i$ $(i = x + y) \approx 0$) (Parvin *et al.*, 2012; Dattoli *et al.*, 1993; Penzkofer, 1988; Davis, 1996; Dhedan *et al.*, 2022):

$$g_0 = \frac{16\pi\, k^2\, N_u\, I}{\lambda_u\, I_0 \gamma \left(\sqrt{1 + \in_s^2}\right)(1 + k^2)} \tag{14}$$

where I is the current of the electron beam.

The gain and gain factor in the stimulated emission process is considered small, so it is necessary to reduce all the causes of loss in the laser device, including the loss caused by its absorption by the resonator mirrors. Mirrors for the SR-FEL in ultrashort wavelength must have high reflectivity and resistance against coherent photons.

Many layers of dielectric coatings with high reflectivity are used to coat the mirrors instead of metallic coatings (such as aluminum oxide, hafnium oxide, and hybrid systems combining fluoride and oxide materials) since dielectric coatings do not absorb light, and nearly 100% of the incident light becomes reflective without any loss.

These successive layers of thickness (t) are $\lambda/4$, and successive refractive indexes (high then low, as shown in Figure 3) are successively deposited on the glass substrate. Because of the difference in the phase that occurs at the point of contact of any two layers, all the reflected rays are in one phase and interfere constructively. Usually, more than twenty layers are used to obtain a reflectivity of approximately 99.9% (Wieduwilt *et al.*, 2014; Zegadi *et al.*, 2022).

Figure 3: Successive refractive indexes (high, then low).

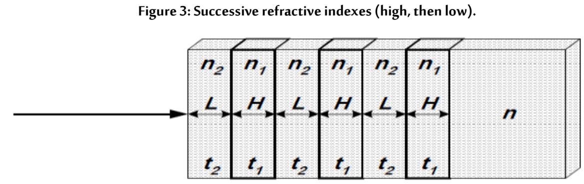

The reflectivity of the reflected light in the case of a multi-layered mirror is calculated as follows:

$$R = \frac{n_2^{q+1} - n\, n_1^{q-1}}{n_2^{q+1} - n\, n_1^{q+1}} \tag{15}$$

where n is the refractive index of the substrate, n_1 the high dielectric layer refractive index, n_2 the low dielectric layer refractive index, and q the number of layers.

While the reflectivity of the metal mirror is dependent on the density of metal ρ (g/cm3) and the wavelength λ (in micrometer) of the laser used, reflectivity is as follows:

$$R = 100 - 3.65\sqrt{\frac{\rho}{\lambda}} \tag{16}$$

The mode-locked pulse duration τ following a Lorentzian distribution, is given by the equation (Parvin *et al.*, 2012; Dattoli *et al.*, 1993; Penzkofer, 1988; Davis, 1996; Kawamura *et al.*, 1987):

$$\tau = \frac{2.773}{\sqrt{1+\epsilon_s^2}}\left(\frac{\lambda\, L_u}{c\, \lambda_u}\right) \tag{17}$$

In the SR-FEL resonator, the pulses are equal to the round-trip time τ_r. This achieves the gain switching necessary to produce a series of pulses, which requires a suitable gain broadening. When the bunching frequency v is tuned to the FSR, the repetition time of the pulse becomes equal to τ_r.

$$v = FSR = \frac{1}{\tau_r} = \frac{C}{2L} \tag{18}$$

3. Results and discussion of the simulation

An executable program was constructed using Matlab 2019 software (as shown in Figure 4) to simulate and analyze the generation of shorter pulses of FEL. It contained several parameters to produce shorter pulses of femtosecond duration.

Figure 4: The implementation of an executable program to produce shorter pulses in fs duration and summary of the values of the optimum parameters for the FEL.

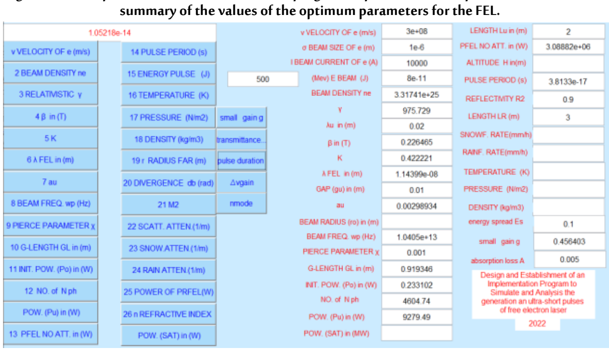

Table 1 shows the results of the simulation for the relation between the energy spread $\in_s$ vs. the small signal gain g_0 and transmittance T when the wavelength of the electron λ_u is equal to 0.02, 0.03, and 0.04.

Table 1: The results of simulation for $\in_s$ vs g_0 and T.

$\in_s$	$\lambda_u = 0.02$ $\lambda = 11.4\,nm$ $k = 0.422221$		$\lambda_u = 0.03$ $\lambda = 42.11\,nm$ $k = 0.654025$		$\lambda_u = 0.04$ $\lambda = 190.2\,nm$ $k = 4.01353$	
	g_0	T	g_0	T	g_0	T
0.1	0.456403	0.0568732	3.80327	0.5087	10.2715	1.38191
0.2	0.449776	0.0559785	3.74810	0.501252	10.1229	1.36185
0.3	0.439345	0.0545704	3.66124	0.489526	9.88896	1.33027
0.4	0.425890	0.0527539	3.54921	0.474402	9.58717	1.28953
0.5	0.410280	0.0506466	3.41923	0.456855	9.23696	1.24225
0.6	0.393347	0.0483606	3.27821	0.437817	8.85696	1.19095
0.7	0.375805	0.0459925	3.13212	0.418095	8.46318	1.13779
0.8	0.358215	0.0436178	2.98562	0.398317	8.06822	1.08447
0.9	0.340986	0.0412919	2.84211	0.378944	7.68124	1.03223
1	0.324392	0.0390517	2.70389	0.360284	7.30844	0.981898

Figure 5-a shows the effect of changing the energy spread $\in_s$ on the small signal gain g_0, which has an inverse relationship according to equation 14. A decrease in the value of the small signal gain g_0 due to increasing values of the energy spread $\in_s$ is noted. This effect becomes more evident at high values of the electron wavelength λ_u. This is due to a decrease in the number N_u values according to equation 2 and a decrease in the homogenous broadening $\left(\frac{\Delta\omega}{\omega}\right)_{hom}$ according to equation 8. All these decrease the average number of coherent photons resulting from the passage of accelerated electrons through the β magnetic field.

Table 1 shows an increase in the value of the wavelength of the electron λ_u as a result of an increase in the wavelength values of the output laser λ and k according to equations 9 and 11. It is also noted that at the short wavelength of the resulting laser beam (λ = 11.4 nm), the gain g_0 is smaller compared to that at a longer wavelength (λ = 190.2 nm).

Figure 5-b shows the effect of changing the energy spread $\in_s$ on the transmittance T. Where the relation is inverse according to equations 13 and14, a decrease in the value of the transmittance T due to an increase in the energy spread $\in_s$ value is noted. The effect is more evident at higher values of electron wavelength λ_u, resulting from an increase in the gain values, and thus the transmittance T according to equation 13.

Tables 2, 3, and 4 show the results of the simulation for the relation between the energy spread $\in_s$ vs. the mode-locked pulse duration τ, the gain bandwidth Δv_{gain}, and the number of n_{mode} when the wavelength of the electron λ_u is equal to 0.02, 0.03, and 0.04.4.

Table 1: The simulation results for ∈s vs. τ ∆vgain and nmode when λu = 0.02 m.

$\in_s$	$\lambda_u = 0.02$m	$\tau_r = 20ns$	$L = 3$m
	$\tau(fs)$	$\Delta v_{gain} s^{-1} T$	n_{mode} M
0.1	10.5218	95.0407	1.9008
0.2	10.3689	96.4419	1.9288
0.3	10.1283	98.733	1.9746
0.4	9.81797	101.854	2.0370
0.5	9.45792	105.731	2.1146
0.6	9.06737	110.286	2.2057
0.7	8.66279	115.436	2.3087
0.8	8.25713	121.108	2.4221
0.9	7.85980	127.230	2.5445
1	7.47715	133.741	2.6748

Table 2: The simulation results for ∈s vs. τ∆vgain and nmode when λu = 0.03 m.

$\in_s$	$\lambda_u = 0.03$m	$\tau_r = 20ns$	$L = 3$m
	$\tau(fs)$	$\Delta v_{gain} s^{-1} T$	n_{mode} M
0.1	25.8203	38.7292	0.7745
0.2	25.4452	39.3001	0.7860
0.3	24.8547	40.2338	0.8046
0.4	24.0932	41.5056	0.8301
0.5	23.2096	43.0856	0.8617
0.6	22.2512	44.9414	0.8988
0.7	21.2583	47.0403	0.9408
0.8	20.2629	49.3514	0.9870
0.9	19.2878	51.8462	1.0369
1	18.3488	54.4995	1.0899

Table 3: The simulation results for ∈s vs. τ∆vgain and nmode when λu = 0.04 m.

$\in_s$	$\lambda_u = 0.04$m	$\tau_r = 20ns$	$L = 3$m
	$\tau(fs)$	$\Delta v_{gain} s^{-1} T$	n_{mode} M
0.1	87.4701	11.4325	0. 2286
0.2	86.1993	11.601	0.2320
0.3	84.1991	11.8766	0.2375
0.4	81.6191	12.252	0.2450
0.5	78.6259	12.7185	0.2543
0.6	75.3791	13.2663	0.2653
0.7	72.0157	13.8859	0.2777
0.8	68.6434	14.568	0.2913
0.9	65.3403	15.3045	0.3060
1	62.1592	16.0877	0.3217

Figure 5-c shows the effect of changing the energy spread $\in_s$ on the pulse duration τ. Where the relation is inverse according to equation 17, there is a decrease in the value of the pulse duration τ as a result of an increase in the energy spread $\in_s$ value. The effect is more evident at high values of the electron wavelength λ_u, where short pulses between $\tau = 7.47715\, fs$ and $\tau = 87.4701\, fs$ are generated by the Fabry–Perot resonator.

Figure 5-d and Figure 5-e show the effect of changing the energy spread $\in_s$ on the gain bandwidth Δv_{gain} and the number of n_{mode} when the wavelength of the electron λ_u is equal to 0.02, 0.03, and 0.04. Where a direct relation is present according to equations 7, 14, and 17, there is an increase in the values of the gain bandwidth Δv_{gain} and the number of n_{mode} as a result of increasing energy spread $\in_s$ values. The effect is more evident at high values of electron wavelength λ_u.

Figure 5: The effect of changing the energy spread $\in_s$ on the small signal gain g_0, transmittance T, pulse duration τ, gain bandwidth Δv_{gain} and number of n_{mode}.

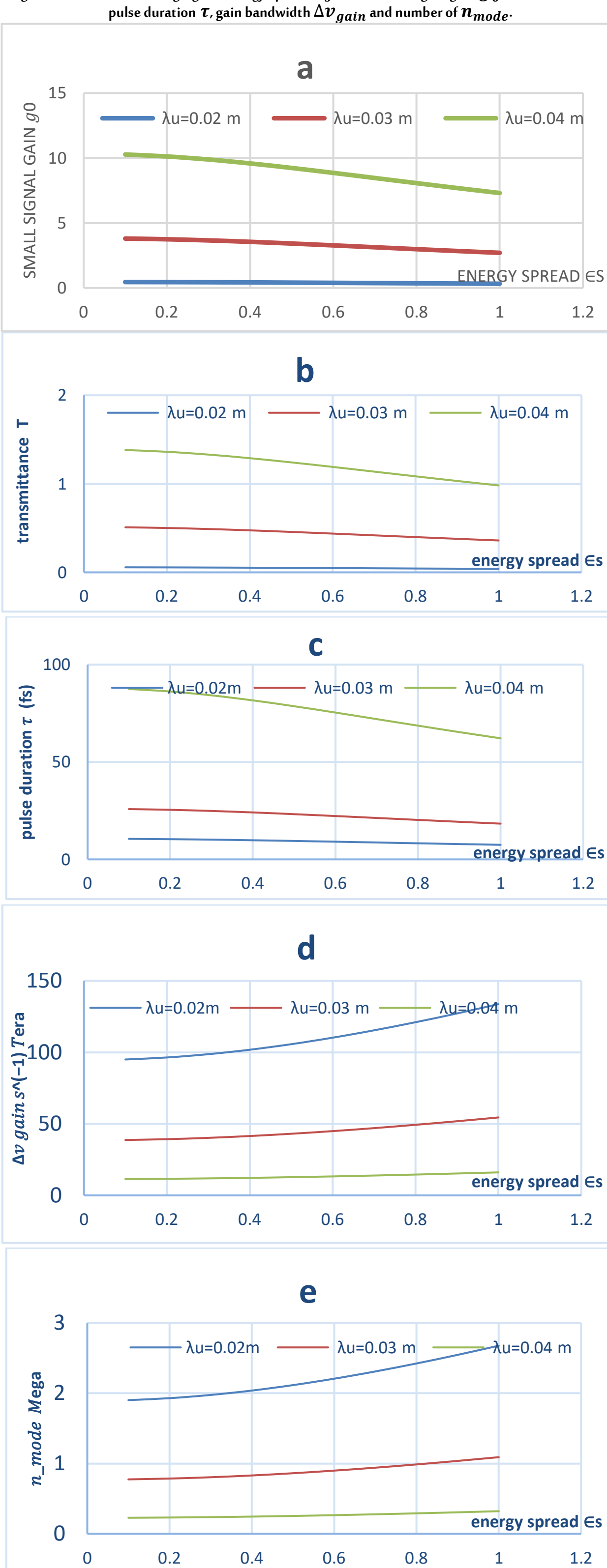

Table 5: The simulation results for the relation between the length of an ideal Fabry–Perot cavity L vs. the bunching frequency v and the round-trip time.

Table5: The results of simulation for L vs. v and τ_r.

L	v(MHz)	$\tau_r(ns)$
1	150	6.66
2	75	13.3
3	50	20
4	37.5	26.66
5	30	33.33
6	25	40
7	21.4	46.66
8	18.7	53.33
9	16.6	60
10	15	66.66

Figure 6-a and Figure 6-b show the effect of changing the length of the resonator L on the bunching frequency v and the round-trip time τ_r. There is an inverse relation with the bunching frequency v and a direct relation with the round trip-time τ_r according to equation 18. In a Fabry–Perot resonator, the condition of resonance requires a match between v and FSR, so the corresponding parameters were determined for τ_r and gain switching. The round-trip time $\tau_r = 20ns$ was chosen (as shown in Table 2), corresponding to the length $L = 3\ m$ used in the simulation.

Figure 6: shows the effect of changing length of resonator L on both the bunching frequency and the round-trip time τ_r.

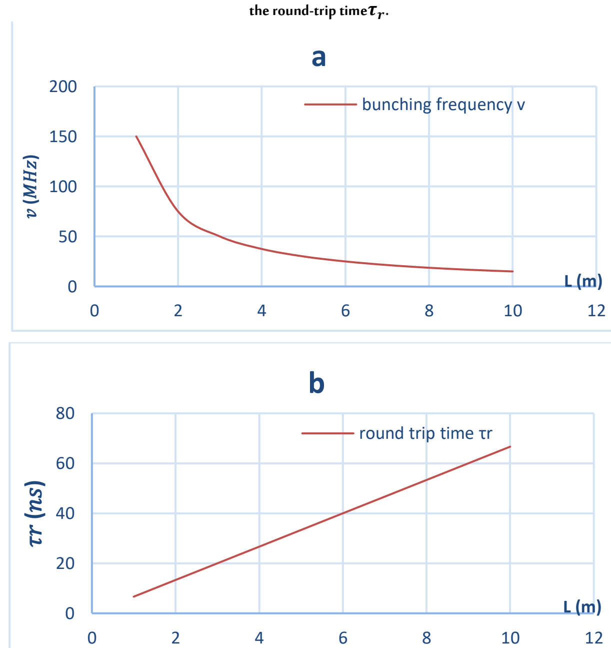

4. Conclusions

From the analysis of the obtained simulation results, it can be concluded that the small signal gain g_0 is affected by the energy spread $\in_s$; thus, the set of parameters of the laser resonator SR-FEL can be controlled. The main goal of this paper was to generate short pulses between 7.4–87.4 fs with the Fabry–Perot resonator using the fewest modes (n_{mode}) possible because there is an increase in the values of the gain bandwidth Δv_{gain} and the number of n_{mode} as a result of increasing the energy spread.

Biographies

Thair Abdulkareem Khalil Al-Aish

Department of Physics, College of Education for Pure Sciences, Ibn Al-Haitham, University of Baghdad, Baghdad, Iraq, 009647801693969, thair.ak.i@ihcoedu.uobaghdad.edu.iq

Dr. Al-Aish is a university of Baghdad graduate and an Iraqi assistant professor. He has published 20 Scopus-indexed articles with global publishers. Many countries cite his work. He teaches a laser subject at the college for bachelor's, master's, and doctoral students. He supervises masters and doctoral students. He is a supervisor at the optics and laser lab, computer lab, and information and media unit manager. He has participated in conferences in Iraq, Greece, Lebanon, and France. ORCID: 0000-0003-2479-5840

Hanady Amjed Kamil

Directorate of Education of First Karkh, Ministry of Education, Baghdad, Iraq, 009647813038914, hanadyamjedkamil@gmail.com

Kamil is a university of Baghdad graduate and an Iraqi assistant lecturer. She obtained a master's degree in Laser Physics. She has published 7 Scopus-indexed articles with global publishers. Many countries cite her work. She is interested in researching the interaction of a laser beam with matter in various applications. She teaches physics at the Directorate of Education of First Karkh, Ministry of Education, Baghdad, Iraq. She has participated in conferences in Iraq, Greece, Lebanon, and France. ORCID: 0000-0003-4485-1475.

References

Al-Aish, T.A. and Jawad, R.L. (2017). Design and simulate a new defense system of free electron laser DSFEL. *Engineering and Technology Journal*, **35**(2B), 166–72.

Al-Aish, T.A.K. (2017). Analysis and study of the effect of atmospheric turbulence on laser weapon in Iraq. *Baghdad Science Journal*, **14**(2), 426–37. DOI: 10.21123/bsj.2017.14.2.0427.

Al-Aish, T.A.K. and Kamil, H.A. (2022). Simulation and analysis the effect of the Lorentz force in a free electron laser. *Ibn AL-Haitham Journal for Pure and Applied Sciences*, **35**(2), 7–16. DOI:10.30526/35.2.2775.

Al-Aish, T.A.K., Jawad, R.L. and Kamil, H.A. (2019). Design and simulation a high-energy free electron laser HEFEL. In: *AIP Conference Proceedings*, AIP Publishing LLC, Beirut, Lebanon, 10–12/04/2019. DOI: 10.1063/1.5116995.

Ali, M.A., Al-Aish, T.A.K. and Kamil, H.A. (a2022). Analyzing and simulating the mechanism of laser medical therapy. In: *AIP Conference Proceedings*, AIP Publishing LLC, Athens, Greece, 28–30/05/2021. DOI: 10.1063/5.0092605.

Ali, M.A., Al-Aish, T.A.K. and Kamil, H.A. (b2022). A simulation breakdown the blood clot using a free electron laser system. In: *AIP Conference Proceedings*, AIP Publishing LLC, Athens, Greece, 28–30/05/2021. DOI: 10.1063/5.0092607.

Benson, S.V., Douglas, D., Neil, G.R. and Shinn, M.D. (2011). The Jefferson Lab free electron laser program. In: *Journal of Physics: Conference Series*, IOP Publishing. Virginia, USA, 8–11/06/2011. DOI 10.1088/1742-6596/299/1/012014.

Dattoli, G., Renieri, A. and Torre, A. (1993). *Lectures on the Free Electron Laser Theory and Related Topics*. London, UK: World Scientific.

Davis, C.C. (1996). *Lasers and electro-optics: Fundamentals and Engineering*. New York, USA: Cambridge University Press.

Dhedan, Z.A., Al-Aish, T.A.K. and Kamil, H.A. (2022). Design and simulation of a new system for producing laser beams without resonator "NSPLBR". In: *AIP Conference Proceedings*, AIP Publishing LLC, Athens, Greece, 28–30/05/2021. DOI: 10.1063/5.0092603.

Haarlammert, T. and Zacharias, H. (2009). Application of high harmonic radiation in surface science. *Current Opinion in Solid State and Materials Science*, **13**(1-2), 13–27.

Hannon, F.E. (2008). *A High Average-Current Electron Source for the Jefferson Laboratory Free Electron Laser*. PhD Thesis, Lancaster University, Lancaster, United Kingdom.

Kamil, H.A. and Al-Aish, T.A.K. (2022). Determine the hazard level and biological effects for visible laser pointers. In: *AIP Conference Proceedings*, AIP Publishing LLC, Athens, Greece, 28–30/05/2021. DOI: 10.1063/5.0092595.

Kamil, H.A., Ahmed, M.S. and Al-Aish, T.A.K. (2019). Rain formation by free electron laser pulse system FELPS. In: *AIP Conference Proceedings*, AIP Publishing LLC, Beirut, Lebanon, 10–12/04/2019. DOI: 10.1063/1.5138570.

Kawamura, Y., Toyoda, K. and Kawai, M. (1987). Observation of periodical short pulse trains in free‐electron laser oscillations. *Applied Physics Letters*, **51**(11), 795–7.

Kryukov, P. and Letokhov, V. (1972). Fluctuation mechanism of ultrashort pulse generation by laser with saturable absorber. *IEEE Journal of Quantum Electronics*, **8**(10), 766–82.

Mahmood, H.K. and Al-Aish, T.A.K. (2020). Design and stimulated the detectors of high-power lasers DHPL. In: *AIP Conference Proceedings*, AIP Publishing LLC, Athens, Greece, 28–30/05/2021. DOI: 10.1063/5.0092603.

Mehravaran, H., Parvin, P. and Dorranian, D. (2010). Changeover in the molecular and atomic fluorine laser transitions. *Applied optics*, **49**(15), 2741–8.

Moulton, P.F. (1986). Spectroscopic and laser characteristics of Ti:Al_2O_3. *JOSA B*, **3**(1), 125–33.

Parvin, P., Mortazavi, S.Z. and Korabaslo, M.N. (2012). Possibility for mode-locked operation of a femtosecond UV storage ring free-electron laser using a low-loss Fabry–Perot resonator. *Optics and Laser Technology*, **44**(7), 2161–7.

Parvin, P., Zaeferani, M.S., Mirabbaszadeh, K. and Sadighi, R. (1997). Measurement of the small-signal gain and saturation intensity of a XeF discharge laser. *Applied optics*, **36**(6), 1139–42.

Penzkofer, A. (1988). Passive Q-switching and mode-locking for the generation of nanosecond to femtosecond pulses. *Applied physics B*, **46**(1), 43–60.

Varro, S. (2012). *Free Electron Lasers*. Rijeka, Croatia: BoD–Books on Demand.

Wieduwilt, T., Dellith, J., Talkenberg, F., Bartelt, H. and Schmidt, M.A. (2014). Reflectivity enhanced refractive index sensor based on a fiber-integrated Fabry-Perot microresonator. *Optics express*, **22**(21), 25333–46.

Zegadi, R., Lorrain, N., Meziani, S., Dumeige, Y., Bodiou, L., Guendouz, M. and Charrier, J. (2022). Theoretical demonstration of the interest of using porous germanium to fabricate multilayer vertical optical structures for the detection of SF6 gas in the mid-infrared. *Sensors*, **22**(3), 844.

The Scientific Journal of King Faisal University

Basic and Applied Sciences

Prevalence of Pathogenic Bacteria on Face Masks from Wet Markets in Makkah during the COVID-19 Pandemic

Mohammad Melebari[1], Tariq Alpakistany[2], Taher M. Taha[1,3], Abdullah S. Alsalman[4]

[1] Department of Biology, Faculty of Science, Al-baha University, Al Baha, Saudi Arabia
[2] Ministry of Health, King Faisal Medical Complex, Taif, Saudi Arabia
[3] Department of Botany and Microbiology, Faculty of Science, Al-Azhar University, Assiut, Egypt
[4] Nuclear Science Research Institute, King Abdulaziz City for Science and Technology, Riyadh, Saudi Arabia

LINK	RECEIVED	ACCEPTED	PUBLISHED ONLINE	ASSIGNED TO AN ISSUE
https://doi.org/10.37575/b/sci/220040	23/10/2022	01/12/2022	01/12/2022	01/12/2022
NO. OF WORDS	**NO. OF PAGES**	**YEAR**	**VOLUME**	**ISSUE**
5512	6	2022	23	2

ABSTRACT

The Coronavirus disease 2019 (COVID-19) pandemic compelled people worldwide to use face masks to limit the spread of the disease. Improper use of masks may increase the transmission of pathogenic bacteria, causing co-infection that may result in an increase in complications of COVID-19 and a rise in the death rate. This study aims to determine the presence of pathogenic bacteria on the surfaces of masks worn by workers while working at several markets (meat, fish, fruit, and vegetable markets) in Makkah, Saudi Arabia, during the COVID-19 pandemic. The pathogenic bacteria on the masks of some workers in different markets in Makkah were identified and confirmed by growth media and an automated system. Pathogenic bacteria were detected in 99% of the studied samples. The most commonly detected bacteria on masks were *E. coli,* followed by *Staphylococcus epidermidis*, and *Staphylococcus aureus*. A few samples included additional bacterial species, such as *Klebsiella pneumoniae*. To the best of our knowledge, this is the first study to investigate harmful bacteria on the masks of a random group of non-healthcare workers. Improper mask use by various populations might result in significant cross-contamination with pathobionts.

KEYWORDS
COVID-19, face masks, bacterial contamination, infection, hygiene, wet market

CITATION
Melebari, M., Alpakistany, T., Taha, T.M. and Alsalman, A.S. (2022). Prevalence of pathogenic bacteria on face masks from wet markets in Makkah during the COVID-19 pandemic. *The Scientific Journal of King Faisal University: Basic and Applied Sciences*, **23**(2), 33–8. DOI: 10.37575/b/sci/220040

1. Introduction

Coronavirus disease 2019 (COVID-19) is caused by a novel virus (SARS-CoV-2). This disease emerged in Wuhan, China, and was identified in December 2019 (Li *et al.*, 2020; Phelan *et al.*, 2020). The pandemic has had noticeable effects on people, cultures, lifestyle, and economic and public health (Mukhtar, 2020; Yoosefi *et al.*, 2021; Giuntella *et al.*, 2021; Azuma *et al.*, 2021). Consequently, various regulations and habits were changed worldwide to prevent the spread of the disease (Zarocostas, 2020). The public health sector is one of the most sensitive areas affected by COVID-19, which is considered an extremely infectious disease (Alimohamadi *et al.*, 2020). COVID-19 is transmitted by droplets loaded with viruses released from infected individuals through sneezing, coughing, and exhaling, similar to other respiratory viral infections (Anderson *et al.*, 2020; Setti *et al.*, 2020; and Somsen *et al.*, 2020). A single infected person can infect up to three people (Chen *et al.*, 2019). Globally, approximately 409 million confirmed cases and over 5.8 million deaths had been documented as of February 13, 2022 (World Health Organization (WHO), 2022). To limit the spread of this virulent virus, wearing face masks was recommended by health authorities in many countries, such as the USA, the UK, Germany, China, Singapore, and Hong Kong (Feng *et al.*, 2020). According to WHO (2022), using face masks can help prevent the spread of COVID-19 and consequently limit the number of deaths. However, other factors can play a role in the spread of COVID-19 infection.

Bacterial co-infection is very common in various infections, such as viral respiratory infections, and can significantly affect the rate of morbidity and mortality (Gupta *et al.*, 2008; Morris *et al.*, 2017; Westblade *et al.*, 2021). Undesirable effects of several cases associated with COVID-19 infections showed that the viral infection was not the only cause of the adverse outcomes. Bacterial co-infection can be a critical factor in the patient health situation (Nasir *et al.*, 2021; Singh *et al.*, 2021), and the possibility of death is amplified when patients with COVID-19 have bacterial co-infection (Silva *et al.*, 2021; Shafran *et al.*, 2021). Bacterial pathogens can infect humans through food, water, or living vectors (Doron and Gorbach, 2008). Hand contact is considered one of the most common modes of pathogens transmission (Pittet *et al.*, 2006; Kutter *et al.*, 2018). It can spread pathogens among people and on surfaces such as food, tools, clothes, and personal belongings (Sze-To *et al.*, 2014; Mitchell *et al.*, 2015; Aljamali *et al.*, 2021).

Although masks are supposed to be a preventing tool (Dehaghi *et al.*, 2020; Dehgani-Mobarak *et al.*, 2020; Saijonkari *et al.*, 2020), they could be one of the harmful pathogen vehicles (Chughtai *et al.*, 2019). Improper use of masks might lead to bacterial transmission, which can cause co-infection cases in patients (Simatupang *et al.*, 2021). Furthermore, several unsuitable practices have been observed in various communities using masks. Such practices include touching the outer surface of masks with bare hands while working, attempting to put masks on and take them off multiple times while performing assigned work, and reusing masks repeatedly for extended periods, in some cases for days, with no regard for sanitation or contamination (Simatupang *et al.*, 2021). These diverse behaviors could be salient factors since they could transmit pathogenic organisms from individual to individual, product to person, and surface to surface.

During the pandemic, few studies have been conducted on the prevalence of pathogenic bacteria on the surfaces of face masks, and there is a need to demonstrate the diversity of pathogenic bacteria on the surfaces of masks worn while working. Therefore, this study aims to detect the prevalence of pathogenic bacteria on the surfaces of masks worn by workers while working at different markets (meat, fish, fruit, and vegetable markets) in Makkah, Saudi Arabia, during the COVID-19 pandemic.

Corresponding Author: Mohammad Melebari 00966556558455, melebari@bu.edu.sa

2. Material and Methods

2.1. Collection of Samples:

Cotton swabs (Sigma-Aldrich, Bangalore, India) were used to swab the outer surfaces of face masks worn by workers in the central market of Makkah, which is one of the main and biggest cities in the western region of Saudi Arabia. The central market was divided into four individual sections (fruits, vegetables, fish, and meat). Samples were collected between 10:30 am and 1:30 pm on Friday, as this is when the marker is the busiest and most crowded. It is the first day of the weekend in Saudi Arabia.

Samples were collected in April 2021, when wearing masks was mandatory for the whole country as per government guidelines due to the rise in COVID-19 infections. During the collection of samples, data such as mask type (surgical or textile), wearing duration, and market type were recorded. A total of 100 samples were taken from the central market's four sections (27 from the fruit market, 26 from the vegetable market, 27 from the fish market, and 20 from the meat market).

2.2. Detection of Bacterial Pathogens:

All the experiments were conducted following the methods proposed by Saikia and Joshi (2014). First, within 5 hours, all the swabs were directly streaked onto four different types of culture media: blood agar, MacConkey agar, HiCrome Staph Selective Agar, and eosin methylene blue (EMB) agar (HiMedia, Mumbai, India)). Second, plates were incubated at 37°C for 24 hours. In the third stage, the colonies grown on EMB agar and HiCrome Staph Selective Agar were identified based on their cultural characteristics by following the manufacturer's instructions. Metallic colonies on EMB were classified as E. coli. Green colonies and blue colonies on HiCrome Staph Selective Agar were classified as Staphylococcus aureus and Staphylococcus epidermidis, respectively. Blood agar and MacConkey agar media were used to verify the hemolytic pattern of staphylococci and the lactose fermentation ability of lactose fermenters, respectively.

2.3. MicroScan Automated Identification:

The Gram staining step was performed on samples (n = 13) that showed no characteristic features on culture media, such as metallic colonies on EMB or green and blue colonies on HiCrome Staph Selective Agar. All the samples (n = 13) were Gram-negative. These samples were prepared for MicroScan analysis according to the manufacturer's instructions. Briefly, using the rapid inoculation technique, a single fresh colony from the overnight cultures on blood agar was rapidly standardized for MicroScan antimicrobial sensitivity testing (AST) and identification tests. After inoculation, the solution was transferred onto the N66 panels and loaded into the instrument for overnight treatment. Finally, MicroScan (Walkaway 96 plus) Gram-positive and -negative cards automatic identification technology was used to identify all the isolates (Osei *et al.*, 2020).

2.4. Statistical Analysis:

Statistical Package for the Social Sciences (SPSS) version 26 was used to code and input the data (IBM Corp., Armonk, NY, USA). The mean, standard deviation, median, minimum, and maximum were used to describe the quantitative data. Conversely, the frequency (count) and relative frequency (%) were used to summarize the categorical data. The non-parametric Kruskal–Wallis and Mann–Whitney tests were utilized to compare quantitative variables (Chan, 2003a). The Chi-square (c2) test was used to compare categorical data. The exact test was employed instead when the anticipated frequency was less than 5 (Chan, 2003b). Statistical significance was defined as p-values less than 0.05.

3. Results and Discussion

The existence of bacterial species on the surfaces of surgical and textile face masks was examined in 100 samples collected from four different local markets in Makkah, Saudi Arabia. The distribution of bacterial species on the masks collected from the markets is shown in **Table 1**.

Table 1: Distribution of bacterial strains in different markets

Bacterial strain	Fish (n = 27)	Fruits (n = 27)	Vegetables (n = 26)	Meat (n = 20)	Total (n = 100)
E. coli	21	13	18	16	68
Staphylococcus epidermidis	15	17	23	7	62
Staphylococcus aureus	13	10	17	9	49
Klebsiella pneumoniae	0	1	1	1	3
Klebsiella rhinoscleromatis	0	0	1	1	2
Klebsiella ozaenae	0	1	0	1	2
Acinetobacter baumanii	0	0	1	0	1
Acinetobacter lwoffii	0	0	0	1	1
Mannheimia haemolytica	1	0	0	0	1
Providencia rustigianii	1	0	0	0	1
Pantoea agglomerans	0	0	1	0	1
Pseudomonas putida	0	1	0	0	1

Of the 100 samples, 99 positive samples revealed the existence of at least one bacterial species. Only one sample showed no bacterial growth on any of the growth media used. The maximum recorded number of bacterial species on a single mask (four species) was collected from the vegetable market. The total number of bacterial species detected per mask sample was one, two, and three, representing 26%, 53%, and 19% of the collected samples, respectively.

The most prevalent pathogenic bacteria was *E. coli*, detected in 68% of the samples, followed by *Staphylococcus epidermidis*, detected in 62% of the samples, and *Staphylococcus aureus,* detected in 49%. *Klebsiella pneumoniae* was detected in 3% of samples, while *Klebsiella rhinoscleromatis* and *Klebsiella ozaenae* were recorded in only 2% of the samples. Some bacterial species, such as *Acinetobacter baumanii, Acinetobacter lwoffii, Mannheimia haemolytica, Providencia rustigianii*, and *Pseudomonas putida*, were detected in only 1% of the samples. It was found that the mask-wearing duration did not affect the mask bacterial flora. Some samples with a short mask-wearing duration showed the existence of many bacterial species, whereas others with a long mask-wearing duration contained just a few bacterial species, as shown in **Figure 1**.

Figure 1: Prevalence of pathogens on textile and surgical masks

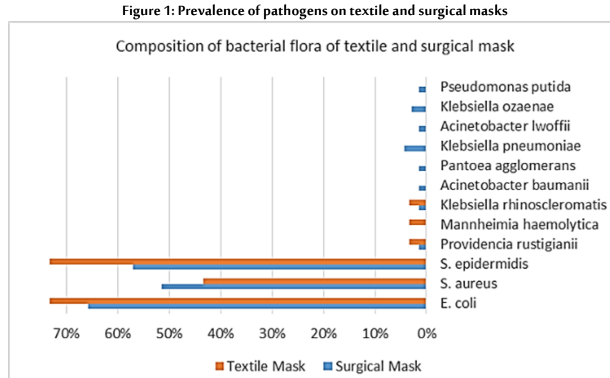

The total number of bacterial isolates per market were 62, 51, 43, and 36 in the vegetable market (26 samples), fish market (27 samples), meat market (20 samples), and fruit market (27 samples), respectively, as shown in **Chart 1**.

Chart 1: Total number of bacterial isolates per each market

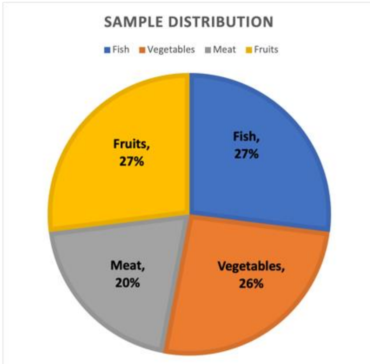

Among the studied samples, it was found that the most commonly used mask was the surgical mask, representing 70% of the collected samples, while textile masks represented 30%, as shown in **Chart 2**.

Chart 2: Most commonly used mask: surgical and textile masks

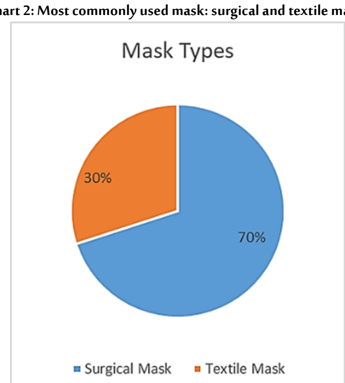

The statistical analysis showed no significant effect of mask type on bacterial flora. However, some bacterial species, namely, *Acinetobacter baumanii, Acinetobacter lwoffii, Pantoea agglomerans*, and *Pseudomonas putida*, were detected on surgical masks but not on textile masks. Conversely, *Mannheimia haemolytica* was detected on textile masks but not on surgical masks, as shown in **Figure 1**. The statistical analysis also showed a significant variation ($p<0.05$) in S. epidermidis among the studied markets, and it was more commonly found in the vegetable market. However, no significant changes were observed in the distribution of other bacterial isolates in all the analyzed markets. Furthermore, the statistical analysis revealed that surgical masks were ($p<0.05$) utilized much more commonly than textile masks.

Several studies have demonstrated the usefulness of face masks in limiting the spread of airborne viruses (Liang *et al.*, 2020; MacIntyre and Chughtai, 2015; Suess *et al.*, 2012). However, a limited number of studies have investigated their bacterial loads in the population, particularly during the COVID-19 pandemic (Delanghe *et al.*, 2021). The present study indicated that *E. coli* was the most prevalent bacterium. There are several reports about the involvement of E. coli in some skin diseases, such as necrotizing fasciitis (Afifi and El-Hindawi, 2008; Krebs *et al.*, 2001; Li *et al.*, 2006), cellulitis of upper or lower limbs (Brzozowski and Ross, 1997; Corredoira *et al.*, 1994; Yoon *et al.*, 1998), neonatal omphalitis (Fraser *et al.*, 2006), burn injuries (Rodgers *et al.*, 2000), and surgical site infections (Tourmousoglou *et al.*, 2008). Moreover, *E. coli* is involved in other internal infections, such as urinary tract infections (Bannon *et al.*, 2016; Flores-Mireles *et al.*, 2015) and acute diarrheal disease (Torres *et al.*, 2001). *Staphylococcus epidermidis* and *Staphylococcus aureus* are among the normal human and animal skin flora involved in skin health. However, some of them are also known as skin pathogens that cause skin diseases such as acne vulgaris and atopic dermatitis (Findley and Grice, 2014; Bjerre *et al.*, 2017; Byrd *et al.*, 2017).

Furthermore, three detected species belonging to the genus *Klebsiella*, namely, *Klebsiella pneumoniae, Klebsiella rhinoscleromatis,* and *Klebsiella ozaenae*, are involved in many respiratory diseases, such as *pneumonia, ozena*, and *rhinoscleroma*, respectively (Janda and Abbott, 2006). The existence of bacterial species such as *E. coli, Staphylococcus aureus*, and *Klebsiella pneumoniae* on face masks is a critical finding. The detection of bacterial flora recorded in this study partially agrees with that recorded by Delanghe *et al.* (2021). They recorded the existence of strains belonging to the genera *Bacillus, Staphylococcus*, and *Acinetobacter*. The difference in the findings may be due to the variation in population and mask-wearing duration.

A previous study showed variations in the composition of the bacterial flora on textile and surgical masks (Delanghe *et al.*, 2021). However, we observed no significant difference between the two types of masks. The conflicting results may be due to differences in mask-wearing duration. In the current study, in several cases, most masks were worn for more than 6 hours or more than 24 hours, whereas the mask-wearing duration in the study conducted by Delanghe *et al.* (2021) was only 4 hours.

Another reason for pathobiont transmission is speech volume (Patel *et al.*, 2020), and it has been demonstrated that high speech volumes increase the possibility of pathogen transmission, including COVID-19. The finding of the current study is in accordance with that of Patel *et al.* (2020). The chosen markets being considered places with high speech volumes for prolonged periods is another reason behind having 99% positive samples. The mask itself can be a favorable habitat for bacterial accumulation (Abbasi *et al.*, 2020), particularly in confined and congested areas with inadequate ventilation (Tuñón-Molina *et al.*, 2021). Furthermore, improper habits associated with using masks observed during the study, such as touching the mask surface and beneath the mask to scratch the face or nose, may increase the microbial load of the mask (Simatupang *et al.*, 2021). It can consequently transfer bacteria to other organs, such as the eyes and mouth, or the objects present in various markets, such as food, shopping bags, bills, payment machines, and tools. On average, humans touch their face, including the mouth, nose, and eyes, more than 20 times per hour (Kwok *et al.*, 2015). That could be the main reason for infection (Shen *et al.*, 2020) with a wide range of different viruses such as Coronavirus, Ebola virus, swine flu, and seasonal flu (Sudharsan *et al.*, 2020).

There is no doubt about the importance of using masks, especially during the COVID-19 pandemic. Several studies have highlighted masks' essential role in protecting the public from different infections and diseases (Greenhalgh *et al.*, 2020; Liang *et al.*, 2020; MacIntyre and Chughtai, 2015). However, the current study's findings show that the primary purpose of using masks might be influenced by community behavior (Simatupang *et al.*, 2021). The public still needs to be more educated about the proper use of masks and their necessity to achieve the main purpose of using masks.

The pathogenic bacteria detected in this study are related to fecal contamination, hand washing, or personal hygiene issues. This highlights the need to educate communities about the proper methods of washing hands and self-hygiene. Health authorities worldwide and other related local organizations must take serious actions to encourage the public at different levels, specifically non-educated communities, to focus on the adverse effects of bad habits that might lead to serious health issues. The guidance and information should be simplified and clarified to be easily understood. For instance, in the current study, most workers in the chosen market do not speak the native or local language of the country fluently, making it exceedingly difficult to understand the essential role of safety and hygiene guidance. Many people and workers might be wearing masks only because of the new rules and systems that have been implemented in some countries since the start of this pandemic, and they might not know the reasons for and benefits of those rules. We noticed several inappropriate actions from our observation, such as wearing a "half mask" and touching the mask before handling products and shopping bags. According to Lee *et al.* (2020), in a study of 1500 participants, more than 90% did not follow hand hygiene before using masks, and more than 95% did not follow the correct hand hygiene after taking masks off.

All these behaviors can affect the purpose of using masks. Consequently, masks can be a transmission tool for several pathogens. People and communities must learn and follow the proper use of masks to avoid spreading COVID-19 and other pathogens. All the health sectors worldwide must educate communities and consider the variety of backgrounds, cultures, and education.

4. Conclusion

Face masks have been used increasingly during the COVID-19 pandemic to prevent the spread of this lethal disease. Improper use of masks may lead to contamination of the mask with pathogenic bacteria. The findings of this study confirmed the existence of bacterial species on 99% of the samples collected from some workers in wet markets, including vegetable, fruit, fish, and meat markets. Some of these bacteria, such as *Klebsiella pneumoniae, Klebsiella ozaenae, Klebsiella rhinoscleromatis,* and *Staphylococcus aureus*, are strong pathogens and may cause dangerous diseases. Bacteria prevalence on the masks may be due to the crowded nature of these markets and workers' lack of awareness about the right way to use a mask. Educating people about the proper way to use a mask and providing instructions in different languages within multilingual and multicultural communities may reduce the contamination of masks with bacteria. Statistical studies about the prevalent respiratory and skin bacterial diseases during the COVID-19 pandemic are needed to evaluate their relation to mask use.

Biographies

Mohammad Melebari

Department of Biology, Faculty of Science, Albaha University, Al Baha, Saudi Arabia, 00966556558455, melebari@bu.edu.sa

Dr. Melebari is a Saudi assistant professor at Al Baha University. He obtained a B.Sc. (Biology Department) in 2007 from Umm Al Qura University and an M.Sc. (2012) and Ph.D. (2019) (Food Microbiology) from The University of Guelph, Canada. He has been the head of the Biology Department since January 2020. He is interested in the area of pathogenic bacteria detection and identification in food and different natural resources in addition to bacteriophages.

Tariq Alpakistany

Ministry of Health, King Faisal Medical Complex, Taif, Saudi Arabia, 00966503213967, talpakistany@moh.gov.sa

Mr. Alpakistany obtained a B.Sc. in Microbiology from Umm Al Qura University and an MSc in Molecular Bacteriology and an MSc in Hospital and Healthcare Administration from Taif University. He works at the Ministry of Health, King Faisal Hospital, Taif. He is a professional Saudi instructor on several public health topics.

Taher M. Taha

Department of Biology, Faculty of Science, Albaha University, Al Baha, Saudi Arabia, 00966531636590, tmohamed@bu.edu.sa

Dr. Taha is an Egyptian associate professor at Al Baha University. He obtained a B.Sc. (Botany Department) in 1993 from Cairo University. In 2000, he obtained an M.Sc. (Microbial Phycology) from Al Azhar University, Egypt. He obtained a Ph.D. (Biotechnology) from Okayama University, Japan. The title of his thesis was Involvement of Iron-Oxidation and Iron Reduction Enzyme Systems in Sulfur Oxidation of Iron-Oxidizing Bacterium Acidithiobacillus ferrooxidans. He has published around 30 papers on botany, microbiology, and biotechnology.

Abdullah S Alsalman

Nuclear Science Research Institute, King Abdulaziz City for Science and Technology, Riyadh, Saudi Arabia, 00966506903121, aalsalman@kacst.edu.sa

Mr. Alsalman is a Saudi professional in plant development and using techniques of biotechnology, Assist. a leader team project in nuclear science institute with the IAEA to achieving the country goals as well as how to benefit from nuclear techniques in the fields of development the agricultural crops to enhancing agricultural sustainability and biodiversity in the agricultural sector. He was a Co-Monitor in projects on Removal of Heavy Metals and Radionuclides from Industrial Water Waste Areas by Using Resistant Bacteria to Irradiation. He achieved third place in The National Olympiad for Scientific Creativity (Ibdaa 2022).

References

Abbasi, S.A., Khalil, A.B. and Arslan, M. (2020). Extensive use of face masks during COVID-19 pandemic: (micro-) plastic pollution and potential health concerns in the Arabian Peninsula. *Saudi Journal of Biological Sciences*, **27**(12), 3181–6.

Afifi, R.Y. and El-Hindawi, A.A. (2008). Acute necrotizing fasciitis in Egyptian patients: a case series. *International Journal of Surgery*, **6**(1), 7–14.

Alimohamadi, Y., Sepandi, M., Taghdir, M. and Hosamirudsari, H. (2020). Determine the most common clinical symptoms in COVID-19 patients: A systematic review and meta-analysis. *Journal of Preventive Medicine and Hygiene*, **61**(3), E304.

Aljamali, N.M., Jawd, S.M. and Hussein, H.A. (2021). Review on Preventive Instructions for Controlling Infectious Diseases. *International Journal of Industrial Biotechnology and Biomaterials*, **7**(1), 22–8.

Anderson, E.L., Turnham, P., Griffin, J.R. and Clarke, C.C. (2020). Consideration of the aerosol transmission for COVID-19 and public health. *Risk Analysis*, **40**(5), 902–7.

Azuma, K., Nojiri, T., Kawashima, M., Hanai, A., Ayaki, M., Tsubota, K. and TRF-Japan Study Group. (2021). Possible favorable lifestyle changes owing to the coronavirus disease 2019 (COVID-19) pandemic among middle-aged Japanese women: An ancillary survey of the TRF-Japan study using the original "Taberhythm" smartphone app. *Plos one*, **16**(3), e0248935.

Bannon, J., Melebari, M., Jordao Jr, C., Leon-Velarde, C.G. and Warriner, K. (2016). Incidence of top 6 Shiga toxigenic Escherichia coli within two Ontario beef processing facilities: challenges in screening and confirmation testing. *Aims Microbiol*, **2**(3), 278–91.

Bjerre, R.D., Bandier, J., Skov, L., Engstrand, L. and Johansen, J. D. (2017). The role of the skin microbiome in atopic dermatitis: a systematic review. *British Journal of Dermatology*, **177**(5), 1272–8.

Brzozowski, D. and Ross, D. C. (1997). Upper limb Escherichia coli cellulitis in the immunocompromised. *Journal of Hand Surgery*, **22**(5), 679–80.

Byrd, A. L., Deming, C., Cassidy, S.K.B., Harrison, O.J., Ng, W.I. and Conlan, S. (2018). Staphylococcus aureus and Staphylococcus epidermidis strain diversity underlying pediatric atopic dermatitis. A study using metagenomic shotgun sequencing to identify strain-level differences in S. aureus and S. epidermidis colonization in pediatric AD patients. *Sci Transl Med.*, **9**(397), eaal4651.

Chan Y.H. (2003a). Biostatistics 102: quantitative data--parametric & non-parametric tests. *Singapore Medical Journal*, **44**(8), 391–6.

Chan Y.H. (2003b). Biostatistics 103: qualitative data - tests of independence. *Singapore Medical Journal*, **44**(10), 498–503.

Chen T, Dai Z, Mo P, Li X, Ma Z, Song S, Chen X, Luo M, Liang K, Gao S, Zhang Y, Deng L, Xiong Y. (2020). Clinical Characteristics and Outcomes of Older Patients with Coronavirus Disease 2019 (COVID-19) in Wuhan, China: A Single-Centered, Retrospective Study. *J. Gerontol A Biol. Sci. Med. Sci.*, **16**(9), 1788–95. DOI:

10.1093/gerona/glaa089

Chughtai, A.A., Stelzer-Braid, S., Rawlinson, W., Pontivivo, G., Wang, Q., Pan, Y. and MacIntyre, C.R. (2019). Contamination by respiratory viruses on outer surface of medical masks used by hospital healthcare workers. *BMC Infectious Diseases*, **19**(1), 1–8.

Corredoira, J.M., Ariza, J., Pallares, R., Carratala, J., Viladrich, P.F., Rufi, G. and Gudiol, F. (1994). Gram-negative bacillary cellulitis in patients with hepatic cirrhosis. *European Journal of Clinical Microbiology and Infectious Diseases*, **13**(1), 19–24.

Dehaghi, B.F., Ghodrati-Torbati, A., Teimori, G., Ghavamabadi, L.I. and Jamshidnezhad, A. (2020). Face masks vs. COVID-19: a systematic review. *Investigacion Y Educacion En Enfermeria*, **38**(2), n/a.

Dehgani-Mobaraki, P., Zaidi, A.K. and Levy, J.M. (2020). Face masks are an essential tool to mitigate the ongoing SARS-CoV-2 pandemic: a call to action. *Rhinology Online*, **3**, 157–9.

Delanghe, L., Cauwenberghs, E., Spacova, I., De Boeck, I., Van Beeck, W., Pepermans, K. and Lebeer, S. (2021). Cotton and surgical face masks in community settings: Bacterial contamination and face mask hygiene. *Frontiers in Medicine*, **8**(n/a),1477.

Doron, S. and Gorbach, S.L. (2008). Bacterial infections: Overview. *International Encyclopedia of Public Health*, **273**(n/a),n/a.

Feng, S., Shen, C., Xia, N., Song, W., Fan, M. and Cowling, B.J. (2020). Rational use of face masks in the COVID-19 pandemic. *The Lancet Respiratory Medicine*, **8**(5), 434–6.

Findley, K. and Grice, E.A. (2014). The skin microbiome: a focus on pathogens and their association with skin disease. *Plos pathogens*, **10**(11), e1004436.

Flores-Mireles, A.L., Walker, J.N., Caparon, M. and Hultgren, S.J. (2015). Urinary tract infections: Epidemiology, mechanisms of infection and treatment options. *Nature reviews microbiology*, **13**(5), 269–84.

Fraser, N., Davies, B.W. and Cusack, J. (2006). Neonatal omphalitis: a review of its serious complications. *Acta Paediatrica*, **95**(5), 519–22.

Giuntella, O., Hyde, K., Saccardo, S. and Sadoff, S. (2021). Lifestyle and mental health disruptions during COVID-19. *Proceedings of the National Academy of Sciences*, **118**(9).

Greenhalgh, T., Schmid, M.B., Czypionka, T., Bassler, D. and Gruer, L. (2020). Face masks for the public during the covid-19 crisis. *Bmj*, **369**(n/a)n/a.

Gupta, R.K., George, R. and Nguyen-Van-Tam, J.S. (2008). Bacterial pneumonia and pandemic influenza planning. *Emerging Infectious Diseases*, **14**(8), 1187.

Janda, J. M. and Abbott, S. L. (2006). The Genera Klebsiella and Raoultella. *The Enterobacteria*, **2**(n/a), 115–29.

Krebs, V.L.J., Koga, K. M., Diniz, E.M.D.A., Ceccon, M.E.J. and Vaz, F.A.C. (2001). Necrotizing fasciitis in a newborn infant: a case report. *Revista do Hospital das Clínicas*, **56**(n/a), 59–62.

Kutter, J. S., Spronken, M. I., Fraaij, P.L., Fouchier, R.A. and Herfst, S. (2018).

Kwok, Y. L.A., Gralton, J. and McLaws, M.L. (2015). Face touching: un hábito frecuente que tiene implicaciones para la higiene de las manos. *Am. J. Infectar*, **43**(n/a), 112–4.

Li, D.M., De Lun, L. and Chen, X.R. (2006). Necrotising fasciitis with Escherichia coli. *The Lancet Infectious Diseases*, **6**(7), 456.

Liang, M., Gao, L., Cheng, C., Zhou, Q., Uy, J.P., Heiner, K. and Sun, C. (2020). Efficacy of face mask in preventing respiratory virus transmission: A systematic review and meta-analysis. *Travel medicine and infectious disease*, **36**(n/a), 101751.

MacIntyre, C.R. and Chughtai, A.A. (2015). Facemasks for the prevention of infection in healthcare and community settings. *Bmj*, **350**(n/a),n/a.

Mitchell, A., Spencer, M. and Edmiston Jr, C. (2015). Role of healthcare apparel and other healthcare textiles in the transmission of pathogens: a review of the literature. *Journal of Hospital Infection*, **90**(4), 285–92.

Morris, D.E., Cleary, D.W. and Clarke, S.C. (2017). Secondary bacterial infections associated with influenza pandemics. *Frontiers in microbiology*, **8**(n/a), 1041.

Mukhtar, S. (2020). Psychological health during the coronavirus disease 2019 pandemic outbreak. *International Journal of Social Psychiatry*, **66**(5), 512–6.

Nasir, N., Rehman, F. and Omair, S.F. (2021). Risk factors for bacterial infections in patients with moderate to severe COVID-19: A case-control study. *Journal of medical virology*, **93**(7), 4564–9.

Osei Sekyere, J., Sephofane, A.K. and Mbelle, N.M. (2020). Comparative evaluation of CHROMagar COL-APSE, MicroScan Walkaway, ComASP Colistin, and Colistin MAC Test in detecting colistin-resistant Gram-negative bacteria. *Scientific Reports*, **10**(1), 1–13.

Patel, K. P., Vunnam, S.R., Patel, P.A., Krill, K.L., Korbitz, P.M., Gallagher, J. P., Suh, J. E. and Vunnam, R. R. (2020). Transmission of SARS-CoV-2: an update of current literature. *European Journal of Clinical Microbiology & Infectious Diseases: Official Publication of the European Society of Clinical Microbiology*, **39**(11), 2005–2011.

Phelan, A.L., Katz, R. and Gostin, L.O. (2020). The novel coronavirus originating in Wuhan, China: Challenges for global health governance. *Jama*, **323**(8), 709–10.

Pittet, D., Allegranzi, B., Sax, H., Dharan, S., Pessoa-Silva, C.L., Donaldson, L. and Boyce, J.M. (2006). Evidence-based model for hand transmission during patient care and the role of improved practices. *The Lancet Infectious Diseases*, **6**(10), 641–52.

Rodgers, G. L., Mortensen, J., Fisher, M. C., Lo, A., Cresswell, A. and Long, S. S. (2000). Predictors of infectious complications after burn injuries in children. *The Pediatric Infectious Disease Journal*, **19**(10), 990–5.

Saijonkari, M., Booth, N., Isojärvi, J., Finnilä, J. and Mäkelä, M. (2020). Face masks for preventing respiratory infections in the community: A systematic review. *Medrxiv*, **n/a**(n/a), n/a

Saikia, P. and Joshi, S.R. (2014). A study on the occurrence of non-O157 Shiga toxin producing Escherichia coli isolates in retail chicken meats marketed in North-East India. *Proceedings of the National Academy of Sciences, India Section B: Biological Sciences*, **84**(2), 337–42.

Setti, L., Passarini, F., De Gennaro, G., Barbieri, P., Perrone, M.G., Borelli, M., ... and Miani, A. (2020). Airborne transmission route of COVID-19: Why 2 meters/6 feet of inter-personal distance could not be enough. *International Journal of Environmental Research and Public Health*, **17**(8), 2932.

Shafran, N., Shafran, I., Ben-Zvi, H., Sofer, S., Sheena, L., Krause, I., ... and Sklan, E.H. (2021). Secondary bacterial infection in COVID-19 patients is a stronger predictor for death compared to influenza patients. *Scientific Reports*, **11**(1), 1–8.

Shen, K.L., Yang, Y.H., Jiang, R.M., Wang, T.Y., Zhao, D.C., Jiang, Y. and Wang, X. F. (2020). Updated diagnosis, treatment and prevention of COVID-19 in children: experts' consensus statement (condensed version of the second edition). *World Journal of Pediatrics*, **16**(3), 232–9.

Silva, D.L., Lima, C.M., Magalhães, V.C., Baltazar, L.M., Peres, N.T., Caligiorne, R.B. and Santos, D.A. (2021). Fungal and bacterial co-infections increase mortality of severely ill COVID-19 patients. *Journal of Hospital Infection*, **113**(n/a), 145–54.

Simatupang, M. M., Veronika, E. and Sitepu, O. (2021). Potential Self-contamination: Improper Hygiene Procedure of Using Masks. *KEMAS: Jurnal Kesehatan Masyarakat*, **17**(2), n/a.

Singh, V., Upadhyay, P., Reddy, J. and Granger, J. (2021). SARS-CoV-2 respiratory co-infections: Incidence of viral and bacterial co-pathogens. *International Journal of Infectious Diseases*, **105**(n/a), 617–20.

Somsen, G.A., van Rijn, C., Kooij, S., Bem, R.A. and Bonn, D. (2020). Small droplet aerosols in poorly ventilated spaces and SARS-CoV-2 transmission. *The Lancet Respiratory Medicine*, **8**(7), 658–9.

Sudharsan, B., Sundaram, D., Breslin, J.G. and Ali, M.I. (2020). Avoid touching your face: A hand-to-face 3d motion dataset (covid-away) and trained models for smartwatches. In: *10th International Conference on the Internet of Things Companion*, Malmo Sweden, 07/10/2020. (pp. 1–9).

Suess, T., Remschmidt, C., Schink, S.B., Schweiger, B., Nitsche, A., Schroeder, K., ... and Buchholz, U. (2012). The role of facemasks and hand hygiene in the prevention of influenza transmission in households: results from a cluster randomised trial; Berlin, Germany, 2009-2011. *BMC Infectious Diseases*, **12**(1), 1–16.

Sze-To, G.N., Yang, Y., Kwan, J.K., Yu, S.C. and Chao, C.Y. (2014). Effects of surface material, ventilation, and human behavior on indirect contact transmission risk of respiratory infection. *Risk analysis: an official publication of the Society for Risk Analysis*, **34**(5), 818–30.

Torres, M. E., Pırez, M.C., Schelotto, F., Varela, G., Parodi, V., Allende, F., ... and Ingold, E. (2001). Etiology of children's diarrhea in Montevideo, Uruguay: associated pathogens and unusual isolates. *Journal of Clinical Microbiology*, **39**(6), 2134–9.

Tourmousoglou, C.E., Yiannakopoulou, E.C., Kalapothaki, V., Bramis, J. and Papadopoulos, J. S. (2008). Surgical-site infection surveillance in general surgery: a critical issue. *Journal of chemotherapy*, **20**(3), 312–8.

Transmission routes of respiratory viruses among humans. *Current opinion in virology*, **28**(n/a), 142–51.

Tuñón-Molina, A., Takayama, K., Redwan, E.M., Uversky, V.N., Andrés, J. and Serrano-Aroca, Á. (2021). Protective face masks: Current status and future trends. *ACS Applied Materials & Interfaces*, **13**(48), 56725–51.

Westblade, L.F., Simon, M.S. and Satlin, M.J. (2021). Bacterial coinfections in coronavirus disease 2019. *Trends in Microbiology*, **29**(10), 930–41.

WHO.int. (2022). *Weekly Epidemiological Update on COVID-19 - February 15 2022*. Available at: https://www.who.int/publications/m/item/weekly-epidemiological-update-on-covid-19---15-february-2022 (accessed on 18/02/2022)

Yoon, T.Y., Jung, S.K. and Chang, S.H. (1998). Cellulitis due to Escherichia coli in three immunocompromised subjects. *British Journal of Dermatology*, **139**(5), 885–8.

Yoosefi Leb, J., Abbas, J., Moradi, F., Salahshoor, M.R., Chaboksavar, F., Irandoost, S.F. and Ziapour, A. (2021). How the COVID-19 pandemic effected economic, social, political, and cultural factors: A lesson from Iran. *International Journal of Social Psychiatry*, **67**(3), 298–300.

Zarocostas, J. (2020). How to fight an infodemic. *The Lancet*, **395**(10225), 676.

The Scientific Journal of King Faisal University

Basic and Applied Sciences

Design and Establishment of an Implementation to Simulate and Analyse the Tertiary Undulator of the FEL

Thair Abdulkareem Khalil Al-Aish[1] and Hanady Amjed Kamil [2]

[1] Department of Physics, College of Education for Pure Sciences Ibn Al-Haitham, University of Baghdad, Baghdad, Iraq
[2] Directorate of Education of First Karkh, Ministry of Education, Baghdad, Iraq

LINK	RECEIVED	ACCEPTED	PUBLISHED ONLINE	ASSIGNED TO AN ISSUE
https://doi.org/10.37575/b/sci/220036	01/11/2022	01/12/2022	01/12/2022	01/12/2022
NO. OF WORDS	**NO. OF PAGES**	**YEAR**	**VOLUME**	**ISSUE**
2565	4	2022	23	2

ABSTRACT

This paper discusses how the power of the free electron laser (FEL) beam was increased without increasing the size of the laser device by using a new model with a different technique for the undulator; the purpose of this technique is to make full use of the undulator magnets in a three-row system instead of the two-magnet system. This technique reduces the size of the laser device by decreasing the undulator's length and controlling the path of electrons within the rows of the undulator magnets. From the analysis of the obtained simulation results, it can be concluded that it is possible to make the FEL device with double the power output without increasing the size of the device; this will increase future applications of the FEL in the civil and military fields.

KEYWORDS

Laser, coherent photons, wavelength, output power, magnets, SASE

CITATION

Al-Aish, T.A.K. and Kamil, H.A. (2022). Design and establishment of an implementation to simulate and analyze the tertiary undulator of the free-electron laser. *The Scientific Journal of King Faisal University: Basic and Applied Sciences*, **23**(2), 39–42. DOI: 10.37575/b/sci/220036

1. Introduction

The scientific and technological development witnessed in various fields of life is the result of many important scientific discoveries. One of the most crucial of these discoveries is the laser beam and its use as a tool with high accuracy in solving problems and reaching the best solutions. Therefore, it has become necessary for researchers and scientists to develop laser-generating devices to suit those applications.

Since the invention of the laser by Theodore Maiman in 1960, scientists and researchers have been racing to develop a device that generates a laser beam with distinctive specifications to suit all civil and military applications (Madey, 1971).

The most important specifications of the desired laser are the control of the wavelengths and power of the output laser beam. The best type of laser that produces a laser beam with these characteristics is the free-electron laser (FEL), which was invented 10 years later by John Madey in 1970. The FEL differs from other types of lasers in regard to its physical form. The most effective medium is emitting electrons from an electronic gun. These electrons can be accelerated to reach a certain energy (300–500 MeV) and then enter the undulator (two rows of magnets) to make these electrons move in a sinusoidal motion in order to release coherent photons, which then reach a certain threshold level in a resonator with suitable specifications and eventually leads to the formation of the required laser beam.

The control of the electrons' energy and the specifications of the undulator are the distinguishing features of the FEL, whereby the wavelength and the power of the output laser beam are controlled. However, the size of the FEL device is a problem in some of its applications; consequently, researchers are working on reducing the size of the device by developing some of its parts (Al-Aish and Jawad, 2017; Kamil and Al-Aish, 2022; Zhang *et al.*, 2013; Varro, 2012; Hannon, 2008).

This paper explores how the power of the FEL beam was increased without increasing the undulator length by using a new model with a different undulator technique; this technique's purpose is to make full use of the undulator magnets in a three-row system instead of the two-magnet system. This technique reduces the size of the laser device by shortening the undulator's length and controlling the path of electrons within the rows of the undulator magnets.

2. Technique and implementation of the work

The FEL self-amplified spontaneous emission(SASE) consists of three main parts (electrons gun, linear accelerator, and undulator) as shown in Figure 1. It illustrates that the original undulator consists of two rows of magnets and that the coherent photons can be increased by increasing the undulator length. This paper demonstrates that a rise in the number of coherent photons was achieved without changing the undulator length. Moreover, a new row of magnets was added, making a total of three rows, as shown in Figure 2 (Mahmood and Al-Aish, 2022; Al-Aish, 2017; Kamil *et al.*, 2019; Mansfield, 2005; Al-Aish and Kamil, 2022).

Figure 1: The three main parts of the FEL.

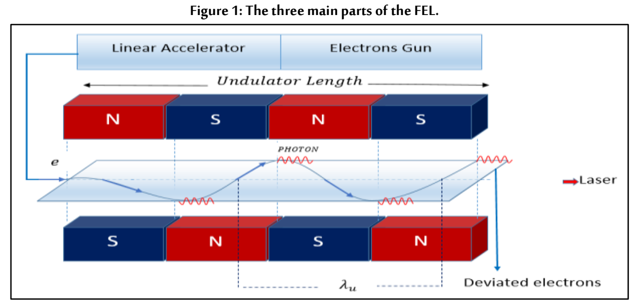

To calculate the effect of the additional new path on the output laser specification, an executable program called TUFEL was constructed using the Matlab 2019 software, as shown in Figure 3. It contains several parameters to simulate the change in the movement of the electrons, from accelerated linear motion to sinusoidal motion of the synchrotron beam formation.

Corresponding Author: Thair Abdulkareem Khalil Al-Aish 009647801693969, thair.ak.i@ihcoedu.uobaghdad.edu.iq

Figure 2: The triple undulator of the FEL.

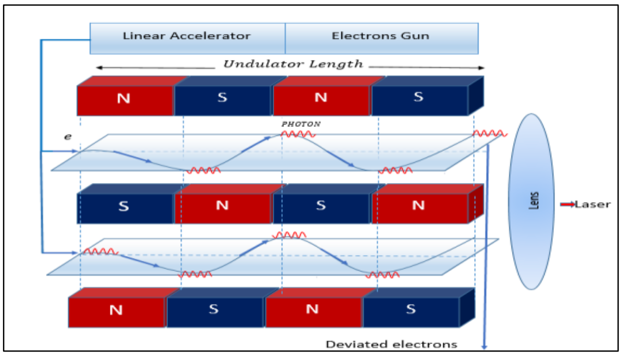

Figure 3: The implementation of the executable program TUFEL to simulate and analyse the tertiary undulator of the free electron laser.

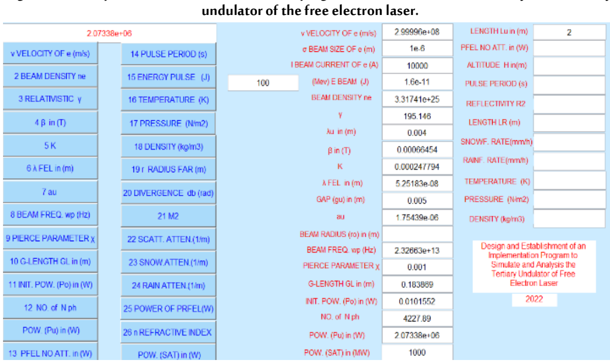

The electrons will move to the first (original) path and the second (new) path through bending magnets. Thus, the number of coherent photons N_{PH} will double as a result of the electrons passing through two paths instead of one path.

The number of coherent photons N_{PH} generated as one electron passes through the original path depends on the number N_u of electron wavelengths λ_u resulting from the oscillation of the electron during its passage through the length of the undulator L_u. The number N_u is calculated by the following equation (Al-Aish and Kamil, 2022; Bergman *et al.*, 2017; Steiniger *et al.*, 2014; Dhedan *et al.*, 2022; Ali *et al.*, a2022):

$$N_u = \frac{L_u}{\lambda_u} \tag{1}$$

Each λ_u generates two coherent photons. Therefore, the N_{PH} for one electron in the first path is given by the equation:

$$N_{PH} = \rho\, E_e\, \lambda / h\, c \tag{2}$$

Where: ρ represents the Pierce parameter, E_e represents the energy of the electrons' beam, c represents the velocity of light, h represents Planck's constant, and λ represents the wavelength of the output laser. λ is calculated using the equation below:

$$\lambda = 4.095 \times 10^{-14} \times \left(\frac{\lambda_u}{{E_e}^2}\right)\left(1 + \left(4354.77 \times {\lambda_u}^2\, B^2\right)\right) \tag{3}$$

Where: B is the intensity of the magnetic field.

Thus, due to the passage of electrons through two paths instead of one path, the number of coherent photons N_{PH} will double.

$$N_{PH} = 2\, \rho\, E_e\, \lambda / h\, c \tag{4}$$

The transmission of an electron beam through the undulator will lead to the generation of a coherent photon beam to form the output laser, which has power formed by the following equation (Ali *et al.*, b2022; Pflueger, 2018; Colson, 1976; Romaniuk, 2009; Al-Aish *et al.*, 2019):

$$P_u = \left(\frac{c\, E_e\, \rho^2\, N_{PH}}{9\, \lambda}\right) e^{(21.57\, \rho\, L_u/\lambda_u)} \tag{5}$$

The saturation power P_{sat} is given by the equation:

$$P_{sat} = \frac{\rho\, I_{beam}\, E_e}{e} \tag{6}$$

Where I_{beam} is the current of the electron beam.

3. Results and discussion of simulation

The main goal of this paper is to reduce the undulator length in order to reduce the size of the FEL device while maintaining or increasing the power of the output laser.

Therefore, the results shown in this paper are concentrated in support of this goal, as shown in Table 1. The standard values of the other parameters of the FEL are shown in Table 2.

Table 1: The results of simulation for (N_{PH}, P_u, and λ).

λ_u(m)	N_u(m)	λ (nm)	N_{PH} (one path)	N_{PH} (two path)	P_u(W) (one path)	P_u(W) (two path)
0.004	1000	52.51	4227.89	8455.78	2073380	4146760
0.006	666.6	78.78	6342.27	12684.54	56936.3	113872.6
0.008	500	105.30	8477.71	16955.42	9435.06	18870.12
0.010	400	134.22	10805.3	21610.6	3208.92	6417.84
0.012	333.3	172.47	13884.5	27769	1563.51	3127.2
0.014	285.7	233.79	18820.8	37641.6	935.531	1871.026
0.016	250	338.81	27275.5	54551	636.469	1272.938
0.018	222.2	514.17	41392.4	82784.8	471.706	943.412
0.02	200	791.33	63705	127410	371.18	742.36

Table 2: The standard values of the other parameters of the free-electron laser.

L_u	2 m		σ	1e-6 m		ρ	0.001
I_{beam}	10000 Amp		E_e	100 Mev		Mass of e	9.1e-31 kg
n_e	3.3 e+19		c	3e+8 m/s		P_{sat}	1000 MW

According to Equation (1), the number of electron wavelengths N_u is inversely proportional to the wavelength of the electron λ_u, as shown in Table 1. Figure 4 shows the decrease in N_u against the increase of λ_u while the length of undulator L_u remains a constant.

Figure 4: The decrease in N_u due to the increase of λ_u while the length of undulator L_u remains a constant.

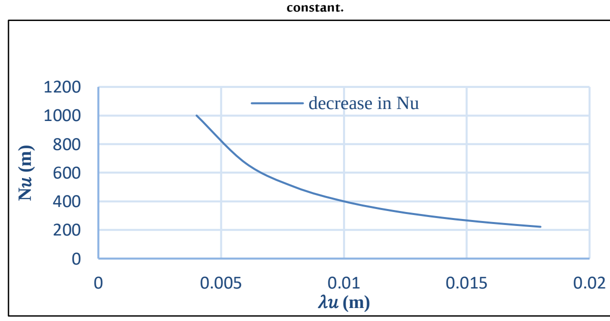

The number of coherent photons N_{PH} in the original first path represents the original photons, which will then increase by forming a new second path parallel to the first one; thus, the coherent photons will double due to their passage through the second path. According to Equation (2), the number of coherent photons N_{PH} is directly proportional to the wavelength λ of the output laser, as shown in Table 1. Figure 5a shows this increase in N_{PH} due to the increase of λ as a result of an increase in λ_u according to Equation (3). Figure 5b shows the relation between λ and λ_u.

Figure 5a: The increase in N_{PH} due to the increase of λ as a result of an increase in λ_u.

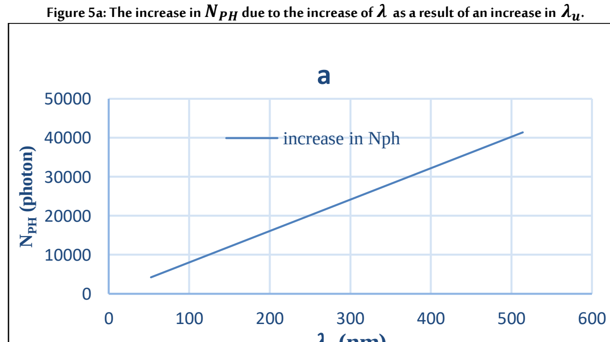

Figure 5b: The relation between λ and λ_u.

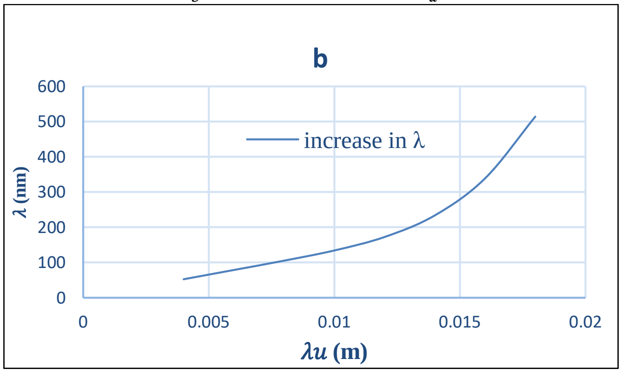

The undulator length L_u represents a group of wavelengths λ_u. By increasing the wavelengths λ_u (represented by the second path), the number of coherent photons N_{PH} will be increased according to Equation (4). Figure 6a shows the increase in N_{PH} as a result of an increase in λ_u.

The power of the output laser from undulator P_u will decrease as a result of the increase of λ according to Equation (5). Figure 6b shows the decrease in (P_u). On the other hand, the increase in laser power P_u can be observed in the case of two paths.

Figure 6a: The increase in N_{PH} due to the increase in λ_u.

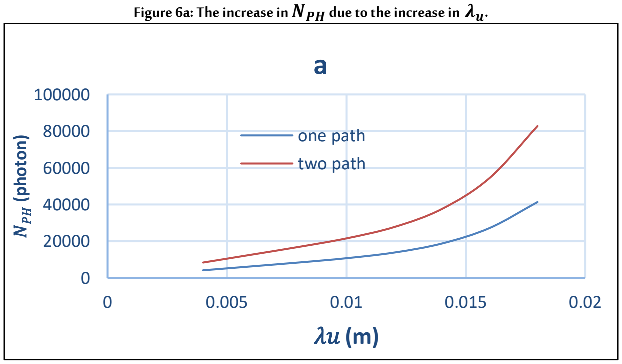

Figure 6b: The increase in P_u as a result of using the second path.

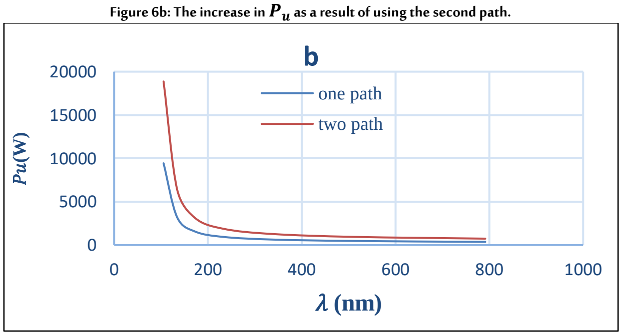

Finally, it is important to clarify that all results of the laser beam power P_u for the first and second paths had the least saturation power P_{sat}, which is 1000 MW according to Equation (6).

4. Conclusions

From the analysis of the obtained simulation results, it can be concluded that the increase in the number of photons as a result of adding the second path led to an increase in the output power of the laser beam without changing the undulator length.

Accordingly, it is possible to make the FEL device with a doubled output power without increasing the size of the device. This will help improve the future applications of the FEL in the civil and military fields.

Biographies

Thair Abdulkareem Khalil Al-Aish

Department of Physics, College of Education for Pure Sciences Ibn Al-Haitham, University of Baghdad, Baghdad, Iraq, 009647801693969, thair.ak.i@ihcoedu.uobaghdad.edu.iq

Dr. Al-Aish is a University of Baghdad graduate and an Iraqi assistant professor. He has published 20 Scopus-indexed articles with global publishers. His work is cited by many countries. He teaches the subject of laser at a college for bachelor's, master's and doctoral students. He supervises master's and doctoral students. He is a supervisor of the optics and laser lab and the computer lab and a manager of the information and media unit. He has participated in conferences in Iraq, Greece, Lebanon, and France. ORCID: 0000-0003-2479-5840

Hanady Amjed Kamil

Directorate of Education of First Karkh, Ministry of Education, Baghdad, Iraq, 009647813038914, hanadyamjedkamil@gmail.com

Kamil is a University of Baghdad graduate and an Iraqi assistant lecturer. She obtained a master's degree in Physics-laser. She has published seven Scopus-indexed articles with global publishers. Her work is cited by many countries. She is interested in research related to studying the interaction of the laser beam with matter in various applications. She teaches physics at the Directorate of Education of First Karkh, Ministry of Education, Baghdad, Iraq. She has participated in conferences in Iraq, Greece, Lebanon and France. ORCID: 0000-0003-4485-1475

References

Al-Aish, T.A. and Jawad, R.L. (2017). Design and simulate a new defense system of free electron laser DSFEL. *Engineering and Technology Journal*, **35**(2B), 166–72.

Al-Aish, T.A.K. (2017). Analysis and study of the effect of atmospheric turbulence on laser weapon in Iraq. *Baghdad Science Journal*, **14**(2), 426–37. DOI: 10.21123/bsj.2017.14.2.0427.

Al-Aish, T.A.K. and Kamil, H.A. (2022). Simulation and analysis the effect of the Lorentz force in a free electron laser. *Ibn AL-Haitham Journal for Pure and Applied Sciences*, **35**(2), 7–16. DOI:10.30526/35.2.2775.

Al-Aish, T.A.K., Jawad, R.L. and Kamil, H.A. (2019). Design and simulation a high-energy free electron laser HEFEL. In: *AIP Conference Proceedings*, AIP Publishing LLC, Beirut, Lebanon, 10-12/04/2019. DOI: 10.1063/1.5116995.

Ali, M.A., Al-Aish, T.A.K. and Kamil, H.A. (a2022). Analyzing and simulating the mechanism of laser medical therapy. In: *AIP Conference Proceedings*, AIP Publishing LLC, Athens, Greece, 28-30/05/2021. DOI: 10.1063/5.0092605.

Ali, M.A., Al-Aish, T.A.K. and Kamil, H.A. (b2022). A simulation breakdown the blood clot using a free electron laser system. In: *AIP Conference Proceedings*, AIP Publishing LLC, Athens, Greece, 28-30/05/2021. DOI: 10.1063/5.0092607.

Bergman, U., Yachandra, V.K. and Yano, J. (2017). *X-Ray Free Electron Lasers: Applications in Materials, Chemistry and Biology*, Cambridge, UK: Royal Society of Chemistry.

Colson, W.B. (1976). Theory of a free electron laser. *Physics Letters A*, **59**(3), 187–90. DOI: 10.1016/0375-9601(76)90561-2.

Dhedan, Z.A., Al-Aish, T.A.K. and Kamil, H.A. (2022). Design and simulation of a new system for producing laser beams without resonator "NSPLBR". In: *AIP Conference Proceedings*, AIP Publishing LLC, Athens, Greece, 28-30/05/2021. DOI: 10.1063/5.0092603.

Feng, C. and Deng, H.X. (2018). Review of fully coherent free-electron lasers. *Nuclear Science and Techniques*, **29**(11), 1–15. DOI: 10.1007/s41365-018-0490-1.

Hannon, F.E. (2008). *A High Average-Current Electron Source for the Jefferson Laboratory Free Electron Laser*. PhD Thesis, Lancaster University, Lancaster, United Kingdom.

Kamil, H.A. and Al-Aish, T.A.K. (2022). Determine the hazard level and biological effects for visible laser pointers. In: *AIP Conference Proceedings*, AIP Publishing LLC, Athens, Greece, 28-30/05/2021. DOI: 10.1063/5.0092595.

Kamil, H.A., Ahmed, M.S. and Al-Aish, T.A.K. (2019). Rain formation by free electron laser pulse system FELPS. In: *AIP Conference Proceedings*, AIP Publishing LLC, Beirut, Lebanon, 10-12/04/2019. DOI: 10.1063/1.5138570.

Madey, J.M. (1971). Stimulated emission of bremsstrahlung in a periodic magnetic field. *Journal of Applied Physics*, **42**(5), 1906–13. DOI:10.1063/1.1660466.

Mahmood, H.K. and Al-Aish, T.A.K. (2022). Design and stimulated the detectors of high-power lasers DHPL. In: *AIP Conference Proceedings*, AIP Publishing LLC, Athens, Greece, 28-30/05/2021. DOI: 10.1063/5.0092603.

Mansfield, R.P. (2005). *High Energy Solid State and Free Electron Laser Systems in Tactical Aviation*. PhD Thesis, Naval Postgraduate School, California, USA.

Pflueger, J. (2018). Undulator technology. In: *Proceedings of the CAS–CERN Accelerator School: Free Electron Lasers and Energy Recovery Linacs*, CERN Yellow Reports: School Proceedings, Hamburg, Germany, 31–10/06/2018. DOI: 10.23730/CYRSP-2018-001.55.

Romaniuk, R.S. (2009). POLFEL-free electron laser in Poland. *Photonics Letters of Poland*, **1**(3), 103–5.

Steiniger, K., Debus, A., Irman, A., Jochmann, A., Pausch, R., Schramm, U. and Bussmann, M. (2014). All-optical free-electron lasers using Traveling-Wave Thomson-Scattering. In: *5th International Particle Accelerator Conference,* IPAC2014, Dresden, Germany, 15–20/07/2014. DOI: 10.18429/JACoW-IPAC2014-WEPRO053.

Varro, S. (2012). *Free Electron Lasers*. Rijeka, Croatia: BoD–Books on Demand.

Zhang, T., Wang, G.L., Yao, H.F., Wang, D., Wang, W.T., Wang, C. and Wang, S.H. (2013). Numerical investigations of transverse gradient undulator based novel light sources. In: *Proceedings of the 35th International Free-Electron Laser Conference,* New York, USA, 26–30/08/2013.

The Scientific Journal of King Faisal University

Basic and Applied Sciences

Acute Transfusion Reactions in a Tertiary Care Hospital: The Saudi Context

Ammar Alsughayir[1], Mohrah Alalshaikh[2], Yasser Almaki[3], Leenah Almass[2], Mohammed Alnamnakani[1], Imran Ahad Pukhta[1], Alyazeed Alsaif[1], Sarah Abo Baker[1] and Abdullah Albarghash[1]

[1] Transfusion Division, King Fahad Medical City, Riyadh, Saudi Arabia
[2] Clinical Laboratory Sciences Department, Applied Medical Sciences, King Saud University, Applied Medical Sciences, Riyadh, Saudi Arabia
[3] Blood Bank Division, King Saud University Medical City, Riyadh, Saudi Arabia

LINK	RECEIVED	ACCEPTED	PUBLISHED ONLINE	ASSIGNED TO AN ISSUE
https://doi.org/10.37575/b/med/220034	26/10/2022	01/12/2022	01/12/2022	01/12/2022
NO. OF WORDS	**NO. OF PAGES**	**YEAR**	**VOLUME**	**ISSUE**
4226	5	2022	23	2

ABSTRACT

Although blood transfusion is a life-saving procedure, it can be associated with complications in rare cases. An acute transfusion reaction (ATR) is a complication where recipients exhibit an adverse reaction within 24 hours of a blood transfusion. This study aimed to determine the incidence of ATRs. This retrospective study reviewed the ATRs for all patients who received blood products over three years (2018, 2019, 2020). Of 81,498 transfusion episodes investigated, 132 (0.16%) were associated with ATRs. The most frequent adverse reactions were allergic reactions (62.9%, n = 83), followed by febrile non-haemolytic transfusion reactions (FNHTR) (32.6%, n = 43). Among blood products, it was found that allergic reactions were associated with platelet transfusions (40.9%, n = 34) and FNHTR with packed red blood cell transfusions (79.0%, n = 34). Serious complications such as acute haemolytic transfusion reaction and transfusion-related lung injury were not reported. The low percentage of recorded ATRs may indicate an underestimation of the true incidence due to under-reporting. Accurate reporting of ATRs is a crucial element of the haemovigilance system and would improve blood transfusion safety and enhance patient management.

KEYWORDS

FNHTR; allergic reactions; TACO; haemovigilance; urticarial rash

CITATION

Alsughayir, A., Alalshaikh, M., Almaki, Y., Almass, L., Alnamnakani, M., Pukhta, I.A., Alsaif, A., Abo Baker, S. and Albarghash, A. (2022). Acute transfusion reactions in a tertiary care hospital: The Saudi context. *The Scientific Journal of King Faisal University: Basic and Applied Sciences*, **23**(2), 43–7. DOI: 10.37575/b/med/220034

1. Introduction

Blood transfusion remains unquestionably a life-saving procedure. Its direct aid in achieving vital therapeutic outcomes in treating patients outweighs the infrequent, though possible, adverse events that can ensue. These adverse events have been reduced historically through the universal development of enhanced guidelines in blood transfusion services. These range from strict policies in selecting blood donors and screening donated blood for transfusion-transmissible infections to establishing hospital transfusion committees and direct feedback on transfusion adverse reactions to monitoring systems. These monitoring systems are now globally known and designated as haemovigilance, formally defined as the set of surveillance procedures covering the transfusion chain from blood donations to blood transfusions (Jain and Kaur, 2012). This vital concept of monitoring blood transfusion practices and events can help us define and understand the possible adverse events or reactions following a transfusion and aid in developing techniques and procedures that prevent their recurrence (Prakash, Basavaraj, and Kumar, 2017).

Acute transfusion reactions (ATRs) may differ in severity depending on the type and susceptibility of the patient. These reactions are defined as any unfavourable transfusion-related reaction that occurs to a recipient during or after the transfusion of blood or its components. ATRs occur during or within 24 hours of transfusion and are classified as immune- or non-immune-mediated adverse reactions. They include acute haemolytic transfusion reaction (AHTR), transfusion-related acute lung injury (TRALI), transfusion-associated circulatory overload (TACO), febrile non-haemolytic transfusion reaction (FNHTR), anaphylactic reactions and allergic transfusion reactions.

The international haemovigilance system was founded in 2009, and many developed countries have established haemovigilance systems at various levels. In Saudi Arabia (SA), establishing a national haemovigilance system is an important goal of the Saudi Society of Transfusion Medicine and the Ministry of Health (Hindawi, 2020). However, studies have reported that ATRs in Saudi hospitals are very rare, and only a small number of studies were found in the literature (Ali, Ibraham, and Joseph, 2005; Badawi *et al.*, 2021; Hindawi *et al.*, 2016). Measuring adverse transfusion events provides healthcare providers insights into blood transfusion safety and consequently enables them to improve it. This study aims to report and analyse ATR events over three years at a tertiary care hospital in Riyadh, SA.

2. Materials and Methods

This retrospective cross-sectional study was conducted at King Fahad Medical City, a tertiary hospital in Riyadh, SA. The institutional ethics committee approved the study (registration number: H-01-R-012). Reported transfusion reactions documented due to different transfused blood products, namely, leucodepleted packed red blood cells (PRBC), platelets and fresh frozen plasma (FFP), over three years (from January 2018 to December 2020) were analysed. When a transfusion reaction was reported to the blood bank, a transfusion reaction form was provided to medical staff. ATRs were examined using a standard transfusion reaction investigation protocol, which includes: clerical checking; an inspection of a post-transfusion blood sample for any evidence of haemolysis and comparison of the same with a pre-transfusion sample if available; rechecking of the patient's pre- and post-transfusion samples for blood grouping; carrying out direct antiglobulin and auto-control tests for the patient's pre- and post-transfusion samples; examining the patient's pre- and post-transfusion samples with the donor sample to recheck compatibility; repeating the antibody screen with a 3-cell panel and, in the event of a positive result, carrying out an antibody identification test using an 11-cell panel; and performing a bacteriological culture.

In addition to information obtained through the protocol, other data (age, sex, type and number of transfused products, symptoms and the diagnosed adverse reaction) were retrieved from the transfusion reaction reports. Acute reaction reports adequately filled out and confirmed by a haematologist were included. Those reports which

Corresponding Author: Mohrah Alalshaikh 00966504445584, malalshaikh@ksu.edu.sa

did not describe the symptoms and type of the adverse reaction were excluded, as were delayed adverse reaction reports. For statistical analysis, Microsoft Excel 2016 was used for data analysis and to obtain the event percentages.

3. Results

This retrospective study collected data on a total of 81,498 transfused blood components over the study period (from 2018 to 2020). The most transfused blood components were PRBC units (56%), followed by platelets and FFP (both 22%), as seen in Table 1.

Table 1. Number and type of transfused blood components over the study period.

Issued blood components	Number of units (2018)	Number of units (2019)	Number of units (2020)	Total (%)
PRBC	14278	15270	15925	45473 (56%)
Platelets	5999	6103	5790	17892 (22%)
FFP	6149	6040	5944	18133 (22%)
Total transfused units per year	26426	27413	27659	81498

Patients who developed ATR events ranged widely in age (1 to 94 years); 46.21% were male, and 53.79% were female. Of the total transfused units, 132 adverse events were reported, setting the average rate of transfusion reactions at 0.16%. The rates of allergic reactions and FNHTR were approximately 0.1% and 0.05%, respectively.

As illustrated in Table 2, most of these events were associated with PRBCs (43.2%). The highest reported types of ATRs were allergic reactions (62.9%), followed by FNHTR (32.6%). Most of the allergic reactions were associated with platelets (40.9%), followed by FFP (36.1%), while 79.0% of FNHTR events were associated with PRBCs. Moreover, allergic reactions affected more females than males (59% vs 41%). The opposite was noted with FNHTR, which was observed more in males than females (56% vs 44%). Three cases of anaphylactic reactions were reported, representing 2.3% of all cases. No TRALI or AHTR were reported.

Table 1. Types and percentages of the reported ATRs and their association with specific blood components.

Type of ATR	Component transfused				Incidence (per 10,000 components)
	PRBC	Platelets	FFP	Total (n=132)	
Allergic reactions	19	34	30	83(62.9%[B])	10.2
FNHTR	34	5	4	43 (32.6%)	5.3
Anaphylactic	1	0	2	3 (2.3%)	0.4
Hypotension	1	0	0	1 (0.8%)	0.1
TACO	1	0	0	1 (0.8%)	0.1
Others	1	0	0	1 (0.8%)	0.1
Total	57 (43.2%[A])	39 (29.5%)	36 (27.3%)	132	16.2

A Percentage of adverse reactions of total adverse transfusion reactions was noted.

B Percentage incidence of adverse transfusion reaction after transfusion of the blood component.

ATRs, acute transfusion reactions; FNHTR, febrile non-haemolytic transfusion reaction; TACO, transfusion-associated circulatory overload; PRBC, packed red blood cells; FFP, fresh frozen plasma.

The clinical presentations reported in these events covered a wide range of symptoms; the 12 symptoms reported are illustrated in Figure 1. Urticaria was the most frequent symptom, comprising 21% of the reported symptoms. Rash, fever, chills or flushing were also frequent, with percentages ranging between 12% and 14% of the total reported symptoms. Swelling of the face and pain in the chest or back were the least frequent symptoms experienced by only six and seven patients, respectively. All ATRs were reported following the standard hospital procedure and verified by blood bank haematologists.

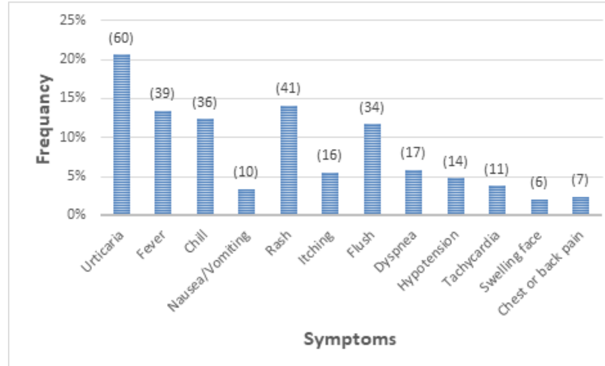

Figure 1. Distribution of ATR symptoms.

4. Discussion

This study provides a retrospective analysis of the ATR incidence resulting from the transfusion of 81,498 blood components over three years. This study's incidence rate of ATRs is 0.16%, comparable to another study from SA, which reported a rate of 0.2% (Hindawi *et al.*, 2016). These percentages are similar to those reported from other countries and range from 0.14% to 1.2% (Borhany *et al.*, 2019; Cho, Choi, Kim, Alghamdi, and Kim, 2016; Saha, Krishna, Prasath, and Sachan, 2020).

Allergic reactions and FNHTR are the most common adverse reactions seen with transfusion (Borhany *et al.*, 2019; Kumar, Thapliyal, Coshic, and Chatterjee, 2013; Saha *et al.*, 2020). Similarly, this study found that the most frequent reactions of 132 reported ATRs were allergic reactions (63%), followed by FNHTR (32%). Urticaria and skin rash were the most common symptoms, correlating with the high rate of allergic reactions (Cho *et al.*, 2016; Pahuja, Puri, Mahajan, Gupta, and Jain, 2017). However, some studies reported a higher percentage of FNHTR than allergic reactions (Grandi, Grell, Areco, and Barbosa, 2018; Prakash *et al.*, 2017). Several factors were associated with FNHTR, such as age, gender and the number and type of transfused components (Menis *et al.*, 2015). The rate of FNHTR was lower than that detected in other studies (Kumar *et al.*, 2013; Pahuja *et al.*, 2017; Prakash *et al.*, 2017), which could be explained by the use of leucodepleted blood (Bianchi *et al.*, 2016). FNHTR can result from patients' leucocyte antibodies reacting with donors' leucocyte antigens, leading to the release of endogenous cytokines or leucocyte cytokines accumulated in the blood products. Consistent with our results, the frequency of FNHTR was higher with red cell transfusions than with platelets (Menis *et al.*, 2015). Moreover, compared with FNHTR, allergic reactions are associated more with platelets and plasma transfusion than red cells (Saha *et al.*, 2020). The severity of these adverse reactions ranged from mild non-systemic to severe and life-threatening systemic reactions. The frequency of severe anaphylactic reactions was low, representing 2% of the total allergic reactions (Grandi *et al.*, 2018). In this study, of the total adverse events, three events (2.3%) presented clinically with hypotension, bradycardia, urticaria and dyspnoea. Two events were ATRs from an FFP transfusion and a PRBC transfusion.

Syndromes of acute respiratory distress, TACO and TRALI, occur during or within six to 12 hours of transfusion (International Society of Blood Transfusion Working Party on Haemovigilance in collaboration with The International Haemovigilance Network and AABB, 2018; Vlaar *et al.*, 2019). TACO was described as one of the leading causes of transfusion-related fatalities (44%) (FDA, 2019). Only one TACO reaction after a PRBC transfusion was observed in this study period. The presenting symptoms were chills, dyspnoea and chest pain. These findings are in contrast to other studies, which reported a higher percentage, such as the study by Saha *et al.* (2020), where six TRALI events were detected among 140 ATR events (4.3%). However, no TACO events were seen in other studies (Borhany *et al.*, 2019; Prakash *et al.*, 2017).

Like TACO, TRALI is one of the leading causes of transfusion-related mortality (FDA, 2019). Although TRALI can result from the red blood cell component, most severe cases are related to plasma-rich components (Peters, Stein, and Velar, 2015). In the majority of cases, donors' antibodies were detected, reacting against recipients' human leucocyte antigens (HLA) class I/II and/or human neutrophil antigens (HNA) (Peters *et al.*, 2015). HNA and HLA may develop when the immune system is exposed to foreign HNA or HLA antigens, such as during pregnancy or transfusion. The incidence of TRALI has reduced significantly following the use of plasma-rich components from men and women who have not been pregnant or have tested negative for HLA antibodies (Otrock, Liu, and Grossman, 2017). In SA, the vast majority of donors are men, with women representing only 2% of the total donors (Alsughayyir *et al.*, 2022). These mitigation strategies have played an essential role in reducing the incidence rate of TRALI. No TRALI event was detected in our study, which is consistent with the study conducted in Jeddah, SA, by Hindawi et al. (2016). Moreover, the use of leucodepleted blood components can play a role in reducing the incidence of TRALI (Simancas-Racines *et al.*, 2019). Nevertheless, this adverse effect can occur even when leucodepleted products are used (Maulydia, Airlangga, Imam, Siregar, and Hendriana, 2022).

The fatal risk of blood transfusion from ABO incompatibility transfusion events can cause severe AHTR and has significantly reduced in the last few decades (Storch, Rogerson, and Eder, 2020). In our study, no AHTR was reported in the three-year study period. This may be due to the hospital protocol, which includes verifying patients' ABO type using a second or historical sample. In addition, no bacterial sepsis event was reported, which may indicate the implementation of quality measures at different steps of the blood transfusion chain.

Moreover, only one event of isolated hypotension reaction associated with PRBC transfusion was reported in the study period, in contrast to other studies, which detected a higher incidence rate (Hendrickson *et al.*, 2016; Saha *et al.*, 2020).

As this study is retrospective, adverse events may have been under-reported. Compared with international studies, the low incidence of total ATRs and some specific adverse events, such as TACO and isolated hypotension, may indicate the under-reporting of transfusion reaction events. Furthermore, as there are few published national studies, a statistical comparison of the results of this study with other Saudi studies was not possible. However, our data can help evaluate the safety of transfused blood in the country and identify areas for improvement.

In conclusion, our results showed that the most frequent ATRs are allergic reactions and FNHTR. Adequate reporting of ATR events should be emphasised, as this would help improve the haemovigilance system and, consequently, blood safety. This study adds to the published national data to allow benchmarking. Moreover, the upcoming Saudi National Haemovigilance Project could utilise the published data in developing national and local benchmarks for ATRs.

Biographies

Ammar Alsughayir

Department of Pathology and Laboratory Medicine, King Fahad Medical City, Riyadh, Saudi Arabia, 00966541235322, aalsughayir@kfmc.med.sa

Dr Ammar AlSughayir is a King Saud University graduate, Saudi haematopathologist and transfusion medicine consultant. He is a knowledgeable and talented certified clinical pathologist with twenty years of experience providing medical diagnostic services in clinical laboratories and blood banks and developing and renovating the diagnostic services to be comparable with the highest international standards. He has published several articles and authored books and chapters. He has presented at national and international conferences. He is a board member of several scientific societies and an active member of many international associations. ORCID: 0000-0003-3606-0542

Mohrah Alalshaikh

Clinical Laboratory Sciences Department, Applied Medical Sciences, King Saud University, Applied Medical Sciences, Riyadh, Saudi Arabia. 00966504445584, malalshaikh@ksu.edu.sa

Mohrah Alalshaikh is a Saudi teaching assistant. She teaches immunohaematology and haematology courses for undergraduate students. She has an MSc in Transfusion and Transplantation Sciences from the University of Bristol, United Kingdom. Currently, she is a PhD candidate at King Saud University. She has several publications in high-quality journals in the transfusion field. She collaborates with several Saudi research centres and hospitals, such as Heath Science Research Center, Princess Nourah Bint Abdulrahman University and Prince Sultan Medical City. ORCID: 0000-0001-8471-7452.

Website: https://faculty.ksu.edu.sa/ar/malalshaikh

Yasser Almalki

Department of Blood Bank, King Khalid Hospital at King Saud University Medical City, Riyadh, Saudi Arabia. 00966566579680, yalmalki@ksu.edu.sa

A senior laboratory specialist, Yasser Almalki, is a King Saud University graduate. He has majored in Clinical Laboratory Sciences, with a Master's in Biomedical Sciences from the University of Tasmania, Australia. He worked at King Khalid Hospital as a laboratory specialist from 2010 to 2019 and then as a senior laboratory specialist from 2019. He is registered with the Saudi Commission for Health Specialities (SCHFS) as a senior laboratory specialist since 2019.

Leenah Almass

Clinical Laboratory Sciences Department, Applied Medical Sciences, King Saud University, Applied Medical Sciences, Riyadh, Saudi Arabia. 00966532700952, inahmass@gmail.com

Leenah Almass is a student at the clinical laboratory science department at the Applied Medical Science College at King Saud University, Riyadh, SA. She was selected as one of the most talented students in college. She is interested in researching blood and genetic disorders like sickle cell disease, thalassemia and leukaemia and their physiology at the cellular and genetic levels. She is also interested in gene-editing techniques like CRISPR-Cas9 and how they can be used to treat genetic disorders. She is also involved in improving processes to make them more accessible and methods to lessen the side effects caused by chemotherapy and other therapies for delivering gene-edited cells more safely.

Mohammed Alnamnakani

Department of Pathology and Laboratory Medicine, King Fahad Medical City, Riyadh, Saudi Arabia, 00966557777038, malnamnakani@gmail.com

Dr Mohammed Alnamnakani is the director of pathology and laboratory medicine at King Fahad Medical City. He is certified by the American Board in Anatomic and Clinical Pathology. His primary focus is on transformation, artificial intelligence and digital solutions. He is a team player in human capital development and change management. He is very keen on emotional intelligence and leadership courses. He has many website case reviews and has published several papers in his speciality. He is looking forward to more publications and interactive courses.

Imran Ahad Pukhta

Department of Transfusion Medicine Service, King Fahad Medical City, Riyadh, Saudi Arabia, 00966533095845, imranpukhta@gmail.com

Dr. Imran Ahad Pukhta had his postgraduate education at Acharya Shri Chander College of Medical Sciences, University of Jammu, Kashmir. He earned his M.D. degree in Pathology in 2008. He has been an assistant speciality consultant at the blood bank and head of the transfusion service section for nine years. He played an essential role in the CAP accreditation of his department. ORCID: 0000-0002-3385-0808

Alyazeed Saad Alsaif

Department of Transfusion Medicine Services at King Fahad Medical City, Riyadh, Saudi Arabia, 00966555440778, yss54@hotmail.com

Alyazeed Saad Alsaif is a Saudi post-graduate from the Royal Melbourne Institute of Technology, College of Applied Medical Science, Melbourne, Australia. He earned his master's degree in transfusion medicine in 2017. He works as a medical technologist in the blood bank department and as a blood bank supervisor, supervising transfusion medicine and blood donor practice. He has participated in many awareness campaigns for laboratories and international blood donor days. Moreover, he participated with his colleagues to achieve national and international accreditation for his institution. ORCID: 0000-0003-4737-4483.

Sarah Bakr Abobakr

Department of Transfusion Medicine Services, King Fahad Medical City, Riyadh, Saudi Arabia, 00966553448447, sb.1991@hotmail.com

Sarah Bakr Abobakr graduated from King Saud University, College of Applied Medical Science. She earned her bachelor's degree in clinical laboratory science in 2014. She works as a medical technologist at the blood bank and as a quality coordinator, having initiated three quality projects in the same field. She has participated in many awareness campaigns for laboratories and international blood donor days. Moreover, she participated with her colleagues to achieve national and international accreditation for her institution. ORCID: 0000-0002-0981-9894.

Abdullah Khalid Albarghash

Department of Transfusion Medicine Services, King Fahad Medical City, Riyadh, Saudi Arabia, 00966540081221, iabdullah.khalid0@gmail.com

Abdullah Khalid Albarghash graduated from Prince Sattam Bin Abdulaziz University, College of Applied Medical Science, Alkharj. He earned his bachelor's degree in clinical laboratory science in 2016. He works as a medical technologist in the blood bank department and as a blood bank senior. He has participated in many awareness campaigns for laboratories and international blood donor days. Moreover, he participated with his colleagues to achieve national and international accreditation for his institution. ORCID: 0000-0003-0632-5255

Acknowledgements

The authors extend their appreciation to the Deanship of Scientific Research at King Saud University for funding this work through the Undergraduate Research Support Program. We would also like to thank the Deanship of Scientific Research and the Researcher Support and Services Unit at King Saud University for their technical support.

References

Ali, S.I., Ibraham, R.C. and Joseph, L. (2005). Transfusion related acute lung injury. *Journal of the Pakistan Medical Association*, **55**(7), 304–06.

Alsughayyir, J., Almalki, Y., Alalshaik, M., Aljoni, I., Kandel, M., Alfhili, M.A., and Alabdullateef, A. (2022). Demography and blood donation trends in Saudi Arabia: A nationwide retrospective, cross-sectional study. *Saudi Journal of Biological Sciences*, **29**(12), n/a. https://doi.org/10.1016/j.sjbs.2022.103450.

Badawi, M.A., Saaty, R., Altayyari, S.T., Khalil, R., Moria, F., Zaher, G., Alnajjar, S. and Hindawi, S.I. (2021). Improving detection rates of suspected acute transfusion reactions through active surveillance. *Iraqi Journal of Hematology*, **10**(2), 165–9. https://doi: 10.4103/ijh.ijh_31_21.

Bianchi, M., Vaglio, S., Pupella, S., Marano, G., Facco, G., Liumbruno, G.M., and Grazzini, G. (2016). Leucoreduction of blood components: An effective way to increase blood safety. *Blood Transfusion*, **14**(2), 214–27. DOI: 10.2450/2015.0154-15.

Borhany, M., Anwar, N., Tariq, H., Fatima, N., Arshad, A., Naseer, I. and Shamsi, T. (2019). Acute blood transfusion reactions in a tertiary care hospital in Pakistan - an initiative towards haemovigilance. *Transfusion Medicine*, **29**(4), 275–8. DOI: 10.1111/tme.12541.

Cho, J., Choi, S.J., Kim, S., Alghamdi, E. and Kim, H.O. (2016). Frequency and pattern of noninfectious adverse transfusion reactions at a tertiary care hospital in Korea. *Annals of Laboratory Medicine*, **36**(1), 36–41. DOI: 10.3343/alm.2016.36.1.36.

FDA. (2019). *Transfusion/Donation Fatalities – Fatalities Reported to FDA Following Blood Collection and Transfusion: Annual summary for fiscal year 2019*. Available at: https://www.fda.gov/media/147628/download (Accessed on 8/3/2022).

Grandi, J.L., Grell, M.C., Areco, K.C.N. and Barbosa, D.A. (2018). Hemovigilance: The experience of transfusion reaction reporting in a teaching hospital. *Revista Da Escola de Enfermagem*, **2018**(52), 1–7. DOI: 10.1590/S1980-220X2017010603331.

Hendrickson, J.E., Roubinian, N.H., Chowdhury, D., Brambilla, D., Murphy, E.L., Wu, Y., Ness, P.M., Gehrie, E.A., Snyder, E.L., Hauser, R.E., Gottschall, J.L., Kleinman, S., Kakaiya, R. and Strauss, R.G. (2016). Incidence of transfusion reactions: A multicenter study utilizing systematic active surveillance and expert adjudication. *Transfusion*, **56**(10), 2587–96. DOI: 10.1111/TRF.13730

Hindawi, S.I. (2020). Evolution of blood transfusion medicine in Saudi Arabia. *Transfusion*, **60**(S1) 2–3.

Hindawi, S.I., Badawi, M.A., Raj, E.T., Gholam, K.A., Al-Weail, S.O. and Azher, F. (2016). The use of transfusion quality indicators as a tool for hemovigilance system implementation at a tertiary care center in Saudi Arabia. *Saudi Medical Journal*, **37**(5), 538–43. DOI: 10.15537/smj.2016.5.15084

International Society of Blood Transfusion Working Party on Haemovigilance in Collaboration with the International Haemovigilance Network and AABB. (2018). *Transfusion-Associated Circulatory Overload (TACO) Definition (2018)*. Available at: https://www.aabb.org/docs/default-source/default-document-library/resources/taco-2018-definition.pdf?sfvrsn=e1bcfce4_0 (Accessed on 12/02/2022).

Jain, A. and Kaur, R. (2012). Hemovigilance and blood safety. *Asian Journal of Transfusion Science*, **6**(2), 137–8. DOI: 10.4103/0973-6247.98911

Kumar, P., Thapliyal, R., Coshic, P. and Chatterjee, K. (2013). Retrospective evaluation of adverse transfusion reactions following blood product transfusion from a tertiary care hospital: A preliminary step towards hemovigilance. *Asian Journal of Transfusion Science*, **7**(2), 109–15. DOI: 10.4103/0973-6247.115564

Maulydia, M., Airlangga, P.S., Imam, M., Siregar, T. and Hendriana, D.R. (2022). Transfusion-related acute lung injury (TRALI) in post-partum bleeding patients: A case report. *Bali Journal of Anesthesiology*, **6**(2), 119–22. DOI: 10.4103/bjoa.bjoa

Menis, M., Forshee, R.A., Anderson, S.A., Mckean, S., Gondalia, R., Warnock, R., Johnson, C., Mintz, P.D., Worrall. C.M., Kelman. J.A. and Izurieta, H. S. (2015). Febrile non-haemolytic transfusion reaction occurrence and potential risk factors among the U.S. elderly transfused in the inpatient setting, as recorded in Medicare databases during 2011-2012. *Vox Sanguinis*, **108**(3), 251–61. DOI : 10.1111/vox.12215.

Otrock, Z.K., Liu, C. and Grossman, B.J. (2017). Transfusion-related acute lung injury risk mitigation: An update. *Vox Sanguinis*, **112**(8), 694–703. DOI: 10.1111/VOX.12573.

Pahuja, S., Puri, V., Mahajan, G., Gupta, P. and Jain, M. (2017). Reporting adverse transfusion reactions: A retrospective study from tertiary care hospital from New Delhi, India. *Asian Journal of Transfusion Science*, **11**(1), 6–12. DOI: 10.4103/0973-6247.200779

Peters, A.L., Van Stein, D. and Vlaar, A.P. (2015). Antibody-mediated transfusion-related acute lung injury; from discovery to prevention. *British Journal of Haematology*, **170**(5), 597–614.

DOI: 10.1111/BJH.13459

Prakash, P., Basavaraj, V. and Kumar, R. (2017). Recipient hemovigilance study in a university teaching hospital of South India: An institutional report for the year 2014–2015. *Global Journal of Transfusion Medicine*, **2**(2), 124–9. DOI: 10.4103/gjtm.gjtm_32_17

Saha, S., Krishna, D., Prasath, R. and Sachan, D. (2020). Incidence and analysis of 7 years' adverse transfusion reaction: A retrospective analysis. *Indian Journal of Hematology and Blood Transfusion*, **36**(1), 149–55. DOI: 10.1007/s12288-019-01174-x

Simancas-Racines, D., Arevalo-Rodriguez, I., Urrutia, G., Buitrago-Garcia, D., Núñez-González, S., Martínez-Zapata, M.J., Madrid, E., Bonfill, X. and Hidalgo-Ottolenghi, R. (2019). Leukodepleted packed red blood cells transfusion in patients undergoing major cardiovascular surgical procedure: Systematic review and meta-analysis. *Cardiology Research and Practice*, **2019**(n/a), 1–10. DOI: 10.1155/2019/7543917

Storch, E.K., Rogerson, B. and Eder, A.F. (2020). Trend in ABO-incompatible RBC transfusion-related fatalities reported to the FDA, 2000-2019. *Transfusion*, **60**(12), 2867–75. DOI: 10.1111/trf.16121

Vlaar, A.P., Toy, P., Fung, M., Looney, M.R., Juffermans, N.P., Bux, J., Bolton-Maggs, P., Peters, A.L., Silliman, C.C., Kor, D.J. and Kleinman, S. (2019), A consensus redefinition of transfusion-related acute lung injury. *Transfusion,* **59**(7), 2465–76. DOI: 10.1111/trf.15311

المجلة العلمية لجامعة الملك فيصل
The Scientific Journal of King Faisal University

العلوم الأساسية والتطبيقية
Basic and Applied Sciences

تسجيل جديد لأنواع نادرة من اللافقاريات البحرية في شرقي المتوسط، سوريا

New Records of Rare Species of Marine Invertebrates in the Eastern Mediterranean, Syria

ازدهار علي عمار و يارا بسيم حميشة
قسم البيولوجيا البحرية، المعهد العالي للبحوث البحرية، جامعة تشرين، اللاذقية، سوريا

Izdihar Ali Ammar and Yara Baseem Hmaesha
Department of Marine Biology, High Institute of Marine Research, Tishreen University, Lattakia, Syria

LINK الرابط	RECEIVED الاستقبال	ACCEPTED القبول	PUBLISHED ONLINE النشر الإلكتروني	ASSIGNED TO AN ISSUE الإحالة لعدد
https://doi.org/10.37575/b/sci/220044	28/10/2022	01/12/2022	01/12/2022	01/12/2022

NO. OF WORDS عدد الكلمات	NO. OF PAGES عدد الصفحات	YEAR سنة العدد	VOLUME رقم المجلد	ISSUE رقم العدد
5211	6	2022	23	2

الملخص

يساعد الاستمرار في إجراء البحوث وبذل مزيدٍ من الجهود الحقليّة في الكشف عن وجود أنواعٍ جديدةٍ ونادرةٍ من الحيوانات اللّافقارية (invertebrates) في المياه الإقليمية السوريّة - شرق البحر الأبيض المتوسط، والتعرّف على صفاتها البيولوجيّة والبيئيّة. تقدّم هذه المقالة معلوماتٍ عن أربعة أنواعٍ من السرطانات البحريّة (crabs) إحداها غريبٌ (alien) ونوعين من نجوم البحر (starfish)، ونوعٍ من قنافذ البحر(sea urchins)، ونوعين من الأخطبوط (octopus) وتوثّق وجودها للمرة الأولى في البحر السوريّ – شرق البحر الأبيض المتوسط، وقد جُمعَت من قبل الصيّادين بواسطة شباك الصّيد من المنطقة الشاطئيّة (coastal area) والمنطقة متوسّطة العمق (20 – 630 متراً) من مناطق رأس البسيط واللاذقية وبانياس خلال العامين 2020 و 2021، وهذه الأنواع هي: Actaea savignii (H. Milne Edwards,1834), Dromia personata Linnaeus, 1758, Geryon longipes A. Milne-Edwards, 1882, Homola barbata(Fabricius, 1793), Peltaster placenta (Müller and Troschel, 1842), Chaetaster longipes (Bruzelius, 1805), Sphaerechinus granularis (Lamarck, 1816), Tremoctopus violaceus delle Chiaje, 1830, Ocythoe tuberculata Rafinesque 1814. يعدّ توثيق وجود هذه الأنواع أمراً مهمّاً جداً من الناحيتين البيئيّة و العلميّة، ويستدعي تسجيل المزيد منها التنسيق مع العاملين في قطّاع الصّيد البحريّ في سوريا.

Abstract

Conducting further research and exerting more effort into field studies will aid the detection and recording of new, rare species of invertebrates in the Mediterranean and allow the examination of their biological and environmental characteristics. This article provides information on four species of sea crab (one of which is alien), two species of sea star, one species of sea urchin and two species of octopus, which have all been documented for the first time in Syrian waters. Samples were collected by fishing nets from a coastal area at medium depths (20–630 meters) from Ras al-Basit, Lattakia and Banias during 2020 and 2021. These species are: *Actaea savignii* (H. Milne Edwards, 1834); *Dromia personata* (Linnaeus, 1758);*Geryon longipes* (A. Milne-Edwards, 1882); *Homola barbata* (Fabricius, 1793); *Peltaster placenta* (Müller and Troschel, 1842); *Chaetaster longipes* (Bruzelius, 1805); *Sphaerechinus granularis* (Lamarck, 1816); *Tremoctopus violaceus* (Delle Chiaje, 1830);*Ocythoe tuberculate* (Rafinesque, 1814). Documenting the presence of these rare species is very important from an environmental and scientific perspective, and recording more of them requires coordination with the marine fishing sector in Syria.

KEYWORDS
الكلمات المفتاحية
Cephalopods, crustaceans, echinoderms, marine biodiversity, non-indigenous species,zoobenthos
رأسيات الأرجل، القشريّات، شوكيات الجلد، التنوّع الحيويّ البحريّ، أنواع غير أصيلة، قاعيّات حيوانيّة

CITATION
الإحالة
Ammar, I.A. and Hmaesha, Y.B. (2022). Sajilaat jadidat lil'anwae alnaadirat min allaafiqariaat albahriat fi sharq albahr al'abyad almutawasit, Surya'New records of rare species of marine invertebrates in the eastern Mediterranean, Syria'. *The Scientific Journal of King Faisal University: Basic and Applied Sciences*, **23**(2), 48–53. DOI: 10.37575/b/sci/220044 [in Arabic]

عمار، ازدهار علي و حميشة، يارا بسيم. (2022). تسجيل جديد لأنواع نادرة من اللافقاريات البحرية في شرقي المتوسط، سوريا. *المجلة العلمية لجامعة الملك فيصل: العلوم الأساسية والتطبيقية*، **23**(2)، 48–53.

1. مقدمة

تمتلك مُحيطات العالم وبحاره أكبر موائل(*habitats*) للأحياء على الأرض وتحتوي على أقدم أشكال الحياة فيها. توفّر هذه البيئات البحريّة عدداً كبيراً من متطلّبات الإنسان وحاجاته(Townsend *et al.,* 2018: 1). تُعدّ الحيوانات القاعيّة (*benthic fauna*) مُكوّناً رئيساً في النّظم البيئيّة البحريّة كلّها، فهي غذاءٌ رئيسٌ لجميع الأنواع التي تتغذّى من القاع، بالإضافة إلى الأهميّة الاقتصاديّة للعديد منها في مجال الاستثمار والاستزراع. لا يزال جزءٌ كبيرٌ من محيطات العالم غيرَ مستكشَفٍ، في الوقت الذي تشهد فيه هذه البيئات تغيّراتٍ في المناخ، وكثيراً من الاضطرابات بفعل الأنشطة البشريّة، مثل: الصّيد الجائر، والتلوّث، وتغيير الموائل وتخريبها، والغزو البيولوجي (*bio - invasion*). وتؤثّر جميعها على العمليات البيئيّة والتنوّع الحيويّ البحريّ (*marine biodiversity*) (Canonico *et al.,* 2019: 2).

في البحر الأبيض المتوسط (*Mediterranean*) الذي يبدو الأكثر تأثراً(Lejeusne *et al.*, 2010: 250)، ويعدّ نقطةً ساخنةً (*hot spot*)للتنوّع الحيويّ البحريّ(Coll *et al.,* 2010:1)، تؤثّر عديدٌ من العوامل على انتشار الحيوانات القاعيّة وتوزّعها فيه: كنمط القاع، والعمق(depth)، والملوحة (*salinity*)، والشفافية (*transparency*)، ودرجة الحرارة (*temperature*) (Stachowitsch and Gallmetzer, 2016: 29). يعدّ غزو الأنواع غير الأصيلة (*non-indigenous species*) عاملاً مزمناً سيستمرُّ في تغيير التنوّع البيولوجي للبحر الأبيض المتوسط وخاصّةً في حوضه الشرقيّ، والذي يمكن أن ينتشر بسرعة شمالاً وغرباً بسبب ارتفاع درجة حرارة مياهه بشكلٍ عام.

ولا بدّ من الإشارة إلى أنّ معظم الأنواع الغريبة في شرقي البحر المتوسط وسوريا هي من أصول هندية – هادية، ومن البحر الأحمر، وصلت عبر قناة السويس، كما أنّ وجود بعضها الآخر يعود إلى انتقالها من خلال مياه التوازن Ballast water، و الحشف البحريّ Maeine Fouling ، ودخولها في بيئاتها الجديدة (Zenetos *et al.,* 2018: 209). يملك عديدٌ من هذه الأنواع الغريبة تأثيراً سلبياً، وتصنّف على أنّها غازيةٌ، وهي مسيطرةٌ في مختلف الموائل والأعماق(Katsanevakis *et al.*, 2014: 662) والبعض منها لا يزال وجوده نادراً (Zenetos *et al.*, 2022: 197). لقد تمّ إنجاز عديدٍ من الدّراسات لتسجيل هذه الأنواع في المنطقتين الشاطئيّة Littoral وتحت الشاطئيّة Sublittoral (Ammar, 2019: 180) في سوريا، التي تواجه الأحياء القاعيّة البحريّة فيها، بالإضافة إلى الغزو من قبل أنواعٍ غريبةٍ، مخاطر الصّيد الجائر، والتلوّث، وارتفاع حموضة المياه. وتهدّد هذه العوامل كلّها الأنواع الأصيلة

Corresponding Author: Izdihar Ali Ammar 00963998694090, izdiammar@gmail.com المؤلف المراسل: ازدهار علي عمار

بالانقراض.

يعدّ توثيق وجود الأنواع النّادرة، والأنواع المُوصى بحمايتها، وتلك المهدّدة بالانقراض (threatened species)، ودراسة توزّعها الجغرافيّ، أمراً مهمّاً وضروريّاً من الناحية العلميّة، لزيادة المعرفة بالتنوّع البيولوجي، ولإدارة هذه الأنواع، باعتبارها توفّر معلوماتٍ مبكرةً عن التغييرات التي تطرأ على توزعها، أو توسع انتشارها في موائل أخرى، كما توفّر هذه التسجيلات معلومات عن الحالة، والخصائص البيولوجيّة والبيئيّة للأنواع التي تشهد انخفاضاً في غزارتها، أو تلك التي تمّ إهمالها بسبب وجودها المحدود وعددها القليل.

في العديد من الدراسات المنجزة حول الأنواع النادرة في البحر الأبيض المتوسط، تمّ الحصول على العيّنات والأنواع بعدّة طرائق، أهمّها منصّات التواصل الاجتماعي ومنصّات العلوم العامّة من خلال قيام علماء الطبيعة والغوّاصين والمستجمّين بمشاركة صورٍ لبعض الأنواع فيها، وقد ساهمت هذه الطريقة بشكل فعّال في توثيق وجود الأنواع النادرة، والتي يصعب الحصول عليها بطريقة المسح العلميّ المنتظم (Follett and Strezov, 2015: 1)، وأنواع نادرة أخرى قد تمّ تسجيلها خلال المسوحات العلمية باستخدام مجموعة متنوّعة من الوسائل مثل شباك الجرّ التجريبية (*trawl*) في قاع البحار والمحيطات، وشباك العوالق الحيوانيّة (Zooplankton)، والملاحظة البصرية بالغوص تحت الماء، وخاصّة في الموائل والنظم البيئيّة غير المستكشفة، مثل الكهوف البحريّة والمياه العميقة(deep sea)، تؤكّد جميع المعطيات المتوفّرة أهميّة التنسيق والتعاون مع قطاع المصايد السمكية في اكتشاف الأنواع النادرة (Steins *et al.*, 2020: 146).

تمّ ذكر العديد من الأنواع النادرة في البحر الأبيض المتوسط في مقالات جماعية مشتركة(collective articles)، كان الهدف منها تجميع التسجيلات الحديثة والمعلومات المتعلّقة بهذه الأنواع وفق التقسيمات الجغرافية لمناطق البحر المتوسط (غرب المتوسط، مركز المتوسط، بحر الدرياتيك، شرقي المتوسط والبحر الأسود) (Santin *et al.*, 2021: 199; Tsagarakis *et al.*, 2021: 627)، كما تمّ توثيق العديد من الأنواع الجديدة والنادرة الموجودة في موائل خاصّة كالمحميات (marine protected areas) والكهوف – UNEP/MAP SPA/RAC, 2022: 19)، وفي أحدث دراسة على التنوّع الحيويّ في الحوض الشرقي للبحر المتوسط سُجّل وجود ثلاثة وثلاثين نوعاً من اللافقاريات البحريّة المعرّضة للخطر هي تسعة أنواع من الإسفنجيات (*Spongia*)، وتسعة عشر نوعاً من الزهريات (*Anthozoa*) (حيود مرجانية coral reefs، قلم البحرsea pen وشقائق البحرsea anemon)، ونوعان من الرخويات (*Mollusca*)، ونوع من عضديات الأرجل (*Brachiopoda*)، ونوعان من شوكيات الجلد (*Echinodermata*) (Mytilineou *et al.*, 2016: 794).

يتضمّن البحث الحالي تسجيل وجود تسعة أنواع نادرة من اللّافقاريات البحريّة في مناطق وأعماق مختلفة من البحر السوري، تنتمي أربعة أنواع منها للقشريات (Crustacea)، ونوعين من الرخويات رأسيات الأرجل (Cephalopoda)، وثلاثة أنواع من شعبة شوكيات الجلد، بالإضافة إلى توصيف حالة الرخوي بطني القدم (*gastropod*) *Tonna galea*، كنوع موصى بحمايته، والكركند *Polycheles typhlops* (lobster) كنوع مهدّد بالانقراض (Chan, 2011).

2. هدف البحث

تسجيل وجود بعض الأنواع القاعيّة النادرة، والتعريف ببعض صفاتها البيولوجية والبيئيّة، مما يسمح بإضافة معلومات حول التنوّع الحيويّ في سوريا، ويساهم في إدارة الأنواع ذات الأهميّة الاقتصاديّة منها.

3. مواد البحث وطرائقه

تمّ الحصول على الأنواع المسجّلة في هذا البحث من حصيلة الصيد لبعض المراكب العاملة في المياه الإقليمية السوريّة للبحر الأبيض المتوسط من أعماق مختلفة تراوحت مابين (20 – 630 متراً) في رأس البسيط شمالاً E35.877783, N35.794267 وN 35.865836, E 35.866614،ومقابل مدينتيّ اللاذقيةN 35.32144,E 35.45189، وبانياسN 35.267332, E35.923825 (الشّكل 1) خلال الفترة 2020 –2021 باستخدام شباك قاعية مختلفة trawl, trammel net, gillnet، صنّفت العيّنات بالاعتماد على المراجع العالمية (FAO., 2016; Galil *et al.*, 2002; Riedl 2011; Bariche, 2012)، والتوصيف الوارد في السجلّ العالمي للأنواع البحريّة (WoRMS, 2022)، أجريت القياسات المورفومترية والوزنية للعيّنات في المختبر، كما تمّ تصويرها باستخدام كاميرا موبايل من نوع Xiami Note.9.s بدقة 48.0 Mega Pixel،وحفظت نماذج منها بالفورم ألدهيد (5%)في مختبر البيولوجيا البحريّة في المعهد العالي للبحوث البحريّة.

الشّكل 1: مو اقع تسجيل الأنواع في البحر السوري (شرقي البحر المتوسط)

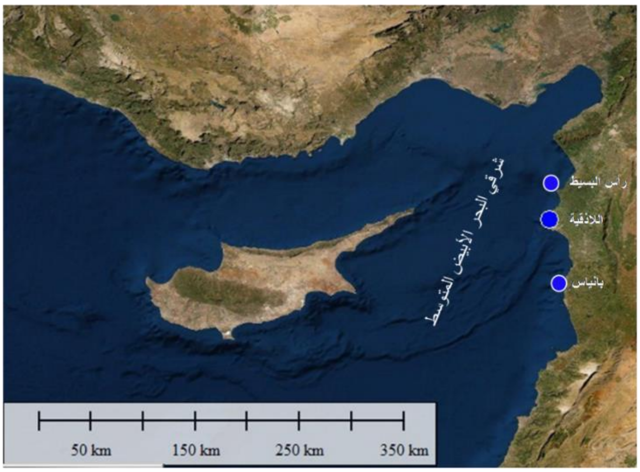

4. النتائج والمناقشة

يبين الجدول (1) بعض المعلومات الأساسية لكل نوع من الأنواع القاعيّة المتوسطية والغريبة النادرة المسجّلة في سوريا للمرّة الأولى خلال الفترة 2020 – 2021، وجميعها تمّ صيدها حيّة بالشباك القاعيّة، مع الإشارة إلى أنّ اعتبار النّوع الغريب يعتمد على مجموعة من الصفات أهمّها: أصله الجغرافي (Geographical origin)، ونمط البيئة، والدول التي يوجد فيها (Zenetos *et al.*, 2020: 873).

الجدول 1: الأنواع القاعيّة النادرة والجديدة في سوريا وبعض المعلومات الرئيسية عنها: عدد الأفراد، تاريخ الجمع، العمق، المكان، غريب أومحلي.

Species	No. of individuals	Date of collecting	Depth (m)	Locality	Native/Alien species
Crustaceans – Crabs					
Actaea savignii (H. Milne Edwards,1834)	2	15l03l2020	20	Banias	Alien
Dromia personata Linnaeus, 1758	1	24\03\2021	60	Latakia	Native
Geryon longipes A. Milne-Edwards, 1882	1	27\04\2021	360	Latakia	Native
Homola barbata (Fabricius, 1793)	1	23\02\2021	630	Latakia	Native
Molluscs- Cephalopods					
Ocythoe tuberculata (Rafinesque, 1814)	4	27\04\2021	500	Latakia and Al-bassit	Native
*Tremoctopus violaceus*delleChiaje, 1830	2	06\06\2021	130	Banias	Alien
Echinoderms-Urchins					
Sphaerechinus granularis (Lamarck, 1816)	4	24\03\2021	60	Al-bassit	Native
Echinoderms-Sea stars					
Peltaster placenta (Müller and Troschel, 1842)	1	17\05\2021	90	Latakia	Native
Chaetaster longipes (Bruzelius, 1805)	1	07\12\2020	>300	Banias	Native

النّوع*Actaea savignii* (H. Milne Edwards,1834)
Crustacea: Malacostraca: Decapoda: Xanthidae

ينتمي هذا النّوع من السرطانات الصغيرة إلى فصيلة الـXanthidae السّامّة، و ينتشر في المحيط الهندي وغرب الهادي وشرقاً نحو اليابان وأستراليا (Davie, 2015)، كما يظهر في البحر الأحمر، وصل إلى شرقيّ البحر المتوسط عبر قناة السويس، وقد سُجّل وجوده فيها في العام 1924(WoRMS, 2022) وسُجّل وجوده في البحر الأبيض المتوسط كنوع مهاجر(*Lessepsian migrant*) للمرّة الأولى في لبنان عام 2006 (Crocetta and Bariche, 2015: 696)، وظهر لاحقاً في العام 2010 في حيفا، وفي العام2011 في

تركيا (Karhan *et al.*, 2013: 145)، وهذا هو التّسجيل الأوّل له في الشّاطئ السوري.

العيّنة المدروسة: جمع فردان من الـ *Actaea savignii* بشباك الصيد القاعيّة من القاع الصّخري من عمق 20 متراً تقريباً خارج ميناء الصّيد في بانياس خلال شهر آذار من العام 2020 مترافقاً مع أنواع من الأسماك البوقية والصّول الغريبة أيضاً الشّكل(2)، بلغ طول الدّرقة للفرد الكبير 2.4 سم وعرضها 3.1. وبهذا التّسجيل تكون قد استُكمِلت خارطة توثيق وجوده في الشّاطئ الشّرقي للبحر المتوسط.

النّوع *Geryon longipes* A. Milne-Edwards, 1882
Arthropoda: Malacostraca: Decapoda: Geryonidae

من سرطانات المياه العميقة، يعيش هذا النّوع القاعيّ في أعماق مختلفة تصل إلى 2000 متر تقريباً، إنّه نوع متوسطيّ، ينتشر في شرقيّ البحر المتوسط و اليونان والأدرياتيك وبحر إيجه وشمال المحيط الأطلسي(Türkay, 2015) وهو من الأنواع ذات القيمة التجاريّة ويتمّ استهلاكه كغذاء (Cortes Pujol *et al.*,2019). العيّنة المدروسة: فرداً واحداً ذكراً، تمّ جمعُه بشباك الجرف القاعيّة من القاع الطّيني على عمق360 متراً مقابل اللاذقيّة، بلغ طول الدّرقة 5.8 سم وعرضها 11.2. إنّه التّسجيل الثّاني لهذا النّوع في شرقيّ المتوسط (WoRMS, 2022)، يعدّ تسجيل وجوده في سوريا أمراً هامّاً ويستدعي المزيد من البحث والمتابعة.

النّوع*Homola barbata* (Fabricius, 1793)
Arthropoda: Malacostraca: Decapoda: Homolidae

ينتشر هذا النّوع في شرق المحيط الأطلسي، وشماله، وفي البحر الأبيض المتوسط في الأدرياتيك، وبحر إيجة، وبحر اليونان وشرقيّ المتوسط (Bianchi*et al.*, 2022: 167). العيّنة المدروسة: فرد واحد تمّ جمعه باستخدام شباك الجرف القاعي من القاع الطّيني،على عمق 630متراً من منطقة المياه الإقليميّة السوريّة مقابل اللاذقيّة خلال شهر شباط2021،بلغ طول الدرقة2.5 سم وعرضها 1.2. وهو التّسجيل الثّاني لهذا النّوع في شرقيّ المتوسط.

النّوع *Dromia personata* Linnaeus, 1758
Arthropoda: Malacostraca: Decapoda: Dormiidae

ينتمي هذا النّوع إلى فاونا البحر الأبيض المتوسط و شرق المحيط الأطلسي، سُجّل وجوده في بحر إيجه،والأدرياتيك، واليونان، وخليج قابس (Türkay, 2015)، يعيش على المستندات القاعيّة الصّخرية والحصوية على أعماقٍ مختلفةٍ بدءاً من المناطق الضّحلة وحتى عمق 110 أمتار، يغطّي جسمَه بجزءٍ من الإسفنج الحيّ للتّمويه (الشّكل2)، لمخالبه لونٌ زهريّ مميّز يساعد على التّصنيف والتعرّف على النّوع، درقته بيضاويّة الشّكل يصل طولها حتى 5 سموعرضها 6.5، يتغذّى على بقايا النباتات الميّتة وبقايا الحيوانات، إنّه التّسجيل الثّاني لهذا النّوع في شرقيّ المتوسط (Corsini-foka and Pancucci-papadopoulou, 2012: 359). العيّنة المدروسة: فرد واحد تمّ جمعه من عمق60 متراً من الجرف الصّخريّ شمال اللاذقيّة خلال شهر آذار2021بواسطة شباك قاعيّة، يبلغ طول الدّرقة 2.2 سم وعرضها 2.8(الشّكل2).

وهناك أنواع أخرى من القشريّات تصنّف على أنّها نادرة أو مهدّدة في البحر الأبيض المتوسط، عُثر عليها في حصيلة الصّيد بشباك الجرف في المناطق العميقة مقابل اللاذقيّة وبانياس، مثل كركند المياه العميقة Deep sea lobster*Polycheles typhlops* (Heller, 1862)(الشّكل3).

توزيع هذا النّوع P. typhlops عالميّ، وهو من أكثر أنواع القشريّات المميّزة لمجتمعات المياه العميقة في البحر المتوسط، سُجّل وجوده في أعماق مختلفة وفي عدّة مناطق من العالم، تمّ رصد وجوده بغزارة في المياه العميقة مقابل اللاذقيّة خلال آذار/2020 ونيسان/2021، في أعماق تراوحت مابين 600 – 650 متراً، وكان قد سُجّل وجوده للمرّة الأولى في العام 2016 في المنطقة نفسها.

إنّه من الأنواع المهدّدة بالانقراض(Chan, 2011)، ويعدّ تزايد أعداده في الشّاطئ السّوري مؤشّراً إيجابياً على إعادة بناء التّجمّعات الأحيائية في القاع العميق في شرق البحر المتوسط وسوريا، وتظهر في معظم الأحيان أفراد من بعض الأنواع النادرة من السرطانات البحريّة والأنواع المهدّدة بالانقراض كصيد عَرَضِي Bycatch في شباك الجرف، أهمّها النّوعان *Calppa granulata*و*Parathenope angular*عثر عليهما في القاع الطّيني على عمق630 متراً، بالإضافة إلى وجود نادر للنّوع *Munida rugusa* (فرد واحد) في القاع الطّيني وعلى العمق نفسه، ولا تعرف أيّة قيمة غذائية له، يستمرّ ظهور هذه الأنواع وبأعداد قليلة جدّاً منذ العام 1992.

يضاف إلى ذلك نوعان من الأخطبوط من الرخويات رأسيات الأرجل (Cephalopoda)، يُسجّلان للمرّة الأولى في المياه الإقليميّة السوريّة في اللاذقيّة وبانياس هما:

النّوع *Tremoctopus violaceus* delle Chiaje, 1830
Mollusca: Cephalopoda: Octopoda: Tremoctopodidae

يطلق عليه اسم Blanket octopus (أخطبوط البطانية)، هو أخطبوط كبير،ينتشر على نطاق واسع في المحيطات والبحار الاستوائية (Finn, 2014: 240)،وجوده نادر في البحر الأبيض المتوسط، والتمايز الشّكلي بين الجنسين في هذا النّوع كبير جدّاً،حيث يصل طول الإناث إلى مترين بينما تنمو الذّكور إلى حوالي 24 ملم، تملك الذّكور والإناث الصغيرة التي يقلّ طولها عن 7 سم مخالباً، ومن المتوقّع أن تعمل هذه المخالب كآليّة دفاعيّة وربّما كوسيلة لالتقاط الفريسة، تعمل الشبكة بين ذراعي أنثى الأخطبوط الناضجة كوسيلة دفاعيّة أيضاً، فهي تجعل الحيوان يبدو أكبر حجماً، ويمكن فصلها بسهولة إذا عضّه حيوان مفترس.يوجد *T. Violoceus* في خليج المكسيك و شمال المحيط الأطلسي، سُجّل وجوده في فرنسا واليونان، كما سُجّل حديثاً في جنوب إيطاليا (Famulari *et al.*, 2022: 1).

العيّنة المدروسة: جُمِع فردان من إناث*T. violaceus*من المياه البحريّة مقابل بانياس (N 35.267332, E35.923825) للمرّة الأولى في 6 حزيران/2021 بواسطة شباك الصّيد من عمق 130 متراً، ونوع القاع طينيّ، بلغ الطّول الكلّي للفرد الكبير 33.5 سم، بينما بلغ طول البرنس 15.4(mantle) سم وعرضه 3.3 (الشّكل2). إنّ تسجيل وجود هذا النّوع في بانياس يؤكّد وجوده في شرقي البحر المتوسط.

النّوع *Ocythoe tuberculata* Rafinesque 1814
Mollusca: Cephalopoda: Octopoda: Ocythoidae

يطلق عليه أخطبوط كرة القدم Football octopus، يعدّ هذا الأخطبوطمن الأنواع النادرة في البحار والمحيطات العالميّة، ينتشر في البحار الدّافئة والمعتدلة، وخاصّة في نصف الكرة الشماليّ، وهو من الأنواع المكتشفة حديثاً في البحر الأبيض المتوسط (Tsagarakis *et al.*, 2021:627)، لا يتوفّر الكثير من المعلومات حول أهمّيته وخصائصه البيئيّة والبيولوجيّة، وقد تمَّ تسجيل وجوده في تركيا ومؤخّراً في إيطاليا(Battaglia and Stipa, 2021: 627)، تكون الإناث كبيرة الحجم، والذّكور قزمة، هو أخطبوط سابح، جُمع بوسائل جمع مختلفة (FAO, 2016: 238)، وفي سوريا تمّ صيد فرد واحد في دراسة منفصلة من شاطئ رأس البسيط في الشّمال السّوري سنة 2020 من عمق5 – 10 أمتار بواسطة شباك الصّيد (بحث جاري)، كما جرى صيد عدد قليل من أفراد هذا النّوع من المياه البحريّة السوريّة مقابل اللاذقيّة (N 35.488059, E 35.745165) بتاريخ 27 نيسان من العام2021من عمق 500 متر من القاع الرّخو،عن طريق الصّيادين باستخدام الشّباك القاعيّةtrammel net.

العيّنة المدروسة: أربعة أفراد تمّ تصويرها، ووزنها وإجراء القياسات المورفومترية لها في المختبر، حيث كانت العينات إناثاً (الشّكل2). بلغ الطّول الكلّي لأكبر فرد 21 سم، بينما بلغ طول البرنس 5.2 سم وعرضه 2.5، كما بلغ وزنه 44.48 غ.

أظهرت المعطيات الحقلية أيضاً وجود بعض الأنواع النّادرة من شوكيات الجلد (*Echinodermata*) التي يُسجّل وجودها للمرّة الأولى في المياه البحريّة السورية أهمّها نوعان من نجوم البحر ونوع من قنافذ البحر:

النّوع *Peltaster placenta* (Müller and Troschel, 1842)
Echinodermata: Asteroidea: Valvatida: Goniasteridae

نجمة متوسطة الحجم، يبلغ قطرها ثمانية سنتيمترات، خماسية الشّكل و لها قُبّة، يتكوّن هيكلها من صفائح كبيرة متجاورة، ذات لون برتقاليّ زاهٍ، القرص المركزي واضح ومزيّن بصفائح مُضلّعة الشّكل ولوحة كبيرةبلون برتقاليّ باهت (Serrano *et al*., 2017: 116).

P. placenta واسعة الانتشار في المحيط الأطلسي (WoRMS, 2022) وفي البحر الأبيض المتوسط (Kaspiris and Tortonese, 1982: 27)، تمّ توثيق وجودها على جانبي المحيط الأطلسي في أعماق تراوحت مابين2 – 1007 أمتار، تتغذّى على الشّعاب المرجانية النّاعمة الصّغيرة،بالإضافة إلى أنواع من الإسفنجيات الزّجاجية، تستخدم للزينة بسبب شكلها المميّز، ولم تتمّ دراستها من النّاحية الصّناعية أو أيّة ناحية أخرى. العيّنة المدروسة: فرد واحد يبلغ قطره7.5 سم تقريباً، عثر عليه في القاع الطّيني مقابل اللاذقيّة، جمع بشباك الجرف من عمق 90 متراً في شهر أيّارمن عام 2021.

النّوع *Chaetaster longipes* (Bruzelius, 1805)
Echinodermata: Asteroidea: Valvatida: Chaetasteridae

هو نجم بحر كبير إلى حدّ ما، أذرعه طويلة ونحيلة،والقرص المركزي صغير جدّاً، كما تكون الخطوط الشعاعية رفيعة، أسطوانية، وعليها نقوش خشنة مرتّبة بشكل شبكيّ منتظم،يتلوّن باللونين البرتقاليّ والأصفر، كما يبدو بلون بنيّ أحياناً. يوجد هذا النّوع بشكل رئيسيّ في المحيط الأطلسي وغرب البحر الأبيض المتوسط (Mah, 2021)، وتمّ توثيق وجوده في اليونان (Koukouras, 2007: 70) من الحوض الشّرقي للبحر المتوسط، يعيش بشكل أساسي في أعماق تزيد عن 40 متراً وحتّى أكثر من1000.العيّنة المدروسة: فرد واحد لونه بنّي، يبلغ قطره 13 سم تقريباً، تمّ جمعه بشباك الصّيد من أعماق تزيد عن 300 متر في بانياس بتاريخ 7 كانون الأول 2020 من القاع الطّيني وفق الإحداثيات (N35.267332 E35.92382)، يُسجّل وجوده للمرّة الأولى في البحر السوري خلال هذا البحث.

النّوع *Sphaerechinus granularis* (Lamarck, 1816)
Echinodermata: Echinoidea:Camarodonta: Toxopneustidae

قنفذ البحر الحبيبيGrainy Sea Urchin:شكله كرويّ محبّب، يتراوح حجمه ما بين8 – 13 سم، الأشواك قصيرة وثخينة، الهيكل كرويّ مسطّح، لونه ورديّ-أرجوانيّ، وأشواكه بيضاء. تتمتّع أفراد هذا النّوع بقيمة غذائية عالية؛ وعلى الرّغم من صغر حجمها إلّا أنّ غددها الجنسيّة من الممكن أن تؤكل.

يرعى *S. granularis* الطّحالب المرجانيّة القشريّة الموجودة على الصّخور، كما يتغذّى على جذور وبقايا الأعشاب البحريّة، خاصّة الـ*Posidonia oceanica*.هو نوع معتدل، وشبه استوائيّ، ينتشر في شمال وشرق المحيط الأطلسي والبحر المتوسط، على أعماق2 – 130 متراً، وقد سُجّل وجوده في كل من المملكة المتحدة، إسبانيا،فرنسا، اليونان، بحر الأدرياتيك وبحر إيجه(Koukouras *et al*., 2007: 77).يعيش هذا النّوع في الشواطئ الصّخرية، وكذلك في القيعان الحصويّة المغطّاة بالطّحالب الحمراء الكلسيّة. العيّنة المدروسة: أربعة أفراد من هذا النّوع جُمعت من القاع الصّخري (حافّة صخريّة)، شمال رأس البسيط،من عمق60 متراً، خلال شهر آذار/2021 باستخدام شبكة صيد قاعيّة، وتراوحت أقطارها مابين 9 – 11 سم تقريباً، تميّزت هذه الأفراد بتباين ألوانها من الورديّ إلى البنّيّ والأسود (الشّكل2)،وهذا هو التّسجيل الأوّل لهذا النّوع في سوريا.

الشّكل 2: الأنواع القاعيّة النّادرة والمسجّلة للمرّة الأولى في سوريا

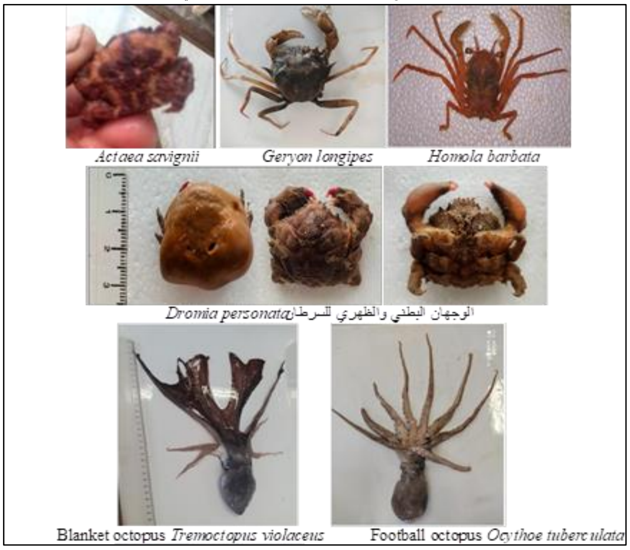

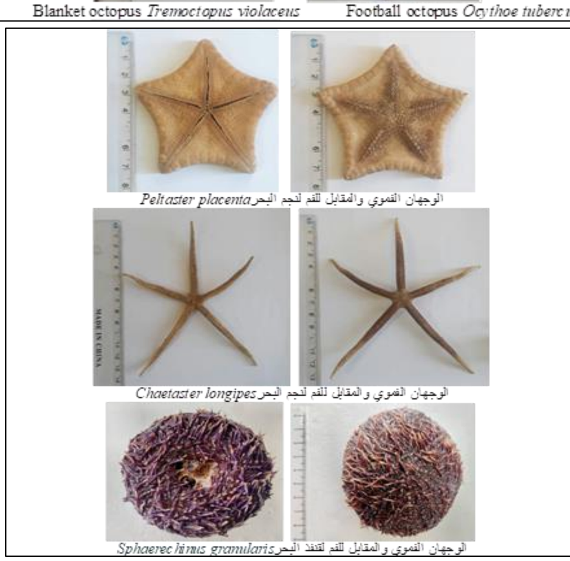

التونا العملاقة (Giant tun*Tonna galea (*Linnaeus, 1758: من الرخويات-بطنيات القدم (*Gastrpda*) المرغوبة للأكل والزّينة، سجّل وجودها على أعماق – 798 163 متراً في شرقي البحر المتوسط وحوض الليفانتين (Otero*et al*., 2022: 130)، ونظراً لأهميتها وتعرّضها للاستنزاف؛ فقد تمّ ذكرها في اثنتين من الاتفاقيّات والمعاهدات القانونية الدّولية هما: اتفاقية برن بشأن الحفاظ على الحياة البرّية الأوروبّية والموائل الطّبيعية Bern Convention، وبروتوكول اتفاقية برشلونة للحماية من التلوّث في البحر الأبيض المتوسط Barcelona Convention(Cuttelod*et al*., 2011: 91)، إلا أنّها تظل مستهدفة ومهددة. لا تزال تظهر الـ*Tonna galea* في المياه البحريّة السوريّة بأعداد مقبولة، وعلى أعماق مختلفة تتراوح مابين 8– 630 متراً. يظهر الشّكل (3) صورة لفرد من هذا النّوع، أبعاده 15 و 17 سم، ووزنه 1 كغ تقريباً.

الشّكل 3:كركند المياه العميقة *Polycheles typhlops* والتونا العملاقة *Tonna galea* من القيعان العميقة في سوريا

الوجهان البطني والظهري لقوقعة *Tonna galea*	كركند المياه العميقة *Polycheles typhlops*

قد تعزى ندرة هذه الأنواع في شرقي البحر الأبيض المتوسط لعدد من الأسباب أهمّها: انتشارها في نطاق ضّيق، أو التراجع في أعدادها، أو أن تُهمَل بعض الأنواع بسبب غزارتها المنخفضة وندرة مشاهدتها، بالإضافة إلى ضعف إمكانيات الصّيد (Tsagarakis *et al.*, 2021: 629)، كما أنّ السلوك اليومي للعديد من الحيوانات القاعيّة التي تختبئ نهاراً وتنشط ليلاً يزيد من صعوبة كشفها، والحصول عليها، أو وجودها في مناطق عميقة حيث تكون عمليات الصيد محدودة، والأبحاث العلمية نادرة؛ لعدم توفر الإمكانيات المادّية. لقد ساعد التواصل مع الصّيادين العاملين في المياه العميقة في الحصول على معظم العينات، كما ساهمت زيادة الحديث عن ظاهرة الغزو البيولوجي بالأنواع الغريبة في البحر الأبيض المتوسط عبر مواقع التواصل الاجتماعي والمواقع الالكترونية(Kousteni *et al.*, 2022: 13)، وظهور المزيد من الأنواع غير الملاحظة سابقاً في شباك الصيد؛ في زيادة الاهتمام والتواصل بين الباحثين والصيّادين؛ لتحديد الأنواع التي تلاحظ للمرّة الأولى، ومعرفة أثرها البيئيّ والصحيّ.

على الرّغم من أنّ هذه الدراسة كشفت عن وجود المزيد من الأنواع النادرة من القاعيات الحيوانية، وقدّمت بعض المعلومات عنها في المياه البحريّة السوريّة الممتدّة على البحر الأبيض المتوسط، الأمر الذي يشكّل إضافة معرفية هامّة على مستوى التنوّع الحيويّ البحريّ في البحر الأبيض المتوسط والجزء الشرقي منه على وجه الخصوص، إلاّ أنّ المعلومات حول توزّع الكائنات الحيّة في أعماق البحر السوري جزئية، ولا تزال الأعمال البحثية في مجال تصنيف وتوزّع حيوانات أعماق البحار، والبيئات الخاصّة كالكهوف البحريّة، بما في ذلك المجموعات الرئيسية للحيوانات القاعيّة اللافقارية والأسماك المرافقة مستمرّة ومطلوبة، لذلك فإنّه من المتوقّع حدوث تغييرات في التنوّع، وظهور المزيد من الأنواع في المستقبل القريب، كما أنّ الصّعوبات اللوجستية التي تواجه الباحثين في الأعمال الحقلية، والحصول على العينات، تؤكّد الحاجة إلى التّعاون الوثيق بين قطاع صيد الأسماك والأوساط العلمية للكشف عن المزيد من الأنواع النادرة، وتقييم حالتها، والتعرّف على بيئاتها الحقيقية وخصائصها البيولوجيّة.

نبذة عن المؤلفين

ازدهار علي عمّار

قسم البيولوجيا البحرية، المعهد العالي للبحوث البحرية، جامعة تشرين، اللاذقية، سوريا، izdiammar@gmail.com، 00963998694090

أ.د. عمّار، دكتوراه (سوريا)، سوريّة، أستاذ دكتور، رئيس قسم ونائب عميد سابق في المعهد العالي للبحوث البحرية، أعمالها في لغتين: العربية والانكليزية.الدكتورة عمّار عضو في هيئة تحرير مجلّة وادي الرافدين لعلوم البحار ومجلّات Discovery، نشرت 75 ورقة في Web of Science, Scopus, Google Scholar,...،أبحاثها مقتبسة في 33 دولة منها: ايطاليا، وروسيا، و فرنسا و اليونان، شاركت بـ 25 ورقة في مؤتمرات علمية، أشرفت على 23 رسالة ماجستير ودكتوراه، شاركت في 15 بحثاً مع هيئات علمية خارجية مثل UNEP/MAP، RAC?SPA، IFREMER وهيئات بحثية محلّية مثل HCSR وAEC. رقم الأوركيد (ORCID): 0000-0001-8567-0756.

يارا بسيم حميشة

قسم البيولوجيا البحرية، المعهد العالي للبحوث البحرية، جامعة تشرين، اللاذقية، سوريا، izdiammar@gmail.com، 00963998694090

حميشة، ماجستير (سوريا)، سوريّة، باحثة في مجال التنوّع الحيويّ البحري والتصنيف الحيواني في قسم البيولوجيا البحرية، تشارك في أبحاث خاصّة بالطفيليات الخارجية على أنواع من الأسماك البحرية، شاركت في العديد من الأعمال الحقلية خلال العامين 2020 و2021 لجمع عينات من الأحياء البحرية القاعيّة في المياه البحرية السوريّة، وهي مدرّسة لمادة الأحياء الدقيقة والتلوّث في كليّة العلوم بجامعة تشرين، مهتمّة وناشطة في المجال البيئيّ وتنمية الموارد البشرية، اتّبعت عدّة دورات في مجال التصنيف الحيواني و التّقانة الحيوية البحرية والميكروبيولوجيا البحرية.

المراجع

Ammar, I.A. (2019). Updated list of alien macrozoobenthic species along the Syrian coast. *International Journal of Aquatic Biology*, **7**(**4**), 180–94. DOI: 10.22034/ijab.v7i4.556

Bariche,M.(2012).*Field Identification Guide to the Living Marine Resources of the Eastern and Southern Mediterranean*. Rome: FAO Species Identification Guide for Fishery Purposes.

Battaglia, P. and Stipa, M.G. (2021). New record of the football octopus *Ocythoe tuberculata* Rafinesque 1814, from the southern Tyrrhenian Sea (Italy). *Mediterranean Marine Science*,**22**(3), 627–52.DOI: 10.12681/mms.26669.

Bianchi, C.N., Gerovasileiou, V.M. and Froglia. C. (2022). Distribution and ecology of decapod crustaceans in Mediterranean marine caves: A review. *Diversity*, **14**(3), 176.DOI: 10.3390/d14030176

Canonico, G., Buttigieg, P.L., Montes, E., Muller-Karger, F.E., Stepien, C., Wright, D., Benson, A., Helmuth, B., Costello, M., Sousa-Pinto, I., Saeedi, H., Newton, J., Appeltans, W., Bednaršek, N., Bodrossy, L., Best, B.D., Brandt, A., Goodwin, K.D., Iken, K., Marques, A.C., Miloslavich, P., Ostrowski, M., Turner, W., Achterberg, E.P., Barry, T., Defeo, O., Bigatti, G., Henry, L-A., Ramiro-Sánchez, B., Durán, P., Morato, T., Roberts, J.M., García-Alegre, A., Cuadrado, M.S. and Murton, B. (2019). Global observational needs and resources for marine biodiversity. *Frontiers in Marine Science*, **6**(367), 1–20.

Chan, T.Y. (2011). *Polycheles typhlops*. *The IUCN Red List of Threatened Species*. Available at: https://www.iucnredlist.org/species/ (accessed on 24/12/2022).

Clark, A.M. and Downey, M.E. (1992). *Starfishes of the Atlantic*. *Chapman & Hall Identification* Guides. 3rd edition. London, UK: Chapman & Hall.

Coll, M., Piroddi, C., Steenbeekand, J., Kaschner, K., Ben Rais Lasra, F. and Voultsiadou, E. (2010). The biodiversity of the Mediterraneansea: estimates, patterns, & threats. *PLoS ONE*, **5**(8), n/a. DOI: 10.1371/journal.pone.0011842

Corsini-foka, M. and Pancucci-Papadopoulou, M.A. (2012). Inventory of crustacea decapoda and stomatopoda from Rhodes Island (eastern Mediterranean sea), with emphasis on rare and newly recorded species. *Journal of Biological Research-Thessaloniki*, **18**(n/a), 359 –71.

Cortes Pujol, M.A., Guijarro, B. and Beatriz, G. (2019). Spatial and temporal trends of *Geryon longipes* in the western mediterranean sea. In: R.R.Granjel, O.Godoy, I.Badenhausser and N.Gross (eds.)*How the Interaction Network Determines the Herbivory Effects on Plant Coexistence 1*. Spain,Barcelona:Meeting of the Iberian Ecological Society (SIBECOL).

Crocetta, F. and Bariche, M. (2015). Six new records from Lebanon, with general implications for Mediterranean alien fauna in new Mediterranean biodiversity records (October 2015). *Mediterranean Marine Science*, **16**(3), 696–8.

Cuttelod, A., Seddon, M. and Neubert, E. (2011). *European Red List of Non-Marine Molluscs*. Luxembourg: Publications office of the European Union.

Davie, P. (2015). *Actaea savignii (H. Milne Edwards, 1834)*. *World Register of Marine Species*.Available at: https://www.marinespecies.org/aphia. (accessed on 23/12/2022).

Famulari, S., Savoca, S., Panarello, G., Iaria, C., Spanò, N. and Capillo, G. (2022). New record of a female violet blanket octopus (*Tremoctopus violaceus*, delleChiaje, 1830) in the Strait of Messina, southern Italy. *International Journal of Environmental Studies*, **n/a**(n/a), 1–6.DOI: 10.1080/00207233.2022.2062109.

FAO. (2016). *Cephalopods of the World. An Annotated and Illustrated Catalogue of Cephalopod Species Known to Date*.In: P.Jereb, C.F.E. Roper, M.D.Norman, J.K. Finn and S.Yapici, (eds.) FAO Species Catalogue for Fishery Purposes. Rome, Italy: FAO.

Finn, J.K. (2014). *Family Tremoctopodidae*. In: P.Jereb, C.F.E. Roper, M.D.Norman and J.K.Finn. (eds.) *Cephalopods of the world. An Annotated and Illustrated Catalogue of Cephalopod Species Known to Date. Octopods and Vampire Squids*. FAO Species Catalogue for Fishery Purposes. Rome, Italy: FAO.

Follett, R. and Strezov, V. (2015). An analysis of citizen science based research: usage and publication patterns. *PLoS ONE*,**10**(11), n/a.DOI: 10.1371/journal.pone.0143687

Galil, B.S., Froglia, C. and Noël, P. (2002).*CIESM Atlas of Exotic Species in the Mediterranean*. 2nd edition. Monaco: CIESM publishers.

Karhan, Ü.S., Yokeş, M.B., Clark, P.F. and Galil, B.S. (2013). First Mediterranean record of Actaeasavignii (H. Milne Edwards, 1834) (Crustacea:

MG., Kurt, T., Tiralongo, F., Tsiamis, K., Vella, A., Vella, N., Zava, B. and Gerovasileiou, V.M. (2021). New records of rare species in the Mediterranean sea. *Mediterranean Marine Science*, **22**(3), 627–52. DOI: 10.12681/mms.26669

Türkay, M.K. (2015). *Personal Decapoda Distribution Database for Europe*. Available at:https://doi.org/10.14284/205(accessed on 25/12/2022).

Bouafif, C. and Ouerghi, A. (2022). UNEP/MAP – SPA/RAC.In: *The 3rd Mediterranean Symposium on the Conservation of Dark Habitats*, Genova, Italy, 21–22/09/2022.

WoRMS Editorial Board (2022). *World Register of Marine Species*. Available at: marinespecies.org (accessed on 19/12/2022).

Zenetos, A.G., Corsini-Foka, M., Crocetta, F., Gerovasileiou, V.M., Simboura, N., Tsiamis, K. and Pancucci- Papadopoulou, M-A. (2018). Deep cleaning of alien and cryptogenic species records in the Greek seas (2018 update). *Management of Biological Invasions*, **9**(n/a),209–26.DOI: 10.3391/mbi.2018.9.3.04.

Zenetos, A.G., Albano, P.G., López Garcia, E., Stern, N., Tsiamis, K. and Galanidi, M. (2022). Established non-indigenous species increased by 40% in 11 years in the Mediterranean Sea. *Mediterranean Marine Science*, **23**(1), 196–212.DOI: 10.12681/mms.29106

Zenetos, A.G., Ovalis, P., Giakoumi, S., Kontadakis, C., Lefkaditou, E., Mpazios, G., Simboura, N. and Tsiamis. K. (2020). Saronikos Gulf: A hotspot area for alien species in the Mediterranean sea. *BioInvasions Records*, **9**(44), 873–89. DOI: 10.3391/bir.2020.9.4.21

Decapoda: Brachyura: Xanthidae), an additional erythraean alien crab.*BioInvasions Records*, **2**(2), 145–8.

Kaspiris, P. and Tortonese, E. (1982). Echinoderms from the western seas of Greece. *Thalassographica*, **n/a**(2), 27–32.

Katsanevakis, S., Acar, Ü., Ammar, I., Balci, B.A., Bekas, P., Belmonte, M., Chintiroglou, C.C., Consoli, P., Dimiza, M., Fryganiotis, K., Gerovasileiou, V.M., Gnisci, V., Gülşahin, N., Hoffman, R., ISSARIS, Y., Izquierdo-Gomez, D., Izquierdo-Munoz, A., Kavadas, S., Koehler, L., Konstantinidis, E., Mazza, G., Nowell, G., Önal, U., Özen, M.R., Pafilis, P., Pastore, M., PErdikaris, C., Poursanidis, D., Prato, E., Russo, F., Sicuro, B., Tarkan, A.N., Thessalou-Legaki, M., Tiralongo, F., Triantaphyllou, M., Tsiamis, K., TunÇer, S., Turan, C., Türker, A. and Yapici, S. (2014). New Mediterranean biodiversity records (October, 2014). *Mediterranean Marine Science*, **15**(3), 675–95.

Kousteni, V., Tsiamis, K., Gervasini, E., Zenetos, A.G., Karachle, P.K. and Cardoso, A.C. (2022). Citizen scientists contributing to alien species detection: the case of fishes and mollusks in European marine waters. *Ecosphere,* **13**(1), n/a. DOI: 10.1002/ecs2.3875

Koukouras, A., Sinis, A.I., Bobori, D., Kazantzidis, S. and Kitsos, M.-S. (2007). The Echinoderm (Deuterostomia) fauna of the Aegean Sea, and comparison with those of the neighbouring seas. *Journal of Biological Research*, **n/a**(7), 67–92.

Lejeusne, C., Chevaldonné, P., Pergent-Martini, C., Boudouresque, C.F. and Pérez, T. (2010). Climate change effects on a miniature ocean: The highly diverse, highly impacted Mediterranean sea. *Trends in Ecology and Evolution*, **25**(4),250–60.

Mah, C.L. (2022). *World Asteroidea Database. Chaetaster longipes (Bruzelius, 1805). Accessed through: World Register of Marine Species*. Available at:http://www.marinespecies.org. (accessed on 23/12/2022).

Mytilineou, C., Akel, E., BabalI, N., Balistreri, P., Bariche, M., Boyaci, Y., Cilenti, L., Constantinou, C., Crocetta, F., Çelik, M., Dereli, H., Dounas, C., Durucan, F., Garrido, A., Gerovasileiou, V., Kapiris, K., Kebapcioglu, T., Kleitou, P., Krystalas, A., Lipej, L., Maina, I., Marakis, P., Mavrič, B., Moussa, R., Peña-rivas, L., Poursanidis, D., Renda, W., Rizkalla, S., Rosso, A., Scirocco, T., Sciuto, F., Servello, G., Tiralongo, F., Yapici, S. and Zenetos, A.G. (2016). New Mediterranean biodiversity records (November, 2016). *Mediterranean Marine Science*, **17**(3), 794–821.DOI: 10.12681/mms.1976

Otero, M.M., Jimenez, C., Kiparissis, S., Mytilineou, C., Papadopoulou, N., Smith, C.J., Thasitis, I., Anastasiadou, Ch., Lefkaditou, E., Makovsky, Y. and Schüler, M. (2022). Deep-sea vulnerable benthic fauna. In: M.M.Otero andC.Mytilineou (eds.) *Deep-sea Atlas of the Eastern Mediterranean Sea*. IUCN-HCMR DeepEastMed Project. Malaga: IUCN Gland.

Riedl, R. (2011). *Fauna und Flora des Mittelmeeres* 'Fauna and Flora of the Mediterranean'. Wien: Seifer Verlag GmbaH. [in German].

Santin, A., Aguilar, R., Akyol, O., Begburs, C. R., Benoit, L., Chimienti, G., Crocetta, F., Dalyan, C., de la Linde Rubio, A., Dragicevic, B., Dulcic, J., Giglio, G., Gönülal, O., Kebapcioglu, T., Kesici, N. B., Kiparissis, S., Kousteni, V., Mancini, E., Mastrototaro, F., Menut, T., Montesanto, F., Peristeraki, P., Poursanidis, D., Renoult, J.P., Sánchez-Tocino, L., Sperone, E. and Tiralongo, F. (2021). New records of rare species in the Mediterranean sea (March 2021). *Mediterranean Marine Science*, **22**(1), 199–217. DOI: 10.12681/mms.25295

Serrano, A., González-Irusta, J.M., Punzón, A., García-Alegre, A., Lourido, A., Ríos, P., Blanco, M., Gómez-Ballesteros, M., Druet, M. and Cartes, J.E. (2017). Deep-sea benthic habitats modeling and mapping in a NE Atlantic Seamount (Galicia Bank). *Deep Sea Research*, **126**(n/a), 115–27. DOI: 10.1016/j.dsr.2017.06.003.

Stachowitsch, M. and Gallmetzer, I.J.M.E. (2016). *The Mediterranean Sea. Its History and Present Challenges*.In: S. Goffredo, Z. Dubinsky (eds.) Dordrecht, Heidelberg.New York, London: Springer.

Steins, N.A., Kraan, M.L., van der Reijden, K.J., Quirijns F.J. and Broekhoven, W. (2020). Integrating collaborative research in marine science: Recommendations from an evaluation of evolving science-industry partnerships in Dutch demersal fisheries. *Fish and Fisheries*, **21**(1),146–61. DOI: 10.1111/faf.12423

Townsend, M., Davies, K., Hanley, N., Hewitt, J.E., Lundquist, C.J. and Lohrer, A.M. (2018). The challenge of implementing the marine ecosystem service concept. *Frontiers in Marine Science*, **5**(359), n/a. DOI: 10.3389/fmars.2018.00359

Tsagarakis, K., Agius Darmanin, S., AL Mabruk, S.A., Auriemma, R., Azzurro, E., Badouvas, N., Bakiu, R., Bariche, M., Battaglia, P., BettI, F., Borme, D., Cacciamani, R., Calì, F., Corsini-foka, M., Crocetta, F., Dalyan, C., Deidun, A., Digenis, M., Domenichetti, F., Dragičević, B., Dulčić, J., Durucan, F., Guy-Haim, T., Kesici, NB., Lardi, P-I., Manitaras, Y., Michailidis, N., Piraino, S., Rizgalla, J., Siapatis, A., Soldo, A., Stipa,

إرشادات التسليم (المجلة العلمية لجامعة الملك فيصل)

Submission Guidelines (The Scientific Journal of King Faisal University)

1. General Information

- The Journal publishes in English and Arabic.
- There are no submission or publication fees.
- It takes up to 100 days from submission to publication.
- Manuscripts must be submitted to the appropriate managing editor:
  - The Managing Editor of Basic and Applied Sciences: secretary-b@kfu.edu.sa. The associate editor will check if the author has followed the Submission Instructions. If not, the manuscript will be sent back to the author. If the instructions are followed, the associate editor will create an account and send the author the username and password to log in using our online submission system (ScholarOne): https://mc04.manuscriptcentral.com/sjkfub.
  - The Managing Editor of Humanities and Management Sciences (educational manuscripts only): sjkfu-assed@kfu.edu.sa. The associate editor will check if the author has followed the Submission Instructions. If not, the manuscript will be returned to the author. If followed, the associate editor will create an account and send the author the username and password to log in using our online submission system (ScholarOne): https://mc04.manuscriptcentral.com/sjkfuh.
  - The Managing Editor of Humanities and Management Sciences (non-educational manuscripts): sjkfu-hm@kfu.edu.sa. The associate editor will check if the author has followed the Submission Instructions. If not, the manuscript will be returned to the author. If followed, the associate editor will create an account and send the author the username and password to log in using our online submission system (ScholarOne): https://mc04.manuscriptcentral.com/sjkfuh.

2. Pre-Submission Guidelines

- **Content**: Authors must ensure a clearly articulated academic contribution to the field, clarity of abstracts, quality of and conformity to the stated aims and scope of the Journal and readability of their manuscripts.
- **Manuscript Word Limit**: Manuscripts must not exceed 8,000 words, considering all inclusions (e.g. references, tables, figures).
- **Abstract Word Limit**: Abstracts must not exceed 200 words.
- **Title Word Limit**: Manuscript titles must not exceed 15 words.
- **Keyword Limit**: Keywords must not exceed six words and must not be used in the manuscript title.
- **Number of Tables and Figures**: Tables, figures, abbreviations and footnotes must be kept to a minimum. Tables and figures must not exceed six, each.
- **Reference Limit**: There must be no more than 40 references unless the manuscript is a review article or equivalent.
- **Quotations**: A quotation must not exceed 50 words. Longer quotations required due to the nature of the academic field must be justified in the cover letter.
- **Appendixes**: Appendixes are not allowed. If readers would like to access appendixes, they can reach out to corresponding authors.
- **Linguistic Quality**: Manuscripts must be written at an acceptable language level.
- **Plagiarism**: The Journal maintains a strict plagiarism policy.
- **Reviewers**: Authors must suggest five reviewers, who are specialised in the field of the manuscript, are not affiliated with authors' institutions, are at least associate professors and have not worked on joint projects with authors. Reviewers' names, phone numbers, email addresses, academic field, academic rank and institutions must be provided.
- **Documents Required**: Title page (with author details) and main document (without author details):
  - **Title Page**: It must consist of the following: the manuscript title, author details, minor and major field of the topic, 80-word bio and acknowledgements (optional). Below are explanations of how the author details and bio are written.
  - **Main Manuscript**: It must be submitted in MSWord format. It must consist of the following: manuscript title, abstract, keywords, main body and references.
- **Author Details**: Author details must be included in the following order: full name, department, college, university, city and country (or the equivalent). In the absence of an employer, one may write 'Independent Researcher'. Ranks (e.g. Dr and Prof.) must not be included. A star '*' should be placed next to the corresponding author's name. Below is an example:

  Abdulrahman Essa Al Lily*
  Department of Curriculum and Teaching Methods, College of Education, King Faisal University, Al Ahsa, Saudi Arabia
- **Bio**: The bio must be in the following format: the author's name, under which is written the author's department, college, university, city, country (or equivalent), the author's contact number and email address, under which is written an 80-word description of the author. Author's names and affiliations are not part of the 80-word count. If the author has an ORCID number or personal website, this can be included at the end of the description. Below is an example:

  Abdulrahman Essa Al Lily
  Department of Curriculum and Teaching Methods, College of Education, King Faisal University, Al Ahsa, Saudi Arabia, 00966000000000, scijkfu@kfu.edu.sa
  Prof. Al Lily is an Oxford graduate, Saudi professor, a dean of research, former national-centre director, editor-in-chief (Scopes) and bestselling author (Amazon). He has coined various theories (e.g. 'Multiple Stupidities', "Retroactivism' and 'On-the-Go Sourcing') and 3 notions ('Crowd-Authoring', 'Crowd-Reflecting' and 'Door-Knocking'). His work is translated into 7 languages (including Spanish, Filipino, Indonesian, Chinese and Italian). His interviews is in 5 languages (including, French, Spanish and German). He has published 24 ISI/Scopus-indexed articles with the globally largest publishers (Elsevier, Springer, Taylor & Francis, Wiley, SAGE, Cogent, Palgrave, Nature Research & Oxford). His work is cited by 35 countries (Including Hungary, Serbia, Russia, Peru, Korea, Colombia, Switzerland, Netherlands, Sweden, Finland and Latvia) in 6 languages (including Turkish and Lithuanian). He has worked as a consultant for such institutions as Wikipedia and the University of Hanover. He worked during the summer in New Zealand and Italy. He has participated in conferences in Singapore, Greece, Spain, US, Japan & Bulgaria.
  ORCID: 0000-0002-5116-422X. Website: https://abdulallily.wordpress.com/

3. Post-Reviewing Guidelines

- **Page Settings**: Page size is A4. Margins are 2.5 cm, each side. Any standard font is acceptable.
- **Headings**: There must be no more than three levels of headings. The first level of headings must be numbered: 1., 2., 3., etc. The second level of headings must be numbered: 1.1., 1.2., 1.3., etc. The third level of headings must be numbered: 1.1.1., 1.1.2., 1.1.3, etc. The headings for abstracts, bios and references must not be numbered.
- **Tables and Figures**: Captions must be above tables and figures. In the body, 'see above' or 'see below' must not be used. Instead, use 'see Table 1' or 'see Figure 1'.
- **Measuring Units**: In the case of using local measuring units in the manuscript, the equivalent of international units must be included. Scientific rather than provincial terms must be used. Currencies must be in U.S. dollars.
- **Footnotes**: Footnotes must be kept to a minimum. They must be referred to in the text in uppercase numbers. Footnotes must appear at the bottom of the page on which they are introduced.
- **References**: Authors must follow the APA style of referencing. References must be arranged alphabetically. The reference list must not be numbered. Non-English references must be "romanised" into English.
- **Digital Object Identifier (DOI)**: If a reference has a DOI, it must be included.

Proofreading Certificates: Once accepted, manuscripts must be sent by authors to an accredited proofreading company. A proofreading certificate must be submitted to the Journal. A suggested company is: proofreadmyessay.co.uk

1. معلومات عامة

- **أخلاقيات البحث**: لا تقبل المجلة استلام أي ورقة أو تحكيم يتضمن أي نوع من أنواع التحامل أو العدوانية أو التطرف أو التشدق الأيديولوجي (سواء كان ذلك موجها لشخص، أو مدرسة فكرية، أو طائفة، أو جنس، أو أيديولوجية بعينها). كما لا تقبل استلام الأبحاث أو تقييمات المحكمين التي تحمل أفكاراً تناهض الأمن الفكري والمجتمعي، أو تُعزز الإرهاب والأفكار المتطرفة، أو تحضّ عليها تصريحاً أو تلميحاً.
- **أوقات العمل**: تقوم المجلة بمهمة استلام الأوراق العلمية على مدار العام، وفي حالة وجود توقف سيتم وضع رد تلقائي على البريد الإلكتروني.
- **رسوم النشر**: المجلة لا تتقاضى أي أجر أو رسوم مالية مقابل عملية النشر العلمي واجراءاته (النشر مجاناً لجميع الباحثين).
- **لغة النشر**: تقبل المجلة أبحاثاً مكتوبة باللغة العربية أو اللغة الإنجليزية.
- **مدة النشر**: بعد انضمام المجلة إلى المعرف الرقمي العالمي الموحد (DOI) أصبح بإمكان أي بحث جديد مرسل للمجلة أن ينشر على الموقع الإلكتروني للمجلة برقم المعرف الرقمي (DOI) في غضون فترة لا تزيد عن 100 يوم عمل منذ تسليمه للمجلة وإعطائه رقم قيد.
- **آلية تسليم الورقة**: يجب تسليم الورقة للمحرر المناسب، وفقاً للآتي:
  - تسلم أوراق العلوم الأساسية والتطبيقية إلى سعادة محرر فرع العلوم الأساسية والتطبيقية: secretary-b@kfu.edu.sa. سيقوم المحرر بتدقيق الورقة للتأكد من اتباعها لـ "تعليمات النشر". في حال عدم اتباع التعليمات، فستعاد الورقة للمؤلف. في حال اتباع التعليمات، فسيقوم المحرر بإنشاء حساب للمؤلف وتزويده باسم المستخدم وكلمة السر لتسليم ورقته من خلال نظام التسليم الإلكتروني (ScholarOne): https://mc04.manuscriptcentral.com/sjkfub.
  - تسلم أوراق العلوم الإنسانية والإدارية (الأبحاث التربوية فقط) إلى سعادة محرر فرع العلوم الإنسانية والإدارية للقضايا التربوية: sjkfu-assed@kfu.edu.sa. سيقوم المحرر بتدقيق الورقة للتأكد من اتباعها لـ "تعليمات النشر". في حال عدم اتباع التعليمات، فستعاد الورقة للمؤلف. في حال اتباع التعليمات، فسيقوم المحرر بإنشاء حساب للمؤلف وتزويده باسم المستخدم وكلمة السر لتسليم ورقته من خلال نظام التسليم الإلكتروني (ScholarOne): https://mc04.manuscriptcentral.com/sjkfuh.
  - تسلم أوراق العلوم الإنسانية والإدارية (الأبحاث غير التربوية) إلى سعادة محرر فرع العلوم الإنسانية والإدارية للقضايا غير التربوية: sjkfu-hm@kfu.edu.sa. سيقوم المحرر بتدقيق الورقة للتأكد من اتباعها لـ "تعليمات النشر". في حال عدم اتباع التعليمات، فستعاد الورقة للمؤلف. في حال اتباع التعليمات، فسيقوم المحرر بإنشاء حساب للمؤلف وتزويده باسم المستخدم وكلمة السر لتسليم ورقته من خلال نظام التسليم الإلكتروني (ScholarOne): https://mc04.manuscriptcentral.com/sjkfuh.
- **الرسائل العلمية**: تقبل المجلة الأوراق المستلة من الرسائل العلمية، على أن يتم النص على ذلك.
- **الحقوق الفكرية**: جميع حقوق الطبع والنشر محفوظة للمجلة، ولا يسمح بإعادة طبع أو نشر أي جزء من المجلة أو نسخه بأي شكل وبأي وسيلة كانت إلكترونية أو آلية بما في ذلك التصوير والتسجيل والإدخال في أي نظام حفظ معلومات أو استعادتها دون الحصول على موافقة كتابية من رئيس هيئة التحرير.
- **آراء المؤلفين**: الآراء المضمنة في الأوراق المنشورة تعبر عن وجهات نظر كتابها ولا تعبر بالضرورة عن وجهة نظر المجلة.
- **فلسفة الأوراق العلمية**: لا تستقبل المجلة الأوراق العلمية التي لا تراعي المحاور الآتية ولا تحقق مدى عاليا في كل محور:
  - مدى احتمالية اقتباس الورقة من قِبل بحوث أخرى في كلاريفيت وسكوبس خلال عامين قادمين؛ حيث إن هذا يعد أحد المتطلبات المهمة لتصنيف المجلة في قاعدة بيانات سكوبس.
  - مدى فائدة الورقة للقارئ الدولي ومدى اتساع جمهور الورقة خارج نطاق المكان والزمان واللغة. يُعرف القارئ الدولي هنا بأنه "شخصية اعتبارية محايدة (سواء شخص، مجموعة، جهة، مؤسسة أو مُنظمة) لا تشترك مع المؤلف في الحدود الزمانية والمكانية واللغوية التي كُتبت بها الورقة".
- **ضرورة اتباع الإرشادات**: وفقاً لسياسة المجلة، فإنه يتوجب على أصحاب السعادة الباحثين ضبط ورقتهم وفقاً لملف "إرشادات التسليم"، واتباعها *حرفياً* وبدقة متناهية وعالية *جداً*، حيث إن عدم الالتزام بها بأي وجه من الأوجه سيمثل عائقاً لنشر الورقة. نؤكد الضرورة القصوى للاتباع الحرفي والدقيق لهذه الإرشادات. إن المجلة تسعى جاهدة أن تكون مصنفة في عدد من قواعد البيانات المتميزة عالمياً مما يتطلب دقة عالية في ضبط الورقة، وعليه وجب توخي الحذر التام في كيفية ضبط الورقة وفقاً للمطلوب، حيث إن آلية صياغة المراجع، على سبيل المثال، هي العنصر الأهم لقواعد البيانات العالمية. في حالة قيام المؤلف بإرسال الورقة إلى المجلة، وتبين لهيئة التحرير وجود بعض الإرشادات لم يتم اتباعها، فإنه سيتم إرجاع الورقة للمؤلف، وسيتم إخباره بعدم اتباعه للإرشادات، بدون تحديد أي من الإرشادات لم يتم اتباعها، وذلك لأن الوقت للأسف لا يتسع للمجلة لأن تزود كل مؤلف بتغذية فردية عن أي من الإرشادات لم يتم مراعاتها، كما أنه بناء على سياسة المجلة فإن السادة الباحثين هم المعنيون بالدرجة الأولى من التأكد من اتباع كافة الإرشادات. ولذلك ننصح سعادة المؤلف الرئيس، بعد الانتهاء من ضبط الورقة، بأن يقوم بإرسال الورقة للمؤلفين الآخرين (وأيضاً لزميل من غير المؤلفين) للتأكد من أن جميع الإرشادات قد اتبعت. كما ننصح أصحاب السعادة المؤلفين أن يقوموا أيضاً بالاستعانة بطرق واستراتيجيات أخرى يرون أنها قد تساعدهم في التأكد من اتباع كافة الإرشادات؛ فعلى سبيل المثال، القيام بطباعة ملف "إرشادات التسليم"، ثم وضع علامة "صح" بجانب كل فقرة من الإرشادات للتأكد من تغطية جميع الإرشادات. تؤكد المجلة لأصحاب السعادة المؤلفين أنها من خلال خطتها الاستراتيجية الحالية تسعى لأن تكون منار التميز في العالم العربي (بجميع ما يتطلبه التميز من عمل شاق ودقة)، وهذا قد يزيد العبء على المجلة والمؤلف والمحكمين وجميع "أصحاب الشأن" على حد سواء. سيمنح المؤلف فرصتين كحد أعلى لاتباع التعليمات، وفي حالة عدم قيامه بذلك، فإن هيئة التحرير ستقوم بطي قيد البحث، حتى وإن أوصى المحكمون بقبول البحث. اتباع التعليمات تحمل نفس الماهية التي تحملها القيمة العلمية للورقة.
- **متعارضات**: في حالة تضارب توصيات المحكمين مع إرشادات النشر، فيتم استبعاد توصيات المحكمين وتعتمد إرشادات النشر، مع ضرورة إعلام المحرر بهذا التضارب.

2. شروط لا يتم استلام الورقة دونها

- **المستندات المطلوبة**: يجب تسليم ملفين على صيغة الوورد (DOC)، وهما كالتالي:
  - الملف الأول تحت مسمى "بيانات الباحث" (Title Page): يجب ترتيب هذا الملف كالتالي:
    - عنوان الورقة بالعربي (غير مطلوب إذا كانت الورقة باللغة الإنجليزية).
    - بيانات المؤلف بالعربي (على أن يتضمن اسم المؤلف، اسم القسم، اسم الكلية، اسم الجامعة، اسم المدينة، واسم الدولة، البريد الإلكتروني، رقم الواتساب). في حالة عدم وجود قسم أو كلية أو جامعة، يكتب ما يعادلها. في حالة عدم الانتساب لجامعة، يكتب "باحث مستقل" (غير مطلوب إذا كانت الورقة باللغة الإنجليزية).
    - عنوان الورقة بالإنجليزي.
    - بيانات المؤلف بالإنجليزي (على أن يتضمن اسم المؤلف، اسم القسم، اسم الكلية، اسم الجامعة، اسم المدينة، واسم الدولة، البريد الإلكتروني، رقم الواتساب). في حالة عدم الانتساب لجامعة، يكتب "Independent Researcher".
    - تحديد تخصص الورقة: 1) التخصص العام، 2) التخصص الدقيق ، 3) التخصص الأدق من الدقيق.
    - نبذة من 80 كلمة عن كل مؤلف. أدناه توضيح عن كيفية كتابة النبذ (إذا كانت الورقة بالعربي فتكتب النبذة بالعربي، وإذا كانت الورقة بالإنجليزي، فتكتب النبذة بالإنجليزي).
    - شكر وتقدير (اختياري).

- الملف الثاني تحت عنوان "ملف البحث" (Main Document): تتبع المجلة سياسة التحكيم المزدوج مجهول الهوية، وعليه يجب على المؤلف عدم تضمين ما يكشف هويته في "ملف البحث"، حيث ان "ملف البحث" سيرسل كما هو للمحكمين. يجب ترتيب الملف كالتالي:
  - عنوان الورقة بالعربي (غير مطلوب إذا كانت الورقة باللغة الإنجليزية).
  - ملخص الورقة بالعربي (غير مطلوب إذا كانت الورقة باللغة الإنجليزية).
  - الكلمات المفتاحية بالعربي (غير مطلوب إذا كانت الورقة باللغة الإنجليزية).
  - عنوان الورقة بالإنجليزي.
  - ملخص البحث بالإنجليزي.
  - الكلمات المفتاحية بالإنجليزي.
  - مضمون البحث.
  - المراجع.

- **"نبذة عن المؤلف"**: يجب تزويد نبذة عن كل مشارك في البحث. تتضمن النبذة الاسم، ثم أدناه اسم القسم، الكلية، الجامعة، المدينة، الدولة (أو ما يوازيه)، رقم الواتساب مع فتح الخط الدولي، البريد الإلكتروني، ثم أدناه نبذة عن الباحث (من 80 كلمة لكل باحث، علماً أن اسم الباحث و مكان العمل لا يحسب من هذه الـ 80 كلمة). إذا كان لدى الباحث رقم أوركيد و/أو صفحة شخصية، فيدرج في نهاية النبذة. يجب أن تتضمن النبذة جنسية المؤلف، وأعلى درجة علمية حصل عليها (مثلاً، ماجستير، دكتوراه) واسم الجامعة التي حصل منها على هذه الدرجة. يمكن للمؤلف الكتابة في النبذة عن نشاطه البحثي واهتماماته البحثية ومدى التأثير الوطني والعالمي الذي حققه ومدى قدرته على التواصل خارج نطاق مكان عمله وشيء من نشاطه في المؤتمرات والدورات التدريبية. النبذة هي وسيلة مهمة يستطيع الباحث من خلالها التعريف بنفسه وتسويق ذاته؛ فينبغي أن تحظى باهتمام عال من قبل المؤلف. ترتب النبذ وفقاً لترتيب المؤلفين. أدناه مثال على ذلك:

  عبدالرحمن عيسى الليلي
  قسم المناهج وطرق التدريس، كلية التربية، جامعة الملك فيصل، الأحساء، المملكة العربية السعودية، 00966000000000،
  scijkfu@kfu.edu.sa
  أ.د. الليلي دكتوراه (أكسفورد)، سعودي، أستاذ دكتور، عميد بحث علمي، مدير مركز وطني، رئيس هيئة تحرير (سكوبس)، أعماله في 7 لغات (منها، إسباني، فلبيني، إندونيسي، صيني، إيطالي)، مقابلاته في 5 لغات (منها، فرنسي، إسباني، ألماني)، مؤسس عدد من النظريات (منها، "Multiple Stupidities" و"Retroactivism" و"On-the-Go Sourcing") و 3 منهجيات ("Crowd-Authoring" و"Crowd-Reflecting" و"Door-Knocking")، أكثر مبيعاً (أمازون)، نشر مع أكبر دور نشر (Nature Research, Cogent, Palgrave, Elsevier, Springer, Taylor & Francis, Wiley, Sage, Oxford)، نشر 24 ورقة في ISI و/أو سكوبس، أبحاثه مقتبسة من قبل 35 دولة (منها المجر، صربيا، روسيا، بيرو، كوريا، كولومبيا، سويسرا، هولندا، السويد، فنلندا، لاتفيا) في 6 لغات (منها، التركية و الليتوانية)، عمل خلال الصيف في نيوزلندا وايطاليا. شارك بأوراق في مؤتمرات سنغافورة، اليونان، اليابان، بلغاريا وغيرها. عمل مستشاراً لمؤسسات منها الويكيبيديا و جامعة هانوفر.
  رقم الأوركيد (ORCID): 0000-0002-5116-422X
  الموقع الشخصي: https://abdulrahmanallily.wordpress.com

- **عدد كلمات الورقة**: ألا يتجاوز عدد كلمات الورقة 8000 كلمة في أي حال من الأحوال (شاملة كل شيء، بما في ذلك المراجع والجداول والأشكال والملخص وبيانات المؤلفين والهوامش والرومنة وكل شيء).
- **الملخص**: ألا يزيد الملخص عن 200 كلمة. لا يسمح بإدراج مراجع أو اقتباسات في الملخص.
- **عدد كلمات العنوان**: ألا يزيد عنوان الورقة عن 15 كلمة.
- **عدد الكلمات المفتاحية**: أن تحتوي الورقة على ست كلمات مفتاحية باللغة العربية وترجمتها بالإنجليزية، ويجب ألا يكون قد سبق ذكرها في العنوان، كما يجب ألا تزيد كل كلمة مفتاحية عن كلمتين.
- **عدد الجداول والرسومات**: ينبغي تقليص عدد الجداول والرسومات والاختصارات والحواشي السفلية، قدر المستطاع. يجب ألا تتضمن الورقة أكثر من (6) جداول و (6) صور/أشكال. علماً أن عدم وجود أشكال بالورقة لا يعني أن عدد الجداول يمكن أن يزيد عن (6)، وعدم وجود جداول بالورقة لا يعني أن عدد الأشكال يمكن أن يزيد عن (6). يجب ألا يزيد عدد السطور عن 20 وعدد الأعمدة عن 7 في كل جدول من الجداول.
- **الجودة اللغوية**: يجب أن يكون البحث مكتوبًا بمستوى لغوي صحيح مقبول. كما يجب على المؤلف الضغط على أيقونة "المراجعة اللغوية" في ملف الوورد للتأكد من عدم وجود أخطاء لغوية.
- **عدد المراجع**: يجب ألا يزيد عدد المراجع عن 40 مرجعًا (إلا في حالة كون الورقة "مراجعة أدبية").
- **الاقتباس**: يجب أن تكون نسبة الاقتباس غير المشروع 0%.
  - يسري ذلك على نوعي الاقتباس: الاقتباس الذاتي و الاقتباس من الآخرين. ويقصد بالاقتباس الذاتي أن ينقل الباحث من عمل آخر له قام بنشره من قبل دون أن يشير إلى النقل.
  - يستثنى من الاقتباس غير المشروع تلك العبارات والجمل المتداولة التي لا تُمثل انتهاكا لحقوق الآخرين، ولا تطعن في الأصالة العلمية؛ مثل عبارة:
    والجدول يُوضح معاملات متغيرات الدراسة التي وضعت في قائمة الاستقصاء التي اعتمد عليها الباحث في تجميع البيانات الأولية.
  - في حالة الاقتباس الحرفي ولجعل الاقتباس مشروعاً، فيجب ألا يزيد عن 30 كلمة، وتوضع في علامة تنصيص، ويذكر اسم المرجع ورقم الصفحة. مثال على ذلك:
    ويجدر الإشارة إلى أنه "يعد التعليم عن بعد في زمن الكورونا مختلفاً بشكل أساسي وجوهري عن "التعليم عن بعد" التقليدي من عدة أوجه، أولها كونه مفاجئا وغير مخطط له مسبقاً" (العلي، 2020: 15).
  - غير مسموح بالاقتباس الحرفي إلا في حالة الضرورة القصوى والمبررة؛ حيث مفترض من المؤلف أن يعيد صياغة أي اقتباس بأسلوبه الشخصي.
  - في حالة كون أن طبيعة التخصص تتطلب اقتباسات مطولة، فيجب تبرير ذلك في الخطاب الموجه للمجلة أثناء التسليم.
- **العبارات غير الأكاديمية**: يجب أن تكون اللغة المكتوب بها الورقة لغة علمية أكاديمية مباشرة تبتعد عن الإسهاب الذي لا علاقة له بالورقة من الناحية العلمية، وأيضا تبتعد عن تكرار الجمل والمعاني المعلومة بالضرورة؛ ومن الأمثلة على ذلك ما يرد في مقدمة البحث وخاتمته لدى بعض الباحثين: (فإن أكن أصبت فمن الله وحده وله المنة على ذلك، وإن تكن الثانية فمن نفسي ومن الشيطان، والله الهادي إلى سواء السبيل..)، (أحمد الله أن أعانني ويسر لي إتمام هذا البحث بعدما لاقيت فيه من عناء وجهد طيلة شهور متتابعة، فإن أصبت فإمساك بمعروف، وإن تكن الأخرى فتسريح بإحسان..)، (حفظه الله ورعاه وسدد على طريق الخير خطاه..)، (رحمه الله وطيب ثراه..)، ونحو ذلك، ويستثنى من ذلك ما يتعلق بالأنبياء والمرسلين: (صلى الله عليه وسلم)، (عليه السلام).
- **المرفقات/الملاحق**: ألا تتضمن الورقة مرفقات، وفي حال ضرورة المرفقات فإنها توضع في المتن، أو يتم وضع رابط للمرفقات على الإنترنت (يتم تزويد الملحقات فقط في حالة طلب المحكمين لها).

3. إجراءات يطلب من المؤلف عملها فقط بعد صدور قرار المحكمين

- **مقاس الصفحة**: يكون مقاس الصفحة A4، على عمود واحد، الهوامش 2.5 سم من جميع الجهات، ويكون نوع الخط من الخطوط الدارج استخدامها، ويكون حجم الخط مقبولا.
- **جودة اللغة**: يجب التأكد من الخلو التام من وجود أي ملاحظات لغوية.
- **العناوين**:
  - لا يزيد عدد مستويات العناوين عن ثلاثة. أي يسمح فقط بعناوين أساسية، وفرعية وفرعية فرعية فقط. أي كون هناك عناوين فرعية فرعية فرعية غير مسموح لتجاوزها ثلاثة مستويات. الأساسية والفرعية. يجب ترقيمها كالتالي: 1.، 2.، 3.، وتحت 1. يكون 1.1.، 1.2.، 1.3.، وتحت 1.1. يكون 1.1.1.، 1.1.2.، 1.1.3.، وهكذا. يجب ألا يتم ترقيم عنوان الملخص،

والنبذة عن المؤلف والمراجع.

- المجلة لا تستقبل عناوين الأبحاث التي تدور حول فرد بعينه أو قصيدة بعينها أو كتاب بعينه؛ مثل: "المفارقة الشعرية في شعر أبي الحسن القيرواني"، "حجيّة المنجز الكلامي في مقدّمة دلائل الإعجاز لعبد القاهر الجرجاني"، "هرمية المصطلح البلاغي والنقدي عند الجاحظ"، "النسق البنيوي في قصيدة أبي ذؤيب الهذلي في رثاء أولاده الخمسة".
- نظرا لكون المجلة العلمية لجامعة الملك فيصل مجلة متعددة التخصصات تندرج ضمن المنصات العالمية للبحث العلمي فإن هذا يتطلب من الباحثين كتابة عنوان الورقة وملخصها باللغة العلمية المباشرة بصياغة سهلة بعيدة عن التعقيد مما ييسر لكل قارئ في مختلف التخصصات فهم مضمون الورقة وعنوانها وملخصها.
- لا تنشر المجلة الأوراق التي تتحدد بذكر مدينة أو محافظة بعينها في العنوان البحثي (يمكن الاكتفاء بذكر اسم الدولة فقط إذا لزم الأمر)، وذلك لأن تخصيص اسم مدينة بعينها يحدد من نسبة الاستشهادات للورقة بعد نشرها، لأنه غالباً ما تكون هذه المدينة غير معلومة أو غير ذات اهتمام من القراء، وهذا يتعارض مع سياسة المجلة في استقطاب الأوراق ذات العمومية والانتشار الواسع. واذا أراد الباحث أن يخصص محافظة أو مدينة ما، فيمكنه الإشارة لذلك في ملخص الورقة وحدودها المكانية وليس في العنوان.

- **التواريخ والأرقام**: يجب أن تكون جميع تواريخ الورقة بالميلادي وبأرقام إنجليزية (سواء في المتن أو المراجع).
- **الجداول**: يتم كتابة رقم وعنوان الشكل أو الجدول أعلاه. في المتن، يتم الإشارة إلى الجدول أو الشكل دائماً برقمه سواءً قبل أو بعد وضعه، وترقم الجداول تسلسليا حسب تسلسل ذكرها في المتن.
- **العملات**: يجب كتابة القيمة بالدولار بين قوسين، بعد أي قيمة مذكورة بالريال السعودي أو أي عملة أخرى.
- **الاختصارات**: عند استخدام رموز لاختصار مصطلح، فيجب أن يذكر نص المصطلح كاملا في أول مرة يرد فيها في نص البحث. علما أن المسموح به ثلاث اختصارات على الأكثر.
- **المقاييس الرياضية**: يجب استخدام الاختصارات المقننة دوليا بدلا من كتابة الكلمة كاملة مثل سم، ملم، كلم و% (لكل من سنتمتر، مليمتر، كيلومتر والنسبة المئوية، على الترتيب). يفضل استخدام المقاييس المترية وفي حالة استخدام وحدات أخرى يكتب المعادل المتري لها بين أقواس مربعة. في حالة ذكر وحدات قياس أو أسماء دارجة إقليميا للكائنات الحية في المتن يذكر عقبها مباشرة المقابل لها بالوحدات القياسية أو الاسم اللاتيني للكائن. يجب أن تكون جميع العملات بالدولار الأمريكي.
- **الحواشي**: يفضل تقليص الحواشي، ولكن في حالة الحاجة لها، فيشار إلى الحاشية في المتن بأرقام بين قوسين مرتفعة عن السطر، ترقم الحواشي داخل المتن وتكتب حواشي كل صفحة أسفلها مفصولة عن المتن بخط ولا تجمع في نهاية المتن. يعاد ترقيم الحواشي ابتداءً من الرقم 1 مع بداية كل صفحة جديدة.
- **الهوامش السفلية**: تأخذ المراجع المدرجة في الحواشي السفلية ترقيماً متسلسلاً لكل صفحة بحيث يوضع رقم الحاشية بين قوسين علويين ()، وتكون جميع العناصر البيليوجرافية لكل مرجع مرتبة وفقا للترتيب المذكور في قائمة المراجع، سواء ذكرت البيانات كاملة أو مختصرة، كما يجب التأكد من أن جميع المراجع الواردة في المتن والحواشي مذكورة في قائمة المراجع، كما يجب ألا تكون هنالك مراجع بالقائمة لم يشر إليها في المتن.
- **روابط المراجع**:
  - **للمراجع العربية**: في حالة الرغبة في إدراج رابط لمرجع عربي، فيكتب بعد المرجع "متوفر بموقع:" ثم يدرج الرابط، وبعد الرابط يفتح قوس ويكتب "تاريخ الاسترجاع:" ثم يدرج التاريخ على هذه الصيغة "2020/07/27"، ثم يغلق القوس.
  - **للمراجع الإنجليزية**: في حالة الرغبة في إدراج رابط لمرجع إنجليزي، فيكتب بعد المرجع "Available at:" ثم يدرج الرابط، وبعد الرابط يفتح قوس ويكتب "accessed on" ثم يدرج التاريخ على هذه الصيغة "2020/07/27"، ثم يغلق القوس.
- **ترتيب قائمة المراجع**: يجب ترتيب المراجع هجائياً. ويجب عدم ترقيم قائمة المراجع.
- **مرجعان لمؤلف في سنة واحدة**: في حالة وجود مرجعين لمؤلف واحد في سنة واحدة، فللتمييز بينهما يكتب حرف بجانب التاريخ كالآتي: (2020أ)، (2020ب)، وبالإنجليزي (2020a)، (2020b)
- **DOI للمرجع**: عند استعمال مراجع لها رقم DOI، يجب ذكر هذا الرقم.
- **المراجع داخل المتن**: بخصوص آلية كتابة المراجع داخل المتن:
  - إذا كان المرجع في بداية الجملة، يكتب اسم عائلة الباحث/الباحثين يليها تاريخ النشر بين قوسين. مثال: "ذكر الصالح والأحمد (2020) بأن..."
  - إذا كان المرجع في نهاية الجملة، فيكتب بين قوسين اسم عائلة الباحث/الباحثين، ثم فاصلة، ثم تاريخ النشر. مثال: "وهذا هو أساس المشكلة (الصالح والأحمد، 2020)."
  - في حالة كون المرجع لأكثر من باحثين فيكتب اسم عائلة الباحث الأول متبوعا بكلمة "وآخرون". مثال: "ذكر المحمد وآخرون (2020) بأن..." أو "وهذا ما يسمى بالتعليم المدمج (العلي وآخرون، 2020)."
  - يجب تدوين رقم الصفحة المقتبس منها داخل المتن. أدناه أمثلة على كيفية عمل هذا التدوين:
    - "وهذه من القضايا الأساسية التي ستساهم في تطور التعليم العالي" (المحمد، 2020: 15).
    - ذكر المحمد (2020: 15) أن هذه "من القضايا الأساسية التي ستساهم في تطور التعليم العالي".
    - ذكر المحمد (2020) أن هذه "من القضايا الأساسية التي ستساهم في تطور التعليم العالي" (ص. 15).
- **المراجع في قائمة المراجع**: لا يتم استخدام كلمة "وآخرون" (.et al) في قائمة المراجع.
- **صفحات الويكيبيديا**: لا يسمح باقتباس صفحات الويكيبيديا.
- **تعريف الرومنة**: يجب رومنة/ترجمة قائمة المراجع العربية. يقصد بالرومنة النقل الصوتي للحروف إلى الإنجليزية، أي تحويل منطوق الحروف العربية إلى حروف إنجليزية. تتم الرومنة عن طريق مترجم قوقل (http://translate.google.com)، حيث إن في كتابة أي جملة في مترجم قوقل (مثلاً: " إنجازات جامعة الملك فيصل منذ تأسيسها")، فستكون رومنة هذه الجملة متوفرة بأسفل النص " iinjazat jamieat almalik faysal mundh tasisiha"، وترجمتها متوفرة على الجنب (Achievements of King Faisal University since its foundation). رومنة المراجع العربية لا يعني حذف المراجع العربية. فالمراجع العربية والمرومنة تبقى سوياً. توضع أولاً المراجع العربية، يليها المراجع المرومنة والإنجليزية. تدمج المراجع المرومنة والإنجليزية سوياً وترتب هجائياً.
- **تعديلات هيئة التحرير على عنوان الورقة**: يحقّ لهيئة التحرير إعادة صياغة عنوان الورقة في المرحلة الأخيرة للنشر (قبل الإحالة لعدد)، وذلك وفقاً لمقتضيات التوجه التطويري العام للمجلة حالياً، والذي يتطلب الاقتصار على نشر العناوين: "الموجزة، والبسيطة، والواضحة، والعامة التي لا تشتمل على صف دراسي بعينه أو جامعة أو محافظة أو مدينة بعينها في العنوان" وبالتالي سيتم استبعاد أية كلمة غير ضرورية من العنوان لأن هذه المصطلحات تحدّ من نسبة انتشار البحث، وشموليته، وتقلل من نسبة اقتباسه واستشهاداته من قبل الباحثين.
- **شهادة مراجعة لغوية**: في حالة قبول الورقة للنشر، فإنه سيطلب من المؤلف إرسال ورقته لشركة معتمدة لمراجعة الورقة من قبل متحدثي اللغة الإنجليزية كلغة أم، وموافاة المجلة بشهادة إثبات مراجعة لغوية من قبل الشركة. إذا كانت الورقة باللغة العربية، فإن المراجعة تكون لعنوان الورقة والملخص باللغة الإنجليزية. وإذا كانت الورقة باللغة الإنجليزية، فإن المراجعة تكون على الورقة كاملة. تكون هذه المراجعة اللغوية كمرحلة أخيرة قبل نشر الورقة وبعد إدخال كامل ملاحظات المحكمين والمحررين وهيئة التحرير. أدناه إحدى هذه الشركات والتي تقوم بالمراجعة اللغوية خلال 24 ساعة: https://proofreadmyessay.co.uk

4. آلية كتابة الدوريات والمجلات في المراجع (يطلب عملها فقط في حالة قبول الورقة للنشر)

4.1. كتابة الدوريات والمجلات العربية في قائمة المراجع

يبدأ كل مرجع باسم العائلة للمؤلف الأول، ثم فاصلة، ثم الاسم الأول واسم الأب للمؤلف الأول، ثم فاصلة، ثم اسم العائلة للمؤلف الثاني، ثم فاصلة، ثم الاسم الأول واسم الأب للمؤلف الثاني، ثم حرف العطف "و" ثم اسم العائلة للمؤلف الثالث، ثم فاصلة، ثم الاسم الأول واسم الأب للمؤلف الثالث، ثم نقطة، ثم فتح قوس، ثم التاريخ، ثم إغلاق القوس، ثم نقطة، ثم عنوان البحث، ثم نقطة، ثم اسم المجلة يكون مكتوبا بشكل مائل، ثم فاصلة، ثم رقم المجلد مكتوبا بشكل عريض، ثم فتح قوس، ثم

يكتب رقم العدد، ثم يغلق القوس، علماً أنه لا يوجد مسافة بين رقم المجلد ورقم العدد، ثم فاصلة، ثم رقم أول صفحة للبحث، ثم علامة "-" ثم رقم آخر صفحة للبحث. (مع مراعاة أن حرف العطف "و" يوضع دائما قبل المؤلف الأخير أيًّا كان عدد المؤلفين). أدناه مثال على ذلك:

الأحمد، محمد عبدالرحمن، العلي، إسماعيل صلاح والصالح، أحمد محمد. (2020). إنجازات جامعة الملك فيصل منذ تأسيسها. *المجلة العلمية لجامعة الملك فيصل: فرع العلوم الإنسانية والإدارية*، **13**(2)، 213-223.

في حالة عدم وجود تاريخ، فتكتب العبارة التالية "د.ت." في مكان التاريخ، سواء في المتن أو المرجع. على سبيل المثال:

الأحمد، محمد عبدالرحمن، العلي، إسماعيل صلاح والصالح، أحمد محمد. (د.ت.). إنجازات جامعة الملك فيصل منذ تأسيسها. *المجلة العلمية لجامعة الملك فيصل: فرع العلوم الإنسانية والإدارية*، **13**(2)، 213-223.

في حالة عدم وجود رقم مجلد، فتكتب العبارة التالية "بدون رقم مجلد" في مكان رقم المجلد. على سبيل المثال:

الأحمد، محمد عبدالرحمن، العلي، إسماعيل صلاح والصالح، أحمد محمد. (2020). إنجازات جامعة الملك فيصل منذ تأسيسها. *المجلة العلمية لجامعة الملك فيصل: فرع العلوم الإنسانية والإدارية*، **بدون رقم مجلد** (2)، 213-223.

في حالة عدم وجود رقم عدد، فتكتب العبارة التالية "بدون رقم عدد" في مكان رقم العدد. على سبيل المثال:

الأحمد، محمد عبدالرحمن، العلي، إسماعيل صلاح والصالح، أحمد محمد. (2020). إنجازات جامعة الملك فيصل منذ تأسيسها. *المجلة العلمية لجامعة الملك فيصل: فرع العلوم الإنسانية والإدارية*، **13**(بدون رقم عدد)، 213-223.

في حالة عدم وجود أرقام صفحات، فتكتب العبارة التالية "بدون أرقام صفحات" في مكان أرقام الصفحات، أو رقم مسلسل البحث في مجلات الأونلاين. على سبيل المثال:

الأحمد، محمد عبدالرحمن، العلي، إسماعيل صلاح والصالح، أحمد محمد. (2020). إنجازات جامعة الملك فيصل منذ تأسيسها. *المجلة العلمية لجامعة الملك فيصل: فرع العلوم الإنسانية والإدارية*، **13**(2)، بدون أرقام صفحات.

4.2. كتابة الدوريات والمجلات الإنجليزية في قائمة المراجع

يبدأ كل مرجع باسم العائلة للمؤلف الأول، ثم فاصلة، ثم الحرف الأول من الاسم الأول للمؤلف الأول، ثم نقطة، ثم الحرف الأول لاسم الأب للمؤلف الأول، ثم نقطة، ثم فاصلة، ثم اسم العائلة للمؤلف الثاني، ثم فاصلة، ثم الحرف الأول من الاسم الأول للمؤلف الثاني، ثم نقطة، ثم الحرف الأول لاسم الأب للمؤلف الثاني، ثم نقطة، ثم حرف العطف "and" (وليس "&") ثم اسم العائلة للمؤلف الثالث، ثم فاصلة، ثم الحرف الأول من الاسم الأول للمؤلف الثالث، ثم نقطة، ثم الحرف الأول لاسم الأب للمؤلف الثالث، ثم نقطة، ثم فتح قوس، ثم التاريخ بالميلادي، ثم إغلاق القوس، ثم نقطة، ثم عنوان البحث بحروف صغيرة (صمول small؛ يستثنى من ذلك الكلمة الأولى وأسماء الأشخاص وأسماء الأماكن وأسماء الجنسيات واللغات والأسابيع والشهور فيبقى الحرف الأول منها بحروف كبيرة، كابتل capital)، ثم نقطة، ثم اسم المجلة يكون مكتوبا بشكل مائل والحرف الأول من كل كلمة يكون كبيرا (كابتل capital؛ يستثنى من ذلك أدوات التنكير والتعريف مثل "a" و "an" و "the" وحروف الجر مثل "to" و "of" و "in" وأدوات الربط "and" و "but" و "or" فيبقى الحرف الأول منها بحروف صغيرة، إلا إذا كانوا في بداية اسم المجلة فيكون الحرف الأول منها بحروف كبيرة)، ثم فاصلة، ثم رقم المجلد مكتوبا بشكل عريض، ثم فتح قوس، ثم يكتب رقم العدد، ثم يغلق القوس، علماً أنه لا يوجد مسافة بين رقم المجلد ورقم العدد، ثم فاصلة، ثم رقم أول صفحة للبحث، ثم علامة "-" ثم رقم آخر صفحة للبحث. أدناه مثال على ذلك:

Al Ahmed, K.A., Al Muhammed, S.F. and Al Saleh, A.F. (2020). The history of agriculture in Al Ahsa. *The Scientific Journal of King Faisal University: Humanities and Management Sciences*, **13**(2), 213-222.

في حالة عدم وجود تاريخ، فيكتب "n/a". على سبيل المثال:

Al Ahmed, K.A., Al Muhammed, S.F. and Al Saleh, A.F. (n/a). The history of agriculture in Al Ahsa. *The Scientific Journal of King Faisal University: Humanities and Management Sciences*, **13**(2), 213-222.

في حالة عدم وجود رقم مجلد، فيكتب "n/a". على سبيل المثال:

Al Ahmed, K.A., Al Muhammed, S.F. and Al Saleh, A.F. (2020). The history of agriculture in Al Ahsa. *The Scientific Journal of King Faisal University: Humanities and Management Sciences*, **n/a**(2), 213-222.

في حالة عدم وجود رقم عدد، فيكتب "n/a". على سبيل المثال:

Al Ahmed, K.A., Al Muhammed, S.F. and Al Saleh, A.F. (2020). The history of agriculture in Al Ahsa. *The Scientific Journal of King Faisal University: Humanities and Management Sciences*, **13**(n/a), 213-222.

في حالة عدم وجود أرقام صفحات، فيكتب "n/a". على سبيل المثال:

Al Ahmed, K.A., Al Muhammed, S.F. and Al Saleh, A.F. (2020). The history of agriculture in Al Ahsa. *The Scientific Journal of King Faisal University: Humanities and Management Sciences*, **13**(2), n/a.

4.3. رومنة/ترجمة الدوريات والمجلات غير الإنجليزية في قائمة المراجع

يبدأ كل مرجع باسم العائلة للمؤلف الأول، ثم فاصلة، ثم الحرف الأول من الاسم الأول للمؤلف الأول، ثم نقطة، ثم الحرف الأول لاسم الأب للمؤلف الأول، ثم نقطة، ثم فاصلة، ثم اسم العائلة للمؤلف الثاني، ثم فاصلة، ثم الحرف الأول من الاسم الأول للمؤلف الثاني، ثم نقطة، ثم الحرف الأول لاسم الأب للمؤلف الثاني، ثم نقطة، ثم حرف العطف "and" (وليس "&") ثم اسم العائلة للمؤلف الثالث، ثم فاصلة، ثم الحرف الأول من الاسم الأول للمؤلف الثالث، ثم نقطة، ثم الحرف الأول لاسم الأب للمؤلف الثالث، ثم نقطة، ثم فتح قوس، ثم التاريخ بالميلادي، ثم إغلاق القوس، ثم نقطة، ثم عنوان البحث (مرومن) بحروف صغيرة (صمول small)، ثم فتح علامة تنصيص واحدة، ثم عنوان البحث مترجما بحروف صغيرة (صمول small؛ يستثنى من ذلك الكلمة الأولى وأسماء الأشخاص وأسماء الأماكن وأسماء الجنسيات واللغات والأسابيع والشهور فيبقى الحرف الأول منها بحروف كبيرة، كابتل capital)، ثم إغلاق علامة التنصيص، ثم نقطة، ثم اسم المجلة مترجما (أو مرومن) يكون مكتوبا بشكل مائل والحرف الأول من كل كلمة يكون كبيرا (كابتل capital؛ يستثنى من ذلك أدوات التنكير والتعريف مثل "a" و "an" و "the" وحروف الجر مثل "to" و "of" و "in" وأدوات الربط "and" و "but" و "or" فيبقى الحرف الأول منها بحروف صغيرة، إلا إذا كانوا في بداية اسم المجلة فيكون الحرف الأول منها بحروف كبيرة)، ثم فاصلة، ثم رقم المجلد مكتوبا بشكل عريض، ثم فتح قوس، ثم يكتب رقم العدد، ثم يغلق القوس، علماً أنه لا يوجد مسافة بين رقم المجلد ورقم العدد، ثم فاصلة، ثم رقم أول صفحة للبحث، ثم علامة "-" ثم رقم آخر صفحة للبحث، ثم نقطة، ثم تكتب "[in Arabic]" أدناه مثال على رومنة المرجع العربي:

Al Ahmed, M.A., Al Ali, I.S. and Al Salah, A.M. (2020). Iinjazat jamieat almalik faysal mundh tasisiha 'Achievements of King Faisal University since its foundations'. *The Scientific Journal of King Faisal University: Humanities and Management Sciences*, **13**(2), 213-223. [in Arabic]

في حالة كون المرجع بلغة غير العربية وغير الإنجليزية، وهذه اللغة تستخدم حروف غير إنجليزية، فتتم رومنة العنوان بالطريقة نفسها التي تتم بها رومنة العناوين العربية. ولكن، في حالة كون الدورية بلغة غير العربية وغير الإنجليزية، ولكن هذه اللغة تستخدم الحروف الإنجليزية نفسها، فلا حاجة لرومنة عنوان البحث، ويكتفى بإبقاء العنوان في لغته الأصل ووضع الترجمة في علامة تنصيص. فعلى سبيل المثال، في حالة كون الدورية باللغة

الألمانية، فيبدأ المرجع باسم العائلة للمؤلف الأول، ثم فاصلة، ثم الحرف الأول من الاسم الأول للمؤلف الأول، ثم نقطة، ثم الحرف الأول لاسم الأب للمؤلف الأول، ثم نقطة، ثم فاصلة، ثم اسم العائلة للمؤلف الثاني، ثم فاصلة، ثم الحرف الأول من الاسم الأول للمؤلف الثاني، ثم نقطة، ثم الحرف الأول لاسم الأب للمؤلف الثاني، ثم نقطة، ثم حرف العطف "and" (وليس "&") ثم اسم العائلة للمؤلف الثالث، ثم فاصلة، ثم الحرف الأول من الاسم الأول للمؤلف الثالث، ثم نقطة، ثم الحرف الأول لاسم الأب للمؤلف الثالث، ثم نقطة، ثم فتح قوس، ثم التاريخ بالميلادي، ثم إغلاق القوس، ثم نقطة، ثم عنوان البحث باللغة الألمانية (صمول small)، ثم فتح علامة تنصيص واحدة، ثم عنوان البحث مترجما بحروف صغيرة (صمول small؛ يستثنى من ذلك الكلمة الأولى وأسماء الأشخاص وأسماء الأماكن وأسماء الجنسيات واللغات والأسابيع والشهور فيبقى الحرف الأول منها بحروف كبيرة، كابتل capital)، ثم إغلاق علامة التنصيص، ثم نقطة، ثم اسم المجلة مترجما يكون مكتوبا بشكل مائل والحرف الأول من كل كلمة يكون كبيرا (كابتل capital؛ يستثنى من ذلك أدوات التنكير والتعريف مثل "a" و "an" و "the" وحروف الجر مثل "to" و "of" و "in" وأدوات الربط "and" و "but" و "or" فيبقى الحرف الأول منها بحروف صغيرة، إلا إذا كانوا في بداية اسم المجلة فيكون الحرف الأول منها بحروف كبيرة)، ثم فاصلة، ثم رقم المجلد مكتوبا بشكل عريض، ثم فتح قوس، ثم يكتب رقم العدد، ثم يغلق القوس، علماً أنه لا يوجد مسافة بين رقم المجلد ورقم العدد، ثم رقم أول صفحة للبحث، ثم علامة "-" ثم رقم آخر صفحة للبحث، ثم نقطة، ثم تكتب "[in German]" أدناه مثال على ذلك:

Al Ahmed, M.A., Al Ali, I.S. and Al Salah, A.M. (2020). Erfolge der King Faisal University seit ihrer gründung 'Achievements of King Faisal University since its foundations'. *The Scientific Journal of King Faisal University: Humanities and Management Sciences*, **13**(2), 213-223. [in German]

5. آلية كتابة المؤتمرات والندوات والملتقيات في المراجع (يطلب عملها فقط في حالة قبول الورقة للنشر)

5.1. كتابة المؤتمرات والندوات والملتقيات العربية في قائمة المراجع

يبدأ كل مرجع باسم العائلة للمؤلف الأول، ثم فاصلة، ثم الاسم الأول واسم الأب للمؤلف الأول، ثم فاصلة، ثم اسم العائلة للمؤلف الثاني، ثم فاصلة، ثم الاسم الأول واسم الأب للمؤلف الثاني، ثم حرف العطف "و" ثم اسم العائلة للمؤلف الثالث، ثم فاصلة، ثم الاسم الأول واسم الأب للمؤلف الثالث، ثم نقطة، ثم فتح قوس، ثم التاريخ، ثم إغلاق القوس، ثم نقطة، ثم عنوان البحث، ثم نقطة، ثم يكتب "في:" ثم يكتب اسم المؤتمر بشكل مائل، ثم فاصلة، ثم اسم مكان انعقاد المؤتمر، ثم فاصلة، ثم اسم مدينة المؤتمر، ثم فاصلة، ثم اسم دولة المؤتمر، ثم فاصلة، ثم تاريخ انعقاد المؤتمر، ثم نقطة. (مع مراعاة أن حرف العطف "و" يوضع دائما قبل المؤلف الأخير أيًّا كان عدد المؤلفين). أدناه مثال على ذلك:

الأحمد، محمد عبدالرحمن، العلي، إسماعيل صلاح والصالح، أحمد محمد. (2020). الموهبة في التعليم العالي. في: *الملتقى الوطني الأول لمنسقي الموهوبين، جامعة الملك فيصل*، الأحساء، المملكة العربية السعودية، 03-05/03/2020.

5.2. كتابة المؤتمرات والندوات والملتقيات الإنجليزية في قائمة المراجع

يبدأ كل مرجع باسم العائلة للمؤلف الأول، ثم فاصلة، ثم الحرف الأول من الاسم الأول للمؤلف الأول، ثم نقطة، ثم الحرف الأول لاسم الأب للمؤلف الأول، ثم نقطة، ثم فاصلة، ثم اسم العائلة للمؤلف الثاني، ثم فاصلة، ثم الحرف الأول من الاسم الأول للمؤلف الثاني، ثم نقطة، ثم الحرف الأول لاسم الأب للمؤلف الثاني، ثم نقطة، ثم حرف العطف "and" (وليس "&") ثم اسم العائلة للمؤلف الثالث، ثم فاصلة، ثم الحرف الأول من الاسم الأول للمؤلف الثالث، ثم نقطة، ثم الحرف الأول لاسم الأب للمؤلف الثالث، ثم نقطة. ثم فتح قوس، ثم التاريخ بالميلادي، ثم إغلاق القوس، ثم نقطة، ثم عنوان البحث بحروف صغيرة (صمول small؛ يستثنى من ذلك الكلمة الأولى وأسماء الأشخاص وأسماء الأماكن وأسماء الجنسيات واللغات والأسابيع والشهور فيبقى الحرف الأول منها بحروف كبيرة، كابتل capital)، ثم نقطة، ثم يكتب "In:"، ثم يكتب اسم المؤتمر يكون مكتوبا بشكل مائل والحرف الأول من كل كلمة يكون كبيرا (كابتل capital؛ يستثنى من ذلك أدوات التنكير والتعريف مثل "a" و "an" و "the" وحروف الجر مثل "to" و "of" و "in" وأدوات الربط "and" و "but" و "or" فيبقى الحرف الأول منها بحروف صغيرة، إلا إذا كانوا في بداية اسم المجلة فيكون الحرف الأول منها بحروف كبيرة)، ثم فاصلة، ثم اسم مكان المؤتمر، ثم فاصلة، ثم اسم مدينة المؤتمر، ثم فاصلة، ثم اسم دولة المؤتمر، ثم فاصلة، ثم تاريخ انعقاد المؤتمر، ثم نقطة. أدناه مثال على ذلك:

Al Ahmed, K.A., Al Muhammed, S.F. and Al Saleh, A.F. (2020). Giftedness and creativity. In: *The First National Symposium for the Coordinators of the Gifted*, King Faisal University, Al Ahsa, Saudi Arabia, 03-05/03/2020.

5.3. رومنة/ترجمة المؤتمرات والندوات والملتقيات غير الإنجليزية في قائمة المراجع

يبدأ كل مرجع باسم العائلة للمؤلف الأول، ثم فاصلة، ثم الحرف الأول من الاسم الأول للمؤلف الأول، ثم نقطة، ثم الحرف الأول لاسم الأب للمؤلف الأول، ثم نقطة، ثم فاصلة، ثم اسم العائلة للمؤلف الثاني، ثم فاصلة، ثم الحرف الأول من الاسم الأول للمؤلف الثاني، ثم نقطة، ثم الحرف الأول لاسم الأب للمؤلف الثاني، ثم نقطة، ثم حرف العطف "and" ثم اسم العائلة للمؤلف الثالث، ثم فاصلة، ثم الحرف الأول من الاسم الأول للمؤلف الثالث، ثم نقطة، ثم الحرف الأول لاسم الأب للمؤلف الثالث، ثم نقطة. ثم فتح قوس، ثم التاريخ بالميلادي، ثم إغلاق القوس، ثم نقطة، ثم عنوان البحث (مرومن) بحروف صغيرة (صمول small)، ثم فتح علامة تنصيص واحدة، ثم عنوان البحث مترجما بحروف صغيرة (صمول small؛ يستثنى من ذلك الكلمة الأولى وأسماء الأشخاص وأسماء الأماكن وأسماء الجنسيات واللغات والأسابيع والشهور فيبقى الحرف الأول منها بحروف كبيرة، كابتل capital)، ثم إغلاق علامة التنصيص، ثم نقطة، ثم يكتب "In:"، ثم يكتب اسم المؤتمر مترجما (أو مرومن) يكون مكتوبا بشكل مائل والحرف الأول من كل كلمة يكون كبيرا (كابتل capital؛ يستثنى من ذلك أدوات التنكير والتعريف مثل "a" و "an" و "the" وحروف الجر مثل "to" و "of" و "in" وأدوات الربط "and" و "but" و "or" فيبقى الحرف الأول منها بحروف صغيرة، إلا إذا كانوا في بداية اسم المجلة فيكون الحرف الأول منها بحروف كبيرة)، ثم فاصلة، ثم اسم مكان المؤتمر مترجما (أو مرومن)، ثم فاصلة، ثم يكتب اسم مدينة المؤتمر بالإنجليزي، ثم فاصلة، ثم اسم دولة المؤتمر بالإنجليزي، ثم فاصلة، ثم تاريخ انعقاد المؤتمر، ثم نقطة، ثم يكتب "[in Arabic]" أدناه مثال على رومنة المرجع العربي:

Al Ahmed, K.A., Al Muhammed, S.F. and Al Saleh, A.F. (2020). Al'iibdae fi altaelim aleali 'Creativity in higher education'. In: *The First National Symposium for the Coordinators of the Gifted*, King Faisal University, Al Ahsa, Saudi Arabia, 03-05/03/2020. [in Arabic]

في حالة كون المرجع بلغة غير العربية وغير الإنجليزية، وهذه اللغة تستخدم حروف غير إنجليزية، فتتم رومنة العنوان بالطريقة نفسها التي تتم بها رومنة العناوين العربية. أما في حالة كون المرجع بلغة غير العربية وغير الإنجليزية، ولكن هذه اللغة تستخدم الحروف الإنجليزية، فلا حاجة لرومنة عنوان البحث، ويكتفى بإبقاء العنوان في لغته الأصل ووضع الترجمة في علامة تنصيص. فعلى سبيل المثال، في حالة كون المرجع باللغة الفرنسية، فيبدأ المرجع باسم العائلة للمؤلف الأول، ثم فاصلة، ثم الحرف الأول من الاسم الأول للمؤلف الأول، ثم نقطة، ثم الحرف الأول لاسم الأب للمؤلف الأول، ثم نقطة، ثم فاصلة، ثم اسم العائلة للمؤلف الثاني، ثم فاصلة، ثم الحرف الأول من الاسم الأول للمؤلف الثاني، ثم نقطة، ثم الحرف الأول لاسم الأب للمؤلف الثاني، ثم نقطة، ثم حرف العطف "and" ثم اسم العائلة للمؤلف الثالث، ثم فاصلة، ثم الحرف الأول من الاسم الأول للمؤلف الثالث، ثم نقطة، ثم الحرف الأول لاسم الأب للمؤلف

الثالث، ثم نقطة. ثم فتح قوس، ثم التاريخ بالميلادي، ثم إغلاق القوس، ثم نقطة، ثم عنوان البحث باللغة الفرنسية (صمول small)، ثم فتح علامة تنصيص واحدة، ثم عنوان البحث مترجما بحروف صغيرة (صمول small؛ يستثنى من ذلك الكلمة الأولى وأسماء الأشخاص وأسماء الأماكن وأسماء الجنسيات واللغات والأسابيع والشهور فيبقى الحرف الأول منها بحروف كبيرة، كابتل capital)، ثم إغلاق علامة التنصيص، ثم نقطة، ثم يكتب "In:"، ثم يكتب اسم المؤتمر مترجما يكون مكتوبا بشكل مائل والحرف الأول من كل كلمة يكون كبيرا (كابتل capital؛ يستثنى من ذلك أدوات التنكير والتعريف مثل "a" و "an" و "the" وحروف الجر مثل "to" و "of" و "in" وأدوات الربط "and" و "but" و "or" فيبقى الحرف الأول منها بحروف صغيرة، إلا إذا كانوا في بداية اسم المجلة فيكون الحرف الأول منها بحروف كبيرة)، ثم فاصلة، ثم اسم مكان المؤتمر مترجما، ثم فاصلة، ثم يكتب اسم مدينة المؤتمر بالإنجليزي، ثم فاصلة، ثم اسم دولة المؤتمر بالإنجليزي، ثم فاصلة، ثم تاريخ انعقاد المؤتمر، ثم نقطة، ثم يكتب "[in French]". أدناه مثال على رومنة المرجع الفرنسي:

Al Ahmed, K.A., Al Muhammed, S.F. and Al Saleh, A.F. (2020). Créativité dans l'enseignement supérieur 'Creativity in higher education'. In: *The First National Symposium for the Coordinators of the Gifted*, King Faisal University, Al Ahsa, Saudi Arabia, 03-05/03/2020. [in French]

6. آلية كتابة الكتب في قائمة المراجع (يطلب عملها فقط في حالة قبول الورقة للنشر)

ملاحظات:

- إذا كانت طبعة الكتاب هي الطبعة الأولى، فلا يكتب أي شيء بخصوص رقم الطبعة.
- تصاغ مراجع التقارير والدراسات الصادرة عن وزارات ومؤسسات حكومية وغير حكومية بالطريقة نفسها التي تصاغ بها الكتب.

6.1. كتابة الكتب العربية في قائمة المراجع

يبدأ كل مرجع باسم العائلة للمؤلف الأول، ثم فاصلة، ثم الاسم الأول واسم الأب للمؤلف الأول، ثم فاصلة، ثم اسم العائلة للمؤلف الثاني، ثم فاصلة، ثم الاسم الأول واسم الأب للمؤلف الثاني، ثم حرف العطف "و" ثم اسم العائلة للمؤلف الثالث، ثم فاصلة، ثم الاسم الأول واسم الأب للمؤلف الثالث، ثم نقطة، ثم فتح قوس، ثم التاريخ، ثم إغلاق القوس، ثم نقطة، ثم عنوان الكتاب بخط مائل، ثم نقطة، ثم اسم مدينة الناشر، ثم فاصلة، ثم اسم دولة الناشر، ثم نقطتين رأسيتين، ثم اسم الناشر. (مع مراعاة أن حرف العطف "و" يوضع دائما قبل المؤلف الأخير أيًّا كان عدد المؤلفين). أدناه مثال على ذلك:

الأحمد، محمد عبدالرحمن، العلي، إسماعيل صلاح والصالح، أحمد محمد. (2020). *إنجازات جامعة الملك فيصل منذ تأسيسها*. السعودية: مكتبة جرير.

في حالة وجود رقم طبعة، فيكتب التالي:

الأحمد، محمد عبدالرحمن، العلي، إسماعيل صلاح والصالح، أحمد محمد. (2020). *إنجازات جامعة الملك فيصل منذ تأسيسها*. الطبعة الثانية. الرياض، السعودية: مكتبة جرير.

في حالة كون الكتاب مترجمًا، فيكتب بعد اسم المؤلف: "ترجمة: اسم العائلة، الاسم الأول اسم الأب". أدناه مثال على ذلك:

وايت، جولي. ترجمة: الأحمد، محمد عبدالرحمن، العلي، إسماعيل صلاح والصالح، أحمد محمد. (2020). *إنجازات جامعة الملك فيصل منذ تأسيسها*. الطبعة الثانية. الرياض، السعودية: مكتبة جرير.

في حالة كون الكتاب محققاً، فيكتب بعد اسم المؤلف: "تحقيق: اسم العائلة، الاسم الأول اسم الأب". أدناه مثال على ذلك:

الخالد، محمد. تحقيق: الأحمد، محمد عبدالرحمن. (2020). *إنجازات جامعة الملك فيصل منذ تأسيسها*. الطبعة الثانية. الرياض، السعودية: مكتبة جرير.

6.2. كتابة الكتب الإنجليزية في قائمة المراجع

يبدأ كل مرجع باسم العائلة للمؤلف الأول، ثم فاصلة، ثم الحرف الأول من الاسم الأول للمؤلف الأول، ثم نقطة، ثم الحرف الأول لاسم الأب للمؤلف الأول، ثم نقطة، ثم فاصلة، ثم اسم العائلة للمؤلف الثاني، ثم فاصلة، ثم الحرف الأول من الاسم الأول للمؤلف الثاني، ثم نقطة، ثم الحرف الأول لاسم الأب للمؤلف الثاني، ثم نقطة، ثم حرف العطف "and" (وليس "&") ثم اسم العائلة للمؤلف الثالث، ثم فاصلة، ثم الحرف الأول من الاسم الأول للمؤلف الثالث، ثم نقطة، ثم الحرف الأول لاسم الأب للمؤلف الثالث، ثم نقطة، ثم فتح قوس، ثم التاريخ بالميلادي، ثم إغلاق القوس، ثم نقطة، ثم عنوان الكتاب بحروف مائلة والحرف الأول من كل كلمة يكون كبيرا (كابتل capital؛ يستثنى من ذلك أدوات التنكير والتعريف مثل "a" و "an" و "the" وحروف الجر مثل "to" و "of" و "in" وأدوات الربط "and" و "but" و "or" فيبقى الحرف الأول منها بحروف صغيرة، إلا إذا كانوا في بداية اسم المجلة فيكون الحرف الأول منها بحروف كبيرة)، ثم نقطة، ثم اسم مدينة الناشر، ثم فاصلة، ثم اسم دولة الناشر، ثم نقطتين رأسيتين، ثم اسم الناشر، ثم نقطة. أدناه مثال على ذلك:

Al Ahmed, K.A., Al Muhammed, S.F. and Al Saleh, A.F. (2020). *The History of Agriculture in Al Ahsa*. Saudi Arabia: Jarir Bookstore.

في حالة وجود رقم طبعة، فيكتب التالي:

Al Ahmed, K.A., Al Muhammed, S.F. and Al Saleh, A.F. (2020). *The History of Agriculture in Al Ahsa*. 2nd edition. Riyadh, Saudi Arabia: Jarir Bookstore.

6.3. رومنة/ترجمة الكتب غير الإنجليزية في قائمة المراجع

ملاحظة: عند رومنة/ترجمة مراجع الكتب العربية فإنه لا يكتب اسم المحقق.

يبدأ كل مرجع باسم العائلة للمؤلف الأول، ثم فاصلة، ثم الحرف الأول من الاسم الأول للمؤلف الأول، ثم نقطة، ثم الحرف الأول لاسم الأب للمؤلف الأول، ثم نقطة، ثم فاصلة، ثم اسم العائلة للمؤلف الثاني، ثم فاصلة، ثم الحرف الأول من الاسم الأول للمؤلف الثاني، ثم نقطة، ثم الحرف الأول لاسم الأب للمؤلف الثاني، ثم نقطة، ثم حرف العطف "and" (وليس "&") ثم اسم العائلة للمؤلف الثالث، ثم فاصلة، ثم الحرف الأول من الاسم الأول للمؤلف الثالث، ثم نقطة، ثم الحرف الأول لاسم الأب للمؤلف الثالث، ثم نقطة، ثم فتح قوس، ثم التاريخ بالميلادي، ثم إغلاق القوس، ثم نقطة، ثم عنوان الكتاب (مرومن) بحروف مائلة والحرف الأول من كل كلمة يكون كبيرا (كابتل capital)، ثم فتح علامة تنصيص واحدة، ثم عنوان الكتاب مترجما والحرف الأول من كل كلمة يكون كبيرا (كابتل capital؛ يستثنى من ذلك أدوات التنكير والتعريف مثل "a" و "an" و "the" وحروف الجر مثل "to" و "of" و "in" وأدوات الربط "and" و "but" و "or" فيبقى الحرف الأول منها بحروف صغيرة، إلا إذا كانوا في بداية اسم المجلة فيكون الحرف الأول منها بحروف كبيرة) والكلمة غير مائلة، ثم إغلاق علامة التنصيص، ثم نقطة، ثم اسم مدينة الناشر مترجمة، ثم فاصلة، ثم اسم دولة الناشر مترجمة، ثم نقطتين رأسيتين، ثم اسم الناشر مترجما (أو مرومن)، ثم نقطة، ثم تكتب "[in Arabic]" أدناه مثال على رومنة المرجع العربي:

Al Ahmed, M.A., Al Ali, I.S. and Al Salah, A.M. (2020). *Iinjazat Jamieat Almalik Faysal Mundh Tasisiha* 'Achievements of King Faisal University since its Foundations'. Riyadh, Saudi Arabia: Jarir Bookstore. [in Arabic]

في حالة كون الكتاب بلغة غير العربية وغير الإنجليزية، ولكن هذه اللغة تستخدم حروف غير إنجليزية، فتتم رومنة العنوان بالطريقة نفسها التي تتم بها رومنة العناوين العربية. ولكن، في حالة كون الكتاب بلغة غير العربية وغير الإنجليزية، ولكن هذه اللغة تستخدم الحروف الإنجليزية

نفسها، فلا حاجة لرومنة عنوان الكتاب، ويكتفى بإبقاء العنوان في لغته الأصل ووضع الترجمة في علامة تنصيص. فعلى سبيل المثال، في حالة كون الكتاب باللغة الألمانية، فيبدأ المرجع باسم العائلة للمؤلف الأول، ثم فاصلة، ثم الحرف الأول من الاسم الأول للمؤلف الأول، ثم نقطة، ثم الحرف الأول لاسم الأب للمؤلف الأول، ثم نقطة، ثم فاصلة، ثم اسم العائلة للمؤلف الثاني، ثم فاصلة، ثم الحرف الأول من الاسم الأول للمؤلف الثاني، ثم نقطة، ثم الحرف الأول لاسم الأب للمؤلف الثاني، ثم نقطة، ثم حرف العطف "and" (وليس "&") ثم اسم العائلة للمؤلف الثالث، ثم فاصلة، ثم الحرف الأول من الاسم الأول للمؤلف الثالث، ثم نقطة، ثم الحرف الأول لاسم الأب للمؤلف الثالث، ثم نقطة، ثم فتح قوس، ثم التاريخ بالميلادي، ثم إغلاق القوس، ثم نقطة، ثم عنوان الكتاب باللغة الألمانية بحروف مائلة والحرف الأول من كل كلمة يكون كبيرا (كابتل capital)، ثم فتح علامة تنصيص واحدة، ثم عنوان الكتاب مترجما والحرف الأول من كل كلمة يكون كبيرا (كابتل capital؛ يستثنى من ذلك أدوات التنكير والتعريف مثل "a" و "an" و "the" وحروف الجر مثل "to" و "of" و "in" وأدوات الربط "and" و "but" و "or" فيبقى الحرف الأول منها بحروف صغيرة، إلا إذا كانوا في بداية اسم المجلة فيكون الحرف الأول منها بحروف كبيرة) والكلمة غير مائلة، ثم إغلاق علامة التنصيص، ثم نقطة، ثم اسم مدينة الناشر مترجمة للإنجليزي، ثم فاصلة، ثم اسم دولة الناشر مترجمة للإنجليزي، ثم نقطتين رأسيتين، ثم اسم الناشر مترجما للإنجليزي، ثم نقطة، ثم تكتب "[in German]" أدناه مثال على رومنة المرجع الألماني:

Al Ahmed, M.A., Al Ali, I.S. and Al Salah, A.M. (2020). *Erfolge der King Faisal University seit ihrer Gründung* 'Achievements of King Faisal University since its Foundations'. Riyadh, Saudi Arabia: Jarir Bookstore. [in German]

7. آلية كتابة فصل من كتاب في قائمة المراجع (يطلب عملها فقط في حالة قبول الورقة للنشر)

7.1. كتابة فصل في كتاب عربي في قائمة المراجع

يبدأ كل مرجع باسم العائلة للمؤلف الأول، ثم فاصلة، ثم الاسم الأول واسم الأب للمؤلف الأول، ثم فاصلة، ثم اسم العائلة للمؤلف الثاني، ثم فاصلة، ثم الاسم الأول واسم الأب للمؤلف الثاني، ثم حرف العطف "و" ثم اسم العائلة للمؤلف الثالث، ثم فاصلة، ثم الاسم الأول واسم الأب للمؤلف الثالث، ثم نقطة، ثم فتح قوس، ثم التاريخ، ثم إغلاق القوس، ثم نقطة، ثم عنوان الفصل، ثم نقطة، ثم يكتب "في:" ثم يكتب الاسم الأول، ثم اسم الأب، ثم اسم العائلة للمؤلف الأول، ثم فاصلة، ثم يكتب الاسم الأول، ثم اسم الأب، ثم اسم العائلة للمؤلف الثاني، ثم حرف العطف "و"، ثم يكتب الاسم الأول، ثم اسم الأب، ثم اسم العائلة للمؤلف الثالث، ثم يفتح قوس ويكتب "محررون" (أو محرر إذا كان مفردا)، ثم يغلق القوس، ثم اسم الكتاب بخط مائل، ثم نقطة، ثم اسم مدينة الناشر، ثم فاصلة، ثم اسم دولة الناشر، ثم نقطتين رأسيتين، ثم اسم الناشر. (مع مراعاة أن حرف العطف "و" يوضع دائما قبل المؤلف الأخير أيًا كان عدد المؤلفين). أدناه مثال على ذلك:

الأحمد، محمد عبدالرحمن، العلي، إسماعيل صلاح والصالح، أحمد محمد. (2020). الموهبة في التعليم العالي. في: محمد الصالح، إبراهيم العبدالرحمن وصلاح الخالد (محررون) *الإبداع في العالم العربي*. الرياض، السعودية: مكتبة العبيكان.

7.2. كتابة فصل في كتاب إنجليزي في قائمة المراجع

يبدأ كل مرجع باسم العائلة للمؤلف الأول، ثم فاصلة، ثم الحرف الأول من الاسم الأول للمؤلف الأول، ثم نقطة، ثم الحرف الأول لاسم الأب للمؤلف الأول، ثم نقطة، ثم فاصلة، ثم اسم العائلة للمؤلف الثاني، ثم فاصلة، ثم الحرف الأول من الاسم الأول للمؤلف الثاني، ثم نقطة، ثم الحرف الأول لاسم الأب للمؤلف الثاني، ثم نقطة، ثم حرف العطف "and" (وليس "&") ثم اسم العائلة للمؤلف الثالث، ثم فاصلة، ثم الحرف الأول من الاسم الأول للمؤلف الثالث، ثم نقطة، ثم الحرف الأول لاسم الأب للمؤلف الثالث، ثم نقطة، ثم فتح قوس، ثم التاريخ بالميلادي، ثم إغلاق القوس، ثم نقطة، ثم عنوان الفصل بحروف صغيرة (صمول small؛ يستثنى من ذلك الكلمة الأولى وأسماء الأشخاص وأسماء الأماكن وأسماء الجنسيات واللغات والأسابيع والشهور فيبقى الحرف الأول منها بحروف كبيرة، كابتل capital)، ثم نقطة، ثم يكتب "In:"، ثم يكتب الحرف الأول من الاسم الأول للمؤلف الأول، ثم نقطة، ثم الحرف الأول لاسم الأب للمؤلف الأول، ثم نقطة، ثم اسم العائلة كاملاً للمؤلف الأول، ، ثم فاصلة، ثم يكتب الحرف الأول من الاسم الأول للمؤلف الثاني، ثم نقطة، ثم الحرف الأول لاسم الأب للمؤلف الثاني، ثم نقطة، ثم اسم العائلة كاملاً للمؤلف الثاني، ثم حرف العطف "and" (وليس "&")، ثم يكتب الحرف الأول من الاسم الأول للمؤلف الثالث، ثم نقطة، ثم الحرف الأول لاسم الأب للمؤلف الثالث، ثم نقطة، ثم اسم العائلة كاملاً للمؤلف الثالث، ثم يفتح قوس ويكتب "eds." (أو "ed." إذا كان مفردا)، ثم يغلق القوس، ثم اسم الكتاب بخط مائل والحرف الأول من كل كلمة يكون كبيرا (كابتل capital؛ يستثنى من ذلك أدوات التنكير والتعريف مثل "a" و "an" و "the" وحروف الجر مثل "to" و "of" و "in" وأدوات الربط "and" و "but" و "or" فيبقى الحرف الأول منها بحروف صغيرة، إلا إذا كانوا في بداية اسم المجلة فيكون الحرف الأول منها بحروف كبيرة)، ثم نقطة، ثم اسم مدينة الناشر، ثم فاصلة، ثم اسم دولة الناشر، ثم نقطتين رأسيتين، ثم اسم الناشر. أدناه مثال على ذلك:

Al Ahmed, K.A., Al Muhammed, S.F. and Al Saleh, A.F. (2020). Giftedness and creativity. In: A.E. Al Ibrahim, A.L. Al Salim and R.E. Al Rashid (eds.) *Creativity in the Arab World*. Riyadh, Saudi Arabia: Obeikan Bookstore.

7.3. رومنة/ترجمة فصل في كتاب غير إنجليزي في قائمة المراجع

يبدأ كل مرجع باسم العائلة للمؤلف الأول، ثم فاصلة، ثم الحرف الأول من الاسم الأول للمؤلف الأول، ثم نقطة، ثم الحرف الأول لاسم الأب للمؤلف الأول، ثم نقطة، ثم فاصلة، ثم اسم العائلة للمؤلف الثاني، ثم فاصلة، ثم الحرف الأول من الاسم الأول للمؤلف الثاني، ثم نقطة، ثم الحرف الأول لاسم الأب للمؤلف الثاني، ثم نقطة، ثم حرف العطف "and" (وليس "&") ثم اسم العائلة للمؤلف الثالث، ثم فاصلة، ثم الحرف الأول من الاسم الأول للمؤلف الثالث، ثم نقطة، ثم الحرف الأول لاسم الأب للمؤلف الثالث، ثم نقطة، ثم فتح قوس، ثم التاريخ بالميلادي، ثم إغلاق القوس، ثم نقطة، ثم عنوان الفصل (مرومن) بحروف صغيرة (صمول small)، ثم فتح علامة تنصيص واحدة، ثم عنوان الفصل مترجما بحروف صغيرة (صمول small؛ يستثنى من ذلك الكلمة الأولى وأسماء الأشخاص وأسماء الأماكن وأسماء الجنسيات واللغات والأسابيع والشهور فيبقى الحرف الأول منها بحروف كبيرة، كابتل capital)، ثم إغلاق علامة التنصيص، ثم نقطة، ثم يكتب "In:"، ثم يكتب الحرف الأول من الاسم الأول للمؤلف الأول، ثم نقطة، ثم الحرف الأول لاسم الأب للمؤلف الأول، ثم نقطة، ثم اسم العائلة كاملاً للمؤلف الأول، ، ثم فاصلة، ثم يكتب الحرف الأول من الاسم الأول للمؤلف الثاني، ثم نقطة، ثم الحرف الأول لاسم الأب للمؤلف الثاني، ثم نقطة، ثم اسم العائلة كاملاً للمؤلف الثاني، ثم حرف العطف "and" (وليس "&")، ثم يكتب الحرف الأول من الاسم الأول للمؤلف الثالث، ثم نقطة، ثم الحرف الأول لاسم الأب للمؤلف الثالث، ثم نقطة، ثم اسم العائلة كاملاً للمؤلف الثالث، ثم يفتح قوس ويكتب "eds." (أو "ed." إذا كان مفردا)، ثم يغلق القوس، ثم اسم الكتاب (مرومن) بخط مائل والحرف الأول من كل كلمة يكون كبيرا (كابتل capital)، ثم فتح علامة تنصيص واحدة، ثم عنوان الكتاب مترجما والحرف الأول من كل كلمة يكون كبيرا (كابتل capital؛ يستثنى من ذلك أدوات التنكير والتعريف مثل "a" و "an" و "the" وحروف الجر مثل "to" و "of" و "in" وأدوات الربط "and" و "but" و "or" فيبقى الحرف الأول منها بحروف صغيرة، إلا إذا كانوا في بداية اسم المجلة فيكون الحرف الأول منها بحروف كبيرة)، ثم نقطة، ثم اسم مدينة الناشر مترجمة، ثم فاصلة، ثم اسم دولة الناشر مترجما، ثم نقطتين رأسيتين، ثم اسم الناشر مترجما (أو مرومن)، ثم نقطة، ثم تكتب "[in Arabic]" أدناه مثال على رومنة المرجع العربي:

Al Ahmed, K.A., Al Muhammed, S.F. and Al Saleh, A.F. (2020). Al'iibdae fi altaelim aleali 'Creativity in higher education'. In: M. Al Saleh, I. Al

Abdulrahman and S. Al Khalid (eds.) *Al'iibdae Fi Alealam Alearabii* 'Creativity in the Arab World'. Riyadh, Saudi Arabia: Obeikan Bookstore. [in Arabic]

في حالة كون الفصل بلغة غير العربية وغير الإنجليزية، ولكن هذه اللغة تستخدم حروف غير إنجليزية، فتتم رومنة العنوان بالطريقة نفسها التي تتم بها رومنة العناوين العربية. ولكن، في حالة كون الفصل بلغة غير العربية وغير الإنجليزية، ولكن هذه اللغة تستخدم الحروف الإنجليزية نفسها، فلا حاجة لرومنة عنوان الفصل والكتاب، ويكتفى بإبقاء العنوان في لغته الأصل ووضع الترجمة في علامة تنصيص. فعلى سبيل المثال، في حالة كون الفصل باللغة الألمانية، فيبدأ المرجع باسم العائلة للمؤلف الأول، ثم فاصلة، ثم الحرف الأول من الاسم الأول للمؤلف الأول، ثم نقطة، ثم الحرف الأول لاسم الأب للمؤلف الأول، ثم نقطة، ثم فاصلة، ثم اسم العائلة للمؤلف الثاني، ثم فاصلة، ثم الحرف الأول من الاسم الأول للمؤلف الثاني، ثم نقطة، ثم الحرف الأول لاسم الأب للمؤلف الثاني، ثم نقطة، ثم حرف العطف "and" (وليس "&") ثم اسم العائلة للمؤلف الثالث، ثم فاصلة، ثم الحرف الأول من الاسم الأول للمؤلف الثالث، ثم نقطة، ثم الحرف الأول لاسم الأب للمؤلف الثالث، ثم نقطة، ثم فتح قوس، ثم التاريخ بالميلادي، ثم إغلاق القوس، ثم نقطة، ثم عنوان الفصل باللغة الألمانية بحروف صغيرة (صمول small)، ثم فتح علامة تنصيص واحدة، ثم عنوان الفصل مترجما للإنجليزية بحروف صغيرة (صمول small؛ يستثنى من ذلك الكلمة الأولى وأسماء الأشخاص وأسماء الأماكن وأسماء الجنسيات واللغات والأسابيع والشهور فيبقى الحرف الأول منها بحروف كبيرة، كابتل capital)، ثم إغلاق علامة التنصيص، ثم نقطة، ثم يكتب "In:"، ثم يكتب الحرف الأول من الاسم الأول للمؤلف الأول، ثم نقطة، ثم الحرف الأول لاسم الأب للمؤلف الأول، ثم نقطة، ثم اسم العائلة كاملاً للمؤلف الأول، ، ثم فاصلة، ثم يكتب الحرف الأول من الاسم الأول للمؤلف الثاني، ثم نقطة، ثم الحرف الأول لاسم الأب للمؤلف الثاني، ثم نقطة، ثم اسم العائلة كاملاً للمؤلف الثاني، ثم حرف العطف "and" (وليس "&")، ثم يكتب الحرف الأول من الاسم الأول للمؤلف الثالث، ثم نقطة، ثم الحرف الأول لاسم الأب للمؤلف الثالث، ثم نقطة، ثم اسم العائلة كاملاً للمؤلف الثالث، ثم يفتح قوس ويكتب ".eds" (أو ".ed" إذا كان مفردا)، ثم يغلق القوس، ثم اسم الكتاب باللغة الألمانية بخط مائل والحرف الأول من كل كلمة يكون كبيرا (كابتل capital)، ثم فتح علامة تنصيص واحدة، ثم عنوان الكتاب مترجما للإنجليزية والحرف الأول من كل كلمة يكون كبيرا (كابتل capital؛ يستثنى من ذلك أدوات التنكير والتعريف مثل "a" و "an" و "the" وحروف الجر مثل "to" و "of" و "in" وأدوات الربط "and" و "but" و "or" فيبقى الحرف الأول منها بحروف صغيرة، إلا إذا كانوا في بداية اسم المجلة فيكون الحرف الأول منها بحروف كبيرة)، ثم نقطة، ثم اسم مدينة الناشر مترجمة للإنجليزية، ثم فاصلة، ثم اسم دولة الناشر مترجما للإنجليزية، ثم نقطتين رأسيتين، ثم اسم الناشر مترجما للإنجليزية، ثم نقطة، ثم تكتب "[in German]" أدناه مثال على رومنة المرجع الألماني:

Al Ahmed, K.A., Al Muhammed, S.F. and Al Saleh, A.F. (2020). Kreativität in der hochschulbildung 'Creativity in higher education'. In: M. Al Saleh, I. Al Abdulrahman and S. Al Khalid (eds.) *Kreativität in der Arabischen Welt* 'Creativity in the Arab World'. Riyadh, Saudi Arabia: Obeikan Bookstore. [in German]

8. آلية كتابة رسائل الماجستير والدكتوراه في قائمة المراجع (يطلب عملها فقط في حالة قبول الورقة للنشر)

8.1. كتابة رسائل الماجستير والدكتوراه العربية في قائمة المراجع

يبدأ كل مرجع باسم العائلة للمؤلف، ثم فاصلة، ثم الاسم الأول واسم الأب للمؤلف، ثم نقطة، ثم فتح قوس، ثم التاريخ، ثم إغلاق القوس، ثم نقطة، ثم عنوان الرسالة بخط مائل، ثم نقطة، ثم يكتب "رسالة ماجستير" أو "رسالة دكتوراه"، ثم فاصلة، ثم اسم الجامعة، ثم فاصلة، ثم اسم المدينة، ثم فاصلة، ثم اسم الدولة، ثم نقطة. أدناه مثال على ذلك:

الأحمد، محمد عبدالرحمن. (2020). *تأملات في الإبداع*. رسالة دكتوراه، جامعة الملك فيصل، الأحساء، السعودية.

8.2. كتابة رسائل الماجستير والدكتوراه الإنجليزية في قائمة المراجع

يبدأ كل مرجع باسم العائلة للمؤلف، ثم فاصلة، ثم الحرف الأول من الاسم الأول للمؤلف، ثم نقطة، ثم الحرف الأول لاسم الأب للمؤلف، ثم نقطة، ثم فتح قوس، ثم التاريخ بالميلادي، ثم إغلاق القوس، ثم نقطة، ثم عنوان الرسالة بحروف مائلة والحرف الأول من كل كلمة يكون كبيرا (كابتل capital؛ يستثنى من ذلك أدوات التنكير والتعريف مثل "a" و "an" و "the" وحروف الجر مثل "to" و "of" و "in" وأدوات الربط "and" و "but" و "or" فيبقى الحرف الأول منها بحروف صغيرة، إلا إذا كانوا في بداية اسم المجلة فيكون الحرف الأول منها بحروف كبيرة)، ثم نقطة، ثم يكتب "Master's Dissertation" إذا كانت رسالة ماجستير أو "PhD Thesis" إذا كانت رسالة دكتوراه، ثم فاصلة، ثم اسم الجامعة، ثم فاصلة، ثم اسم المدينة، ثم فاصلة، ثم اسم الدولة، ثم نقطة. أدناه مثال على ذلك:

Al Ahmed, K.A. (2020). *The History of Agriculture in Al Ahsa*. PhD Thesis, King Faisal University, Al Ahsa, Saudi Arabia.

8.3. رومنة/ترجمة رسائل الماجستير والدكتوراه غير الإنجليزية في قائمة المراجع

يبدأ كل مرجع باسم العائلة للمؤلف الأول، ثم فاصلة، ثم الحرف الأول من الاسم الأول للمؤلف الأول، ثم نقطة، ثم الحرف الأول لاسم الأب للمؤلف الأول، ثم نقطة، ثم فتح قوس، ثم التاريخ بالميلادي، ثم إغلاق القوس، ثم نقطة، ثم عنوان الرسالة (مرومن) بحروف مائلة والحرف الأول من كل كلمة يكون كبيرا (كابتل capital)، ثم فتح علامة تنصيص واحدة، ثم عنوان الرسالة مترجما والحرف الأول من كل كلمة يكون كبيرا (كابتل capital؛ يستثنى من ذلك أدوات التنكير والتعريف مثل "a" و "an" و "the" وحروف الجر مثل "to" و "of" و "in" وأدوات الربط "and" و "but" و "or" فيبقى الحرف الأول منها بحروف صغيرة، إلا إذا كانوا في بداية اسم المجلة فيكون الحرف الأول منها بحروف كبيرة) والكلمة غير مائلة، ثم إغلاق علامة التنصيص، ثم نقطة، ثم يكتب "Master's Dissertation" إذا كانت رسالة ماجستير أو "PhD Thesis" إذا كانت رسالة دكتوراه، ثم فاصلة، ثم اسم الجامعة، ثم فاصلة، ثم اسم المدينة، ثم فاصلة، ثم اسم الدولة، ثم نقطة، ثم تكتب "[in Arabic]" أدناه مثال على رومنة المرجع العربي:

Al Ahmed, M.A. (2020). *Tamalat Fi Al'iibdae* 'Reflections on Creativity'. PhD Thesis, King Faisal University, Al Ahsa, Saudi Arabia. [in Arabic]

في حالة كون الرسالة بلغة غير العربية وغير الإنجليزية، ولكن هذه اللغة تستخدم حروف غير إنجليزية، فتتم رومنة العنوان بالطريقة نفسها التي تتم بها رومنة العناوين العربية. ولكن، في حالة كون الرسالة بلغة غير العربية وغير الإنجليزية، ولكن هذه اللغة تستخدم الحروف الإنجليزية نفسها، فلا حاجة لرومنة عنوان الرسالة، ويكتفى بإبقاء العنوان في لغته الأصل ووضع الترجمة في علامة تنصيص. فعلى سبيل المثال، في حالة كون الرسالة باللغة الألمانية، فيبدأ المرجع باسم العائلة للمؤلف الأول، ثم فاصلة، ثم الحرف الأول من الاسم الأول للمؤلف الأول، ثم نقطة، ثم الحرف الأول لاسم الأب للمؤلف الأول، ثم نقطة، ثم فتح قوس، ثم التاريخ بالميلادي، ثم إغلاق القوس، ثم نقطة، ثم عنوان الرسالة باللغة الألمانية بحروف مائلة والحرف الأول من كل كلمة يكون كبيرا (كابتل capital)، ثم فتح علامة تنصيص واحدة، ثم عنوان الرسالة مترجما والحرف الأول من كل كلمة يكون كبيرا (كابتل capital؛ يستثنى من ذلك أدوات التنكير والتعريف مثل "a" و "an" و "the" وحروف الجر مثل "to" و "of" و "in" وأدوات الربط "and" و "but" و "or" فيبقى الحرف الأول منها بحروف صغيرة، إلا إذا كانوا في بداية اسم المجلة فيكون الحرف الأول منها بحروف كبيرة) والكلمة غير مائلة، ثم إغلاق علامة التنصيص، ثم نقطة، ثم يكتب "Master's Dissertation" إذا كانت رسالة ماجستير أو "PhD Thesis" إذا كانت رسالة دكتوراه، ثم فاصلة، ثم اسم الجامعة بالإنجليزي، ثم فاصلة، ثم اسم المدينة بالإنجليزي، ثم فاصلة، ثم اسم الدولة بالإنجليزي، ثم نقطة،

ثم تكتب "[in German]" أدناه مثال على ذلك:

Al Ahmed, M.A. (2020). *Überlegungen zur Kreativität* 'Reflections on Creativity'. PhD Thesis, King Faisal University, Al Ahsa, Saudi Arabia. [in German]

9. آلية كتابة موقع إلكتروني في قائمة المراجع (يطلب عملها فقط في حالة قبول الورقة للنشر)

ملاحظة: المراجع المأخوذة من شبكة المعلومات يلزم فيها كتابة العنوان التفصيلي الذي يفتح الصفحة الخاصة بالمرجع مباشرة وليست الصفحة العامة للموقع. يجب ألا يزيد عدد حروف الرابط عن 120 حرف.

9.1. كتابة موقع إلكتروني عربي في قائمة المراجع

يبدأ كل مرجع باسم العائلة للمؤلف الأول، ثم فاصلة، ثم الاسم الأول واسم الأب للمؤلف الأول، ثم فاصلة، ثم اسم العائلة للمؤلف الثاني، ثم فاصلة، ثم الاسم الأول واسم الأب للمؤلف الثاني، ثم حرف العطف "و" ثم اسم العائلة للمؤلف الثالث، ثم فاصلة، ثم الاسم الأول واسم الأب للمؤلف الثالث، ثم نقطة، ثم فتح قوس، ثم التاريخ، ثم إغلاق القوس، ثم نقطة، ثم العنوان بخط مائل، ثم نقطة، ثم يكتب "متوفر بموقع:" ثم يدرج الرابط، وبعد الرابط يفتح قوس ويكتب "تاريخ الاسترجاع:" ثم يدرج التاريخ على هذه الصيغة "2020/07/27"، ثم يغلق القوس. (مع مراعاة أن حرف العطف "و" يوضع دائما قبل المؤلف الأخير أيًّا كان عدد المؤلفين). أدناه مثال على ذلك:

الأحمد، محمد عبدالرحمن، العلي، إسماعيل صلاح والصالح، أحمد محمد. (2020). *إنجازات جامعة الملك فيصل منذ تأسيسها*. متوفر بموقع: https://www.kfu.edu.sa/ar/Departments/Sjournal/Pages/home.aspx (تاريخ الاسترجاع: 2020/07/27)

9.2. كتابة موقع إلكتروني إنجليزي في قائمة المراجع

يبدأ كل مرجع باسم العائلة للمؤلف الأول، ثم فاصلة، ثم الحرف الأول من الاسم الأول للمؤلف الأول، ثم نقطة، ثم الحرف الأول لاسم الأب للمؤلف الأول، ثم نقطة، ثم فاصلة، ثم اسم العائلة للمؤلف الثاني، ثم فاصلة، ثم الحرف الأول من الاسم الأول للمؤلف الثاني، ثم نقطة، ثم الحرف الأول لاسم الأب للمؤلف الثاني، ثم نقطة، ثم حرف العطف "and" (وليس "&") ثم اسم العائلة للمؤلف الثالث، ثم فاصلة، ثم الحرف الأول من الاسم الأول للمؤلف الثالث، ثم نقطة، ثم الحرف الأول لاسم الأب للمؤلف الثالث، ثم نقطة، ثم نقطة، ثم فتح قوس، ثم التاريخ بالميلادي، ثم إغلاق القوس، ثم نقطة، ثم العنوان بحروف مائلة والحرف الأول من كل كلمة يكون كبيرا (كابتل capital؛ يستثنى من ذلك أدوات التنكير والتعريف مثل "a" و "an" و "the" وحروف الجر مثل "to" و "of" و "in" وأدوات الربط "and" و "but" و "or" فيبقى الحرف الأول منها بحروف صغيرة، إلا إذا كانوا في بداية اسم المجلة فيكون الحرف الأول منها بحروف كبيرة)، ثم نقطة، ثم يكتب "Available at:" ثم يدرج الرابط، وبعد الرابط يفتح قوس ويكتب "accessed on" ثم يدرج التاريخ على هذه الصيغة "2020/07/27"، ثم يغلق القوس. أدناه مثال على ذلك:

Al Ahmed, K.A., Al Muhammed, S.F. and Al Saleh, A.F. (2020). *The History of Agriculture in Al Ahsa*. Available at: https://www.kfu.edu.sa/ar/Departments/Sjournal/Pages/home.aspx (accessed on 10/12/2020)

9.3. رومنة/ترجمة موقع إلكتروني غير إنجليزي في قائمة المراجع

يبدأ كل مرجع باسم العائلة للمؤلف الأول، ثم فاصلة، ثم الحرف الأول من الاسم الأول للمؤلف الأول، ثم نقطة، ثم الحرف الأول لاسم الأب للمؤلف الأول، ثم نقطة، ثم فاصلة، ثم اسم العائلة للمؤلف الثاني، ثم فاصلة، ثم الحرف الأول من الاسم الأول للمؤلف الثاني، ثم نقطة، ثم الحرف الأول لاسم الأب للمؤلف الثاني، ثم نقطة، ثم حرف العطف "and" (وليس "&") ثم اسم العائلة للمؤلف الثالث، ثم فاصلة، ثم الحرف الأول من الاسم الأول للمؤلف الثالث، ثم نقطة، ثم الحرف الأول لاسم الأب للمؤلف الثالث، ثم نقطة، ثم فتح قوس، ثم التاريخ بالميلادي، ثم إغلاق القوس، ثم نقطة، ثم العنوان (مرومن) بحروف مائلة والحرف الأول من كل كلمة يكون كبيرا (كابتل capital)، ثم فتح علامة تنصيص واحدة، ثم العنوان مترجما والحرف الأول من كل كلمة يكون كبيرا (كابتل capital؛ يستثنى من ذلك أدوات التنكير والتعريف مثل "a" و "an" و "the" وحروف الجر مثل "to" و "of" و "in" وأدوات الربط "and" و "but" و "or" فيبقى الحرف الأول منها بحروف صغيرة، إلا إذا كانوا في بداية اسم المجلة فيكون الحرف الأول منها بحروف كبيرة) والكلمة غير مائلة، ثم إغلاق علامة التنصيص، ثم نقطة، ثم يكتب "Available at:" ثم يدرج الرابط، وبعد الرابط يفتح قوس ويكتب "accessed on" ثم يدرج التاريخ على هذه الصيغة "2020/07/27"، ثم يغلق القوس، ثم تكتب "[in Arabic]". أدناه مثال على رومنة المرجع العربي:

Al Ahmed, M.A., Al Ali, I.S. and Al Salah, A.M. (2020). *Iinjazat Jamieat Almalik Faysal Mundh Tasisiha* 'Achievements of King Faisal University since its Foundations'. Available at: https://www.kfu.edu.sa/ar/Departments/Sjournal/Pages/home.aspx (accessed on 10/12/2020) [in Arabic]

في حالة كون الموقع بلغة غير العربية وغير الإنجليزية، ولكن هذه اللغة تستخدم حروف غير إنجليزية، فتتم رومنة العنوان بالطريقة نفسها التي تتم بها رومنة العناوين العربية. ولكن، في حالة كون الموقع بلغة غير العربية وغير الإنجليزية، ولكن هذه اللغة تستخدم الحروف الإنجليزية نفسها، فلا حاجة لرومنة عنوان الموقع، ويكتفى بإبقاء العنوان في لغته الأصل ووضع الترجمة في علامة تنصيص. فعلى سبيل المثال، في حالة كون الموقع باللغة الألمانية، فيبدأ المرجع باسم العائلة للمؤلف الأول، ثم فاصلة، ثم الحرف الأول من الاسم الأول للمؤلف الأول، ثم نقطة، ثم الحرف الأول لاسم الأب للمؤلف الأول، ثم نقطة، ثم فاصلة، ثم اسم العائلة للمؤلف الثاني، ثم فاصلة، ثم الحرف الأول من الاسم الأول للمؤلف الثاني، ثم نقطة، ثم الحرف الأول لاسم الأب للمؤلف الثاني، ثم نقطة، ثم حرف العطف "and" (وليس "&") ثم اسم العائلة للمؤلف الثالث، ثم فاصلة، ثم الحرف الأول من الاسم الأول للمؤلف الثالث، ثم نقطة، ثم الحرف الأول لاسم الأب للمؤلف الثالث، ثم نقطة، ثم نقطة، ثم فتح قوس، ثم التاريخ بالميلادي، ثم إغلاق القوس، ثم نقطة، ثم العنوان باللغة الألمانية بحروف مائلة والحرف الأول من كل كلمة يكون كبيرا (كابتل capital)، ثم فتح علامة تنصيص واحدة، ثم العنوان مترجما للإنجليزية والحرف الأول من كل كلمة يكون كبيرا (كابتل capital؛ يستثنى من ذلك أدوات التنكير والتعريف مثل "a" و "an" و "the" وحروف الجر مثل "to" و "of" و "in" وأدوات الربط "and" و "but" و "or" فيبقى الحرف الأول منها بحروف صغيرة، إلا إذا كانوا في بداية اسم المجلة فيكون الحرف الأول منها بحروف كبيرة) والكلمة غير مائلة، ثم إغلاق علامة التنصيص، ثم نقطة، ثم يكتب "Available at:" ثم يدرج الرابط، وبعد الرابط يفتح قوس ويكتب "accessed on" ثم يدرج التاريخ على هذه الصيغة "2020/07/27"، ثم يغلق القوس، ثم تكتب "[in German]". أدناه مثال على ذلك:

Al Ahmed, M.A., Al Ali, I.S. and Al Salah, A.M. (2020). *Erfolge der King Faisal University seit ihrer Gründung* 'Achievements of King Faisal University since its Foundations'. Available at: https://www.kfu.edu.sa/ar/Departments/Sjournal/Pages/home.aspx (accessed on 10/12/2020) [in German]